THE DEVELOPMENT OF AN ABSOLUTE VISCOMETER FOR USE AT ELEVATED CONDITIONS, WITH PARTICULAR REFERENCE TO THE VISCOSITY OF WATER.

by

Jon Wonham, B.Sc.

Thesis submitted for the Degree of Ph.D.

The University of Glasgow.

September, 1967

CONTENTS

Page No

Chapter 4 (cont'd)

PREFACE

This thesis forms a report of the progress made by the author in developing a rotating cylinder viscometer for measurement at elevated temperature and pressure. Initially, some proposals of Whitelaw (5) were tested in a preliminary design of viscometer. Experience gained with this instrument made possible the construction of a viscometer from which the viscosity of liquid water has been obtained in the range 12° to 116°C and at pressures up to 230 Kgf/cm^2.

Important features of this design, which have been successfully applied, include a null technique for measuring the angular deflection of the stationary cylinder and the use of a high pressure mechanical face seal for the shaft driving the rotating cylinder. A vacuum rig was constructed for measuring the torsional properties of suspension wires used in the viscometer. The temperature of this rig could be varied which allowed the torsional stiffness of tungsten wire to be determined experimentally up to 150°C.

Viscosity measurements at 1 atm. pressure were fitted to a modified Arrhenius equation of the form

$$\eta = A e^{\frac{B}{T - T_o}}$$

The standard deviation of experimental values from this equqtion was 7×10^{-3} cP which, at 20°C, amounts to approximately

0.7% of the measured viscosity. The absolute value of viscosity given by this equation was approximately 0.5% higher than the presently accepted standard value at this temperature. At temperatures above 50°C the results obtained appear to be slightly low, the possible reasons for which have been explained.

Results at elevated pressure were made over a similar temperature range although the majority of determinations were made at temperatures below 20°C. These low temperature measurements lend support to the findings of Bett and Cappi (48) rather than those of Horne and Johnson (52) who have made the most recent experimental investigations in this field. The results obtained are regarded as preliminary in so far as a systematic coverage of the whole range has not yet been made.

A second, partially completed, instrument is described which will extend the range of measurement to 400°C and 1000 Kgf/cm^2. A system of radial diffraction gratings producing moire fringes has been incorporated which, it is expected, will improve the precision with which the deflection of the inner cylinder may be obtained.

Since the dynamic method of measuring the torsional stiffness of the wire has been used a number of tests were performed to investigate the effect of varying the mass, inertia and amplitude of a torsional pendulum. The results of these tests are described in a number of Appendices, the main conclusion being that the

amplitude effect is significant and a correction factor may be derived which can be applied to the angular deflection of the wire when it is used statically.

LIST OF SYMBOLS

a	amplitude
A, B & C	constants
d	radial distance between cylinders
D	diameter of inertia ring
e	eccentricity, also emf
E	activation energy of viscous flow
F	torsional stiffness
g	acceleration due to gravity
	also gap between stationary cylinder and guard cylinder
h	stationary cylinder length
	also distance between parallel plates in radial flow viscometer (Chapter 2)
I	angular moment of inertia
J	polar moment of inertia
	also mechanical equivalent of heat
k and K	constants
l	suspension wire length
	also timed fall-tube length (Chapter 2)
L	effective stationary cylinder length
L_F, L_G	lengths of mirror and carrying rod (Chapter 2)
m	mass
M	modified torque due to eccentricity
N	tachometer reading
P	pressure (Chapter 2)

P	pressure drop	Chapter 2
P'	pressure drop along radius r from r_2 to r_1	
r	radial distance	
r_o	radius of oscillating disc	
r_1	inner radius of plate	
r_2	outer radius of plate	
r_F, r_G	radii of mirror, carrying rod	
r_s	radius of sphere	
R	capillary radius	
R_1	inner radius of annulus) annular flow viscometer	
R_2	outer radius of annulus)	
R_b	radius of bulb	
T	periodic time) oscillation viscometers	
T_o	periodic time in vacuum)	
t	time for 1 rev. of rotating cylinder	
R_1, R_2	outer and inner cylinder radii respectively	
Re	Reynolds number	
Re_{crit}	critical value of Reynolds number	
u_1	constant velocity at capillary inlet)	Chapter 2
u_t	terminal velocity - falling body)	
U	surface velocity of moving cylinder	
u, v, w	velocities in co-ordinate directions	
W	mass of falling body (Chapter 2)	
x, y, z	co-ordinate directions	
α	coefficient of linear expansion	
α_m	angular amplitude of oscillation m (chapter 2)	

α_n angular amplitude of oscillation n (Chapter 2)

δ distance on curved scale

Δ logarithmic decrement

Δ_o decrement due to wire damping (Chapter 2)

ϵ small measured distance

η dynamic viscosity

θ angular distance

λ inter-molecular distance) (Chapter 1)
also mean free path)

μ refractive index

ν kinematic viscosity

ρ density

σ standard deviation

τ shear stress
also periodic time - torsion wire calibration.

ω, Ω angular velocity

χ coefficient describing temperature dependence of torsional stiffness

ψ stream function

LIST OF FIGURES

CHAPTER 1

INTRODUCTION

1.1 Motivation

In recent years there has been considerable activity in the measurement of transport properties of water substance. The requirement for accurate property values has been stimulated by the advancement of technology into fields of temperature and pressure which previously were considered to be of purely academic interest. Furthermore, the greater availability of computers has led to progress in formulating properties with a view to making the utilisation of these values more convenient to the engineer, for whom design-calculation by computer is now an every-day event. It can be seen that the provision of tables and formulae describing physical properties is an important service to technology, and that the provision of "raw data", whether this be obtained from theory or by experiment, is an essential activity which is perhaps overlooked by those concerned only with the end product.

In the particular case of water substance, progress in this field has been reviewed and stimulated by the International Conference on the Properties of Steam, the most recent of these being at New York in 1963. As a result of these meetings tables and formulations are published and recommendations are made as to the tolerances which must be applied to each part of the range of properties considered.

It is apparent from examination of these tables that in many cases a fairly wide tolerance has been applied due to the scatter in the various pieces of experimental evidence used or possibly because of a severe lack of experimental values over parts of the field.

Kestin and Whitelaw (1) have given a brief account of the findings of the 1963 Conference with regard to transport properties and have listed the experimental work used as the basis for formulations and tables produced by the Conference. For example, consideration of the viscosity of liquid water in the range from saturation pressure to 800 bar and 0 - 300°C has led to the acceptance of the following tolerances.

$$\text{Saturation pressure} \leqslant p \leqslant 350 \text{ bar} \quad \pm 2.5\%$$

$$350 \text{ bar} < p \leqslant 800 \text{ bar} \quad \pm 4\%$$

It should be realised, however, that particular experimental values, for example those of Swindells, Coe and Godfrey (2) and Roscoe and Bainbridge (3) made at 1 atm pressure and 20°C agree very closely and can have a much finer tolerance applied (in this case ± 0.05%).

The interest in liquid water extends naturally from the previous work carried out in this University, namely that of Kjelland-Fosterud (4), Whitelaw (5) and Ray (6) who measured the viscosity of supercritical steam and that of Latto (7) whose measurements of steam at 1 atm pressure were made over a range extending to 1100°C. These workers all used capillary viscometers for their measurements, but in the examination of alternative methods Fosterud

and Whitelaw both recommended the use of rotational viscometry. Other workers have shown that the rotating cylinder method can be developed to a high degree of accuracy, the best known being Bearden (8) who claims an accuracy of ± 0.01% for his measurement of the viscosity of air at 20°C and at atmospheric pressure.

It has been concluded that the fairly wide tolerances which must be applied to correlations compiled from consideration of the present experimental situation can be improved by making a fresh approach to the problem, preferably by an absolute method. However, because of the need for experimental values from the capillary viscometers, no progress on alternative methods was made until the commencement of the present work.

Having described some of the reasons for undertaking the present task the remainder of this chapter is concerned with the fundamental nature of viscosity and some of the theoretical attempts to evaluate this property from consideration of molecular structure in the liquid state. The lack of success met with so far in the latter approach must strengthen the arguments for developing new experimental techniques, especially in the case of water.

1.2 Nature of viscosity

Motion in 'perfect' fluids is such that there is no internal resistance to change of shape, i.e. layers in contact act on each other with normal forces but no tangential shearing forces. However, real fluids transmit tangential as well as normal stresses and the measure of these frictional forces is expressed by the term 'viscosity', which is a property of the fluid. For the sake of definition, considering the flow of a real fluid between two parallel plates one at rest and the other moving with velocity v, Newton's law of friction is given by

$$\tau = \eta \frac{dv}{dx}$$

where τ is the frictional shear force and η is the constant of proportionality. This factor η is defined as the first coefficient of viscosity or the shear viscosity but is generally referred to simply as 'viscosity'. The second coefficient of viscosity, which should be mentioned for completeness, is concerned with the viscous forces generated by compression (or dilatation). It is a measure of the viscous forces which arise when a volume of fluid is compressed or dilated without change in shape. A determination of this property has been made by Liebermann (9) for water and a number of other liquids. He was unable to relate the values obtained with the first coefficient of viscosity and at 20°C the value obtained for water was about 2.4 times the first coefficient.

Physical properties are a function of the intermolecular forces existing in a fluid, the relationship between the properties and those forces having received much attention both theoretically and experimentally. The behaviour of solids and gases is now fairly well understood from fundamental considerations, and many properties can be predicted theoretically with reasonable accuracy. For instance, in the case of dilute matter, i.e. the low pressure gas, the molecules are widely separated, therefore the interaction is small and their distribution is random. In this case the prediction of the observed macroscopic properties of this phase in terms of the microscopic behaviour is possible by means of statistical mechanics. At the other extreme, a solid crystalline body is characterized by long range order, short intermolecular distances and large interactions. The regularity and orderly arrangement of the molecules in this state greatly simplifies the treatment which can be made. Liquids, however, at first appear to have none of these simplifying features. The molecules are too close to be assumed independent, as in a gas, but they have more freedom than in the solid. Evidence that order exists to some extent in liquids has been provided by Gringrich (10) from x-ray diffraction studies and by the neutron diffraction work of Henshaw (11).

1.3 Molecular interactions

In 1931, London (12) showed that for any two polarizable systems there is an interaction with a negative potential. Consequently two neutral molecules experience an attraction due to their mutual polarization which is generally known as the van der Waal's force. As well as the attractive force there is a repulsive one which dominates at short separation distances. This arises because of interpenetration of the electron clouds of the atoms. In addition to these universally present forces there may be other types of interactional forces such as 'ionic' and 'polar' which add to the complexity of the behaviour. Several attempts have been made to represent the mutual potential energy of a pair of molecules mathematically, for instance, the model proposed by London being

$$U(r) = A \exp(-Br) - \frac{C}{r^6}$$

where the energy of interaction is represented by $\frac{1}{r^6}$ and the energy of repulsion (when the molecules closely approach) being proportional to $\exp(-Br)$ where B is a constant. Another model is the Lennard Jones (11) 6 - 12 potential

$$\text{i.e.} \quad U(r) = 4E\left(\frac{\sigma}{r^{12}} - \frac{\sigma}{r^6}\right)$$

where r is the separation between molecules, E is the minimum energy of interaction and σ is the collision diameter, (i.e. the separation for which the energy of interaction is zero). For simple non-polar

gases these theories have been successfully used to explain both the equation of state and transport phenomena. However, for more complex molecules and for dense gases the theories have not been sufficiently developed for the accurate prediction of properties to be made.

Before discussing theories of the liquid state it is worth considering briefly the behaviour of water compared with other members of the hydride series, H_2S, H_2 Se and H_2 Te. Comparison of the points of fusion of these substances illustrates the anomalous nature of water. The last three members of this series may be considered as normal condensates of neutral molecules since their points of fusion may be derived from the assumption of van der Waal's forces of interaction. If, however, the same type of interaction was to occur in water, the theoretical point of fusion would be found to lie close to - 100°C. The molecular interaction which accounts for this behaviour in water is known as the hydrogen bond. Although hydrogen is classed as a univalent element, which means that it can form only one strong chemical bond with any other element, it can form a second weaker linkage with elements such as fluorine, nitrogen and oxygen. Consequently, in water, the two hydrogen atoms of each molecule can form hydrogen bonds with the oxygen atoms of two other water molecules, while, at the same time, the oxygen can link with two hydrogen atoms of two further molecules. As a result, 5 molecules can associate together as 4 molecules arranged in a

tetrahedron about a given central molecule. The ways in which ice can be made up from this basic structure has been obtained from x-ray data. However, the degree to which hydrogen bonded networks are carried through into the liquid state is not known exactly, although there is much evidence to suggest that such networks, or clusters, of associated molecules do exist in liquid water. Before discussing the problems of arriving at a model for water the following section has been included to provide some general theoretical background for the liquid state.

1.4 The liquid state

The models postulated to describe the liquid state fall into two categories. Firstly, there are those which start from a description of the structure which is usually approximate and simple, leaving the question of how this structure is determined by the molecular properties until it is ascertained that the theory is effective. Secondly there are theories which emphasise initially the process by which the intermolecular forces determine the structure in the hope that a correct mathematical description of this process might also lead to equations whose solutions describe the structure. This second type of theory has closer affinities with the theories of the gaseous state. They are called "distribution function" theories because the equations involve distribution functions specifying the probability of finding sets of molecules in particular configurations. According to Temperley (14) the direct study of the distribution

function g(r), which can be measured experimentally, has practically superseded most other models of the liquid state. Returning to models of the former type, these are called "lattice theories" because the proposed structure often bears some relation to the regular lattice structure of a crystalline solid. These models are still of considerable physical value and detailed analysis using these methods are described by Barker (15) in "Lattice Theories of the Liquid State". These theories include the following:-

(a) The "hole" model in which the liquid is thought of as being like a crystal lattice from which some of the molecules are missing.

(b) The "cell" model in which a typical molecule is supposed to be confined to a small region of the liquid by the repulsive fields of its neighbours. Occasionally it can squeeze between its neighbours and migrate through the fluid, this process being associated with viscous flow.

(c) The "significant structure" or "cybotactic" model in which a typical molecule is supposed to spend a proportion of its time in surroundings resembling a crystal and the remainder in a gas like environment.

The significant structure theory is described in greater detail below because the results of applying the method are convincingly successful, this being partly due to the empirical nature of the

procedure. The theory has been described in several papers by Eyring and his colleagues (16) (17) and (18). It is first necessary to accept that 'holes' are present in liquids. The argument that holes exist is perhaps supported by the fact that glass, which is a metastable liquid, has minute passageways in the structure which allow helium to pass through it. It is postulated that there are three significant structures in the liquid state. The first structure is that of molecules with solid-like degrees of freedom, i.e. in the direction of one or more degrees of freedom, the molecule is bonded and restrained to an equilibrium position much as if it were in a solid state. Secondly, there is positional degeneracy due to the presence of vacant sites accessible to a molecule. In shifting to the new equilibrium position, more or less elastic energy is stored by the molecule due to distortion of the structure. Thirdly, it must be accepted that molecules which have escaped in one direction at least from fitting into the "potential well" made by neighbouring molecules, may, in the liberated state move with "gas-like" degrees of freedom. Thus, it is proposed that a molecule has solid like properties for the short time it vibrates about an equilibrium position, then it instantly transforms to gas-like behaviour as it jumps into the neighbouring vacancy.

It can be shown that the fraction of molecules with gas-like properties is $\frac{V - V_s}{V}$ and that the remaining fraction $\frac{V_s}{V}$ are solid like, where V_s and V are respectively the molar volumes of the solid and the liquid phases.

The viscosity is then given by

$$\eta = \frac{V_s}{V}\eta_s + \frac{V - V_s}{V}\eta_g \qquad \ldots.1.1$$

in which the viscosity of solid like molecules η_s can be calculated using the rate process theory postulated by Eyring (19) and can be expressed as

$$\eta_s = \frac{\lambda_1 \, h \exp\left\{\frac{a' \, E_s \, V_s}{RT\,(V - V_s)}\right\}}{\left(\frac{\lambda^2 \lambda_2 \lambda_3}{6}\right) K \left(1 - e^{-\frac{\Theta}{T}}\right) n \, \frac{V - V_s}{V}} \qquad \ldots.1.2$$

where E_s and Θ are respectively the energy of sublimation and the Einstein temperature of the solid phase, T is absolute temperature, h is Planck's constant and λ is the distance between two successive equilibrium positions between molecules for viscous flow.

The significance of the remaining symbols may be best obtained by reference to the text of Eyring's rate theory. The term η_g is taken as the expression for gas viscosity

$$\eta_g = \frac{1}{3} \, n \, m \, \bar{c} \, \lambda \qquad \ldots.1.3$$

where n is the number of molecules per c.c.

m is the molecular mass

$\bar{c}$ is the average molecular velocity

and λ is the mean free path in this equation.

Equation 1.3 becomes

$$\eta_g = \frac{2}{3\pi^{3/2} d^2} (m k T)^{\frac{1}{2}} \quad \text{.....1.4}$$

where k is Boltzmann's constant and d is the molecular diameter. Equation 1.4 represents the viscosity of a gas composed of hard spheres at low density.

Taking

$$\frac{\lambda^2 \lambda_2 \lambda_3}{\lambda_1} = \frac{V_s}{N} \quad \text{in equation 1.2}$$

where N is Avogadro's Number and substituting equations 1.2 and 1.4 in equation 1.1 gives the final viscosity equation

$$\eta = \frac{Nh}{V} \frac{1}{(1 - e^{-\Theta/t})} \frac{6}{nK} \frac{V_s}{V - V_s} \exp \frac{a' E_s V_s}{(V - V_s) RT}$$

$$+ \frac{V - V_s}{V} \frac{2 (m K T)^{\frac{1}{2}}}{3\pi^{3/2} d^2} \quad \text{.....1.5}$$

This method has been described in some detail since it has been used to calculate the viscosity of argon (17) and also the viscosity of molten sodium and mercury (20) with some success.

The part of equation 1.5 given by

$$\frac{a' E_s V_s}{V - V_s}$$

is termed the activation energy for flow. In order to calculate the viscosity with reasonable accuracy it is necessary to assume some

value of a' and to calculate the value of K which fits the known value of viscosity of the fluid concerned at some particular temperature. The wholly empirical nature of the final fit achieved is the result of choosing a' and K which agree with the best experimental data available. The authors of (20) mention that the theory is being further developed to include a significant structure theory of water. For water the significant structures contemplated are structures analogous to the tetrahedrally bonded ice I structure and the close-packed ice III structure. The proportion of molecules which at a given temperature are in these two forms must be estimated in some way.

In the authors' opinion there is still some way to go before the significant structures theory can be used to predict property values for water. However, this cannot be the sole criterion by which the success of the method is judged, for if such a theory can be shown to fit the existing experimental data with some success, then the theory could well be used as a guide to the properties of substances for which very little experimental data exists.

1.5 The degree of association in water

Returning now to the specific problem of the behaviour of water, it was previously mentioned in Section 1.2 that molecules are associated, as a result of the hydrogen bond, in the liquid state. Workers attempting to explain the behaviour of water have arrived at

different figures for the degree of association which exists. A few of these will be mentioned to illustrate the conflicting figures which have been put forward as a result of approaching the problem in different ways. Bernal and Fowler (21) have, in principle, treated water as a crystalline system. This theory yields an amount of 75% associated molecules at 100°C. The approach of Forslind (22) is similar to the above, except that the theory has been modified to take into account some effects of molecular interaction. He arrives at a figure for the number of associated molecules similar to that given by Bernal and Fowler. However, Grunberg and Nissan (23) have used the energy of activation of viscous flow for water to calculate the degree of dissociation at different temperatures. They found that the fraction of dissociated hydrogen bonds in water was 0.2 at 0°C, 0.6 at 50°C and 0.7 at 100°C. A more recent approach for a suggested water structure has been made by Frank and Wen (24). Their conclusions have been arrived at by considering the effect of ion solutes on the properties of aqueous solutions. Working along similar lines Nemethy and Scherega (25) have estimated that in going from 0° to 100°C the fraction of unbroken H-bonds decreases from 0.529 to 0.325.

For the author, the fact that there is little agreement between the conclusions of different workers is taken to imply that a great deal of progress is yet to be made in predicting properties theoretically. None of the theoretical models describes the behaviour of water exactly and the Nemethy-Scherega model which is

the most recent of those discussed cannot be used with any certainty. However, the general conclusion that structured regions of more ordered molecules exist in liquid water is an important one. These regions are less dense than the free water, thus cluster break-up results in a volume decrease and is therefore enhanced by the application of pressure. Since the structured effect is greater at low temperatures the effect of pressure as a possible structure breaking influence is far greater in this region. This is borne out by the experimental results for the viscosity of compressed water, which is discussed more fully later in the thesis.

CHAPTER 2

TECHNIQUES FOR THE MEASUREMENT OF VISCOSITY OF NEWTONIAN FLUIDS

Before commencing to describe the particular method of viscometry which provided the experimental basis for the present work, the alternative methods available will be discussed. By doing this, the factors affecting the final choice of viscometer may become more obvious and may assist any other researcher faced with a similar situation. Only the more recent developments need to be mentioned since other sources may be consulted for the complete picture, for example, Barr (26), Merrington (27), Dinsdale and Moore (28) and Kestin (29). The latter reviewed the methods available for measuring the viscosity of gases at high pressures and temperatures. It must be realised that a particular method may be only suitable for measurements over quite a small range of viscosity values or, for example, at high temperatures but not high pressures. Almost inevitably the choice of viscometer for a particular set of conditions is limited to a few alternatives, any one of which will require special treatment to be successful. Attention here is confined mainly to methods which are amenable to high pressure measurements.

2.1 Capillary

The most commonly used method in viscometry utilises the flow through a cylindrical tube as described by the Hagen-Poiseille equation. This may be presented in the form

$$\eta = \frac{\pi R^4}{8 \dot{m}} \rho \frac{\Delta P}{L} \qquad \ldots.2.1$$

where the viscosity may be calculated if the density, ρ, the radius of the tube, R, and the length of the tube, L, are known. This method also entails measurement of the pressure drop along the tube, ΔP, and the mass flow rate, $\dot{m}$. Laminar flow may be assumed if the Reynolds Number given by

$$R_e = \frac{2 \rho \bar{u} R}{\eta}$$

has a value less than 2000. Corrections have to be applied due to the fact that fully developed flow cannot occur over the full length of the tube. However, these can be minimised by increasing the length of the tube and, anyway, the magnitude can be estimated by theoretical considerations with reasonable accuracy. These considerations give

$$\frac{X_{99.9\%}}{R. R_e} = 0.24757$$

and

$$\Delta P = \frac{8 \eta u_1 x}{R^2} + \tfrac{1}{2} u_1^2 m$$

where $m_{99.9\%} = 2.262$ and where $x_{99.9\%}$ is the distance along the cylinder from entry to the point where the velocity is 99.9% of the fully-developed value. The solution is based on a constant velocity u_1 across the tube entrance.

2.2 Annular gap

The Navier-Stokes equation which describes fully-developed flow in a cylindrical tube, namely,

$$\frac{dP}{dx} = \eta\left\{\frac{d^2u}{dy^2} + \frac{1}{y}\frac{du}{dy}\right\} \qquad \ldots 2.2$$

(in cylindrical co-ordinates), is also valid for the flow in an annulus provided the gap is small compared with the radius. Applying the appropriate boundary conditions to equation 2.2 namely $u = 0$ at $R = R_1$ and R_2, the solution may be given as

$$\eta = \frac{\pi \Delta P}{8 \dot{m} L}\left[(R_2^4 - R_1^4) - \frac{(R_2^2 - R_1^2)}{\ln \frac{R_2}{R_1}}\right] \qquad \ldots 2.3$$

A limiting Reynolds Number of 2000 must again be applied where R_e may be defined as

$$R_e = \frac{2\rho \bar{u} (R_2 - R_1)}{\eta}$$

The magnitude of the development length with laminar flow has been investigated by Heaton, Reynolds and Kays (30) who show that

$$\frac{x_{99.9\%}}{(R_2 - R_1).\, R_e} = f\left(\frac{R_2}{R_1}\right)$$

and that the pressure drop in the entrance section is also a function of the radius ratio. The values of the appropriate functions may be obtained from this reference.

2.3 Radial flow between parallel plates

An exact solution of the Navier-Stokes equation exists for the flow between infinite plates which, of course, is a hypothetical situation. However, several solutions exist in the case where the discs are of reasonable proportions and where fully developed radial flow can be assumed to exist between the plates. In this case the equation to be solved is a combination of the momentum and continuity equations and may be expressed as

$$-\rho\frac{(\dot{u}r)}{r^3} = -\frac{dP}{dr} + \frac{\eta}{r}\frac{d^2(\dot{u}r)}{dy^2} \qquad \ldots.2.4$$

Equation 2.4 is obtained by making the reasonable approximation that the axial component of velocity V_y can be set to zero. Making this assumption Moses (31) has obtained an exact solution to the equation 2.4. When compared with the solution of Peube (32) which involves expressing the axial velocity component as a power series and which is mathematically more rigorous, Moses found there was little to choose between the two solutions and both agreed closely to his experimental observations. It should be pointed out that the simplest solution to equation 2.4 which can be obtained by neglecting the inertia term $-\rho\left(\frac{\dot{u}r}{r^3}\right)$ which, for flow radially inwards, is given by

$$\eta = \frac{4}{3}\pi\rho\frac{h^3}{\dot{m}}\frac{\Delta P'}{\ln\frac{r_1}{r_2}} \qquad \ldots.2.5$$

This is known as the "creeping flow" solution and in the case of water flowing Moses found it to be as much as 10% in error, depending on the Reynolds Number.

When the first three terms only of the series expansion are considered Peube's solution is

$$\eta = \frac{\frac{\pi \rho h^3 \Delta P'}{\dot{m}} - \frac{27}{560}\left(\frac{\dot{m}}{\pi h}\right)\left(\frac{h^2}{r_2^2} - \frac{h^2}{r_1^2}\right)}{\frac{3}{4} \ln \frac{r_1}{r_2}} \qquad \ldots 2.6$$

This solution is easier to use in viscosity measurements than Moses' solution, which involves elliptical integrals of the first and second kind and can only be conveniently used in conjunction with a digital computer. However, the more recent work of Moses (33) to apply this method in the form of a modified Rankine viscometer is promising for measurement at high pressures.

2.4 Oscillating viscometers

Many shapes, or combination of shapes of oscillating bodies can be used to determine viscosity. In all cases the method of expressing the viscosity in terms of measurable variables is the same - the equation of motion of the oscillating body being solved in conjunction with the equation of motion of the fluid. A comprehensive presentation of the theory of this type of viscometer has been given in a series of papers and reports published by Brown University, Prov. R.I., see references (34) and (35), and their

conclusions may be taken as a realistic guide to the geometries which allow precise determinations to be made.

In practice the sphere and disc have proved to be the most satisfactory oscillating bodies is viscometry. The disc is easier to manufacture but an exact solution of the differential equation exists only in the case of infinite radius. As a consequence the edge effects have to be accounted for by an inexact method. The sphere on the other hand is less easy to manufacture but the solution of the corresponding differential equation is exact in many cases. In practice the sphere or disc is suspended by a torsion wire and, in principle, the viscosity can be obtained by a measurement either of the period or the damping of the torsional oscillation. The values of the various parameters of the suspension system determine which measurement is the more important. It is generally found that both must be measured but that one is more sensitive to viscosity than the other.

At the present time it appears that only three forms of oscillating viscometer are of practical significance.

(i) A disc oscillating between fixed plates.

(ii) A sphere oscillating in a fluid of infinite extent.

(iii) A sphere filled with the test fluid oscillating in a vacuum.

These methods can also be used for relative measurements of viscosity. For instance, instruments in which the oscillation of

a disc in an infinite medium is applied, have been found to give highly reproducable relative measurements, as can be seen from references (36), (37) and (38). This method, however, is not suitable for absolute measurements since the finite width of the edge of the disc implies an approximate theory - in practice, the edge of the disc accounts for a large part of the total drag on the disc. Exact solutions for the infinite disc and cylinder have been given by Kestin and Person (39) on the assumption that the internal friction of the suspension wire is zero.

A disc oscillating between fixed plates:-

The amplitude of decay is measured which is usually expressed as the logarithmic decrement

$$\Delta = \frac{1}{2\pi m} \ln \frac{\alpha_m}{\alpha_n + \alpha_m}$$

The equations of motion of the suspension system and the fluid reduce to

$$\frac{2}{\theta}\left\{\frac{\Delta}{\theta} - \Delta_0\right\} - \frac{C\pi r_0^4 \delta}{I}\left[H_1K_2 + H_2K_1 + \frac{2d}{r}\left\{H_1 + \frac{3\delta}{2r\theta}\right\}\right] = 0 \qquad \ldots 2.7$$

where

$$H_{12} = \left\{1 \pm \left(\frac{3}{2}\right)\Delta - \left(\frac{3}{8}\right)\Delta^2\right\}(2\theta^3)^{-\frac{1}{2}}$$

$$K_1 = \frac{\sin Y}{\cosh X - \cos Y}, \qquad K_2 = \frac{\sinh X}{\cosh X - \cos Y}$$

$$X, Y = (2\theta)^{-\frac{1}{2}}\left[1 \pm \tfrac{1}{2}\Delta + \tfrac{1}{8}\Delta^2\right]\left[\beta_1 + \beta_2\right]$$

$$\beta_{1,2} = \frac{b_{1,2}}{\delta} \quad , \quad \delta = \sqrt{\frac{\eta T_o}{2\pi\rho}} \qquad \text{and } \Theta = \frac{T}{T_o}$$

This set of equations may be solved with the aid of a digital computer.

The constant, C, in equation 2.7 can be obtained in two ways. Newell (40) has shown that when

$$\delta >> \frac{2\, b_1\, b_2}{(b_1 + b_2)}$$

it may be evaluated from the expression

$$C = 1 + \frac{8}{\pi}\left(\frac{2b_1b_2}{b_1 + b_2}\right)\left[\cosh\psi \ln(\cosh\psi + 1) - (\cosh\psi - 1)\ln\sinh\psi\right]$$

$$+ \frac{2}{r}\left(\frac{2b_1b_2}{b_1 + b_2}\right)\left[1 + \frac{3}{2}\left(\frac{d(b_1 + b_2)}{2\, b_1b_2}\right) + 6\int_0^{\infty}\left(\frac{x}{\beta r}\right)\left[\frac{1}{\beta r} - \left(\frac{\partial w}{\partial \eta}\right)_{\eta=0}\right] dx \right. \qquad \ldots\ldots 2.8$$

$\left(\frac{\partial w}{\partial \eta}\right)_{\eta=0}$ is the Laplace transform of the axial gradient of the angular velocity in the field and

$$\beta r = \frac{\delta(b_1 + b_2)}{2b_1b_2}$$

When δ is of the same order of magnitude as

$$\frac{2\, b_1\, b_2}{b_1 + b_2}$$

C varies with $\frac{\delta}{r}$ and must be obtained by using equation 2.7 and

measurements of Δ and θ with a fluid of known viscosity to obtain the curve of C against $\frac{\delta}{r}$. In this case the instrument ceases to be an absolute viscometer.

A sphere oscillating in a fluid of infinite extent

Working formulae for an instrument of this type have been presented by Kestin and Wang (41) and by Moszynski (42) and these may be expressed as

$$\delta = \frac{4\, r_s \left(\frac{\Delta}{\theta} - \Delta_o^{\,1}\right)}{\frac{8\pi r_s^{\,5}}{3 I_s} P_i \rho\theta + \left[\left(\frac{8\pi r_s^{\,5}}{3 I_s} P_i \rho\theta\right)^2 + 16\rho\left(\frac{\Delta}{\theta} - \Delta_o^{\,1}\right)\left(\frac{8\pi r_s^{\,5}}{3 I_s} + \frac{\pi r_s^{\,2} r_F^{\,2} L_F}{3 I_s} + \frac{\pi r^2 r_G^{\,2} L_G}{I_s} + \frac{4\pi r^4}{3 I_s}\,\delta\theta - q_i\right)\right]^{\frac{1}{2}}} \qquad \ldots.2.9$$

where

$$P_i = \frac{\left[1 - \frac{3\Delta}{2} - \left(\frac{3\Delta^2}{8}\right)\right]}{\sqrt{2}\ \theta^{3/2}}$$

$$q_i = \frac{\left[1 + \left(\frac{\Delta}{2}\right) + \left(\frac{\Delta^2}{8}\right)\right]}{\sqrt{2}\ \theta^{\frac{1}{2}}}$$

Equation 2.9 attempts to take account of the viscous drag of the mirror, mirror-holder and stem of the suspension system. Kestin and Whitelaw (43) found that the equation gave absolute values accurate to ± 0.6%, although the equation could be used to provide more precise relative values. In the case where a disc oscillates between fixed plates the contribution of the mirror and stem can be made

negligible compared with the drag exerted by the fluid in the span between the plates. In the case of a sphere oscillating in an infinite medium such an arrangement is not possible. An assessment of the applicability of the oscillating sphere method for gases is given by Kestin and Wang (41).

A sphere filled with test fluid oscillating in vacuum

Equations 2.7 and 2.9 were both obtained from the imaginary part of the complex solution of the appropriate differential equations. A solution of the real part also exists for both of the cases referred to and provides a link between the period of oscillation and the logarithmic decrement. The imaginary solution was used by Kestin and his co-workers for their investigations, because the particular apparatus selected implied that the real solution contained small differences of large numbers.

Kearsley (44) on the other hand, has employed an instrument for which the real solution is more appropriate than the imaginary solution. In this case the period of oscillation is more sensitive to the viscosity than is the logarithmic decrement. The particular geometry investigated is that of a sphere filled with a fluid whose viscosity is to be determined and the appropriate equation is

$$\frac{5}{1 - Z \operatorname{ctg} Z} - \frac{15}{Z^2} = \alpha + \frac{1}{\eta^2 Z^4} \qquad \ldots\ldots 2.10$$

where

$$\alpha = \frac{I_m (Z^4 \phi (Z))}{I_m (Z^4)}$$

$$\frac{1}{\eta^2} = R_e\left(z^4 \phi(z)\right) - \alpha R_e(z^4),$$

$$\frac{1}{\tau} = -\eta I_m(z^2), \qquad D = \frac{2 R_e(z)^2}{I_m(z^2)}$$

R_e and I_m refer to the real and imaginary parts of Z respectively in this equation. Other symbols may be found in the nomenclature. Roscoe and Bainbridge (3) have determined the viscosity of water from observations of the oscillations of a glass vessel filled with liquid. The calculations were based on a formula derived by Roscoe (46) and expressible in the form

$$I_b \Delta = \frac{2}{3} R_b^4 (\pi \eta \rho T)^{\frac{1}{2}} F(\Delta, P) \qquad \ldots\ldots\ldots 2.11$$

where $F \rightarrow 1$ as $\Delta \rightarrow 0$ and P is very great.

2.5 Rotation

The principle of rotating viscometers is that two cylindrical or spherical objects are constructed, one slightly larger than the other, which are then arranged to have the same axis of symmetry so that the gap between them is constant and contains the fluid whose viscosity is to be measured. One object is rotated at a uniform rate and the drag force on the second object is measured. Only the rotating cylinder method has been used with a degree of success because of the difficulties of construction or alignment of anything but the simplest shape. The only other rotational method known to the author is that of rotating concentric spheres used by

Zemplen (47). Since the rotating cylinder method forms the main subject of this thesis it will not be discussed more fully here.

2.6 Falling body

Falling body viscometers are seldom used as primary instruments due to the inapplicability of such theoretical solutions as are available at practical working conditions. They can, however, be used as secondary instruments with considerable precision as has been shown by the work of Bett and Cappi (48) and Cappi (49) in particular.

In principle, the method requires that a spherical body, should fall, due to gravity, through the fluid whose viscosity is to be measured. If the flow is laminar and the Reynolds Number very low, then the inertia terms in the Navier-Stokes equations can be neglected and the equation to be solved becomes

$$\nabla^4 \psi = 0 \qquad \ldots.2.12$$

where ψ is the stream function. A solution to this equation, for flow past a sphere has been obtained by Stokes (50) and in an improved form by Oseen (51) for the particular case when the Reynolds Number

$$(R_e = \frac{2\rho u r_s}{\eta})$$

is less than 1 but this is seldom possible in practice. Most instruments using the principle consist of cylindrical bodies falling along the axis of a round, parallel and vertical tube filled with the

fluid in question. In this case the required solution is for flow through an annulus where one wall moves with respect to another. The appropriate working equation for this problem has been shown by Cappi to be of the form

$$\eta = \frac{W}{2\pi \ell u_t} \left\{ \frac{(R_2 + R_1) \ln \frac{R_2}{R_1} - (R_2 - R_1)}{3 R_2^2 - R_1} \right\} \qquad \ldots 2.13$$

However, this equation does not take into account the shear and pressure forces at each end of the cylindrical body and, so far, these effects have not been accounted for theoretically. Consequently, a working equation of the form

$$\eta = \frac{W}{\ell u} \underline{K}$$

is employed where $\underline{K}$ is the instrument calibration constant and is obtained from measurements with a fluid of known viscosity.

2.7 Rolling ball

For completeness the method by which the viscosity is determined by the time for a ball to roll the length of a tube should be mentioned. This is a relative method first used by Flowers (45) and still in use where the requirements are qualitative rather than quantitative in nature. The method suffers the disadvantage that the flow cannot be expressed mathematically and, in the author's opinion, other than viscous effects may influence the time for the ball to travel the length of the tube. The most recent measurements by this method are by Horn and Johnson (52).

2.8.1 Factors affecting choice of method

Although there is no great virtue in making measurements by an absolute method the use of a primary instrument has definate advantages. In a primary instrument the viscosity can be derived from observations of mass, length and time whereas in the secondary instrument use is made of a calibrating fluid to obtain the instrument constant. Consequently there is introduced the added uncertainty of the value of viscosity of the calibrating fluid. However, in the field investigated by the author, part of the uncertainty in the values found for viscosity up to the present time can be attributed to the variety of secondary instruments used, each covering only part of the range. It was therefore felt that an absolute method was desirable, if not essential, for the present investigation, thus eliminating the methods described in 2.6 and 2.7 from the present discussion. The capillary method is an obvious choice from many points of view, particularly since nearly everything about the practice of this branch of viscometry has been studied in detail. However, this method does not lend itself easily to absolute determinations in the high pressure form, partly because of the requirement for a high pressure manometer for sensing small pressure drops across the capillary and also because of the problem of providing a steady flow rate through the instrument and measuring the mass flow rate. In fact the capillary viscometer is far more amenable to development as a secondary instrument,

particularly in the form of a Rankine viscometer where the flow is induced by the effect of gravity on a mercury pellet in a vertical tube attached to the capillary. In addition it was felt that since existing data has been obtained from predominantly capillary instruments this traditional choice should be given a low priority in the present consideration of available methods.

There would appear to be several advantages in the development of the radial flow method for use at high pressures. Again, this method lends itself particularly to the closed circuit Rankine form of secondary viscometer in the same way as does the capillary. As an absolute method there are some noteworthy advantages over the capillary method. For instance, pressure tappings can be taken at different radii without affecting the flow appreciably. Flat parallel surfaces can be machined with great accuracy and there is less uncertainty than with the bores of capillary tubing which, except for glass or quartz, can be difficult to measure. The problem of providing a steady flow at high pressure is not insurmountable, this having been successfully achieved for capillaries by Tanaka et al (53) and more recently by Rivkin and Levin (54).

The use of an oscillating instrument would appear promising since the precision obtainable with the instrument has been shown to be excellent. However, the oscillating disc method is secondary because of the difficulty in obtaining an edge correction, and the oscillating spherical vessel method would appear to have insurmountable technical difficulties preventing its use as a high pressure method.

There remains the possibility of using the oscillating solid sphere. At the time of starting this work the only assessment of this method was by Moszynski whose results for the absolute viscosity of water were nearly 2% away from the accepted value at 20°C. Since no explanation was given for this behaviour, some apprehension was felt about the suitability of this method for a new investigation.

2.8.2 Method chosen

The method finally chosen for the present investigation was decided as much by force of circumstance as by consideration of the technical merits of each method. The flow between parallel plates was already being investigated by a colleague at the University of Glasgow. As mentioned in Chapter 1 the rotating cylinder method was known to be capable of a high absolute accuracy when used for measurements at atmospheric pressure. In view of the limited choice imposed by the requirement of a primary instrument it was decided to develop the rotating cylinder method for use at elevated conditions. The progress made toward this and the preliminary results obtained for liquid water form the subject matter of this thesis

CHAPTER 3

REVIEW OF LITERATURE

3.1 Application of rotation of a cylinder to viscometry

3.1.1 Historical Aspects: Newton, in Book II of "The Principia" stated the relations between velocity and resistance to flow for a rotating solid cylinder in a uniform and infinite fluid. He also showed that the rate of shear decreases exponentially in the concentric laminar shells of fluid as one moves away from the rotating cylinder and into the fluid. However, he did not apply integral calculus to the problem and hence did not arrive at the complete equation for the flow between concentric cylinders (sometimes called the "Margules' equation" after Margules (55) who was the first to derive this formula) given here as equation 3.7. Nevertheless, Newton arrived at the proper qualitative relationships for viscosities of fluids using the rotational system and it is noteworthy that the original definition of fluid-flow was not for the case of fluid between parallel plates, as is often implied in the literature.

Couette (56), in 1890 devised the first practical rotational viscometer which consisted of a rotating outer cylinder and an inner cylinder which was supported by a torsion wire and rested in a point bearing at the bottom. In this instrument guard rings were utilised to eliminate end-effects. In 1913, Hatschek (57) described a Couette type viscometer with guard rings of improved design which minimised end-effects with very low viscosity fluids. Instruments

employing steady rotation of one or other of the cylinders are often described as Couette or Hatschek viscometers after these two workers. The rotational viscometers which followed, for example, that of MacMichael (58), which employed a disc as the stationary member rather than a cylinder, were aimed at simplicity of procedure in routine investigations rather than absolute accuracy. The Stormer (59) viscometer also falls into this category.

Few absolute determinations of viscosity were made with any great accuracy using the rotating cylinder method until those of Gilchrist (60) and of Harrington (61) on air and the measurements of Leroux (62) on water. The design of the apparatus was, in all cases, similar to that used by Couette. The main problem, arising in the determination of absolute values, is the measurement of small couples produced by the low rates of shearing. This latter precaution is necessary from the theoretical assumption of laminar flow. The problem of providing a suitably sensitive suspension is discussed more fully in 4.3. Houston (63), Kellstrom (64) and Bearden (8) are among other, more recent, workers using this method to measure the viscosity of air, the latter having achieved the highest precision with a claimed accuracy of $\pm$ 0.01% for the viscosity at 20°C. The accuracies achieved by these workers was steadily improved by attention to detail in mechanical construction in order to eliminate errors due to misalignment and end-effects. These problems are discussed more fully in Section 5.1.

None of the workers so far mentioned carried out experiments at elevated pressures except Kellstrom (65) who modified his apparatus to measure the viscosity of air up to 30 Kgf/cm^2. To the authors knowledge the only two investigations using rotating cylinder viscometers for conditions at elevated temperature and pressure are those of Thomas, Harn and Dow (66) who tested lubricating oils up to 3000 Kgf/cm^2 and 250°C and Reamer, Cokelet and Sage (67) who have measured n-pentane and other hydrocarbons at pressures up to 330 Kgf/cm^2.

In recent years the development of rotational viscometers has followed two distinct patterns, depending upon the purpose for which the instruments were intended. Couette's design was suitable primarily for absolute measurements on Newtonian fluids, the virtual elimination of end-effects ensuring that the measured torque was entirely due to the fluid between the concentric surfaces. This ideal situation has been pursued by nearly all workers using instruments where high accuracy is essential. However, the development of rotational viscometers for the general field of rheological measurement has resulted in absolute accuracy being reduced in importance where many other features necessary for sensing non-Newtonian effects have taken priority in the design. In most of these instruments the provision of guard rings would be inconvenient for routine investigation and the basic design has been simplified to the straight "cup and bob" arrangement. Provided the bob is not completely immersed a correction need only be applied for its

bottom surface. This correction can be derived experimentally by making tests on the same fluid with the cup filled to several known levels. Extrapolation of the graph of torque : depth of immersion gives the corrected length of bob to include the end effect. Also solutions of the Navier Stokes equations exist allowing a theoretical correction to be applied for the end surface of the inner cylinder, an example being the solution arrived at by Roscoe (68).

Further consideration of the present objective indicated that the guard ring pattern was likely to provide the best solution. The necessity for pressurising the viscometer requires complete immersion of the inner cylinder with visual access only through a small high-pressure window. In such a design there is no possibility of deriving end-effects or verifying end corrections experimentally by varying the depth of immersion.

Having opted for the guard-ring layout, much has been gained by studying the refinements and considerations of the various instruments used for high-precision measurements. However, although the recorded experience of other workers was useful, the problem of carrying out the measurements at relatively high pressures underlies all practical considerations. In this respect only the viscometers of Thomas et al and Reamer et al have been designed for use at elevated conditions. The accuracy claimed for the measurements of the former of these experimenters was not high, being in the order of ± 4%. Their solution to providing a steady angular velocity to

the rotating cylinder was to completely immerse a small electric motor in the viscometer vessel so that only the electrical conductors had to pass through static seals in the pressure vessel. However, the heat generated by this motor made attainment of steady temperature impossible and this was the main source of error. The torque transmitted to the stationary cylinder was measured by the changing electrical resistance of a helical spring which supported this cylinder. It is doubtful whether this technique was highly accurate as the cylinder needed to be supported in bearings at both ends and some of the viscous effect would be lost in overcoming frictional resistance. The viscometer of Reamer et al can only be described as extremely complicated although the claim that the probable error of measurement does not exceed 0.4% seems justified. Their viscometer and an auxiliary pressure vessel are immersed in a large agitated fluid bath. The test fluid is pressurised through connections to the auxiliary pressure vessel by the injection of mercury. A centrifugal pump circulates the test fluid through the viscometer and auxiliary vessel for the particular case when mixtures are being tested, although it is pointed out that circulation is not employed when pure substances are investigated. A criticism of this arrangement is that no temperature measurement appears to be made of the test fluid, which is assumed to attain the temperature of the bath. In fact, it would appear practically impossible to obtain access to the test fluid in the viscometer to measure its temperature. However, in view of the method of fluid-sealing by close fitting sleeves

on the drive shaft and the presence of other moving parts it seems likely that the test fluid will be at a slightly higher temperature than the bath. Should this be the case the measured viscosity value will obviously be slightly in error. In this viscometer the angular movement of the suspended cylinder is measured electrically by a reluctance gauge technique, the claimed discrimination being 20 seconds of arc. This has allowed accuracies of ± 0.1% to be claimed for the angular deflection. Presumably the electrical equipment associated with this measurement has to be calibrated at the same temperatures at which tests are to be made prior to assembly of the viscometer.

Having discussed some aspects of instrument design the remainder of this review is concerned with the working equation, the equations governing instability and measurements of the viscosity of liquid water.

3.1.2 Derivation of the Margules equation

Consider now tangential annular flow of a Newtonian fluid between concentric cylinders of infinite length, for which the Navier Stokes equations in cylindrical co-ordinates are given in Appendix G. In steady state laminar flow the fluid moves in a circular pattern and the velocity components v_r and v_z are zero. It can also be assumed that there is no pressure gradient in the θ - direction. For this system all terms of the equation of continuity are zero and equations D, E and F reduce to

r component

$$-\rho \frac{v_\theta^2}{r} = -\frac{\partial p}{\partial r} \qquad \ldots.3.1$$

θ component

$$0 = \frac{d}{dr}\left(\frac{1}{r}\frac{d}{dr}(r v_\theta)\right) \qquad \ldots.3.2$$

z component

$$0 = -\frac{\partial p}{\partial z} + \rho g_z \qquad \ldots.3.3$$

Integration of euqation 3.2 with the following boundary conditions

$r = R_2$ (inner radius, inner cylinder stationary), $v_\theta = 0$

$r = R_1$ (outer radius), $v_\theta = \Omega_o R_1$

where Ω_o = angular velocity of rotating outer cylinder, gives

$$v_\theta = \frac{\Omega_o (R_2^2 - r^2)}{r\left[\left(\frac{R_2}{R_1}\right)^2 - 1\right]} \qquad \ldots.3.4$$

The shear stress distribution, $\tau_{r\theta}(r)$, can be obtained using equation J from the list of components of the stress tensor (see Appendix G). This becomes

$$\tau_{r\theta} = -\eta\left[r\frac{d}{dr}\left\{\frac{\Omega_o (R_1^2 - r^2)}{r^2\left(\left(\frac{R_2}{R_1}\right)^2 - 1\right)}\right\}\right]$$

$$= \frac{2\eta\Omega_o R_1^2}{r^2\left(1 - \left(\frac{R_1}{R_2}\right)^2\right)} \qquad \ldots.3.5$$

The torque T required to turn the outer cylinder may be calculated as Force x Lever arm,

$$\text{i.e.} \quad T = 2\pi R_1 L \left(-\tau_{r\theta}\right)_{r=R_1} \cdot R_1$$

$$= \frac{4\pi R_1^2 L \eta \Omega_o}{\left[\left(\frac{R_1}{R_2}\right)^2 - 1\right]} \qquad \ldots.3.6$$

This, of course, is the same value as the torque experienced by the stationary inner cylinder. Where it is required to obtain the viscosity by observation of the torque and the cylinder dimensions equation 3.6 may be conveniently re-written

$$\eta = \frac{T}{4\pi L \Omega_o}\left[\frac{R_1^2 - R_2^2}{R_1^2 R_2^2}\right] \qquad \ldots.3.7$$

The equation for the case when the inner cylinder is rotating and the outer cylinder stationary is identical to 3.7.

3.2 Consideration of the onset of unstable flow

It is necessary to know at what angular velocity of the cylinders the laminar concentric flow assumed in the derivation of equation 3.7, breaks down or becomes unstable. For completeness the problem of instability will be discussed for the general case of either cylinder or both cylinders rotating.

The factors affecting stability are quite different for the cases of inner and outer cylinder rotation. These factors have been discussed in a general manner by Schlichting (69) who has considered

particularly the influence of stabilizing forces on the origin of turbulence, for example centrifugal forces or density variation. For the case of the inner cylinder at rest and the outer cylinder rotating about the axis, the inertia forces have a highly stabilizing effect on the flow in the annulus. A fluid particle from an outer layer opposes being moved inwards because the centrifugal force acting on it exceeds that on a particle nearer the axis of the cylinder. Equally, motion outwards is made more difficult because the centrifugal force acting on an inner particle is smaller than that on a particle further away from the axis.

Schlichting derives what he calls the 'stability equation' which forms the departure of all stability considerations of two-dimensional laminar flows. The terms on the left hand side of the equation are derived from the pressure and inertia terms and those on the right hand side from the viscous terms. When the Reynolds number is large the equation is simplified by omitting viscous terms as compared with inertia terms. The resulting differential equation is known as the frictionless stability equation. The equation to be used in a stability problem depends on whether the inertia terms predominate in which case the simplified equation can be used. Thus instability of the flow in an annulus between concentric cylinders with the inner cylinder rotating and the outer at rest may be predicted using the frictionless stability equation. When the frictionless stability equation is applied to the flow when the outer cylinder rotates and the inner is at rest, laminar flow would appear to persist under all

conditions. However, when the complete stability equation is used it can be shown that the flow becomes unstable. In the following discussion of the literature most solutions to the problem of instability fall naturally under one or other of these headings.

Firstly, it is worth noting some of the observations of early experimenters relating to this problem. Couette (56) found that turbulence occurred with water and air in his apparatus when the outer cylinder rotated at a speed given by

$$R_e = \frac{\Omega a (b - a)}{\nu} = c.\ a.\ 1900$$

where a = 14.393 in. and b = 14.630 in.

Mallock (70) using smaller apparatus was able to reach values of R_e between 4,200 and 32,000 before the laminar conditions broke down. However, Taylor (71), who worked with cylinders of smaller diameter and greater length suggests that the turbulence found by Conette and Mallock was due to insufficient accuracy of construction or end-effects, and showed for the outer cylinder rotating that concentric flow existed at R_e = 12,500 which corresponded to the highest speed of his apparatus. Thus it might first appear that, in the absence of a theoretical solution, the onset of instability could not be accurately predicted by the various workers. However, it can be seen from Figure 1 that the points at which instability occurs follow a definite curve.

3.2.1 Taylor (71) was the first to analyse the general case in which both cylinders rotate in the same or opposite directions. His solution reduces to the following when the outer cylinder is stationary.

$$\frac{\Omega_c^2 \, R_2^2 \, d^3}{\frac{1}{2}(R_1 + R_2)\nu^2} = \frac{\pi^4 f}{0.0571 f^2 + 0.00056} \qquad \ldots\ldots 3.8$$

where Ω_c is the critical speed of the inner cylinder at which turbulence occurs

$$d = R_2 - R_1$$

$$\text{and} \quad f = 1 - 0.652 \frac{d}{R_1}$$

This formula was obtained on the assumption that $\frac{d}{R_1}$ was small but Lewis (72) in an experimental investigation found critical speeds which were in agreement with it up to $\frac{d}{R_1} = 0.71$. The experimental accuracy was improved compared with that of previous workers by ensuring that the length of cylinders was several times larger than the diameter. If the inner and outer cylinders have angular velocities Ω_1 and Ω_2 respectively and if

$$\mu = \frac{\Omega_2}{\Omega_1}$$

it may be shown that Taylor's result applies for $1 > \mu \geq 0$. However, for -ve values of μ the solution ceases to be valid. Meksyn (73) obtained a solution for the case where the cylinders rotate in the same direction using a different mathematical approach. This solution confirmed Taylor's findings and showed complete agreement with

the numerical results. For instance, the numerical factor in Taylor's solution of 0.0571 (see equation 3.8) was found by Meksyn to be 0.0569. In later work Meksyn (74) extended his solution to the case where the cylinders rotate in opposite directions. This solution is valid provided $-\mu$ is not much smaller than 0.5.

Chandrasekhar (75) has pointed out that previous workers had not solved the problem of stability completely since these solutions are valid only when the difference in radii of the two cylinders is small compared to their mean, i.e. when $d = R_2 - R_1 \ll \frac{1}{2}(R_2 + R_1)$.

Making a different approach, Chandrasekhar defines the onset of stability by the critical Taylor number T_c, where the Taylor Number

$$T = \frac{4 A \Omega_1}{\nu^2} d^4$$

In this equation

$$A = \Omega_1 \frac{1 - \mu \frac{R_2^2}{R_1^2}}{1 - \frac{R_2^2}{R_1^2}}$$

Chandrasekhar's more recent paper on instability (76) specifies the complete $T_c : \mu$ relationship over the entire range of μ wh ich is of practical interest. This solution is valid for the wide-gap case, and the results have been confirmed by the experiments of Donnelly (77). Theoretical confirmation of Chandrasekhar's findings has since been provided by Walowit et al (78) who also considered the effect on stability of a radial temperature gradient. In the case of this last investigation they concluded that positive and negative

temperature gradients are de-stabilising and stabilising respectively.

3.2.2 The work on stability of flow so far considered can be used to predict the onset of stability for the case of both cylinders rotating or for just the inner cylinder rotating and the outer cylinder stationary. However, in his later experiments Taylor (79) was able to reproduce experimentally a transition to unstable flow with just the outer cylinder rotating although for this case he had not solved the theoretical problem. The onset of instability varied with the ratio of gap thickness to the cylinder radius and was in good agreement with the findings of Couette and also Wendt (80). Some of Taylor's findings have been summarised by Goldstein (81) in his text on Fluid Dynamics.

To find a theoretical solution for this case of "viscous instability" we must return to Schlichting. The method used by Schlichting (69) was to show the existence of a theoretical limit of stability for the flow between parallel walls. The stability calculation is performed in relation to the velocity profiles which exist when this type of flow is formed. To each profile there corresponds a definite critical Reynolds number $\left(\frac{U\delta^*}{\nu}\right)_{crit}$ where δ^* is the displacement thickness. However, Schlichting found that instability occurs only in the case of early profiles up to $\frac{\delta^*}{h} = 0.161$ and the value of R_{crit} based on the displacement thickness increases from $\left(\frac{U\delta^*}{\nu}\right)_{crit} = 1530$ onwards. At $\frac{\delta^*}{h} = 0.115$ it attains the value of 2220. Thus, referring this result to a

critical Reynolds number formed with the plate distance h it is found that the lowest limit of stability occurs for $\frac{\delta^*}{h} = 0.115$ with $R_{crit} = \frac{2200}{0.115}$ so that $\left(\frac{U h}{\nu}\right)_{crit} = 19300$.

It should be noted that this result is considerably larger than that obtained by Couette. However, Schlichting(82) has extended this method to the stability of flow inside a rotating cylinder with greater success. In this case the velocity profiles were investigated when the outer cylinder is set in motion impulsively. It was assumed that there is no inner cylinder to simplify calculations. The critical Reynolds number based on δ^* was found to increase with increasing $\frac{\delta^*}{R}$ owing to the stabilising influence of centrifugal forces.

Again $(R_e)_{crit}$ for $\frac{\delta^*}{R} \neq 0$ is 1530 as was the case for Couette flow. From Schlichting's results it can be seen that the critical R_e based on the radius of the cylinder has a minimum at $\frac{\delta^*}{R} = 0.091$ and is equal to $\left(\frac{U_m R}{\nu}\right)_{crit} = 66{,}000$ where U_m is the peripheral velocity. Comparison of this result with the experimental results of Taylor, Couette, etc. can be made only at the extrapolated point where $\frac{d}{R} = 1$. Since in most experiments the ratio of the gap thickness d to the radius R is small. It can be seen from Figure 1 that Schlichting's result is low, since extrapolation of measured values to $\frac{d}{R_1} = 1$ gives $\left(\frac{U_m R}{\nu}\right)_{crit} = 200{,}000$. However, since this appears to be the only theoretical solution to the problem the agreement with experiment was considered by Schlichting to be satisfactory. More recently the work of Schultz-Grünow (83)

has shown that theoretically the flow regime when the outer cylinder only rotates is completely stable under steady conditions, however, he has confirmed Schlichting's findings in (82) that turbulence occurred during the starting process. In the experimental investigation by paying particular attention to making sure that the cylinders were exactly concentric and free from vibrations, it was observed that the flow reverts to a laiminar pattern when a steady state had been established. The Reynolds number at which turbulence finally occurred was of the order of 5×10^5 which is considerably higher than that observed by other experimenters. It was observed that turbulence persisted, as in older experiments, when a controlled amount of eccentricity was built into the arrangement which suggests that the causes of turbulence when the outer cylinder rotates and the inner cylinder is stationary are caused by geometrical imperfections.

It might be pointed out here that Schlichting's Figure 17.21 in the 4th edition of Boundary Layer Theory is slightly in error in that Taylor and Wendt observed transition to turbulence when $\frac{d}{R_1} \simeq 0.05$ at R_e something less than 5×10^4 and not at 7×10^4 which is shown in this Figure.

3.3 Viscosity of liquid water

3.3.1 Measurements between 0° and 100° at 1 atm. pressure.

A complete survey of all available measurements on the viscosity of water would be extremely lengthy and has been rendered unnecessary by the correlations compiled from most of the available data from time to time. A well-known correlation covering the range 0 - 100°C was issued by Bingham and Jackson (84) in 1919 and is still widely used; these tables being published, for example, in current editions of the Handbook of Physics and Chemistry (85). A second correlation was made by Dorsey (86) in 1929 which can also be found in Dorsey's (1940) text on the properties of water-substance (87) with the list of workers whose data had been taken into account, In the range 0 - 100°C the Dorsey results are usually slightly in excess of those given by Bingham and Jackson the greatest difference being nearly 0.5% which occurs at around 17°C. It is noteworthy that Dorsey makes special mention of the results of Leroux (62), for which the author ascribes an uncertainty of not more than 0.5% in the range 1.5°C to 44.5°C. These results were unacceptable for the compilation since they were consistently higher than the values observed by other experimenters, the error increasing as the difference between the temperature of water under test and room temperature increased. This was unfortunate because the rotating cylinder viscometer used by Leroux was undoubtedly of a high standard, the error in his results being due to the difficulty he had in measuring the exact temperature of the liquid under test. His procedure was to measure the thermostat

temperature assuming that the whole apparatus was isothermal, which apparently was not the case. Upon examination of these results it can be seen that Leroux achieved a high degree of precision with very little scatter in the experimental values. Had he overcome the problems mentioned his results would have been valuable since most other results have been obtained with capillary viscometers and could therefore contain systematic errors associated with this particular type of instrument. The only other precise determination of the viscosity of water using the rotating cylinder method is that of Drew (88) who made a single determination at 20°C. However, since he makes no mention of the estimated accuracy of his result little importance can be attached to it.

The most precise measurement of the viscosity of water is believed to be that of Swindells, Coe and Godfrey (2) who reported a value of 1.0019 cP ± 0.0003 cP at 20°C using a capillary viscometer. This determination is supported by Roscoe and Bainbridge (3) who state a value of 1.0025 cP ± 0.0005 cP using an oscillating vessel technique. The close agreement between these two determinations, using completely different types of apparatus has resulted in the value of 1.002 cP being accepted as a reference point subject to an uncertainty not exceeding 0.001 cP.

The most recent correlation of dynamic viscosity over the range 0 - 100°C is that of Bruges, Latto and Ray (89). This paper lists the other sets of recommended values which have been issued in

addition to those mentioned earlier of Bingham and Jackson and Dorsey. From this it can be seen that the tables of values of Dorsey and more recently by Weber (90) up to 40°C agree to within 0.3% which suggests that very little had changed in the state of knowledge during the intervening 26 years. However, Bruges correlation lends support more to the correlating formula of the 1964 Skeleton Tables (91) the results for the compilation of which have been described by Kestin and Whitelaw (1). The main difference between the most recent correlations and those prior to 1940 are due to the attempts to take account of observations at pressures greater than 1 atm. A criticism which may be levelled at the use of these two latter correlations to obtain the saturation line is that the result is not in good agreement with earlier correlations except in the range 5° to 40°C. However, the correlations serve different purposes. Bruges correlation allows the viscosity to be calculated from a single equation both along the saturation line and at elevated pressures (with the condition that recommended tolerances are applied). The representation of properties in this form is suited particularly to engineers where data is stored in the form of computer programmes. Where greater accuracy is required for values of viscosity at 1 atm the early correlations of Bingham and Jackson and Dorsey can be used with greater certainty. In fact, the results obtained by capillary viscometers for water between 0° and 100°C are in good agreement generally. The results obtained by Thorpe and Rodger (92) in 1894 and Hardy and Cottington in 1949 being examples which are compared

with values from this viscometer in Chapter 6. The results of these workers agree to within 0.5% between 0° and 100°C. Some attempts have been made to re-correlate the experimental values for water between 0° and 100°C by Kampmeyer (93) on a semi-theoretical basis. However, the main purpose of this work appears to have been to extract values of the activation energy for viscous flow and the correlations don't appear to have been widely accepted.

3.3.2 Measurements at elevated pressure

The earliest recorded measurements on the viscosity of compressed liquid are those of Rontgen (94) in 1884 who used a capillary instrument for measurements up to 29 atm and mostly in the region of 6°C and 11°C. This work was closely followed by that of Warburg and Sachs (95) who also fitted simple equations to express the pressure coefficient of viscosity for water and several liquid hydrocarbons. In 1901 Hauser (96) made measurements on water up to 516 Kgf/cm^2 and 90°C. Three of his results are single determinations at a given temperature and pressure and these don't agree with a set of values obtained at 413 Kgf/cm^2 at intervals of 10°C between 20° and 80°C. However the qualitative conclusions which could be drawn from these experiments were fairly correct, there being a change from a negative to a positive pressure coefficient at approximately 34°C which is in agreement with some more recent work.

A massive contribution to this field was made by Bridgman (97) who measured the effect of pressure on the viscosity of forty-three pure liquids at pressures up to 12,000 Kgf/cm^2. He used a falling

body type instrument at temperatures of 0°, 10.3°, 30° and 75°C over the range 1 to 11,000 Kgf/cm^2 for water. However, he had considerably less success with water than with other liquids due to the electrical conductivity of the water interfering with the operation of the timer through the electric contact arrangement. With water this instrument also presented corrosion problems. These were difficult to solve because when the falling body was made from stainless steel the electrical contact surfaces became covered with a highly insulating film after the contact spark between weight and cylinder had occurred on several successful runs. These difficulties could explain the considerable difference up to 25% between Bridgman's results and those of Bett and Cappi (48) who covered nearly the same range of pressure using a viscometer similar in principle but much improved in design. Cappi's viscometer consisted of a tube containing two sinkers one of high and the other of low density. Measurements were made by inverting the pressure vessel containing the viscometer and timing the fall of each sinker through the fluid separately by an induction - operated electronic timing circuit. The use of two sinkers permits measurements to be made on the density of the fluid as well as the viscosity. The experimental accuracy claimed is ± 1% and the temperature at which the pressure coefficient becomes positive is shown to be 33.5°C.

As a result of studying the viscosity of aqueous solutions Tamman and Rabe (98) inferred that Bridgman's values for water at 10°C are in error and set up their own expressions for the variation

in the viscosity of water with pressure at temperatures of 0°, 10° and 30°C. In 1932 Lederer (99) set up a more complicated equation for water

$$\log_{10}\left(\frac{\eta}{\eta_o}\right) \equiv \log_{10}(1 + KP) = \frac{1.650P}{1000T} + \frac{1369\ P \log_{10} T}{10^8} - 0.1300e^{-f}$$

where $f \equiv 10^{-6}(1350\ t^2) + \frac{691}{P}$

where t is the temperature in °C

T is the temperature in °K

and P is in Kgf/cm^2.

Dorsey (87) has listed values of K computed from this equation and from the expressions of Tamman and Rabe. From plotting these values it would appear that there is fairly good agreement between these computed results and the experimental results of Cohen (100), Bett and Cappi and Bridgman at 0°C. There is poor agreement at 10°C, Tamman being much higher than the experimental values and Lederer much lower.

The early attempts at measuring the viscosity of compressed liquid at temperatures above 100°C were generally unsuccessful and the results have not been used in recent correlations. The results of Sigwart (101) were obtained from an open circuit capillary viscometer similar to that used by Speyerer (102) in which the measurement of pressure drop across the capillary was affected by means of a ring balance. Although he covered the range of temperatures 275 - 380°C and of pressure 25 - 270 Kgf/cm^2 the apparatus was subjected to the difficulties associated with an open circuit viscometer,

namely, the problem of obtaining stable flow and the measurement of the pressure drop along the capillary. The results obtained along the saturation line seem reasonable but the pressure coefficient obtained was completely unacceptable. For instance at 100°C they found that by increasing the pressure by 270 Kgf/cm^2 the viscosity increase was approximately 21%, whereas it is now accepted to be slightly less than 2%. It is astonishing that until 1940 these were the only results available at temperatures above 100°C for the viscosity of compressed liquid, although de Haas (103), Speyerer and Hawkins, Solberg and Potter (104) had made observations along the saturation line. The viscometer of Hawkins et al was used for measurements on compressed water up to 240 kgf/cm^2 however the instrument was insufficiently sensitive to obtain the small changes in viscosity over this range and they concluded that the pressure effect was negligible. Their viscometer was similar to that of Bridgman and involved timing the passage of a falling body in a vertical tube. The timing method was by winding two coils onto the tube and connecting them as part of an a.c. bridge circuit. The fall-body passing through the coil was sufficient to unbalance the bridge and to swing a pen across the chart of a recording milliameter. Although insufficiently sensitive, this method solved the problems encountered by Bridgman and layed the foundation for the much improved falling-body instruments which have since been made.

In 1940 measurements on the viscosity of compressed water were made by Timrot and Khlopkina (105) using a capillary instrument

in which the driving force for the fluid was provided by the movement of mercury in a ring-balance during rotation of the viscometer about its axis. They covered the range 17° - 300°C at pressures up to 500 Kgf/cm^2. A similar range was covered by Schmidt and Mayinger (106) who went to 580 kgf/cm^2 and 200°C also using a capillary instrument. Moszynski (107), using an oscillating sphere has covered the pressure range 1 to 380 Kgf/cm^2 and temperatures between 20° and 300°C. These three workers have been mentioned together since they have also measured the viscosity of steam with the same apparatus and both the steam and liquid water results are in reasonable agreement. This is also the case for Tanaka et al (53) who have covered the range 1 - 1000 kgf/cm at temperatures between 12° and 360°C using a capillary viscometer.

The work of these last four workers has been reviewed by Bruges (89) since the measurements of the former three were used in the correlating equation reproduced here in section 6.1. It is interesting to note that Moszynski observed the temperature at which the pressure gradient became positive as 35°C whereas Bruges' correlation indicated 37°C. Thus a gradual movement away from the value of 33.5° mentioned earlier appears to be taking place. Since none of these workers covered the low temperature region (i.e. 0 - 20°C) the correlation produced does not indicate the large increase in the negative pressure coefficient below 20°C.

Another contribution to the compressed liquid measurements has been made by Weber (108) using a falling ball instrument. The range

covered is 1 to 500 Kgf/cm^2 and 20° to 160°C. The apparatus is similar to that described earlier in his precision measurements on water at atmospheric pressure between 0° and 40°C. The apparatus cannot give absolute values for the viscosity coefficient and the results are listed as being the percentage change in viscosity with pressure assuming that the pressure coefficient is zero along the 32°C isotherm. In view of the variation observed in the temperature at which the pressure coefficient inverts it would seem presumptive to express the results in this way. However, by using the best available data along the saturation line absolute values for high pressure water can be obtained.

The most recently published experimental results are those of Dudziak and Franck (109) who have covered the range 160° to 560°C and 200 and 3500 Kg/cm^2. These are the first to be made on liquid water using the "oscillating-disc-between-fixed-plates" method developed by Kestin and Wang for gases (110) and steam (111). Since the theory for this method has not been developed sufficiently to allow an accurate edge correction to be made, measurements are made relative to the presently accepted experimental data most of which has been mentioned above. A notable difference between the procedure in this work and that of Kestin and Wang and Moszynski is that here the logarithmic decrement has been obtained electrically whereas previously this had always been achieved optically through a high pressure window. Dudziak's method was to apply a small alternating voltage to electrodes on the disc and plates permitting the electrical resistance between these

parts to be measured (since the intermediate water always exhibits a slight conductivity). The resistance variations were proportional to the amplitudes of the small angle oscillations thus the logarithmic decrement of the oscillations could be derived from the recorded resistances. Unfortunately, the published data for water up to 800 Kgf/cm^2 must have a fairly wide tolerance applied to it due to experimental inaccuracies of the various methods used, so that this same tolerance (approximately $\pm$ 5%) must be applied to Dudziak's results. It would appear that the electrical method for determining the decrement of oscillations also requires further development since the average deviation of the experimental values from the smoothed curves is of the order of $\pm$ 3%. However, in the author's opinion the results of this work represent a very considerable achievement in view of the technical problems overcome.

Horne and Johnson (52) have also recently published their results from a rolling ball type viscometer in the ranges 2° - $20^{\circ}C$ and 1 - 2000 Kgf/cm^2. Their object, in concentrating on the low temperature region was to study particularly the structure breaking effect of pressure on water and to allow some decision to be made concerning the discrepancies which exist between the results of Bridgman, Tammann and Rabe and other workers at low temperatures. In the author's opinion Horne and Johnson's choice of experimental technique was unsuitable to achieve this objective since however many precautions were taken, the fact remains that the flow regime around a rolling ball has not yet been theoretically analysed. Furthermore,

even if one does assume that the flow around the ball is laminar, only part of the resistance to movement will be due to the viscosity of the fluid since there will also be a contribution from the rolling contact between ball and tube. This second contribution to the "fall - time" of the ball is obviously critical since the authors admit that in choosing the angle of the tube at which the timings are to be made, steeper inclinations of the tube sacrificed a significant figure in the fall time while less steep inclinations tended to give erratic fall times. The latter observation was attributed to a very slowly moving ball getting retarded by dust particles or slight inhomogeneities on the inner surface of the tube. Since the fall-time has also varied during the test with the various viscosities measured, by the same reasoning it may be deduced that these factors will have also affected the viscosity values obtained. The results recorded, however, are remarkably consistent and the fall times highly reproducable so that the overall picture of the results is convincing.

As a result of this survey the following general conclusions may be drawn. For the very high pressure measurements the falling body method has been developed to a high precision by Cappi and is probably the best solution, although the oscillating disc instrument of Dudziak and Franck has been used for measurements at remarkably high pressures and temperatures. The "moderate" range of pressures and temperatures to 500 Kgf/cm^2 and 300^{o}C has been covered by several reliable workers including Mayinger, Moszynski, Timrot, Tanaka and Weber.

The majority of this work was performed with capillary instruments, however, the oscillating sphere method used by Moszynski and the falling ball results of Weber tend to strengthen the position generally because it means that not all data has been obtained with the same type of instrument. However, the fact that several methods have been used, most of which are not absolute instruments but which require to be calibrated first with a fluid of known viscosity has lead to a fairly large scatter when all of the results are considered together. Thus there remains the need for a reliable absolute viscometer to work systematically through this range allowing those who correlate the results to be more discriminating about the experimental values which should be included in, or rejected from, future correlations.

It may be generalised that the results obtained fall into two groups, those above room temperature and those below. Few workers have covered the complete range and those who have, for instance Bridgman, are not considered now to have produced the most reliable data. For this reason Bruges' correlation which makes use of most of the measurements in the 'moderate' range of temperature and pressure does not show up the rapid increase in the negative pressure coefficient at temperatures below 20°C. Some of those measurements made below 20°C are questionable because of the method used. For instance, some doubt must be cast upon Horne and Johnson's results because of their choice of a rolling ball instrument. Most of the instruments mentioned required to be calibrated with a fluid

of known viscosity. This introduces two uncertainties into the results, the tolerance which must be applied to the calibration itself and the possible effect of advanced temperature and pressure on the dimensions of the instrument. For instance, in some falling body viscometers the drop-tube itself is subjected to the full internal pressure of the test fluid which must inevitably result in a small change in diameter. In the case of Horne and Johnson this problem was overcome by inserting a liner on which the hydrostatic pressure could act from all directions. Moszynski's oscillating sphere method can be considered absolute but for some reason the results he obtained are low when extrapolated to 20°C. Also, the tentative conclusion of Moszynski's that the viscosity of water can be affected by subjecting it to a pressure cycle, which has since been rejected by further measurements of Kestin and Whitelaw (112) using an instrument of similar design, must cause some speculation as to the origin of this phenomenon. That the effect cannot be attributed to dissolved air has also been confirmed by Caw and Wylie (113). It seems, therefore, that pressure cycling in some way affected the absolute accuracy of Moszynski's viscometer.

CHAPTER 4

DESCRIPTION OF APPARATUS

4.1 An account of the stages of development of the viscometer.

4.1.1 The preliminary design.

As mentioned in section 1.1 two previous workers in Glasgow University recommended that the rotating cylinder viscometer could make a useful contribution to the viscosity measurement of compressed water and steam. Parts of their theses were devoted to preliminary design considerations although the pressing need for results from the closed circuit Rankine viscometer prevented them from pursuing the method experimentally. The only experiments were performed by Whitelaw who tested sapphire rollers in a high temperature steam environment to see if these could be used for location of the rotating cylinder in experiments at advanced conditions. However, the tentative conclusions of these workers, particularly of Whitelaw, formed the basis for the first detailed design made by the author, see Figure 2.

The method of assembly and operation can be clearly seen in the illustration. The cover was permanently supported on a tripod stand with levelling screws such that the instrument could be adjusted to stand vertically. The guard cylinders and inner cylinder were first assembled and then by previously warming the outer cylinder, it could be pushed onto the bearing races (which are located on the guard cylinders) and thus shrink fitted into position. The main

pressure vessel could then be lifted into position by a special rig which consisted of 4 tie-bolts screwed into four of the studs in the vessel. These tie bolts passed through the holes in the cover allowing the weight of the vessel to be taken by an overhead frame fitted with pulleys and a balance weight. Once the 8 retaining nuts had been tightened the tie-bolts were removed. It can be seen that the drive shaft is hollow at a point just above the chevron-packed seal allowing the mirror-stem extending from the inner cylinder to hang inside it. The top end of the shaft and the recess in the bottom end of the rotating cylinder were splined so that as the pressure vessel was placed in position the shaft could be located at the same time. In order to be able to observe the angular position of the inner cylinder the hollow part of the drive shaft had three "windows" cut into it, the small torque required to rotate the cylinder being quite adequately transmitted by the three struts which remained.

The drive shaft could be rotated in either direction between 0 and 25 r.p.m. by a fractional H.P. motor with Pye control equipment which was loaned by the electrical department. A 40 : 1 worm gear was necessary which also turned the drive from the horizontal to the vertical plane. Access was provided in the cover for four thermocouple pockets, which allowed the temperature to be measured in the space between the rotating cylinder and the pressure vessel. The angular velocity of the outer cylinder was kept low so that the deflections of the inner cylinder were small and could

be measured directly through the high-pressure sapphire window using a telescope, mirror and illuminated scale technique. Using this method it is necessary to make allowance for refraction at the water/sapphire and sapphire/air interfaces. In this case the observed deflection δ is related to the angular deflection α (see Figure 3) by the relation:-

$$\delta = a \tan 2\alpha + b \tan \beta + c \tan \gamma$$

$$= a \tan 2\alpha + b \tan \left[\sin^{-1} \left(\frac{\sin 2\alpha}{\mu_{ws}} \right) \right] + c \tan \left[\sin^{-1} \left(\frac{\sin 2\alpha}{\mu_{ws} \mu_{sa}} \right) \right]$$

The distance a, b and c must be accurately known and since μ_w the refractive index of water changes with pressure and temperature it is convenient to plot δ against the angle of deflection α for different values of μ_w. The changing refractive index of water can be calculated from the same empirical equation

$$\frac{\mu - 1}{\mu_1 - 1} = \frac{V_1}{V}$$

where μ_1 denotes the index of refraction at specific volume V_1 and μ the refractive index at specific volume V. The refractive index of sapphire has been determined by Malitson et al (114).

At first the viscosity of air was measured with this viscometer under atmospheric conditions. The results, however, were not good, there being far too much scatter in the plots of deflection against rotational velocity for precision determinations to be made. At first this was thought to be purely a matter of vibration due to

possible misalignment in the mechanical set-up, however, after a considerable time spent on adjustments to eliminate this, it was apparent that external vibration was not the sole cause of trouble. It was concluded that the openings in the hollow shaft were the root of the trouble, since it would appear that these were causing a disturbance in the fluid and so causing the mirror stem (and thus the inner cylinder) to vibrate. When the instrument was filled with water, difficulty was encountered measuring the larger angular deflections because of greater dispersion of the light from the scale as the angles of incidence increased. In fact this effect combined with the stirring of the fluid made it quite impossible to achieve the objective and it was decided to construct a new viscometer modified to overcome these difficulties

4.1.2 The first viscometer.

Since the lessons to be learned from the last section were of use to the author and are of little consequence otherwise, the instrument that followed, (see Figure 4 andAppendix C), is hereafter referred to as the 1st viscometer. It had been decided to reach the original objective of a pressure of 1000 Kgf/cm^2 and 375°C in two stages instead of one. Thus the first viscometer was designed for measurements to 250°C and 250 Kgf/cm^2 with the provision that a second viscometer should be constructed at a later date incorporating any lessons learnt from the first viscometer, at the same time extending the conditions to those proposed in the original objective.

The main features of this instrument are that the rotating cylinder is driven by a shaft entering through the side of the vessel and the lower guard cylinder is extended downward to shield the mirror stem from any turbulence in the fluid. The design includes a thermostatic jacket through which a heating fluid is circulated. The angular deflection is no longer measured by observation entirely through the window but by incorporation of the null device described in Appendix B. A separate facility has been provided for measuring the torsional properties of the wire at different temperatures, see Figure 5. Since this viscometer is the subject of the more detailed description to follow it only remains to be said that measurements have been made with this viscometer on compressed liquid water over the range 1 to 230 Kgf/cm^2 and 10° - $120^\circ C$. There is no reason why the temperature should not be increased to $250^\circ C$ subsequently (and, at least, to $180^\circ C$ with the present method of temperature control).

4.1.3 The second viscometer.

In view of the progress made with the first viscometer a second instrument is in the final stages of construction which, it is expected, will enable measurements to be made over the full range envisaged. This viscometer is shown in Figure 6. At temperatures above $200^\circ C$ the problem of obtaining the torsional property of the suspension wire becomes more difficult. In designing the second instrument, therefore, an idea has been incorporated which was first suggested by Kjelland-Fosterud (4). Thus, the

inner cylinder is suspended between two wires, the top one of which is provided only as a sensitive means of support while the bottom wire is a torsion wire calibrated in the normal way. This arrangement, however, enables the torsion wire to be in a tube outside the hottest zone of the viscometer and by having the rotating torsion head at the bottom of the instrument the null method of measuring the angular deflection can again be used. Thus the operating sequence becomes a matter of establishing the null point as seen through the window and then providing a constant angular velocity to the outer cylinder. This will cause the inner cylinder to deflect to some equilibrium position at which point both wires are under torsion. At this stage the torsion head (to which the lower end of the bottom wire is attached) is rotated until the inner cylinder, as seen through the window, is returned to the null position. The torsion is now entirely contained by the lower wire and the angular deflection of the inner cylinder is given by the amount that it was necessary to rotate the torsion head. A radial optical grating attached to the torsion head allows this angle to be determined with a certainty of ± 5 seconds of arc. This feature is more fully described in Appendix J.

4.2 Provision of known angular velocity to the rotating cylinder

Since the angular velocity of the rotating cylinder enters directly into the equation 2.7 used in calculating the viscosity, the time "t" for 1 revolution of the cylinder must be accurately known. The velocity must also remain ostensibly constant over the time required to take a measurement which, for a liquid, has been found to be between five and ten minutes. It should be pointed out that the requirement for measurements on liquids differs from that of gases. With gases the suspended cylinder tends to oscillate about any position at which a reading is required due to the low inherent damping of the system. One therefore has to wait until the cylinder has become sufficiently steady to take a reading or to record the end points of several of these oscillations so that the centre point may be found. Either of these procedures takes a considerable time and therefore the long term stability of the drive is important. For instance, Bearden achieved a drive velocity which remained constant to within 1 part in 10^6 over periods of many hours. However, with liquids, the initial oscillations due to a change of speed soon decay and the angular deflection can be recorded relatively quickly. Several alternative arrangements were examined for a servo-controlled basic drive including the Ward-Lennard arrangement with feed-back from a tachometer offered by Messrs. Lancashire Dynamo and a system using thyristors (i.e. silicon controlled rectifiers) offered by A.E.I. Electronics Division. Surprisingly, the long-term stability of the latter system

is not high, being in the order of 0.5% which was considered unacceptable in this application. The Ward-Lennard arrangement is large and expensive by present standards and could not be expected to control at any one speed to better than 0.1%. It should be noted that both of these sytems are particularly suited for other applications, for instance, where the speed must be maintained under sudden large changes of torque. This, however, is not a problem here. Therefore the idea of using a closed-loop system was abandoned and a satisfactory alternative was found to be a 1/3 H.P., 3-phase synchronous motor supplied from the mains. Tests on this drive are given in Appendix H. The main conclusion being that for periods of up to several hours, at certain times of the day, the speed remained constant to within $\pm$ 0.05%. At other times larger changes occurred but by taking tachometer readings at the beginning and end of a test, the effect of this can be taken into account.

It is a considerable advantage, if not an essential feature, to be able to vary the speed of rotation over a fairly wide range. In this event a speed:deflection curve can be plotted which should be a straight line for Newtonian fluids (the slope of which gives the viscosity). Although early workers used fixed ratio gear boxes the technology of so-called infinitely variable reduction gears has advanced considerably in recent years. The complete range of electrical, mechanical and hydraulic variable

speed methods was reviewed in 1964 by the Engineers' Digest (115). The hydraulic pump installed back-to-back with a hydraulic motor, both of radial piston design, form an excellent reduction unit. The speed can be varied by moving an eccentric which alters the stroke of the radial pistons. The unit chosen for the present work was supplied by Messrs. Carter Gears and makes use of this principle. It is driven at constant speed by the synchronous motor through timing pulleys and stepped-belt, the output being infinitely variable, in either direction of rotation, between zero and 1000 r.p.m. Figure 7 shows the speed stability of the output shaft of this gear when sufficient time had been allowed to elapse for the gear to attain a steady temperature. A fixed-ratio reduction of 29/3 is provided by a worm gear between the hydraulic gear and the viscometer. The tachometer, of which a diagram is shown in Figure 8 is placed on a high speed section of the drive so that the largest speed is measured. Further fixed-ratio reductions in speed occur between the hydraulic gear and the rotating cylinder but in all cases timing pulleys and gears have been used, thus eliminating any possibility of slip. The pick-up for the tachometer was designed by N.E.L. but manufactured in the University. It consists of a Tufnol disc with 120 mild steel inserts equally spaced around the periphery. As each insert passes through a narrow slot in a 'U'-magnet a pulse is generated in a small coil wound on to the magnet. With the present arrangement the pulse needed to be amplified by a factor of 20 before it was acceptable to the Venner

T.S.A.3 counter. With this drive arrangement, for instance, at the maximum hydraulic gear speed available of 1000 r.p.m., the the 5-decade counter can be set to read either 02000 with the 'gate' opening for 1 second or 20000 when the 'gate' is set to open for 10 seconds. Preliminary adjustment of the speed is made on the first setting and thereafter the speed is indicated at 10 second intervals correct to ± 1 count in 20,000. (The counter is accurate to ± 0.001% ± crystal stability, which is not therefore a limitation in this aspect of the overall-accuracy of the instrument).

4.2.2 Various designs of high-pressure rotating seal have been tried. Initially the suggestion of Whitelaw (5) was followed and the chevron seal shown in Figure 9.2 of Appendix C was designed. It was, perahps, hoping for too much that a high pressure could be made to operate successfully in such a limited space as was available in this first design. By making the shaft of small diameter it was calculated that the end loading due to the differential pressure across the seal would be so small as to obviate the need for an additional thrust bearing. Also, it was expected that the area of the shaft in contact with the pressurised chevrons would produce only a small resisting torque. In practice, when the instrument was pressurised or the chevrons were tightened by the follower, the shaft tended to sieze. The difficulty was heightened by the problem of gripping such a small shaft; the collet type coupling shown being only partially successful in this respect.

However, this seal allowed preliminary testing of the

instrument to be made at atmospheric pressure on air and on water at temperatures up to 100°C. However, it was decided that other rotating shaft seals should be considered if the instrument was to be successfully operated at high pressures. The chevron seal is generally applicable to reciprocating motion where the heat of friction is transported away from the contact area by the moving surface. In applying this seal to the rotating shaft there is no such mechanism for heat-removal and local over-heating and subsequent expansion of the chevrons (thus worsening the situation) will inevitably result in failure of the seal.

Radial face seals are commonly used to seal a fluid under pressure on one side of a housing through which a rotating shaft protrudes. The moving seal is effected between a face ring (usually a very hard surface) attached to the shaft and an annular slider (usually carbon or other soft material) fixed to a stationary seal ring. The slider and the face ring have flat surfaces and are pressed together by loading springs and by the sealed pressure acting over the balance-pressure area as shown in Figure 9. The seal ring is attached flexibly to the housing through a static seal and is restrained against rotation. Seals of this basic type have been used extensively in liquid and gaseous environment over wide ranges of speeds, pressure differences and temperatures. Generally those seals can be adjusted to give zero leakage at zero speed, small leakage at operating speed but with a

small but finite wear rate and small friction torque. However, according to Kojabashian and Richardson (116) there is no comprehensive understanding of seal behaviour which could form the basis of a rational design method for these devices. It is generally accepted as a result of experimental work, for example by Denny (117) that face seals support their net closure loads hydrodynamically over major portions of their operating speed ranges, even though the classical hydrodynamic equations prodict zero load capacity for the ostensible flat and parallel sealing surfaces. Several physical mechanisms have been advanced as being the possible cause of hydrodynamic pressure generation such as distortion of the seal faces, accentric rotation and also the effect of surface roughness and microirregularities. Many papers recording the results of investigations into these varying mechanisms have been presented in the First (1961), Second (1964) and Third (1967) International Conference(s) on Fluid Sealing, organised by the British Hydromechanics Research Association, Cranfield, England. A likely explanation is the "micropad" model proposed by Kojabashian and Richardson (116) which suggests that local flat pads or worn regions act effectively as small slider bearings. These support the load by providing net hydrodynamic load capacity for a seal which is quite flat on the average. Microscopic examination of used seal-surfaces and the application of statistical probability theory to the size and distribution of these micropads lends support to these proposals. It may be noted that although a new seal surface

is relatively smooth and flat, as the seal is run in, non-uniform wear of the surface occurs producing a pattern of these exposed and raised areas or so-called micropads.

The seal requirement for this application differs considerably from the industrial requirement to which end the main research task in face-seal development has been directed. One rarely finds test results for sealed pressures in excess of 1500 lbf/in^2. For example, an improved elliptical face seal for use in high temperature pressurised water circulating pumps described by Vilim (118) was designed for an upper pressure limit of 1400 lbf/in^2. Since the torsion head developed by the author for this instrument had been successfully tested at 330 Kgf/cm^2 (see Appendix D) it was hoped that a mechanical face seal could be obtained for use at pressures at least approaching this. Most manufacturers could not quote for any seal to operate at pressures exceeding 1000 lbf/in^2, however, the research department of Messrs. Flexibox promised that their seal type RRNPQ, although advertised with the above limiting condition, would be effective at pressures of 3,500 lbf/in^2 (240 kgf/cm^2) provided the shaft speed was kept below 100 r.p.m.

The modifications to the instrument necessary for the installation of this seal were straight-forward and the completed instrument is shown in Figure 4 and, for the sake of the following discussion, typical configurations for the radial face seal are

shown in Figure 9. Either the seal ring or the face ring can be spring loaded, in the present case the static seal provides the necessary alignment adjustment should this be required. The balance pressure area can be adjusted to give the required pressure across the face-width and for high pressures this balanced configuration is essential. It is thought that at the low rotating speeds used in this viscometer there will not be a hydrodynamic film generated and that a condition of boundary lubrication exists, at the highest pressures anyway. Success of the seal therefore depends on the compatability of the mating surfaces which in this case are tungsten carbide and carbon. Provision of a flow of coolant around the back of the stationary seal ring prevents over-heating of the seal when operating at elevated temperatures.

Mayer (119) has listed suitable formulae for the calculation of friction and leakage in both unbalanced and balanced face seals. He points out, however, that for both types of seal the leakage increases with rougher surface finish, with speed and with other factors such as vibration, while leakage may be expected to decrease with increasing ratio of seal interface pressure to the pressure being sealed (i.e. less leakage through unbalanced seals). Mayer compared the results calculated from these equations with observed values of leakage and friction under test conditions. The results are of particular interest here because they include tests made on the sealing of polybutane at 3000 lbf/in^2 in which the leakage rate was only 0.15 cc/minute for an unbalanced seal and 0.25 cc/minute

for a 0.9 ratio balanced seal (i.e. interface pressure = 0.9 x pressure of fluid being sealed). However, no direct comparison can be made with a simple face seal because Mayer had improved the seal performance by providing radial grooves across part of the face width which, he claims, assists the generation of a hydrodynamic film. These are the only experimental results known to the author where the fluid pressure approaches that to be used in the viscometer and Mayer's observations are particularly encouraging in this respect. The review of fundamental studies in mechanical face seals carried out by Nau (120) is a comprehensive survey of this topic. He points out that, on the basis of other workers' observations, it may be shown that Mayer's operating conditions were well into the region of boundary lubrication effects. Mayer's results are therefore taken as a pointer to the performance of the face seal under the conditions of the present application

The seal ring is usually prevented from rotating by a pin protruding into a recess somewhere on the low pressure side of the static seal, the pin being located in the seal housing. In the first test on the seal the static seal was a PTFE "O"-ring and because of the low friction coefficient there were strong tendencies for the seal ring to rotate and the retaining pin broke the edges away from the recess and eventually destroyed the seal. This difficulty was overcome by replacing the static ring by a standard rubber 'O' ring. PTFE had been previously chosen for all static rings because it was thought that ' Thermex' might be used as a coolant, in which event rubber compounds would have been unsuitable.

4.2.3 The magnetic coupling which forms a part of the second viscometer was considered from the beginning to be the ideal means for putting the steady rotation into the pressure vessel. It was not realised until the previously described sealing method was being installed that permanent magnetic material had been developed which makes this type of coupling a practical proposition. Messrs. Pressure Products Inc (U.K.) have supplied an extremely compact unit with a torque of 4 lb.in, (See Figure 9.5 Appendix C), the pressure tube screwing into the side of the pressure vessel and sealing on a gold-plated wave-ring. A bank of circular ceramic magnets is rotated about the pressure tube by a similar drive arrangement to that already described. The drive shaft inside the pressure tube has a second bank of permanent magnets along its length which 'lock-in' with those on the outside. The application of small resisting torques to the inside tube results in an out-of-phase of the two shafts due to distortion of the magnetic field but no change in the steady angular velocity transmitted. This fact has been confirmed by attaching tachometers to both the initial drive and the inner cylinder.

4.3.1 There are a variety of ways by which the viscous drag on the stationary cylinder may be measured. In all methods the cylinder is supported by some strain-sensitive device, for instance, a coiled spring (Thomas, Hemm and Dow (66)) or a strain gauge attached to a supporting rod could possibly be made sufficiently sensitive (Tucker (121)). Probably the most commonly used suspension

is the single torsion wire, although bifilar and trifilar suspensions have been used in which case the restoring torque is not a function of the mechanical properties of the wire but of the geometry of the suspension. In the case of trifilar suspension the restoring torque is given by

$$T = 3 m g R \tan \left(\frac{R \Theta}{L} \right)$$

where m is the mass of the suspended system, R is the radius at which the wires are attached, L is the length of the wires and Θ is the angle through which the suspended body deflects.

However, this suspension has the disadvantages that the cylinder would undergo a change in vertical position during displacement and the guard cylinder width would have to be large enough to accommodate this. There would also be practical difficulties with adjusting the length of wires to give perfect centering of the cylinder. This would perhaps be a reasonable proposition in an apparatus to operate at atmospheric pressure but in the author's opinion the limited space available inside the pressurised system makes the system prohibitive. Early experimenters provided bearings for the suspended cylinder. Obviously it was necessary to design these with the minimum frictional resistance. Drew (88) who made a single accurate viscosity determination of water at 20°C had the suspended cylinder suspended between agate bearings and an air bearing was utilised by Oldroyde et al (122). Other workers have found it satisfactory to dispense with any supporting bearing

since this is likely to cause a resisting torque of appreciable amount (except for the air-bearing which is impracticable in this high-pressure application). If the cylinder is freely suspended, a sensitive means for adjusting the wire-support must be provided and it must also be ensured that the supporting wire is located very closely to the centre of the cylinder in order that the axis of the cylinder is nearly vertical. In this instrument a single torsion wire has been used and the above precautions closely adhered to. The cover and guard cylinders are firstly assembled, with the inner cylinder, in a separate frame. An accurately-made stand is then fitted to the top of the main pressure vessel which provides the same physical location for the cover that it experiences when actually in position. Final adjustments to the inner cylinder support are made with the coverin this stand. Successful suspension can only be achieved if the instrument itself stands vertically. This has been achieved with the help of a Hilger-Watts precision spirit-level and by introducing packing shims under the 'feet' upon which the main pressure vessel stands. Then, during assembly, the top face of the above mentioned stand is horizontal and the vertical and centering adjustments can be made to the suspension with full knowledge that the cylinder will be central when the viscometer is fully-assembled. It may be noted that the guard cylinders are an excellent guide as to whether successful suspension of the inner cylinder has been achieved, since a suitably placed light and straight edge make small discrepancies very clear to the eye. The vertical hair-line on a

precision cathetometer was also used to check that the cylinder was vertical while in this pre-assembled position.

4.3.2 Having decided to measure the drag upon the stationary cylinder by the deflection of a single torsion wire, it is essential to determine accurately the torsional behaviour of this suspension wire. Firstly, it is worth considering the experiences of others in their choice of wire material and the possible defects or peculiarities to be expected. The equation connecting the torsional constant with the material and physical dimensions is given by

$$\frac{T}{J} = \frac{\Theta G}{\ell} \quad \text{where} \quad J = \frac{\pi d^4}{32} = \frac{\pi a^4}{2}$$

$$\therefore \quad \frac{T}{\Theta} = F = \frac{\pi G a^4}{2\ell}$$

where a = radius of the wire

ℓ = length of wire

G = modulus of rigidity of wire material.

The possibility of predicting the torsional constant of the wire from knowledge of a, ℓ and G should be considered. Unfortunately G is not published with any great accuracy and may only be accepted as an approximate value for engineering calculations. Since wire drawing is normally a cold working process the mechanical properties are normally modified as a result. For example, it has been shown by Kuczynski (123) that materials of close packed hexagonal and other structures have their elastic modulus altered by drawing due to elongation of grains in the longitudinal direction. Tungsten (body centred cubic) is an exception in that its structure

is iso-tropic and unaffected by drawing. Benton (124) made the point that the general torsional behaviour of a wire with varying tension could not be predicted from the experimental observations on a single wire. It seems likely that the converse will be true, i.e. that the behaviour of a particular wire cannot be accurately predicted from readily available data. Bearden (8) reports that pure tungsten wire behaved consistently with negligible zero drift over long periods. Phosphor bronze was also acquired because it is so commonly used in galvanometer and other instrument suspensions and Nimonic 90 for use at high temperatures where creep may be important. It is obvious that the torsional constant of the wire must be measured in some way prior to use in the viscometer.

The torsional constant may be determined statically by accurately measuring the torque necessary to deflect the wire by θ radians. Early workers achieved reasonable success in this way, for example, Drew (88) using silk threads and closely divided scales obtained a result quite close to the value obtained dynamically for the same wire. No doubt, with a suitable electro-magnetic technique and the use of a steel bob at the end of the wire the static method could be developed to much greater accuracy. However, the dynamical method, viz. timing the period of free torsional oscillations of the system, lends itself to much greater precision without the necessity for excessive precautions. Since the oscillations will be damped the following two relationships for damped free-vibrations of a torsional pendulum can be used.

$$\Delta = \frac{C\tau}{2I} \qquad \ldots.1$$

and $$\sqrt{\frac{F}{I} - \left(\frac{C}{2I}\right)^2} = \frac{2\pi}{\tau} \qquad \ldots.2$$

From observations of the amplitude of successive vibrations the logarithmic decrement Δ can be calculated

$$\Delta = \log_e \frac{x_1}{x_2}$$

or considering n oscillations

$$\Delta = \frac{1}{n} \log_e \frac{x_1}{x_n}$$

Thus having observed τ and calculated Δ the damping coefficient C can be determined from (1). This value of C can then be substituted in (2). Equation (2) can be re-written as

$$\frac{\tau_{\text{natural}}}{\tau_{\text{damped}}} = \sqrt{1 - \left(\frac{C}{C_c}\right)^2}$$

where $C_c = \sqrt{4\,IF}$ and is the critical damping coefficient.

A typical value for F = 123.1 dyne cm/radian and for C (calculated from observed $\Delta \simeq 0.001$) = 0.17

giving $$\frac{\tau_n}{\tau_d} = \sqrt{1 - \left(\frac{0.17}{123.1}\right)^2}$$

$$= 1 - \tfrac{1}{2}\left(1.38 \times 10^{-3}\right)^2 + \ldots\ldots\ldots$$

$$= 1 - \tfrac{1}{2} \cdot 1.9 \times 10^{-6}$$

$$= \underline{\underline{1 - 0.95 \times 10^{-6}}}$$

Thus, it can be seen that an error of only 1 in 10^6 is introduced by

calculating F from the undamped vibration formula, viz.,

$$F = \frac{4\pi^2 I}{\tau^2} \qquad \ldots\ldots 3$$

4.3.3 The accuracy of obtaining τ, the period of oscillation, can be greatly increased by observing a large number of oscillations. The counter is accurate to ± 1 count on the 5th decade, therefore, to improve the precision of τ observed the following procedure has been adopted.

e.g. Time for 1 oscillation = 7.5491 ± 1

Time for 10 oscillations = [7]5.4918 ± 1

Time for 100 oscillations = [75]4.9174 ± 1

The figures in [ ] are added by observing the oscillations with a stop-watch simultaneously with the counter. In practice, values for the period are not reproducable to this accuracy due to external influences such as temperature changes and random vibrations from the surroundings. Nevertheless, it is useful to record the period accurate to 6 significant figures, particularly if the effect of amplitude on the period is to be taken into account (see Appendix Biii). Although the damping effect of air is small it is impossible to carry out observations on a freely oscillating system over several hours without the amplitude becoming too small. For this reason a moderate vacuum (c.a. 10^{-4} torr) has been provided for the pendulum which enables several period determinations, over the time required for 100 oscillations, to be made without disturbing the apparatus. Since the torsional properties of the wire are temperature dependent a thermostatic jacket has been

provided for this apparatus (see Figure 5). This calibrating rig will be briefly described with reference to Figure 9.3 in Appendix C.

The upper wire support can be assembled into the top member 4 in exactly the same way that it fits into the viscometer. Thus the wire does not have to be removed from the collets during the transfer from the calibrating rig to the viscometer, which is a considerable advantage. The complete assembly of top member and suspended system is located in the vacuum vessel 2 and is enclosed by the cover 3. The upper member has two alternative positions for height depending on whether the spacer 5 is included. This allows wires of different lengths to be calibrated which is essential since the two viscometers described have different overall dimensions. The complete system is supported by a heavy metal flange 1 which is bolted to a tripod-stand. This stand is mounted on a heavy steel table. The lower member 7 forms part of the vacuum system and contains a triplex-glass window 8 and provision for the plunger 10 and connections 9, 11 and 12 for the Pirani gauge, rotary backing pump and diffusion pump respectively. Although other workers have controlled the pendulum magnetically (e.g. Kestin and Moszynski (125))or used a stand mounted on a large ball-race (Moszynski (107))to provide the initial oscillation, the method used here has been satisfactory. The plunger 10 can be moved slowly inwards using the differential screw until the recess in the bottom end of the mirror stem is 'nudged'. Since the stem is never lying exactly parallel to the plunger it

rotates slightly to rest squarely against the end face. When the plunger is withdrawn the suspended system oscillates both torsionally and as a simple pendulum. Those latter movements can be damped out by cautious removal of the plunger but without destroying the torsional movement which continues long after the other vibrations have died away.

Oscillations have been timed by projecting a spot of light onto the mirror and focusing the reflection onto a photo-cell. The signal has been amplified and used in conjunction with the Schmitt trigger circuit shown in Figure 10 to operate the Venner counter. Once the counter has been "triggered" the photo-cell is shielded from the light until the appropriate number of oscillations have occurred. At this point the light is again allowed to activate the counter and the reading is recorded. In the case where these timings have been made in conjunction with amplitude measurements (see Appendix Biii) a scale was mounted approximately 70 cm from the mirror and the distance which the reflected light spot moved was seen on the scale. However, this could only be carried out for small amplitudes because the angle of access through the thermostatic jacket is quite small. (The effect of amplitude was not thought to be significant when this rig was designed and therefore no special provision was made to its observation). In order to observe up to 100 oscillations the Venner Counter has been used in conjunction with an accurate stop-watch (supplied by Messrs. Camerer-Cuss) in the manner described earlier.

The previous section describes how the torsional constant, F, of the wire is obtained. Having calibrated the wire it is carefully transferred to the viscometer. Since $F = \frac{T}{\theta}$ and F is known, then the torsion, T, exerted by the viscous fluid is given by the measured deflection θ.

Tests, with the preliminary design of viscometer, were made with a fixed support for the torsion wire in which case there was no means for adjusting the angular position of the inner cylinder once the wire had been damped into the collets. This proved to be extremely inconvenient because it was difficult to clamp the wire to nearer than 5° of the required position and this often resulted in the mirror being unfavourably located with respect to the window and scale. It was concluded that a rotating torsion head was essential to enable adjustment of the initial position of the inner cylinder so that the mirror and scale could be accurately lined up. Having made this decision it was an obvious development to adopt this device as a null method for measuring the angular deflection. This device and its application have been adequately described in Appendices C and D.

The scale is a "Chesterman" machine engraved stainless steel and is 200 cm in length and standard at 68°F. It has been mounted on a table in small swivelling clamp blocks set in an arc of radius 300 cm. Once mounted, the scale to viscometer distance was set to 300 cm by means of a specially mounted mild steel bar 300 cm in length.

A Barr and Stroud telescope and pentagonal prism conveniently mounted near the instrument allows the angular movement of the torsion head to be observed on this scale which is suitably illuminated by strip lighting from the front and kept at nearly room temperature by a fan blower. A second scale of engraved perspex is used to maintain the cylinder at some 'reference' point on the scale as seen through a telescope. This scale is illuminated from behind and gives better contrast of the engraving than obtained for the steel scale which is essential since the image through the window often tends to become less distinct after the viscometer has held a sample of water for some time.

4.4 A description of this apparatus would not be complete without noting the particular materials used. Also, since a considerable effort has gone into the problem of both high pressure and low pressure sealing the sealing methods used will be described.

4.4.1 Since the first viscometer is limited to approximately 250°C by the use of a heating fluid passing through the thermostatic jacket it was unnecessary to use a high temperature steel for the pressure vessel. In this instance, Firth Vickers S.80 stainless steel, made to EN57 specification, has been used for all parts coming into contact with the test fluid including the pressure vessel, cover, torsion head and mechanical face-seal housing. The manufacturers of the seal have also used stainless steel to a similar specification. The second instrument has been constructed

mainly from Firth-Vickers FDP quality stainless steel which is austenitic. This material is an 18/8 Niobium stabilised steel suitable for use at temperatures up to 600°C. FDP steel was also used for the inner cylinders of bolt instruments since the design is such that they may be interchanged. Special precautions were taken when machining these cylinders since it was noted by Whitelaw (5) that tests showed that dimensional instability of up to 0.008 in. occurred in similar-sized parts when exposed to temperatures of 500°C for a short time and slowly cooled in air. These changes obviously result from stress-relieving of the material and further tests showed that a final heat treatment of two hours at 1050°C and slow air cooling reduced the change in dimensions to 0.0002 in. at the most. It was necessary to perform this treatment when the cylinders were almost completely machined, i.e. prior to making the final lathe-cut. The main pressure-vessel of the second viscometer was constructed from Firth-Vickers FCB(T) quality stainless steel and was designed on a basis of a stress to rupture in 5000 hours at 600°C and 500 Kgf/cm^2. The magnetic drive was made by Pressure Products Inc (U.K.) to a similar specification.

Provision of suitable studs to hold the cover to the pressure vessel for the second viscometer presented a problem with regard to the choice of material. On the advice of Jessop Saville their G68 high temperature forging alloy has been used. The 0.1% proof stress for this material is 40 T/in^2 at room temperature and

36 T/in^2 at 600°C. The stress to rupture in 100 hours at 650°C is 28T/in^2 and the coefficient of expansion is compatible with that of FCB(T).

As recorded by the author in Appendix C the first testing of the apparatus was by measuring the viscosity of air. This limitation was imposed by the fact that it was impossible to obtain stainless steel bearings of the required size and no manufacturer approached was prepared to make these up as a "special". However, Messrs. Ransome and Marles Ltd. supplied us with stainless steel ball bearings and suggested that we design our own bearings and make them up ourselves. This idea proved remarkably successful and the outer cylinder assembly is shown in Figure 4 which illustrates the viscometer with these bearings in position. Each race consists of one conical surface having a slight radiused recess in which the balls run and a plane conical surface on the other part. By carefully adjusting the screwed ring at the top of the assembly both bearings may be loaded simultaneously to remove any "play" and to put a slight tension on the bearings. No doubt if such bearings were heavily loaded they would fail because stainless steel parts moving relative to each other are notorious for "scuffing" or "picking-up" unless special precautions are taken (such as the application of a graphite paste). In this case the bearing load is light and rotational speeds never exceed 100 r.p.m. The maximum eccentricity of the inner cylinder when assembled in its bearings

and located in the bore of the pressure vessel was observed to be 0.0005 in. Misalignments of this magnitude are almost certain to accumulate unless final dimensions can be machined in-situ. This procedure was adopted by Bearden (8) but would appear to be impracticable in this case.

The gears used to transmit the drive from the shaft to the outer cylinder are straight bevel gears in the first viscometer and spiral bevel in the second. Again this was due to early investigations indicating that only straight bevels could be made economically in such small sizes while at a later stage a manufacturer was discovered who could cut very small spiral-bevels. The advantage of using spiral bevel gears is that at least two teeth are always engaged so that there is no discontinuity as one tooth disengages and the next tooth takes up the drive. In the case of the first instrument this effect has been reduced to negligible proportions by using a stainless steel pinion with 24 teeth and a Tufnol driven gear with 54 teeth. The use of a soft material for the driven gear with a large number of small teeth has almost completely eliminated the effect of vibrations.

The high pressure window was initially obtained only in pure sapphire from the Linde Division of Union Carbide. This has been successfully tested in the 2nd viscometer at pressures up to 13,000 lbf/in^2 and will eventually be used to 1000 Kgf/cm^2. For lower pressure work it has been replaced by a Triplex glass window

of similar dimensions. The sapphire window has been supported by a hardened tool-steel plug while for the lower pressure tests a stainless steel retaining ring has been used. The window is an optically flat disc $\frac{3}{4}$ in. dia. and $\frac{1}{2}$ in. thick. The window seal is of the Poulter (126) type which utilises the Bridgman unsupported area principle. In theory, if the metal retaining plug is lapped to the same degree of flatness as the window then no leakage will occur. This has been found to be the case at pressures above approximately 100 Kgf/cm^2 but at low pressures if the seal has not been established a film of liquid persists and leaking occurs. For this reason a thin film of Araldite epoxy resin has been used to fix the window to the retaining ring in the first viscometer. This procedure was also adopted by Moszynski (107).

The high pressure tubes and fittings including valves are all of stainless steel and were standard items supplied by Aminco. The heating tank and the double walled jacket and connecting tubes for the heating fluid are all copper. Where fabrication has been necessary, for instance, around the top flange, silver solder has been used. Where two soldered joints are fairly close and were made at different times in the manufacturing sequence, brazing has been used for the first joint followed by silver soldering. However, in some cases silver soldering has provded the initial joint while neighbouring joints have been made with soft solder.

This procedure has been necessary because if the same type of solder is used in subsequent operations the solder runs from earlier joints with resulting leakage when the system is filled with fluid. Wherever possible other parts not coming into direct contact with water have been made from mild steel.

The calibrating rig for the torsion wire is almost entirely made from brass except for the heating jacket, which is again fabricated from copper. When initial tests were made using water as the thermostatic fluid several mild steel parts, for instance, the reduction gears for adjusting the torsion head and the heavy flange supporting the vacuum vessel began to corrode badly. These parts were then nickel plated and have since showed no signs of corrosion.

4.4.2 The main seal between the pressure vessel and the cover is the wedge ring or delta ring type of the form described by Niemeier (127). Although this is essentially a high pressure seal it requires a relatively small initial tightening and experiment has shown that it can be capable of supporting a vacuum of better than 10^{-3} torr. The essential design point to be observed here is to ensure that the ring is made slightly larger in diameter than the vee-groove into which it fits. This means that when tightened initially the point of the delta ring is slightly deformed to conform with the mating grooves and one gets the initial seal from the close surface contact rather than from a line contact. Once the internal pressure

is applied, the delta ring operates on the unsupported area principle and the seal becomes even better. A practical difficulty was obtaining a good surface finish at the pointed 'root' of the grooves since the form tool began to 'chatter' when cutting the full depth. The surface produced from this condition is poor and the seal was ineffective. The grooves were later polished to remove all machining marks by a brass ring (in the form of the groove) mounted on a handle. Grinding paste was used between the ring and the groove to remove unwanted machining marks. The best delta-ring dimensions were found by testing several rings in a small high pressure testing vessel. The first ring was too heavy in cross-section, being overall about $\frac{3}{8}$ in. deep. The smaller ring tested showed no signs of leakage and can be seen in Figure 4.

The rotating torsion head was also pressure tested on the above mentioned vessel before being fitted to the viscometer. The problem here was to find a suitable 'O' ring material for the rotating seal since it was discovered that nitrile rubber and silicone rubber were both damaged by rotation at 330 Kgf/cm^2 and the seal was destroyed. At this time P.T.F.E. 'O' rings were becoming available and also the glass-fibre reinforced (so-called glass-filled) material. The combination of a P.T.F.E. 'O' ring and a glass-filled P.T.F.E. anti-extrusion ring have proved a satisfactory combination for this purpose. With the exception of the mechanical face seal and the window all other seals are either lens ring or 'O' rings (backed by anti-extrusion rings).

It should be noted that lens-ring seals need to be heavily loaded or tightened to provide the initial seal. With the torsion head lens ring this operation was made difficult because although the bottom half of the head is machined hexagonal it is almost inaccessible. This was overcome by tightening blocks onto the studs used for holding the retaining cover, so that the faces of the blocks rested like spanner-flats onto opposite faces of the torsion head. A fairly massive torque could then be applied to the lens ring which produced the required effect. The P.T.F.E. cone through which the sheathed thermocouples pass is similar in design to the 'Conax' type seals which are available commercially.

4.5 Method of temperature control

Since two viscometers have been constructed to cover the full range of temperature and pressure under consideration, the different methods of heating each will be described.

4.5.1. The first instrument was designed to cover the temperature range 0° - $250^{\circ}C$ and pressures of 1 - 250 Kgf/cm^2. It was decided that the closest temperature control in this range could be achieved by means of a thermostatically controlled heating jacket through which a heating fluid is circulated. The jacket is of double walled copper construction with three equally spaced inlet connections in the base. The heating fluid then passes up between the inner wall and the pressure vessel before transferring to the annular space between the inner and outer walls near the top. It then passes down through this annulus and out through three more

equally spaced connections at the bottom. The fluid was heated and circulated from a separate vessel similar in overall dimensions to the one containing the viscometer and a system of 0.5 in. bore copper piping was designed to connect the heating tank to the viscometer jacket. It is obvious that equal flows through each of the jacket inlet connections could only be achieved by perfect symmetry in the pipe-layout which in this case is impossible due to the fact that the pipes have had to be designed around other features of the apparatus. To obtain an approximately equal flow, small restricting orifices were fitted into the two tubes through which the fluid was discharging at a higher rate. This was achieved by connecting the pipe system inlet to the mains water supply and collecting the water from all three branches simultaneously. The size of the flow-restricting orifices was obtained by trial and error. The heating tank contained an immersion pump which, for preliminary tests, circulated water as the heating medium. In this set-up there was a free-surface in the tank and water could be added or drained off as required by visually observing this level. Preliminary measurements were made of the viscosity of air using this method and the system operated successfully to just below 100°C. However, it was required to circulate heating fluid to the torsion-wire calibrating rig (which is also jacketed for temperature control) and the modified fluid heating system is shown in Figure 11. With the heating tank completely closed off and experiencing a constant static head of about 4 ft of water the

immersion pump has been fitted into the cover of the vessel and sealed by a static gland. To prevent fluid leaking up the connecting tube joining the pump casing to the motor a small housing containing a lip-seal was fitted. An advantage of this design is that since the driving motor is always remote from the pump in the immersion type, it is a relatively simple matter to prevent the motor from being overheated by provision of a cooling coil on the connecting tube. Unfortunately the shaft is unsupported over a considerable length and due to misalignment and vibration, failure of the lip-seal was accelerated and replacing this seal has caused considerable delay and inconvenience.

The heater is a 3-kW immersion type made as a single unit with separate terminals for each of three 1 kW elements. The heater was manufactured for this specific purpose by Messrs. Duncan Lowe Ltd. with the elements sheathed in Inconel tube and suitable for temperatures exceeding 250°C. The upper 1 kW element is supplied by power switched by the thermostat; the other two elements each have manual control through "Variac" variable transformers. Maximum power for these elements is mainly required during initial heating to the working temperature; at this stage power is reduced to the level where control by the regulator can best meet the remaining heat requirement.

Thermostatic control is by toluene regulator. In order to extend the temperature range of this instrument the toluene has been replaced by anilene which has a boiling point of 186°C. This

has limited operating temperatures with the viscometer to a maximum of 180°C. This regulator is used in conjunction with an A.E.I. proportioning head which damps out fluctuations in power input when the operating temperature has been reached. This device is fitted into the top of the regulator and operates by means of a heated bi-metal strip which withdraws the contact wire when contact is made with the mercury. Ultimately the "on" to "off" time ratio of the heater exactly balances the heat losses, and very fine control is obtained. This regulator was set up to provide a thermostatic control in a similar rig for testing purposes and a Pt/Pt - 10% Rh thermocouple and galvanometer amplifier were used to feed a temperature-dependent signal to an electronic chart recorder. This plot indicated that temperature was held to ± 0.01°C for periods of several hours but that fluctuations of as much as 0.1°C occasionally occurred, probably due to dirty contacts in the regulator or sudden changes in mains voltage. Certainly the controller has proved adequate for the tests described here. The fluctuations described were in the viscometer jacket whereas the large thermal inertia of the viscometer helps to reduce these changes inside the instrument once steady conditions have been reached. The first viscosity on liquid water at atmospheric pressure and up to 100°C were made with water as the heating fluid. After this, the thermostat was filled with Turbotherm 'A' which is a commercially available heating fluid composed of a mixture of

isomeric triaryldi methanes. This liquid has an initial boiling point at 760 mm Hg of approximately 390°C and thus presented no limitation to the present investigation. Temperature stability has been improved and heat losses greatly reduced by covering the exposed surfaces of the rig with several layers of composite corrugated asbestos and aluminium foil. This has proved a satisfactory method of insulation.

The second instrument was designed to extend the range of measurements to 400°C and 1000 Kgf/cm^2. Problems encountered with the first instrument liquid heating system indicated that some other heating system would be necessary unless a pressurised heating circuit, for example, as developed by Sauer (144), could be used. Since this second alternative would have involved a dis-proportionate expense a simple electrically heated jacket has been manufactured to suit the present requirements. This was made by Isopad to the author's specifications. It consists of a base heater, which fits under the main pressure vessel with holes for the legs and high pressure connection to pass through; a main jacket which fits around the outside of the base heater as well as the pressure vessel and a separate heater or mantle for the top of the instrument. The base heater and top mantle are single windings but the main jacket has three separate windings which may be controlled separately. Each of the five windings has a separate rheostat for controlling the power input and tests are to be carried out with

thermocouples placed at intervals around the viscometer to find the settings which make the instrument isothermal. A 7A variable transformer supplies power to all of the windings so that having preset the rheostats to give reasonable isothermal conditions the main adjustments can be made by manual control of the transformer. It is expected that minor 'trimming' of individual heaters (by varying the resistances), will be necessary to obtain the required temperatures along the whole length of the viscometer. The circuit is shown in Figure 12.

4.5.2 Temperature measurement

The choice of method of temperature measurement has been greatly influenced by the machanical difficulty of placing the thermometric device in the close proximity of the test fluid. A further complication in bringing the leads out of the rotating cylinder and through the pressure vessel. After initial considerations chromel/alumel thermocouples sheathed in stainless steel were selected since the outer diameter of the sheath was only 0.021 in and the instrument could be designed to accommodate three or more of these embedded in the lower guard cylinder without difficulty. Sheathed thermocouples have the advantage that they can be sealed into the pressure vessel by a conventional method without straining the thermocouple wires. In addition this method allows the apparatus to be stripped and rebuilt without permanent damage to the thermocouples and without the necessity for re-calibration. An alternative method which has none of these advantages is that of

leading the bare wires through an insulated plug in the pressure vessel wall and sealing the whole assembly by liberal application of an epoxy resin, for instance "Araldite". After the calibration of the chromel/alumel thermocouples, measurements were carried out on the viscosity of water between ambient and 100°C using these thermocouples. It was apparent at this stage that in order to increase the accuracy of the measurements from ± 0.5% to better than ± 0.1%, a better thermometric device would be required. The limitations with regard to access still applied and it was decided to supplement measurements from the base-metal thermocouples with a single platinum/platinum-rhodium thermocouple entering the test fluid in the same manner as with those already in use. The minimum outer diameter of stainless steel sheathed thermocouple available of this type was 0.065 in. The thermocouple wires had been previously annealed and the absolute accuracy had been determined before delivery and quoted to be not worse than ± 1.0°C at 1000°C. In this type, the termination of the sheath no longer necessitated joints in the thermocouple wire and the emerging 'tails' were, in this case, requested to be of sufficient length to be taken straight to the cold junction - thus reducing the occurrence of thermal emf's due to joints etc. to a minimum. After initial measurements of the viscosity of air using uncalibrated Cr/Al thermocouples, these were then calibrated against a standard platinum resistance thermometer prior to measuring the viscosity of water. Some interesting but disappointing faults were discovered in these

thermocouples during calibration which required several experimental precautions to be taken in order to obtain an accuracy of measurement better than 0.1°C. The details are given more fully in Appendix A.

It was decided that if the accuracy of temperature measurement was to be improved to allow a certainty of ± 0.01°C to be achieved the base metal thermocouples would have to be abandoned in favour of the precious metal type. The most recent measurements have therefore been made with the temperature given by a single stainless steel sheathed platinum/platinum - 10% rhodium thermocouple. This thermocouple was calibrated against a standard platinum resistance thermometer while both thermometers were located in the viscometer jacket. A Tinsley vernier potentiometer reading directly to 0.1 μV was used to obtain R_t and e while the thermostat maintained a steady temperature. The procedure is given more fully in Appendix A. More exacting instrumentation has been necessary for measuring the emf from this thermocouple, including a photocell galvanometer amplifier, a thermal compensator and a more sensitive galvanometer.

4.6 Pressure measurement

A diagrammatic sketch of the apparatus used to pressurise the equipment is shown in Figure 13. The Budenberg dead weight tester has been used to raise the pressure in the apparatus and also as a means for measuring and maintaining the pressure during viscosity measurements. The dead weight gauge has a 0.02 in^2 piston area which is based on a piston diameter guaranteed by N.P.L.

to 5 parts in 100,000. The weights used on the gauge tester are annular and are guaranteed to within 2 grains of the nominal weight.

The errors arising from the use of free piston gauges are known, and measurements are based on the following assumptions.

(a) The piston is truly cylindrical and moves in the cylinder with no friction.

(b) The piston and cylinder do not distort under pressure.

(c) There is no leakage of oil past the piston.

The calibration of the piston diameter is sufficiently accurate to allow out of roundness to be neglected. Friction is present in the piston-cylinder assembly but is minimised by rotation of the weight carrier and hence the piston. The investigations of Bett, Hayes and Newitt (128), Dadson (129) and other workers at N.P.L. indicate that up to the maximum pressure used in the present apparatus any distortion error may be neglected. Leakage of oil past the piston is also a function of pressure and causes an effective increase in the area of the piston. It has been shown that provided there is no dimensional change, the effective area may be taken as the mean of the cross-sectional areas of the piston and the cylinder. The makers of the dead weight gauge state that the cylinder is manufactured to fit the piston with a minimum of clearance and it is assumed that any correction required from this source will be less than 0.1% and therefore negligible. The inherent errors of the

dead weight gauge will not significantly affect the measurement of pressure in the present apparatus. A calibrated Bourdon tube is also connected into the high pressure line to give an immediate visual check on the functioning of the pressure system. This is necessary because the telescope for adjusting the null position of the torsion cylinder is some 10 ft. away from the dead weight gauge.

The pressurised fluid in the dead weight gauge and Bourdon tube is castor oil so that an interface between oil and water needs to be provided. The adaptation of a Greer Mercer hydraulic accumulator for this purpose is similar to the manner described by Venart (130). A rubber bag filled with water hangs inside a small hemispherical-ended pressure vessel into which the castor oil is pumped. The water in the bag is then subjected to the same pressure as the oil and is forced into the viscometer. The accumulator used is 1 quart capacity and may be safely subjected to a pressure of 330 kgf/cm^2.

With the exception of the piston cylinder assembly and the mechanical face seal, all joints and seals in the pressure vessel and associated pressure equipment are leak-free. However, the piston cylinder assembly has almost negligible leakage and the leakage from the face seal is very small. The use of the dead weight gauge is advantageous in that the leakage from the face seal is continuously made up by the effective stroke volume of the piston cylinder assembly. Under most running conditions the carrier needed to be raised every 10 minutes or so by injecting more oil into the system.

The use of a magnetic drive on the second viscometer has allowed leakage to be reduced to negligible proportions by the use of almost entirely static seals, the rotating torsion head being the one exception. A Chas. Cooke hand pump with a phosphor-bronze body was fitted with glass-filled P.T.F.E. chevron type packings and has proved suitable for pressurising the vessel directly with water at pressures up to 800 Kgf/cm^2. When higher pressures are required the heating jacket can be raised in temperature slightly without allowing any escape of fluid. The rate of rotation of the torsion head is 1 revolution in 10 minutes and so far the leakage has been extremely small when the assembly is rotating and zero when it is stationary.

4.7 Water and Filling procedure

The availability of a supply of very pure water has been of great assistance. This water is treated for use in a supercritical steam generator and hence its mineral content and electrical conductivity are particularly low. This water is obtained by passing distilled water through a bed of mixed resins. It is then boiled to expel dissolved gases and then admitted to the viscometer which is under vacuum from a Bunsen pump. A cooling coil has been put between the boiler and the viscometer so that there is no excessive cooling of the water as it enters the viscometer. The water is allowed to flow through the instrument for a time once it has been filled and any trapped air is dissolved or dislodged by rotating the outer cylinder. The first viscometer has a vent which is eventually sealed off when the top mirror holder is connected.

The second viscometer has vents both at the top of the apparatus and also at the extremity of the high pressure tube for the magnetic coupling. These are closed by valves once the apparatus has been filled.

Flasks are connected to both the oil and water sides of the pressure system as shown in Figure 14. The by-pass line to each flask is provided so that the high pressure tube may be evacuated before filling with liquid initially. The water flask is filled with gas free pure water from the boiler when required. When the water in the accumulator is expended the vacuum pump can be started above the oil flask while the pressure above the water flask is atmospheric. The oil is gradually pushed out of the accumulator as the rubber bag fills with water. A careful check has to be kept on the amount of oil which has been added to the pressure system because considerable inconvenience can be caused by damage to the rubber interface.

CHAPTER 5

ASSESSMENT OF ERRORS

5.1 Deviation from the ideal viscometer

In order to reproduce the flow for which the theoretical solution is derived the cylinders would need to be infinite in length and perfectly concentric. The effect of limitations imposed by practical considerations will be discussed.

5.1.1 End effects.

Ideally the fluid should be contained in the space between infinite cylinders. In the actual instrument the drag on the ends of the inner cylinder has been greatly reduced by the provision of guard rings. These rings extend some distance from the ends of the inner cylinder with only 0.010 in. clearance at each end. The guard rings are of the same diameter as the inner cylinder and give continuity to the primary flow between the cylinders over the whole length of cylinder upon which the torque is measured. However, a correction of the order of magnitude of the clearance between the inner cylinder and guard rings must be added to the measured length of the inner cylinder to account for drag on the ends. Houston (63) obtained a theoretical solution for a particular configuration where the wall thickness of the guard cylinder was much larger than the inner cylinder, the section of which he treated as a thin sheet. Treating the problem as a two dimensional one (i.e. for the case when the ratio of radius to gap is large) he deduced that 0.47 of the

clearance must be added to each end of the inner cylinder. Using the same reasoning for the case where symmetry exists the correction is 0.5 of the clearance to be added to each end. In the design of the first viscometer care was taken to ensure that symmetry existed. The guard cylinders have a solid face and the ends of the inner cylinder are closed by small plates. Thus the effect of flow in the clearances is shared equally between the guard rings and the inner cylinder. The magnitude of this effect amounts to only 0.34% of the measured drag so that even if the value of 0.47 obtained by Houston was used the difference would only be 0.02% from the correction applied.

For the sake of simplicity many rotating cylinder viscometers have been used without guard cylinders, since in many less-accurate requirements these may be considered unnecessary. However, for this configuration several theoretical solutions exist (e.g. Roscoe (68)) for the torque due to the ends of an immersed cylinder so that corrections may be applied for this if more accurate results are required. Although the method of using a viscometer without guards may be better from the point of view of simplicity (with the provision that an exact correction may be made for the ends) the guards do serve additional purposes, for instance, they assist with mechanical centering of the suspended cylinder during assembly. Also, in this instrument, the extension of the lower guard cylinder serves to shield the mirror stem from turbulence caused by the moving mechanical parts.

In addition to the primary concentric flow which exists in

the annular space there will be fluid velocities modifying this flow due to the proximity at one end of the base of the rotating cylinder and at the top end due to the stationary top cover of the viscometer. The distance which these effects persist along the annular space will vary with the angular velocity of the rotating cylinder and with the gap thickness. It is apparent that the guard cylinders must be long enough for these effects to have become negligible in the space around the suspended cylinder. For instance, the findings of Hatschek (57) that the viscosity of water appeared to increase with higher rates of shear indicates that the effect of the cylinder ends was not eliminated by the short guard cylinders used in his instrument.

According to Couette, each of the guard rings should be about $^{2}/_{5}$ of the length of the suspended cylinder, in which case he considered that disturbance was, for practical purposes, confined to the space between guard rings and the outer cylinder. Considering the relation of the length of the guards to the gap width, Couette (56) and Gilchrist (60) made the guard length approximately 14 $(R_1 - R_2)$ while Leroux (62) worked with 10 $(R_1 - R_2)$. With shorter guards than this Drew (88) found that the elimination of end effects was considerably improved by adding wedge shaped rings to the extremities of the guard cylinders, thus partially closing the gap between the cylinders. The idea underlying this is that the liquid near the ends may have a speed which corresponds with the radius $R_1 - \frac{1}{2}(R_1 - R_2)$ at approximately this same radius instead of

some much smaller radius as would be the case without the attachments.

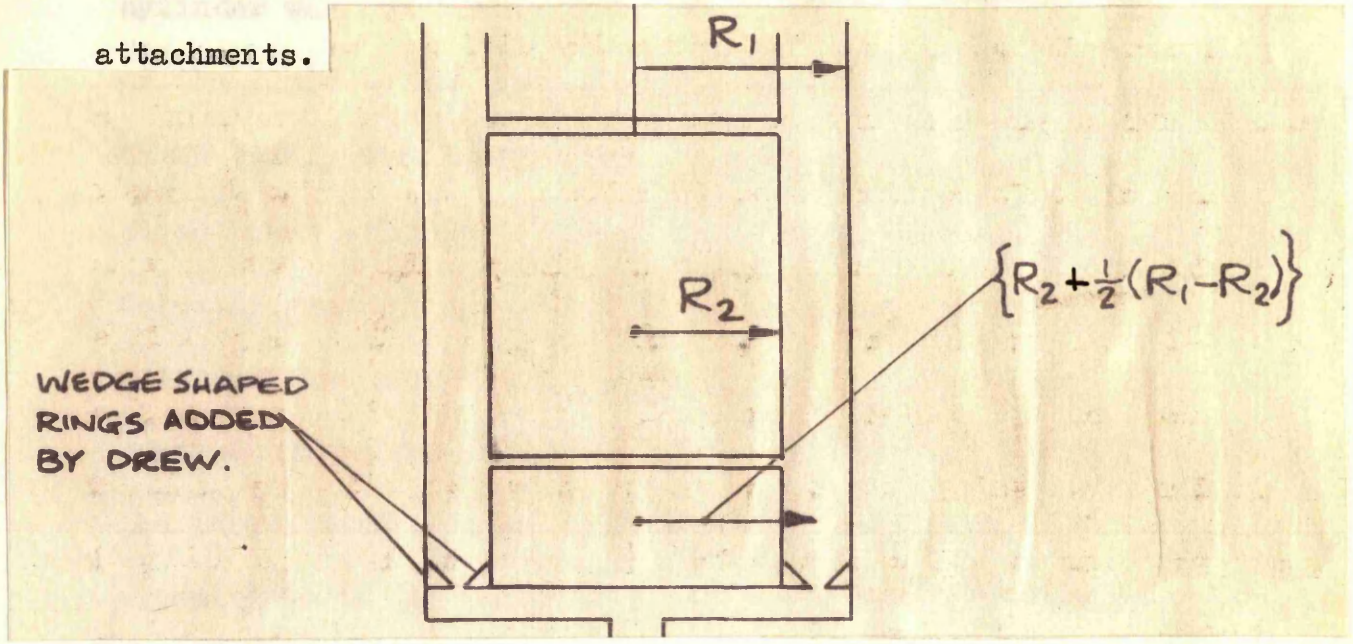

Using this method Drew made an accurate determination of the viscosity of water at 20°C and observed that the relationship between deflection and angular velocity was linear only after the wedge shaped rings had been added.

Several papers describing experimental studies of the flow between rotating cylinders have been scrutinised to see if end effects had been observed and to what extent the quantitative results were altered by it. Taylor (79) in the Part II of this paper measured the distribution of velocity between concentric cylinders when the outer cylinder was rotated and the inner cylinder was at rest by means of small pitot tubes. With a ratio of gap to rotating cylinder radius $\frac{R_1 - R_2}{R_1} = 0.38$ and a cylinder speed of 33 revs/second he showed that although the motion was still not turbulent the velocity distribution under these conditions was somewhat modified. It was shown that the observed velocity of fluid nor the inner

cylinder was greater than the calculated value due to circulation of the fluid by the action of the ends. Several tests are described which verify this explanation, including flow visualisation using a glass outer cylinder. It might be noted that in these tests the velocity gradient was modified to a greater extent near the inner cylinder than near the rotating outer cylinder, where the velocity gradient remained almost the same. One would therefore expect that the torque on the inner cylinder would be altered to a greater extent than on the outer cylinder. The fact that Taylor's torque measurements, which were made on the rotating cylinder, show no appreciable deviation from the theoretical value confirm this observation.

An important difference between Taylor's apparatus and the viscometer described here is that Taylor's outer cylinder was also the container and was closed at both ends, while in the viscometer the rotating cylinder is closed only at the bottom. The flow due to this single rotating end and the stationary boundary at the top would therefore be a velocity outwards at the bottom giving a fluid velocity u_p the inner surface of the rotating cylinder and down the outer surface of the inner cylinder. However, in making this comparison with Taylor, the important fact is that the cylinder speed of 33 revs/sec gives a Reynolds number of 1.1×10^5 whereas the viscometer described here has been designed such that the Reynolds number does not exceed 100. This point also applies to Drew, whose outer cylinder speed was varied between 3.6 and 13.6 revs/sec giving corresponding Reynolds numbers of 1653 to 6246.

Thus ithas been concluded that the small effects observed by these experimenters at high R_e indicates that the effect will be negligible in an instrument designed to operate at very low Reynolds numbers. In fact, tests made with the viscometer have shown no significant deviation from a linear relation between angular deflection and angular velocity, which has been taken to confirm that at very low speeds the end effects are negligible. Should the effect become noticeable at any time or for some particular fluid, the precaution successfully applied by Drew could quite easily be taken.

The more recent measurements by Donnelly (77) confirms the smallness of end effects right up to the point at which instability occurs. Over the range of speeds at which the torque was measured prior to the onset of instability the 'apparent viscosity' of the liquid, as indicated by his instrument fell by approximately 0.5%. The exact figure was not reproducable because this deviation also contains the effect of eccentricity, which varied slightly from day to day. By comparison, section 5.1.3 shows that the viscosity measurements described here were taken over a narrow speed range terminating well short of the point of instability (for either cylinder rotating) which would suggest that in this present instrument the end effect is only a fraction of that observed by Donnelly over his wider range of speed.

5.1.2 Eccentricity

The effect of possible eccentricity of the two cylinders on the measured torque must be considered. The flow created by eccentricity resembles the problem of the lubrication of a journal bearing except that in the bearing the eccentric displacement is not small compared to the gap between the cylinders, although the gap itself is small compared to the radius of curvature. The effect of eccentricity in the viscosity measurement was first considered by Couette (56) in a very rough approximation which resulted in a theoretical increase in viscous drag on the stationary cylinder with eccentricity. Kellstrom (64), however, observed a decrease in the torque on the stationary cylinder due to eccentricity in an experimental investigation. This observation is in agreement with Harrison's (131) theory of the lubrication of a journal bearing, in which it is shown that the movement acting on the stationary cylinder should decrease with eccentricity, while that on the rotating cylinder should increase. Since Harrison's equations were obtained by an approximation neglecting curvature the question of whether the inner or outer cylinder is rotating does not arise. Thus, his result may be applied to viscometers where the torque is measured on either the inner or outer cylinder, whichever is the stationary member. Inglis (132) has presented a further simplification of Harrison's treatment of the problem by means of the approximations that the eccentric displacement is small compared to the width of the gap and that the inertia terms may be neglected. His value

for the modified torque M' on the stationary (outer) cylinder is

$$M' = 2\pi\eta U \frac{(R_2 + d)^2}{d} (1 - C^2 + \ldots\ldots) \quad \ldots 5.1$$

and the torque on the moving (inner) cylinder is given by M where

$$M = -\left(\frac{2\pi\eta U R_2^2}{d}\right) (1 + 2C^2 - \ldots\ldots) \quad \ldots 5.2$$

The total torque on the inner (slightly displaced) cylinder about the original centre is equal and opposite to that on the outer cylinder

$$\therefore \quad M + R\ C d = -M'$$

making the reaction torque on the fluid vanish, as is necessary for constant flow. Here, R is the moment due to the lateral force (per unit height) on the inner cylinder due to the difference of pressure on the opposite sides.

e is the eccentricity

$C = \frac{e}{d}$ where d is the gap between the cylinders

i.e. $R_1 - R_2 = d$

thus

$$R = \frac{6\pi\eta U R_2^2 C}{d^2}$$

and

$$R \times e = \frac{6\pi\eta U R_2^2 e^2}{d^3} \quad \ldots\ldots 5.3$$

Using the equation 5.3 the effect of eccentricity in the present instrument has been calculated. For the maximum angular velocity of the instrument the peripheral velocity of the moving

cylinder U = 6.24 cm/sec and considering the specific case of water at 20°C the effect of e = 0.005 in = 0.0127 cm was found to be 1.36%. If, however, e is limited to a value not exceeding 0.002 in, which is a practical figure in that eccentricities in the pre-assembly stage greater than this can be corrected for, then the resulting error will be only 0.22%. It should perhaps be pointed out here that several errors were noticed in the script of Inglis's paper. For instance, in Part I where curvature is neglected, his equation (3) should read,

$$\eta u = \eta U \left(1 - \frac{y}{h}\right) + \tfrac{1}{2} y \left(y - h\right) \frac{\partial p}{\partial x}$$

In subsequent equations the terms F and G are both wrongly written. They become

$$F = \frac{2\pi U}{d} \left(1 + \frac{c^2}{2} + \ldots\ldots\right)$$

and

$$G = \frac{3\pi U}{d} \left(c^2 + \ldots\ldots\right)$$

N.B. Inglis's notation for the gap is 'g' whereas the present notation of d has been used here.

Inglis's paper was propared particularly with the measurements of Bearden on the viscosity of air by the rotating cylinder method in mind. When considering the equation of motion

$$\frac{\partial p}{\partial x} = \eta \frac{\partial^2 u}{\partial y^2} - \rho u \frac{\partial u}{\partial x}$$

Inglis was able to neglect the last term, which arises from inertia, because for the case of air this can easily be shown to be very small

compared with viscous effects. However, this is not true for liquids and in particular, for water at 20°C the inertia term has been calculated to be about 29% of the viscous term at the highest speeds of rotation and therefore should not be neglected in the analysis. At lower angular velocities, for instance, if the speed is limited to 0.4 of the present maximum, the inertia term has a much smaller effect and can be neglected and equation 5.3 applies. Rather than to solve the full equation of motion in order to work out a more accurate estimate of error this present limitation has been taken to apply.

Previous calculations were made without taking curvature into account. The Part II of Inglis's paper deals with the case of appreciable curvature, and small eccentricity. In this case the viscous torque on the stationary cylinder is given by

$$M' = - \frac{2\pi \eta U (R_2 + d)^2}{d} \left\{ 1 - \frac{d}{2R_2} - c^2 + \frac{9 g c^2}{4 R_2} + \ldots \right\} \quad 5.4$$

Using this equation and the same conditions as before, the torque on the stationary cylinder was calculated to change by 0.20% which is slightly less than the value obtained neglecting curvature.

Intuitively, one would expect that when one cylinder is displaced to an eccentric position a pressure gradient will be generated which tends to restore concentricity. Since the inner cylinder is supported on a single wire it seems reasonable to suppose that initial eccentricity of the inner cylinder may well be removed by slight lateral displacement of the cylinder due to the

pressure gradient produced. If the forces tending to return the cylinder to its initial position are great enough an oscillatory motion would occur. No such oscillations have been observed during tests and it is thought that the practical precautions observed have reduced the effect to a value less than 0.2%.

5.1.3 Stability of flow

The equations governing instability have been given fully in section 3.1.3. However fuller consideration has been given to this equation with regard to this particular instrument. For dynamic similarity $\frac{T}{\rho n^2}$ must be a function os $\frac{n}{\nu}$ for any given pair of diameters, where n is the speed of the rotating cylinder in revs/second and T is the torque. In order to show the effect of rotation on turbulence the theoretical value of T has been calculated for steady motion. Since in this case $T \propto n$, then

$$\frac{T}{\rho n^2} \propto \frac{1}{n}$$

so that with logarithmic co-ordinates the theoretical curve is always a straight line at - 45° to the horizontal axis. To compare these results with those of Taylor (71)(79), Figure 15 has been drawn where $\log_{10} \frac{T}{\rho n^2}$ is plotted against $\log_{10} \frac{n\rho}{\eta}$. A particular set of conditions has been used to calculate the theoretical line and a curve similar to that shown in Figure 1 has been used to calculate the point at which instability is to be expected when the outer cylinder is rotating. At these conditions several

viscosity measurements have been made with the instrument at different cylinder speeds. These experimental points are shown superimposed on Figure 15. It can be seen that whereas the upper limit at which viscosity measurements have been made corresponds to $\log \frac{n}{\nu} \approx 1.2$, instability would not been expected until $\log \frac{n}{\nu} \approx 2.4$ according to Taylor.

The speed at which instability would have occurred had the inner cylinder been rotating has also been calculated using Taylor's theoretical solution. For this case instability would occur for $\log \frac{n}{\nu} \geq 1.73$ and this point has also been plotted on Figure 15. It is of interest to note that had the present viscometer been designed to operate with a rotating inner cylinder and stationary outer cylinder the measurements would have been made much closer to the onset of instability. For instance a 50% increase in the present maximum speed would have caused Taylor vortices to appear. However, for the present design of viscometer it is apparent that possible instability of flow is not a problem and the speed would, in fact, be increased considerably without any trouble from this source.

5.2 Accuracy of direct measurement

Since the viscosity may be calculated from the equation

$$\eta = K F \Theta t \qquad \ldots\ldots 5.5$$

and is also directly dependent on the temperature and pressure recorded, the estimated accuracy with which these factors have been obtained is discussed below

5.2.1 K - the apparatus constant

This constant is given by

$$K = \frac{(R_1^2 - R_2^2)}{L \cdot R_1^2 \cdot R_2^2} \qquad \ldots\ldots.5.6$$

In the present analysis the standard deviation σ has been considered throughout, rather than obtaining a maximum probable error for each variable. At the end the maximum probable error can be calculated from the estimated overall standard deviation obtained from combining individual errors.

The error in K can be obtained by taking partial derivatives in equation 5.6.

$$K = \left[\left(\frac{\partial K}{\partial R_1} \right)^2 (\sigma R_1)^2 + \left(\frac{\partial K}{\partial R_2} \right)(\sigma R_2)^2 + \left(\frac{\partial K}{\partial L} \right)(\sigma L)^2 \right]^{\frac{1}{2}}$$

which reduces to

$$\frac{\sigma K}{K} = \left[\left(\frac{2 R_2^2}{R_1(R_1^2 - R_2^2)} \right)^2 (\sigma R_1)^2 + \left(\frac{2 R_1^2}{R_2(R_1^2 - R_2^2)} \right)^2 (\sigma R_2)^2 + \left(\frac{\sigma L}{L} \right)^2 \right]^{\frac{1}{2}} \ldots$$

$\ldots\ldots.5.7$

Using this equation the value of $\frac{\sigma K}{K}$ has been obtained by two methods. In the first method each dimension was measured a large number of times using slip gauges and an electronic comparator. The standard deviation of each of these sets of measurements from the mean value used to obtain K has been used to obtain σK. The value of $\frac{\sigma K}{K}$ obtained was 2.98×10^{-3}, i.e. approximately 0.3%.

At a later date the standard deviation was re-calculated

using standard deviations obtained from Talyrond plots of the cylinder diameters. These deviations are different because the Talyrond method of calculating the deviation allows out of roundness to be much more accurately taken into account. By this method $\frac{\sigma K}{K}$ has been calculated to be 4.51×10^{-3} which is about 50% greater than the previous estimate. This was because the inner cylinder was much more out-of-round than comparator measurements had indicated. A comparison of the results by the two methods is given in Table 1.

TABLE 1

Cylinder	Standard deviation σ	
	From Talyrond	From comparator
outer	1.07×10^{-4}	1.55×10^{-4}
inner	2.83×10^{-4}	1.50×10^{-4}

The magnification used in the Talyrond method can be varied but in most cases a x400 magnification was used, i.e. a change of 0.00025 in. becomes 0.1 in on the plot. The precedure followed was to draw the mean circumference through the plot so that the sum of areas inside this line were equal to the areas outside. This was achieved by trial and error, the areas being measured by planimeter. The distance, ϵ, between the mean circumference and the plot was then measured at 24 intervals around the circumference. The standard deviation of this dimension has then be calculated from

$$\sigma = \frac{1}{x}\sqrt{\epsilon_1^2 + \epsilon_2^2 + \epsilon_3^2 + \cdots\cdots \epsilon_x^2}$$

The Talyrond method was very revealing of the shortcomings in the method of manufacture for these cylinders. Although the cylinders had been stress-relieved before the final machining operation (which involved removing only a few thousandths of an inch) the plots revealed distortion due to holding of the cylinders in a 3-jaw lathe-chuck. Since, at this time, the cylinders for the second viscometer had not been completed a new sequence of operations for manufacturing the cylinders has been worked out which should reduce the standard deviation to 0.00005 in. or better. In addition to these precautions air-gauging equipment is to be used for giving an independent value for the absolute dimensions of these cylinders. This method of inspection is a fairly recent innovation but is extremely useful where variations in size smaller than 0.0001 in. are to be detected. The principle used is that a master gauging ring or plug is made slightly different in size to the range in which the size of the component is expected to fall. The ring, for example, has two or more small apertures around the circumference through which compressed air can escape. When this ring is pushed over the component to be measured, the film of compressed air between the cylinders has a pressure which can be used, by suitably calibrating the equipment, to give variations from the gauge size very accurately. The great advantage here is that there is an integrating effect over the region at which the air-film pressure is sensed so that the presence of small surface irregularity does not give a misleading measurement.

5.2.2 F - the wire calibration

Since $$F = \frac{I}{\tau^2} \qquad \ldots\ldots 5.8$$

The external error will be the result of errors in the determination of I and in the measure of τ . I is the moment of inertia and for a simple disc of mass M_D is given by $\frac{1}{2} M_D R^2$. For a disc with a hole radius r along its axis

$$I = \tfrac{1}{2} (M_D R^2 - mr^2) \qquad \ldots. 5.9$$

where m is the mass of metal removed in making the hole. For a homogenious material equation 5.9 may be re-written as

$$I = \frac{M}{2} (R^2 + r^2) \qquad \ldots. 5.10$$

where M is the mass of the ring = M_D - m, R is the outer radius and r is the inner radius.

This equation is only valid if the end faces of the ring are parallel and perpendicular to the axis. This condition has been approached by first of all turning the ring accurately in a lathe so that although the ends may not be flat they are perpendicular to the axis. The ring was then ground flat on the end faces and finally lapped. The probable error has therefore been calculated from the estimated errors in M, R and r.

The error analysis will be considered particularly for the rings designated C_2 and D_2 which have the largest inertia. Since these have a large outside diameter and bore, they rest on an aluminium disc and are clamped to the mirror stem with the assistance of a brass spacer. Thus the error in the value of I for these other parts must also be considered.

Re-writing equation 5.10 in terms of the diameters.

$$I = \frac{M (D^2 + d^2)}{8}$$

$$\sigma I = \left[\left(\frac{\partial I}{\partial M} \right)^2 \sigma M^2 + \left(\frac{\partial I}{\partial D} \right)^2 (\sigma D)^2 + \left(\frac{\partial I}{\partial d} \right)^2 (\sigma d)^2 \right]^{\frac{1}{2}}$$

which can be re-written

$$\frac{\sigma I}{I} = \left[\left(\frac{\sigma M}{M} \right)^2 + \left(\frac{2 D}{(D^2 + d^2)} \sigma D \right)^2 + \left(\frac{2d \cdot \sigma d}{(D^2 + d^2)} \right)^2 \right]^{\frac{1}{2}} \quad \ldots.5.11$$

The mass of the ring was obtained with an Oertling automatic chemical balance using calibrated weights allowing an accuracy of $\pm$ 0.1 mg to be obtained. The dimensions of the rings were obtained by slip gauges and a comparator which can discriminate to 1×10^{-5} inch. If the requisite precautions are taken regarding temperature control, this represents the accuracy of the physical measurement. However, each machined part has some degree of our-of-roundness and the standard deviation of the measured dimensions has again been found using the Talyrond plot.

Considering now the experimental error in obtaining the inertia of the mirror stem, which forms a part of the oscillating system. The inertia ΔI was found from several experiments where the relationship

$$\Delta I = I_{A_1} \frac{\tau_{\Delta I}^2}{\tau_1^2 - \tau_{\Delta I}^2}$$

or

$$\Delta I = I_{A_2} \frac{\tau_{\Delta I}^2}{\tau_2^2 - \tau_{\Delta I}^2}$$

has been used. Here $\tau_{\Delta I}$ is the period of oscillation of the mirror stem alone and τ_1 and τ_2 are the periodic times for the pendulum when rings A_1 and A_2 are timed respectively. For the mirror stem used in the first viscometer ΔI has been calculated to be 6.475 ± 0.007 gm cm^2. Since ΔI is small compared with the total inertias of the system, it does not need to know better than this. Using this error and similar estimates of error for the aluminium carrier and the brass spacer the value of $\frac{\sigma_I}{I_{Total}}$ has been estimated to be 1.02×10^{-4} or approximately 0.01%.

Now, $$F = \frac{I}{\tau^2}$$

therefore

$$\frac{\sigma_F}{F} = \left\{ \left(\frac{\sigma_I}{I}\right)^2 + \left(\frac{2\sigma_\tau}{\tau} \right)^2 \right\}^{\frac{1}{2}} \qquad \ldots\ldots 5.12$$

Although the Venner type T.S.A.3 counter is claimed to be accurate to 1×10^{-5} there will be slight variations in performance due to changes in ambient temperature. The standard deviation could therefore be taken as $\pm 5 \times 10^{-5}$ which should allow for changes in room temperature. However, the precision with which τ can be obtained is less than this and varies slightly with such things as vibration from other machinery in the region of the test rig and changes in the response time of the photocell timing device for different experimental conditions. The effect of the latter causes the greatest loss of precision at small amplitudes of oscillation and it can be seen from Figures 18 to 20 that this can amount to

$\pm 2 \times 10^{-3}$ seconds in the period τ of 14 seconds (i.e. approximately $\pm 15 \times 10^{-5}$ or $\pm 0.015\%$).

Using these figures, $\frac{\sigma_F}{F}$ has been estimated as $\pm 1.81 \times 10^{-4}$. It might be noted that the calibration results of rings A_{22}, C_2 and D_2 given in Appendix E(iii) fall within 7×10^{-5} of each other. Although no conclusion can be drawn from so few rings it is thought that this assessment of accuracy may be applied to the most recent calibrations of the wire. However, for the rings made to a less rigorous specification and where the timings were made without estimation of the amplitude effect, it is apparent that errors have entered the experiment which have not been fully accounted for so far. It can be seen from Appendices B and E that the standard deviation was mostly about 9×10^{-4} for the early experiments. Some notes that follow are thought to contain the explanation for this scatter.

For instance, considering the effect of temperature changes in the room of $\pm 3^{\circ}C$ from Appendix E(iii) we know

$$\frac{d\left(\frac{I}{\tau^2}\right)}{dt} = 1.196 \times 10^{-4} \text{ where t is in } {}^{\circ}C$$

$$\therefore \quad \pm 3^{\circ}C \equiv \pm 3.588 \times 10^{-4} \text{ in } \left(\frac{I}{\tau^2}\right)$$

However, since estimated $\sigma F = 9 \times 10^{-4}$ the present scatter cannot be explained by temperature variations alone.

Other possible causes of variation in the observed torsion constant may be listed briefly.

(a) It is possible that inspite of the precautions and adjustments made prior to the timing of oscillations that during, say, the timing of 50 oscillations, the centre of the swing has moved slightly away from the photocell (possibly due to refraction of the light passing through the window) which would mean that the time deduced for one oscillation would be slightly in error.

(b) The internal error in the determination of F has been obtained by timing a series of inertia rings which vary in mass and moment of inertia. Although the aim was to treat the testing of each ring identically, a difficulty in the timing of one particular ring which could mean repeating the test, or removing the suspended system temporarily to clean the mirror, meant that the wire was subjected to many thousands of cycles between the 1st and the 9th inertia ring. Such treatment almost inevitably will cause a work hardening of the material and thus a change in the torsional behaviour. Furthermore, the removal of the suspended system from the vacuum rig and the changing of inertia rings subjects the wire to a considerable handling stresses which could have a similar effect. Since some of these effects may not be permanent, i.e. the wire may return to its initial relaxed state when left unstrained for several days, it is difficult to apply any corrections or to assess the effect of this behaviour quantitatively except by comparing the results for several rings.

For example, the results for the three most accurately made rings may be considered sufficiently accurate with regard to the present state of development of the apparatus. The technique for timing the rings may have to be refined in order to increase the accuracy to $\pm 1 \times 10^{-4}$, which should be attainable. This may involve using a technique similar to that used by Bearden (8) in which the end of each swing is recorded by high-speed cine photography. Thus the peak-to-peak time can be deduced very accurately. A method similar in principle has been developed by Copley (133) using a photocell technique for determining the internal friction of glass fibres. In this arrangement Copley uses 4 photocells arranged equidistant along the arc through which reflected light, from the torsional pendulum, travels. As the amplitude of the oscillation decays the turning point of the swing gets nearer to each photocell in turn. The nearer the photocell is to the turning point of the swing the longer the light dwells on the cell and the stronger is the signal received from the cell. This signal is recorded and the logarithmic decrement can be calculated from counting the number of oscillations which have lapsed between peaks on the record (which corresponds with the amplitude decaying an amount equal to the distance between photocells). Each oscillation gives a distinct line on the record-chart. If an accurate time base could be built in to such a recording system it would seem likely that a method similar to this could be used to determine the periodic time with greater accuracy.

5.2.3 θ - the angular deflection

Although the angular displacement of the torsion head is obtained directly from the mirror and scale arrangement, errors may arise in the operation of the null technique since the suspended cylinder must be moved to the null position (which is some reference point on the lower scale) before the upper scale reading can be made. The lower scale is 150 cm from the viscometer and the divisions are 0.5 mm. Ideally the position of the inner cylinder may be adjusted to ± 0.25 mm although in practice this cannot always be achieved due to the mirror surface being clouded. The precision with which the null position may be obtained is also limited by the reaction of the operator in stopping the motor which rotates the torsion head. In the first viscometer the scale image is moving at a velocity of 0.63 cm/sec relative to the telescope and the operator must therefore must be able to stop the motor with a precision of better than ± 0.1 second if the suspended cylinder is to be placed at the null position within 0.6 mm. In practice several attempts have to be made to do this since during rotation of the torsion head the suspended cylinder lags behind and then over-runs when the motor is stopped. There is usually the tendency for the cylinder to 'creep' towards some equilibrium position after adjustment has been completed which may appear as a slight move away from the null point if this was the position at which the cylinder initially same to rest. It is considered that there is a total experimental uncertainty of ± 0.6 mm in obtaining the null point on the lower scale which represents ± 0.5 minutes of arc of the cylinder. Ways

of improving this aspect of the instrument are being introduced for the second viscometer (see Appendix J). Errors arising in the measurement of deflection may be listed as follows.

(a) Possible errors in reading the upper scale and the smallest distance on the scale which may be resolved.

(b) Errors in the machine dividing of the scale and thermal expansion of the scale.

(c) Errors in the distance of the scale from the viscometer.

(d) Errors in ascertaining the null point from observation of the lower scale image.

Considering (a) there is always the possibility of a gross error if just one reading is made at the required condition. For this reason all absolute viscosity determinations involved several readings at different angular velocities which was a check against a gross error in any individual reading. The total error in the deflection δ due to the top scale reading is taken to be $\pm$ 0.5 mm. This error may be combined with the error mentioned in (d) and discussed earlier which amounts to $\pm$ 0.6 mm. uncertainty in achieving the null point, (this amounts to $\pm$ 1.2 mm. on the upper scale which is twice the distance away). The possible error of $\pm$ 0.5 mm. in reading the lower scale (i.e. $\pm$ 1 mm on to deflection of upper scale) must also be considered.

These three errors have been combined to give the probable error, $\sigma_{N.P.}$, in obtaining the null point. It was found that $\sigma_{N.P.} = 1.64$ mm.

Since the null point must be obtained at least twice to

obtain a deflection δ the probable deviation in δ will be given by $\sigma\delta$ where

$$\sigma\delta = \sqrt{2 \times 1.64^2} = 2.32 \text{ mm}$$

Considering (b) the errors in the machine dividing of the scale are thought to have had a negligible effect on the measured deflection. The scale is described as standard at 20°C and it is certain that the manufacturers error will amount to no more than ± 0.05 mm in the 200 cm overall length of the scale, which is negligible. However, there is a systematic error as a result of the scale being a few degrees above 20°C due to the radiant heat from the strip lamps which provide illumination. This is kept to less than 5°C by a fan blower which keeps the scale cool. The error due to this is of the order of 90×10^{-6}, i.e. less than 1 in 10^4 which for present purposes is insignificant.

The error under heading (c) may be taken to be ±1 mm in the total distance of 300 cm which was achieved in the following way. A steel rod was manufactured with the required length and a frame was made to hold the rod horizontally at the scale height. A small brass fixture was made which fitted into the place normally occupied by the mirror stem which attached to the torsion head. The vertical face of a recess cut into this fixture corresponded to the centre line of the viscometer. Thus the position of the scale was adjusted so that the rod touched the scale at one end and the centre-line located brass face at the other. If this distance is designated r then the angular deflection of the inner cylinder obtained by this method is given by θ where

$$\theta = \frac{\delta}{2r}$$

and

$$\frac{\sigma_\theta}{\theta} = \sqrt{\left(\frac{\sigma_r}{r}\right)^2 + \left(\frac{\sigma_\delta}{\delta}\right)^2} \qquad \ldots.5.13$$

N.B. The assumption is being made that δ is at least 100 cm. This then evaluates to

$$\frac{\sigma_\theta}{\theta} = 2.35 \times 10^{-3}$$

5.2.4 The error in t, the time for 1 revolution of the outer cylinder.

The tachometer is fitted to the fastest moving shaft so that a large number of pulses are produced by the phonic wheel for counting purposes. The amount of reduction between the tachometer and the outer cylinder is positive with no possibility of slip. The time for 1 revolution of the outer cylinder is given by t where $t = \frac{1.624 \times 10^4}{3N}$ and N is the electronic counter reading. The maximum value of N which can be obtained is 2000.0 and most readings are taken when N = 1000.0 (or in this region). The counter is claimed to be accurate to $\pm$ 1 in the last figure so that the error in t will be the error in N which is therefore $\pm 1 \times 10^{-4}$. In addition there are short and long term fluctuations in the speed of the synchronous motor due to changes in mains frequency. This has been discussed more fully in Appendix F. In the short time required to make a measurement, the probable error caused by not being able to record the counter reading and the deflection at the same time is of the order of $\pm 1 \times 10^{-4}$. This error could be eliminated by

chart recording the tachometer reading throughout the period of measurement. This addition to the apparatus may be necessary at some later stage of the development of the instrument. Combining these two sources of error gives a probable error in obtaining t of

$$\frac{\sigma_t}{t} = \pm 1.4 \times 10^{-4}$$

5.2.5 Temperature - errors in measurement.

Some of the temperature measurements at atmospheric pressure were made using three chromel/alumel thermocouples located in the lower guard cylinder. The accuracy of these thermocouples is estimated to be $\pm$ 0.1°C, however, there were experimental difficulties associated with these thermocouples which are fully discussed in section 4.6. These thermocouples were calibrated against a standard platinum resistance thermometer prior to use. At a later date one of these chromel/alumel thermocouples was replaced by a platinum/platinum-10% rhodium thermocouple which again had been calibrated against a standard platinum resistance thermometer.

This was first used in conjunction with the other two chromel/alumel thermocouples using the latter only as a check. However, this procedure was found to be too time-consuming when other readings of deflection and angular velocity needed to be recorded constantly. For this reason quite a large proportion of the 1 atmosphere and elevated pressure results depend upon the temperature recorded by the platinum/platinum-rhodium thermocouple only, for which the estimated accuracy is $\pm$ 0.03°C.

The 1 atm. result were found to fit an equation of the form

$$\eta = A e^{\frac{B}{T - 140}} \qquad \ldots.5.14$$

$$\therefore \quad \frac{d\eta}{dT} = - \frac{AB}{(T - 140)^2} e^{\frac{B}{T - 140}}$$

$$\therefore \quad \frac{d\eta}{\eta} = - \frac{B}{(T - 140)^2} dT \qquad \ldots.5.15$$

where B = 573.59 and T is the temperature in ^{o}K.

The possible uncertainty in the value of temperature recorded will contribute to the overall uncertainty of the viscosity measurement. The uncertainty in η using equation 5.15 is $\pm$ 0.25% at 20°C when the chromel-alumel thermocouples are used, the possible error decreasing at higher temperatures. For the Pt/Pt-Rh thermocouple the worst error should be of the order of $\pm$ 0.1%.

5.2.6 Pressure - errors in measurement

In the experiments with compressed water a dead-weight gauge tester incorporating a free piston balance was used to measure and retain the pressure inside the apparatus. Bett, Hayes and Newitt (128), Johnson and Newall (134) and Dadson (129) have carried out experimental investigations of the errors involved in a free piston balance. Using Dadson's results the maximum possible error in the measurement of pressure at, say, 800 Kgf/cm^2 is found to be of the order of $\pm$ 0.05% when using castor oil as a transmitting fluid. The error due to friction between the piston and the cylinder cannot

be completely eliminated but can be minimised by rotating the piston during an experiment. The pressure coefficient of viscosity is at the most 5×10^{-5} cP/Kgf/cm^2 in the temperature range considered so that an error of ± 0.1% in the pressure would have a negligible effect on the absolute value of viscosity and only a very small effect on the pressure coefficient of viscosity calculated.

5.2.7 Comparison of external and internal errors of measurement

The observations of individual errors listed in 5.2.1 to 5.2.6 may be combined to give the estimated probable error of the measurements which is sometimes called the external error of measurement. Thus, since

$$\eta = K F \theta t$$

$$\therefore \frac{\sigma\eta}{\eta} = \left\{ \left(\frac{\sigma K}{K}\right)^2 + \left(\frac{\sigma F}{F}\right)^2 + \left(\frac{\sigma \theta}{\theta}\right)^2 + \left(\frac{\sigma t}{t}\right)^2 + \left(\frac{\sigma\eta_{temp}}{\eta_{temp}}\right)^2 \right\}^{\frac{1}{2}} \quad \ldots.5.16$$

Using the probable errors listed above this evaluates to

$$\frac{\sigma\eta}{\eta} = \pm 5.7 \times 10^{-3} = 0.57\%$$

Considering the actual measurements made during the course of this work, some 33 experimental results were fitted to an equation of the form

$$\eta = A\, e^{\frac{B}{T - 140}} \quad \ldots.5.17$$

In order to find the equation which fitted the results other equations of the form

$$\eta = A + BT + CT^3 + \ldots\ldots \quad \ldots.5.18$$

were fitted using the method of least squares but even a fifth order equation of this form gave a standard deviation greater than the

exponential fit given by equation 5.17.

The standard deviation of experimental points from the exponential curve was 7.37×10^{-3} CP which is about ± 0.7% in the low temperature range but increasing with the temperature. There is obviously some underlying cause for the disagreement between the estimated probable accuracy and the actual standard deviation of the results about the smooth curve through them. In fact the scatter of the results about a smooth curve is more a matter of the precision obtained than the overall accuracy, however, the two are complementary.

Examination of individual results suggests that the precision attainable should be higher than so far achieved. For instance, most results were obtained from several measurements of the deflection of the inner cylinder while the angular velocity of the rotating cylinder was being increased and decreased in stages from the maximum. The slope of the straight line through these points has been obtained from a least squares fit, the average standard deviation of observations from this fit being in the order of ± .2 mm. This figure is reasonable compared with the estimate in 5.2.3 which is quoted as 2.2 mm. where the total deflection is 100 cm on the upper scale. However, at higher temperatures the deflection attainable was only about 30 cm so that the same precision of ± 2 mm in attaining the null point now represents an overall deviation of 3 times this value. This, it is thought, explains the more or less constant scatter of the results over the temperature range covered and the loss of precision at higher temperatures. The obvious

solution is to have a set of interchangable reduction gears which allow the deflection to be maintained at about 100 cm on the upper scale. Steps have been taken to do this with the second viscometer where quite a wide speed range may be obtained by interchanging pinions in the main reduction gear.

5.3 Experimental Corrections

There are a number of temperature dependent effects which may, or may not, affect the determination of viscosity by the rotating cylinder method. Some of these effects are discussed below and where the results may be substantially altered the correction to the basic equation is derived.

5.3.1 Thermal expansion: The only parts of the viscometer for which the effect of expansion needs to be calculated are the cylinders. The suspension wire is also affected but this is taken into account by the calibration.

Now $\eta = K F \theta t$

and $K = \frac{\text{const.}}{L} \left\{ \frac{1}{(2R_2)^2} - \frac{1}{(2R_1)^2} \right\}$

Both cylinders are machined from FDP quality steel which has a coefficient of linear expansion α of 16×10^{-6} per ^{o}C

$$\therefore \quad K_t = \frac{K_{20}}{(1 + \alpha t)^3} \qquad \text{.....5.19}$$

where t is the amount by which the temperature is above $20^{o}C$,

K_t is the new instrument constant at $(20 + t)^{o}C$

and K_{20} is the constant calculated from dimensions at $20^{o}C$

There will also be a slight change in the gap between the

inner cylinder and the guard rings but this is negligible.

5.3.2 The temperature dependence of the torsional stiffness of the wire has been determined experimentally between 20°C and 150° C. This has been fully described in Appendix E(ii). The rate at which the torsional properties change with temperature has been expressed by the coefficient χ where

$$\left(\frac{I}{\tau^2}\right)_t = \left(\frac{I}{\tau^2}\right)_{20} (1 + \chi t) \qquad \ldots.5.20$$

and the suffixes have the same meaning as in the previous section.

χ was found to be - 1.196 x 10^{-4} per °C for pure tungsten wire. Within the limitations of the experiment the relationship between torsional stiffness and temperature was observed to be perfectly linear.

5.3.3 Effect of non-Hookian behaviour of wire

That this effect exists has been confirmed by observation of the changing torsional behaviour of the wire with amplitude during calibration. The full implication of this effect was only realised in the later stages of the present series of experiments. However, the problem has been dealt with fully in Appendix B(iii) which would suggest that whereas the viscosity may be calculated from

$$\eta = K F \theta t$$

assuming that the wire obeys Hooke's Law, experiment has shown that F is a function of θ. In this case the relationship has been found to be linear so that F can be written

$$F = F_o (1 + k\theta) \qquad \ldots.5.21$$

where F_o is the torsional stiffness at zero deflection of the wire

(i.e. the stiffness given by the torsional pendulum at zero amplitude) and the constant k is found by experiment, θ is in radians.

In the present experiments the correction (at 20°C) is given by $k = -1.40 \times 10^{-2}$ per radian for a wire 9.2 cm in length and 0.0127 mm in diameter at which condition the wire is subject to a direct stress of 25.8 Kgf/cm^2. Numerically, the correction amounts to - 0.23% for a deflection θ of 0.167 radians (i.e. 100 cm on the upper scale). The main bulk of the results had been computed before the correction could be applied to all the deflections observed, however, when this correction was made to a few results there would appear to be an improvement in the absolute accuracy. For instance, the correction to a typical result at 23.20°C amounted to a decrease in the previously observed viscosity of 0.44% and when applied to a result at 47.36°C the correction was a decrease of 0.31% (assuming the same value of k). From the computed smooth curve through the results it would appear that the viscosity at 20°C is 1.0078 CP which is 0.58% higher than the standard value of 1.0020 CP. The application of this correction would therefore go a long way to removing this discrepancy. However, the possibility remains that k is a temperature dependent effect and it is felt that this should be fully investigated before applying a correction to all observations.

5.3.4 Temperature rise in fluid due to shear heating and frictional heat

Although a fairly good temperature stability has been imposed on the viscometer by the thermostatic jacket there remains the possibility of a temperature rise in the test fluid due to the continuous shearing imposed by the rotating cylinder. The amount of this temperature rise depends upon the temperature of the system boundaries, the geometry and speed of the system, fluid properties and time. It is essential to know when this change of temperature becomes significant, in which case an allowance must be made for it.

The rate of energy dissipation by viscous flow is the product of shear stress times the strain rate

$$S \quad \frac{dv}{dr}$$

When the system has operated for a sufficient time, steady state is closely approached and the rate of energy dissipation by viscous flow is equal to the rate of heat conduction to the surroundings. (It is assumed that the thermostat maintains the system boundaries at constant temperature).

The resulting energy balance is given by

$$S \left(\frac{dv}{dr} \right) = \frac{1}{J} \; k \; \frac{d^2t}{dz^2} \qquad \ldots 5.22$$

where J is the mechanical equivalent of heat

k is the thermal conductivity of the material

and z is the distance from the surface of the inner cylinder.

The solution of this equation for parallel plane surfaces

in rectilinear motion for the case of equal boundary temperature is considered here. This solution has been taken from "Viscosity and Flow Measurement" by van Wazer, (135) in which $\bar{T}$, the position average temperature in the gap is given by

$$\bar{T} = T_c + \frac{2 R T_c^2}{3E} \ln \left\{ 1 + \frac{E \eta_c v_c^2}{8 R T_c^2 J k} \right\} \qquad \ldots 5.23$$

where η_c is the viscosity at the boundary temperature T_c and the nominal rate of shear is $\frac{v_c}{R_1 - R_2}$ and where v_c is the linear velocity of the moving boundary = $\Omega_o R_1$ and R is the Universal Gas Constant, E is the activation energy of viscous flow, which for water is not constant due to molecular association. However, the value for E is quoted for water in several texts including that of van Wazer.

To calculate the shear heating effect in water at 20°C at the maximum operating speed of the viscometer the following values have been used.

$E = 4.05 \times 10^3$ cal/gm

$R = 1.986$ cal/gm mole °C

$T_c = 293$°K

$\eta_c = 10^{-2}$ gm/cm.sec

$J = 4.18$ ergs/cal

$k = 816 \times 10^{-7}$ cal/hr °C cm

$= 1.225 \times 10^{-4}$ cal/sec °C cm

Using these figures

$$\frac{E \eta_c v_c^2}{8 R T_c^2 J k} = 4.34 \times 10^{-12}$$

and since $\ln (1 + x) \simeq x$ for this case

$$\bar{T} - T_c = \frac{\eta_c v_c^2}{12 J k}$$

which evaluates to 6.8×10^{-6} °C for the conditions described above.

Thus it can be seen that the shear heating effect is negligible for all practical purposes and is likely to be small compared with frictional heat in the bearings which cannot be readily calculated.

The most serious source of frictional heat is the mechanical face seal in the first viscometer. Although this seal is fairly remote from the test fluid the heat of friction must raise the temperature of the nearby components to some extent, depending upon the pressure being sealed. At low pressure testing this has had no noticeable effect but at high pressures a temperature gradient was set up which increased the temperature indicated by the thermocouple located in the lower guard cylinder. However, due to the temperature gradient the thermocouple is then no longer accurately indicating the fluid temperature, which is slightly further away from the seal. This presented problems in interpreting the high pressure results obtained with the first viscometer, which is discussed more fully in the next chapter. It is expected that the use of a magnetic coupling in the second viscometer will effectively eliminate this particular

problem in future measurements.

5.4 Estimation of overall accuracy

It is expected that the results of measurements made near 20°C should fall within ± 1.7% for 30 ft which was the figure arrived at in the estimation of errors described earlier in this chapter. Since the correction for non-linear behaviour of the wire has not been applied, one may expect the results at 20°C to be slightly high. However, for operation at elevated temperatures there remains a feature of the apparatus which it is felt may have some influence on the results obtained, this being the possible conduction of heat from the viscometer through the legs which support the instrument. Although precautions have been taken to insulate these legs, as can be seen in the assembly drawing, the possibility of conduction remains. The question may be asked as to the necessity for these legs, i.e. why cannot the viscometer pressure vessel stand inside the thermostat without outside contact? The answer is that the legs provide several important functions. The first being that there is a reaction from the hydrostatic thrust on the drive shaft which is trying to push the viscometer away from the thrust race which is mounted independently. This force amounts to about 1000 Kgf at the upper pressures used in the viscometer. Thus the legs have to anchor the viscometer firmly against any tendency to move under this force. Secondly, the levelling of the viscometer is critical if the inner cylinder is to hang in such a way that there is no contact between surrounding components. This has been achieved by placing metal shims beneath the legs

during assembly, a procedure which would be almost impossible if the viscometer stood inside the thermostat, due to inaccessibility. A third reason is that the design of the first viscometer is such that at elevated temperatures the differential expansion between the jacket (copper) and the pressure vessel (stainless steel) can be taken up by a fairly flexible location of the jacket on the legs, (i.e. by 'O' ring seals in this case). A less flexible set-up could cause straining of the flanges through which the seal housing and window penetrate the jacket.

The effect of conduction through the legs can be expected to produce a temperature gradient in the viscometer so that at elevated temperatures the top of the instrument is hotter than the bottom. Thus the mean temperature of the test fluid would be higher than the temperature recorded by the thermocouples in the lower guard cylinder, i.e. one would expect the viscosity recorded to be consistently lower than those of other workers if the temperature gradient is substantial. Should the effect be considerable, then it is thought that the provision of guard heat, possibly in the form of heating tapes wound round the legs, could provide a simple solution to the problem. Alternatively, the placing of thermocouples of some other temperature sensitive device such as a thermistor in closer proximity to the test fluid would lessen the effect of temperature gradients in the instrument. This procedure is feasible in the second viscometer since a greater area of the top cover is free for the provision of thermometer pockets.

It may be concluded that the approach has been to eliminate temperature gradients rather than to allow for them by making a more penetrating investigation. The success of this procedure can only be judged by critical examination of the results obtained.

CHAPTER 6

RESULTS, DISCUSSION OF RESULTS AND CONCLUSIONS

6.1 Measurement of the viscosity of water at stmospheric pressure

The first viscometer was completed in 1965 and some preliminary measurements on the viscosity of air were recorded in the paper included here as Appendix C. At the same time tests were commenced on water which indicated that several modifications needed to be carried out. This included changing the seal on the drive shaft from the one described in Appendix C to the mechanical face seal. Also the silvered mirror attached to the inner cylinder was changed for one of stainless steel after it was discovered that when immersed in hot water the quality of silvered surfaces deteriorated. Tests also indicated that the residual stresses in the coiled tungsten wire used caused some solid friction between the inner cylinder and its surroundings. This was overcome by annealing the wire in hydrogen prior to use, as described in Appendix E(i). These adjustments resulted in a steady improvement in the quality of the results obtained so that during 1966 a number of measurements were made at atmospheric pressure which are included in Table 6.1.

At the same time the calibrating rig was being set up and a number of tests were carried out to determine the effect of temperature on the torsional properties of the wire (see Appendix E(ii)). Other tests on the behaviour of torsion wires had been made prior to this as described in Appendix D.

Further minor difficulties were encountered before results

were obtained at elevated pressures, mainly due to imperfections in one or other of the seals employed. For example, ideally, the window should seal due to the close contact with the retaining ring provided both surfaces are polished to an optical finish. However, this ideal situation only existed at pressures above about 100 Kgf/cm^2. At pressures below this the window tended to leak, not only letting water out but allowing air bubbles in, which caused considerable inconvenience. The mechanical face seals had been provided by the makers with P.T.F.E. 'O' rings which caused a number of seal-failures, mainly due to the fact that when the sealing pressure is removed the 'O' ring retains a semi-permanent "set" in the position taken up at high pressure. This resulted in leaking at lower pressures. All these rings were eventually changed for nitrile or silicone rubber 'O' rings.

At first water was circulated through the thermostat which limited the upper temperature to about 90°C. Later measurements have been made using "Turbotherm - A" heat transfer fluid which has been circulated at temperatures up to 160°C around the calibrating rig jacket and 120°C around the viscometer. Some of the values listed in Table 6.1 were reduced to 1 Kgf/cm^2 by applying a correction to measurements taken at up to 125 Kgf/cm^2 during the high pressure tests. The values for the pressure coefficient of viscosity obtained by Moszynski (42) have been used for calculating this correction.

Nearly all measurements involved observation of the deflection of the inner cylinder, at several speeds, while increasing

and decreasing from the maximum deflection of that particular test. The least squares fit to the speed:deflection data has been used in the calculation giving the viscosity. At all temperatures a correction has been applied for the effect of temperature on the instrument constant K and on the torsional stiffness of the wire F, as described in Chapter 5.

TABLE 6.1

Temperature t °C	η Centipoise	Temperature t °C	η Centipoise
12.53	1.2221	40.65	0.6401
13.22	1.1974	40.68	0.6515
13.24	1.2070	47.36	0.5856
13.64	1.1818	51.56	0.5257
13.74	1.1929	55.68	0.4823
14.12	1.1773	55.95	0.4879
17.29	1.0917	61.38	0.4615
18.50	1.0473	72.68	0.3935
19.30	1.0148	83.01	0.3380
19.64	1.0033	83.89	0.3386
19.70	1.0190	89.73	0.3127
20.42	0.9897	89.81	0.3132
21.87	0.9610	89.85	0.3111
23.20	0.9243	107.92	0.2477
31.99	0.7669	108.01	0.2538
40.26	0.6539	116.56	0.2471
		116.61	0.2344

These results were firstly fitted to equations of the form

$$\eta = A + Bt + Ct^2 + \ldots\ldots \qquad \ldots.6.1$$

up to the 5th order polynomial in t. The best fit of this type was

$$\eta = A + Bt + Ct^2 + Dt^3 + Et^4$$

the standard deviation of experimental points from the equation

0.00740 cP. With higher order equations the standard deviation began to increase.

However, many investigators have studied the dependence of the viscosity of liquids upon temperature and various other relations between viscosity and temperature have been proposed. One of the most widely quoted is the Arrhenius or Andrade (136) equation which in the integrated form may be written

$$\ln \eta = A + \frac{E}{RT} \qquad \text{.....6.2}$$

where A is a constant, R is the gas constant, T the absolute temperature and E is termed the activation energy for viscous flow. Howevever, this equation is not applicable to associated liquids, since E is then a function of temperature and cannot be regarded as a constant in this equation.

Fulcher (137) and Tamman and Hesse (138) derived empirically an equation to describe the temperature dependence of the viscosity of liquids

$$\ln \eta = A' + \frac{B'}{T - T_o} \qquad \text{.....6.3}$$

An equation of similar form has since been developed from the Arrhenius equation by Gutmann and Simmons (139) on the assumption that the activation energy of viscous flow is temperature dependent and described by

$$E = \frac{E_o}{a + \frac{b}{T}} \qquad \text{....6.4}$$

where a and b are constants and E_o is an activation energy for viscous flow which is independent of temperature.

If the results had been fitted directly to an equation of the form 6.3 it would have been necessary, in principle, to solve several sets of three simultaneous equations each arising from experimentally determined values of the viscosity at given temperatures, in order to determine an average value of T_o and the corresponding values of A' and B'.

However, there was a precedent to follow in representing these results. Bruges (89) had used an equation of the form 6.3 which he quotes as

$$\log_{10} \eta = \log_{10} \alpha + \frac{\beta}{(T - T_o)} \qquad \ldots 6.5$$

He correlated other 1 atm. results for water obtaining the following constants (where η is in micropoise)

$$\alpha = 239.4$$

$$\beta = 248.37$$

$$T_o = 140^{\circ}K$$

Bruges (140) had also varied T_o slightly and found that the fit of the equation 6.5 was not greatly affected by this provided α and β were modified to suit. For this reason Bruges' value of T_o has been used to find A' and B' in an equation of the form 6.3 where η is in centipoise

$$\text{i.e. } \eta = A' e^{\frac{B'}{(T - 140)}} \qquad \ldots . 6.6$$

The least squares fit gave

$$A' = 2.38127 \times 10^{-2}$$

$$\text{and} \quad B' = 5.73591 \times 10^{+2}$$

N.B. An equation of the form 6.3 has been used by Barlow, Lamb and Matheson (141) to represent the viscous behaviour of supercooled liquids. Their findings indicate that the value of T_o has some fundamental significance from thermodynamic considerations.

The standard deviation of results from equation 6.6 was 0.00738 cP which is a slight improvement over the fit of the best polynomial equation.

The deviation plot of experimental values from equation 6.6 is shown in Figure 16. It can be seen that this equation fits the results very well, there being no definite trend in the scatter. It can be seen that up to 50°C most results are within about 1% of the smoothed curve. At higher temperatures the scatter has not decreased and therefore expressed as a percentage the deviation is greater. The equation 6.6 was used to obtain viscosity values at 5°C intervals and these have been plotted graphically in Figure 17. Included in this figure are the measurements of Weber (90) and de Haas (103) and the correlation of Bingham and Jackson (84).

From the viscosity values given by equation 6.6 the viscosity relative to the value of 20°C has been calculated and the deviation of other measurements, including those of Thorpe and Rodger (92), Hardy and Cottington (142) and Moszynski (107) have been plotted in Figure 18. It can be seen that from 5°C to 40°C most results agree to ± 0.5% except for Moszynski, who is nearly 1% lower than the smoothed curve at 20°C. At higher temperatures most other values for relative viscosity are greater than obtained in the

present investigation, those of Hardy and Cottington (which are probably the most reliable) being of the order of 1.6% higher at 100°C. Moszynski's experimental result at 85°C is only 0.5% higher than the present work. This has been taken to imply that the absolute accuracy of the instrument at elevated temperatures has been impaired because of a temperature gradient in the instrument due to conduction ofheat through the 'legs'. The possibility of such an occurrence was discussed in section 5.4. The smooth curve gives a value at 20°C of 1.0078 cP which is within 1 standard deviation of the absolute value quoted by Swindells, Coe and Godfrey. The application of the correction suggested in Appendix B(iii) due to the changing torsional stiffness of the wire with deflection would result in the present value at 20°C being in even better agreement with Swindells.

6.2 Measurement of the viscosity of water at elevated pressure

Pressure Kgf/cm^2	50	100	130	150	180	200	230
Temperature °C							
12.65	0.9975	0.9933		0.9905		0.9871	
12.65		0.9938		0.9906		0.9872	
13.74			0.9937		0.9914		0.9885
18.00				0.9960	0.9955	0.9946	

TABLE 6.2 $\frac{\eta_P}{\eta_1}$ measured below 20°C

Pressure Kgf/cm^2	30	50	150	225
Temperature ^{o}C				
55.78		1.0018	1.0067	
55.78		1.0024	1.0060	
89.73		1.0019		1.0141
89.73		1.0015		1.0139
89.73		1.0018		1.0141
107.93	1.0025			1.0189

TABLE 6.3 $\frac{\eta_P}{\eta_1}$ Measured above 20^{o}C

The high pressure results so far obtained are regarded as preliminary in that there has not, so far, been a systematic cover of the whole field. The values recorded in tables 6.2 and 6.3 are mostly the mean of several experimental results. The procedure was to cycle the pressure in the instrument recording the temperature, the tachometer reading and the angular deflection of the inner cylinder for each pressure. Since the temperature was normally changing slightly during this procedure all viscosity values obtained were corrected to a common temperature. The evaluation of results is described more fully in Appendix F(ii). These results have been represented graphically in Figure 19, where the experimental values obtained by other workers are plotted for comparison. It can be seen that the present low temperature results agree with those of Bett and Cappi (48) rather than with Horne and Johnson (52). At higher temperatures the results are in fair agreement with the findings of Moszynski (42). A more

detailed discussion on this finding can be obtained from reference (143)(see Appendix K).

The conclusion to be drawn from the results obtained up to the present may be listed briefly.

1. The results obtained at 1 atm and at temperatures between 12°C and 117°C illustrate the absolute accuracy obtainable from the rotating cylinder viscometer in its present stage of development. The accuracy is expected to be improved considerably as a result of putting into effect certain of the findings of the present investigation. Examples of these being:-

(a) The manufacture of cylinders with greater dimensional accuracy and using air gauging as an inspection technique.

(b) Application of a correction for non-Hookian behaviour of the wire.

(c) The provision of guard heaters around the legs of the viscometer to prevent conduction of heat from the instrument at elevated temperatures.

2. The addition of the second viscometer with several new features will allow not only a greater range of test conditions to be covered but will improve the absolute accuracy of results. The particular featureswhich have a bearing on the present results may be listed:-

(a) The provision of a magnetic coupling to transmit the angular rotation through the pressure vessel means that frictional heating from the rotating seal (experienced

with the first viscometer) is no longer a problem.

(b) The use of a radial optical grating with Moiré fringe counting and fringe interpolation techniques (described in Appendix J), in conjunction with an auto-collimator device for obtaining the null point, will allow the null-method to be used with greater precision.

(c) Preliminary testing of the second viscometer indicates that the inner cylinder is more sensitive to the movement of the torsion head. This improvement is attributed to the use of two suspension wires in the second instrument. Tests on the second instrument have showed no sign of the slight drift of the inner cylinder experienced with the first instrument (discussed in section 5.2.3).

Acknowledgements

The work described in this thesis forms part of a programme of research into the properties of water-substance which is supported by the Central Electricity Generating Board and is being carried out at the Mechanical Engineering Research Annexe, The University of Glasgow.

The author is indebted to Emeritus Professor James Small and Professor R.S. Silver, in whose department he has been privileged to carry out his research and wishes to thank Dr. E.A. Bruges and his other colleagues at the Research Annexe for their assistance. The author also wishes to thank Dr. L. A. Sayce, of the National Engineering Laboratory, for helpful suggestions concerning the application of optical gratings to angular measurement.

It is a pleasure for the author to acknowledge the skill of Mr. W. McKay who has carried out the machining and fabrication of most of the parts used to construct the apparatus described here.

BIBLIOGRAPHY

Chapter 1

Ref.		
1	KESTIN, J. and WHITELAW, J.H.,	Trans. A.S.M.E., J. of Engineering for Power, Jan. 1966, 82.
2	SWINDELLS, COE and GODFREY.	J. Research, N.B.S., V.48 Research Paper No. 2279 (1952).
3	ROSCOE, R and BAINBRIDGE, W.	Proc. Phys. Soc. 1958, LXXII, 585 (1958)
4	KJELLAND-FOSTERUD, E.	Ph.D. Thesis, University of Glasgow, 1958
5	WHITELAW, J.H.	Ph.D. Thesis, University of Glasgow, 1960 also T.R.1 and T.R.3, Mech. Eng. Dept. University of Glasgow, 1960.
6.	RAY, A.K.	Ph.D. Thesis, University of Glasgow, 1963
7	LATTO, B.	Ph.D. Thesis, University of Glasgow, 1964 also T.R.16, Mech.Eng. Dept. University of Glasgow.
8	BEARDEN, J.A.	Phys. Rev. 56, 1023 (1939)
9	LIEBERMANN, L.N.	Phys. Rev. 75, 9, (1949)
10	GRINGRICH, N.S.	Rev. Mod. Phys, 15, 90 (1943)
11	HENSHAW, D.G., HURST, D.G. and POPE, N.K.	Phys. Rev. 92, 1229 (1953)
12	LONDON, F.	Trans. Faraday Soc., 33, 8, (1931)
13	LENNARD-JONES, J.E.	Proc. Phys. Soc, 43, 461 (1931)
14	TEMPERLEY, H.N.V.	Nature 211, 906, August (1966)
15	BARKER, J.A.	Lattice Theories of the Liquid State, Pergamon Press, 1963.
16	EYRING, H., REE, T. and HIRAI, N.	Proc. Nat. Acad. Sci, 44, 683 (1958)
17	EYRING, H. & REE, T	Proc. Nat. Acad. Sci. 47, 1, (1961)

18 FULLER, E.J., REE. T, and EYRING, H. — Proc. Nat. Acad. Sci., 45, 1594 (1959)

19 EYRING, H., — J. Chem. Phys, 4, 283, 1936. Also Glasstone, S., Lander, K.J. and Eyring, H., Theory of Rate Processes, McGraw-Hill, N.Y., 1941.

20 EYRING, H., HENDERSON, D and REE, T. — Progress in Int. Res. on Thermodynamic and Transport Properties, Trans. A.S.M.E., Paper 30, 340 (1962)

21 BERNAL, J.D. and FOWLER, F.J. — J.Chem. Phys. 1933, 1, 515

22 FORSLIND, E. — Proc. 2nd Int. Congress on Rheology, Oxford, 1953 (Butterworth)

23 GRUNBERG, L and NISSAN, A.H. — Trans. Faraday Soc., 45, 125, (1949)

24 FRANK, H.S. and WEN, W.Y. — Discussions of the Faraday Soc, 1957, 24, 133.

25 NEMETHY, G. and SCHERAGA, H.A. — J.Chem. Phys, 36, 12, 3382, June (1962)

CHAPTER 2

26 BARR, G. — "A Monograph ofViscometry", Oxford U.P. (1931)

27 MERRINGTON, A.C. — "Viscometry", published by Edward Arnold & Co., London (1949)

28 DINSDALE, A and MOORE, F. — "Viscosity and its Measurement" Published by The Institute of Physics and the Physical Society (1962)

29 KESTIN, J. — "On the Direct determination of the Viscosity of Gases at High Pressures and Temperatures", Proc. of The 2nd Biennial Gas Dynamic Symposium, Northwestern Univ. Press. (1958)

30 HEATON, H.S. REYNOLDS, W.C. and KAYS, W.M. — Int. J. Heat Mass Transfer, 7, 763 (1964)

31	MOSES, J.Ll.	Proc. Inst. Mech. Engrs. 1965-66, 180, Pt. 3J.
32	PEUBE, J.L.	J. Mécan, 11, 4, December (1963)
33	MOSES, J. Ll.	Ph.D. Thesis, University of Glasgow, (1967)
34	KESTIN, J., and PERSON, L.N.	"Slow oscillations of an infinite disc in a viscous fluid". Brown University Report AF-891/1 (1954)
35	KESTIN, J. and PERSON, L.N.	"Slow oscillations of bodies of revolution in a viscous fluid." Brown University Report AF -891/2 (1954)
36	IWASAKI, H.	Science reports of the Research Institute, Tohoku University, 3, (1951) 247, 6 (1954), 296
37	HOLLIS HALLET, A.C.	Proc. Roy. Soc. A., 210, 404 (1952)
38	MARIENS, P and van PAEMEL.	Appl. Sci. Research, A5, 411, (1955)
39	KESTIN, J. and PERSON, L.N.	"Small oscillations of bodies of revolution in a viscous flow". Proc. of the 9th Int. Congress of Appl. Mech., Brussels (1956)
40	NEWELL, G.F.	Theory of oscillation type viscometers V: disc oscillating between fixed plates. Z.A.M.P., 10, 160 (1959)
41	KESTIN, J. and WANG, H .E.	Corrections for the oscillating disc viscometer. Brown University Report, AFT 891/5 (1955)
42	MOSZYNSKI, J.R.	The viscosity of steam and water at moderate pressures and temperatures. Trans. A.S.M.E., 83C, 111, (1961)
43	KESTIN, J. and WHITELAW, J.H.	The Physics of Fluids, 9, 1966, 1032.
44	KEARSLEY, E.A.	An analysis of an absolute torsional pendulum viscometer. Trans. Soc. of Rheology, 3, 69 (1959)

45	FLOWERS, A.E.	Proc. Am. Soc. Test Mat., 14, 11, 565 (1914)
46	ROSCOE, R.	Viscosity determination by the oscillating vessel method I. Proc. Phys. Soc. 72, 576 (1958)
47	ZEMPLEN	Ann. Physik, 38, 71 (1912)
48	BETT, K.E. and CAPPI, J.B.	Nature, 207, 620 (1965)
49	CAPPI, J.B.	Ph.D. Thesis, The University of London (Imperial College) 1964.
50	STOKES, G.C.	On the effect of the internal friction of fluids on the motion of pendulums. Cambr. Phil. Trans., 9 (1851)
51	OSEEN, C.W.	Arkiv. für mathematik, astronomi och fysik, No. 29 (1910)
52	HORNE, R.A. and JOHNSON, D.S.	J. Phys. Chem., 70, 2182 (1966)
53	TANAKA, K., SASAKI, M., HATTORI, H., KOBAYASHI, Y., HAISHINE, K., SATO, K., and TASHIRO, M.	Viscosity of steam at high pressures and high temperatures. J.S.M.E. Report No. 10 (1963)
54	RIVKIN, S.L. and LEVIN, A. Ya.	Teploenergetika, 13, 4, 79 (1966)

CHAPTER 3

55	MARGULES,	Wien Sitzungsb., 83 (ii), 588 (1881)
56	COUETTE, M.M.	Annales der Chem. et de Phys. 21, p.433 (1890)
57	HATSCHEK, E.	Trans. Faraday Soc. 9, 80 (1913)
58	MacMICHAEL	J. Ind. Eng. Chem., 7 961 (1915)
59	STORMER	Trans. Amer. Ceramic Soc., 11, 597 (1909)
60	GILCHRIST, L.	Phys Rev., 1, 124, (1913)

61	HARRINGTON, E.L.	Phys. Rev., 8, 738 (1916)
62	LEROUX, M.P.	Ann. Physique, 4. 163. (1925)
63	HOUSTON, W.V.	Phys. Rev. 52, 751, (1937)
64	KELLSTROM, G.	Phil. Mag., 23, 313, (1937)
65	KELLSTROM, G.	Die Innere Reibung von Luft in Druckgebiete, Arkiv für Math. Astr. Physik, 27, 1, (1941)
66	THOMAS, B.W., HAM, W.R. and DOW, R.B.	Ind. Engng Chem., 1939, 31, 1267
67	REAMER, H.H., COKELET, G., and SAGE, B.H.	Analyt. Chem. 31, 1422, August (1959)
68	ROSCOE, R.	Brit. J. Appl. Phys. 13, 362, July (1962)
69	SCHLICHTING, H.	"Boundary Layer Theory" (1955), Pergamon Press, London
70	MALLOCK, A.	Phil. Trans., 187A, 41 (1896)
71	TAYLOR, G.I.	Phil. Trans. 223A, 289 (1923)
72	LEWIS, J.W.	Proc. Roy. Soc. A. 117, 388-407
73	MEKSYN, D.	Proc. Roy. Soc. A., 187, 115 (1946)
74	MEKSYN, D.	Proc. Roy. Soc., A., 187, 480 (1946)
75	CHANDRASEKHAR, S.	Mathematika, 1, 5 (1954)
76	CHANDRASEKHAR, S.	Proc. Roy. Soc. A., 246, 301 (1958)
77	DONNELLY, R.J.	Proc. Roy. Soc. A., 246, 312 (1958)
78	WALOWIT, J., TSAO, S. and Di PRIMA, R.C.	Trans. A.S.M.E., J. Appl. Mech. December 1964, 585
79	TAYLOR, G.I.	Proc. Roy. Soc., V 157A, 546 (1936)
80	WENDT, F.	Ingenieur-Archiv, IV, 577, (1933)

81	GOLDSTEIN, S.	"Modern developments in Fluid Dynamics" Vol. I & II, Clarendon Press, Oxford, (1950)
82	SCHLICHTING, H.	Ann. d. Phys, V, 905 (1932)
83	SCHULTZ-GRUNOW, F.	ZAMM, 39, 101 (1959)
84	BINGHAM, E.C. and JACKSON, R.F.	Bull. Bur. Stand., 14, 56 - 86 (SP298, Aug. 1916) (1919)
85	39th Edition	"The Handbook of Physics and Chemistry" Chemical Rubber Publishing Co, Cleveland, Ohio (1957)
86	DORSEY, N.E.	Int. Crit. Tables, 5, 10, (1929)
87	DORSEY, N.E.	"Properties of ordinary water-substance" Reinhold Publishing Corpn. N.Y. (1940)
88	DREW, E.R.	Phys. Rev., 12, 114 (1901)
89	BRUGES, E.A., LATTO, B, and RAY, A.K.	Int. J. Heat Mass Transfer, 9, 465.
90	WEBER, W.	Z. Angew. Phys., 7 (2), 96, (1955)
91	6th Int. Conf. on the Properties of Steam, Supplementary Release on Transport Properties (Nov. 1964) published in Engineer, Lond. 219, (1965)	
92	THORPE, T.E. and RODGER, J.W.	Phil. Trans. A, 185, 443 (1894)
93	KAMPMEYER, P.M.	J. Appl. Phys. 23, 1, January (1952)
94	RONTGEN, W.C.	Annalen der Physik, 22, 510, (1884)
95	WARBURG, E and SACHS, J.	Ann. Phys. 22, 518 (1884)
96	HAUSER, L.	Ann. Phys. (4), 5, 597 (1901)
97	BRIDGMAN, P.W.	Proc. Amer. Acad. Arts Sci. 61, 57 (1926)
98	TAMMAN, G. and RABE, H.	Z. anorg. allgern, chem. 168, 73-85, (1927)

99	LEDERER, E.L.	Koll. Beih, 34, 270-338 (1932)
100	COHEN, R.	Ann. d. Physik (Wied), 45, 666 (1892)
101	SIGWART, K.	Forsch. Gebiete Ingenieurw., 7, 125 (1936)
102	SPEYERER	Zeitschr, V.D.I., No. 273, (1925)
103	de HAAS, M.	Communs Phys. Lab. Univ. Leiden, 12 118 (1894)
104	HAWKINS, G.A. SOLBERG, H.L. and POTTER, A.A.	Trans. A.S.M.E., V.57, 395 (1940)
105	TIMROT, D.L. and KHLOPKINA, A.V.	Experimental investigation of the viscosity of water and steam at high pressures and temperatures. Moscow Thesis by A.V. Khlopkina (1954)
106	SCHMIDT, E and MAYINGER, F.	Techn. Hochschule (Munich) Report, 1961
107	MOSZYNSKI, J.R.	Trans. A.S.M.E., J. Heat Trans. 83 111, (1961)
108	WEBER, W.	Z. Physik, 7, (2), 96 (1955) Also Z. Physik, 15 (4), 342 (1963)
109	DUDZIAK, K.H and FRANCK, E.U.,	Berichte der Bunsengese Uschaft, Band 70, Heft 9/10, 1120 (1966)
110	KESTIN, J. and WANG, H.E.	"The viscosity of five gases" a re-evaluation". Brown Univ. Report AF 891/6 (1956)
111	KESTIN, J. and WANG, H.E.	"The viscosity of superheated steam up to 270°C", Physica, 26, 575 (1960)
112	KESTIN, J and WHITELAW, J.H.	The Physics of Fluids, 9, 5, 1032 (1966)
113	CAW, W.A. and Wylie, R.G.	Nature, 189, 995 (1961)

CHAPTER 4

114	MALITSON, I.H. MURPHY, F.V. and RODNEY, W.S.	J. Optical Soc. of America, 48, 72 (1958)
115	CAHN-SPEYER, P. LAITHWAITE, E.R. and LEZARD, C.V.	Engineers Digest Surveys Nos. 16, 17 and 18 (1964)
116	KOJABASHIAN, C and ROCHARDSON, H.H.	Paper E.4., 3rd Int. Conf. on Fluid Sealing, Cambridge, England, April, (1967)
117	DENNY, D.F.	Wear, 4, 1, 64 (1961)
118	VILIM, P.	Paper B6, 3rd Int. Conf. on Fluid Sealing, Cambridge, England, April (1967)
119	MAYER, E.	Paper E3, Proc. Ist. Int. Conf. Fluid Sealing, B.H.R.A., April, (1961)
120	NAU, B.S.	Paper E5, 3rd Int. Conf. Fluid Sealing, Cambridge, England, April (1967)
121	TUCKER, W.R.	M.Sc. Thesis, University of Glasgow 1963
122	OLDROYD, J.G. STRAWBRIDGE, D.J. and TOMS, B.A.	Proc. Phys. Soc (London), B64, 44 (1951)
123	KUCZYNSKI, G.C.	Nature, 165, April 8th (1950)
124	BENTON, J.R.	Phys. Rev. 12, 100, (1901)
125	KESTIN, J. and MOSZYNSKI, J.R.	Brown University Report No. AF 891/11, Contract AF18(600)1548 (1957)
126	POULTER	Phys. Rev. 35, 297 (1930)
127	NIEMEIER, B.A.	Trans. A.S.M.E., April (1953)
128	BETT, K.E. HAYES, P.F & NEWITT, D.M.	Phil. Trans. V247A, 57, 1954
129	DADSON, R.S.	Symposium on the Transport Properties of Fluids, I.Mech.E. 1957
130	VENART, J.	Ph.D. Thesis, University of Glasgow 1964

CHAPTER 5

131 HARRISON, W.J. Trans. Camb. Phil. Soc. 22, 39 (1913)

132 INGLIS, D.R. Phys. Rev. 56, 1041 (1939)

133 COPLEY, G.J. J. Sci. Instrum. 43, 845 (1966)

134 JOHNSON and NEWALL Trans. A.S.M.E. 75, 301 (1953)

135 Van WAZER, J.R. et al. "Viscosity and Flow Measurement" published by John Wiley & Sons, N.Y. and London.

CHAPTER 6

136 ANDRADE, E.N.da C. Nature, 125, 309 (1930)

137 FULCHER, G.S. J. Amer. Ceram. Soc. 8, 339 (1925)

138 TAMMAN, G and HESSE, W. Z. anorg. Allgem, chem. 156, 245 (1926.

139 GUTMANN, F. and SIMMONS, L.M. J. Appl. Phys. 23, 977 (1952)

140 BRUGES, E.A. Private communication

141 BARLOW, A.J., LAMB, J. and MATHESON, A.J. Proc. Roy. Soc. A292, 322 (1966)

142= HARDY, R.C. and COTTINGTON, R.L. Viscosity of Deuterium Oxide and Water in the range 5° to 125°C. Nat. Bur. of Standards. Research Paper RP1994, 42, June (1949)

143 WONHAM, J. Nature, Vol. 215, 1053, Sept. 2nd (1967)

144 SAUER, R. Unpublished work, Department of Mechanical Engineering, University of Glasgow.

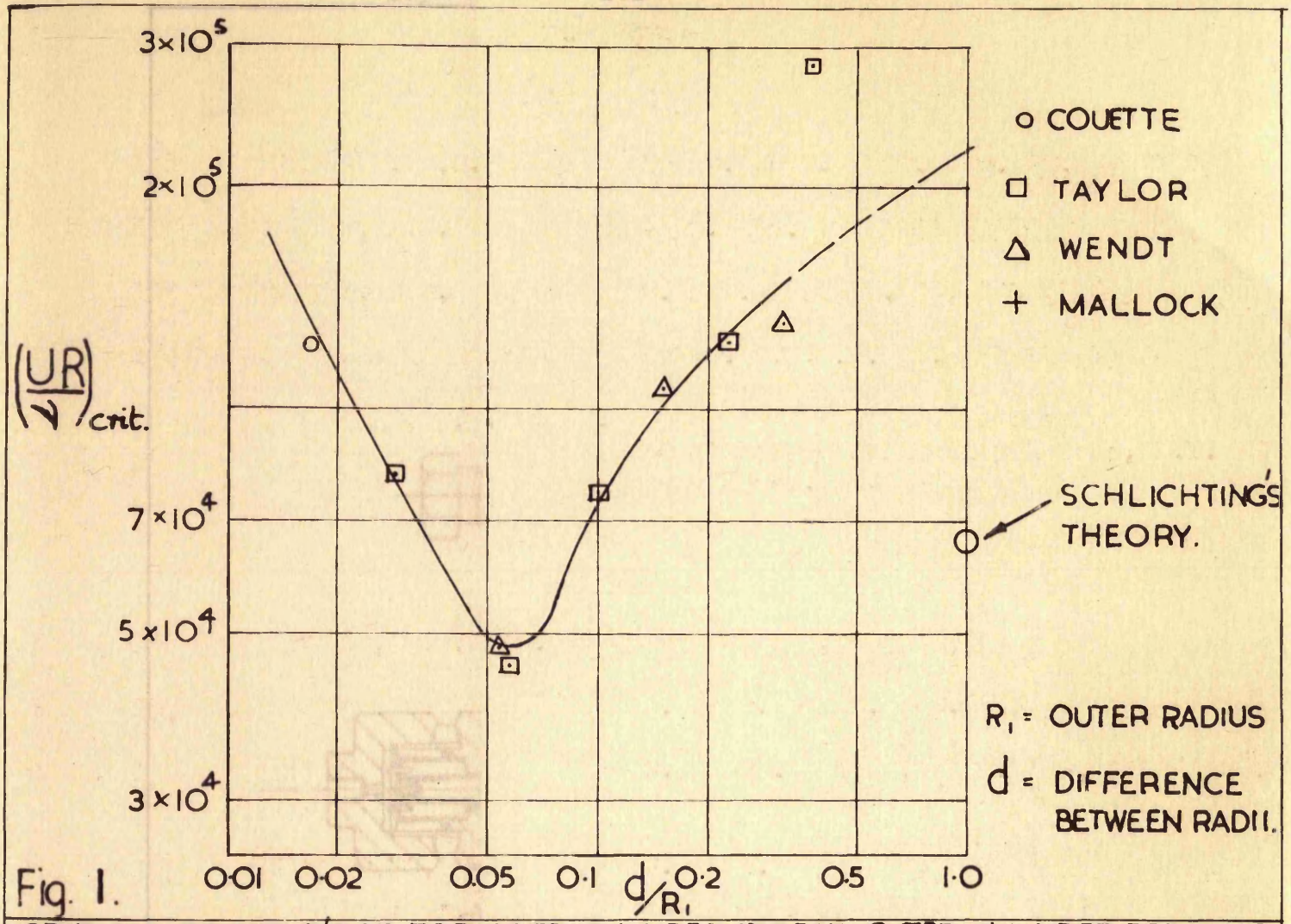

Fig. 1.

CRITICAL REYNOLD'S Nº FOR INNER CYLINDER AT REST OUTER CYLINDER ROTATING.

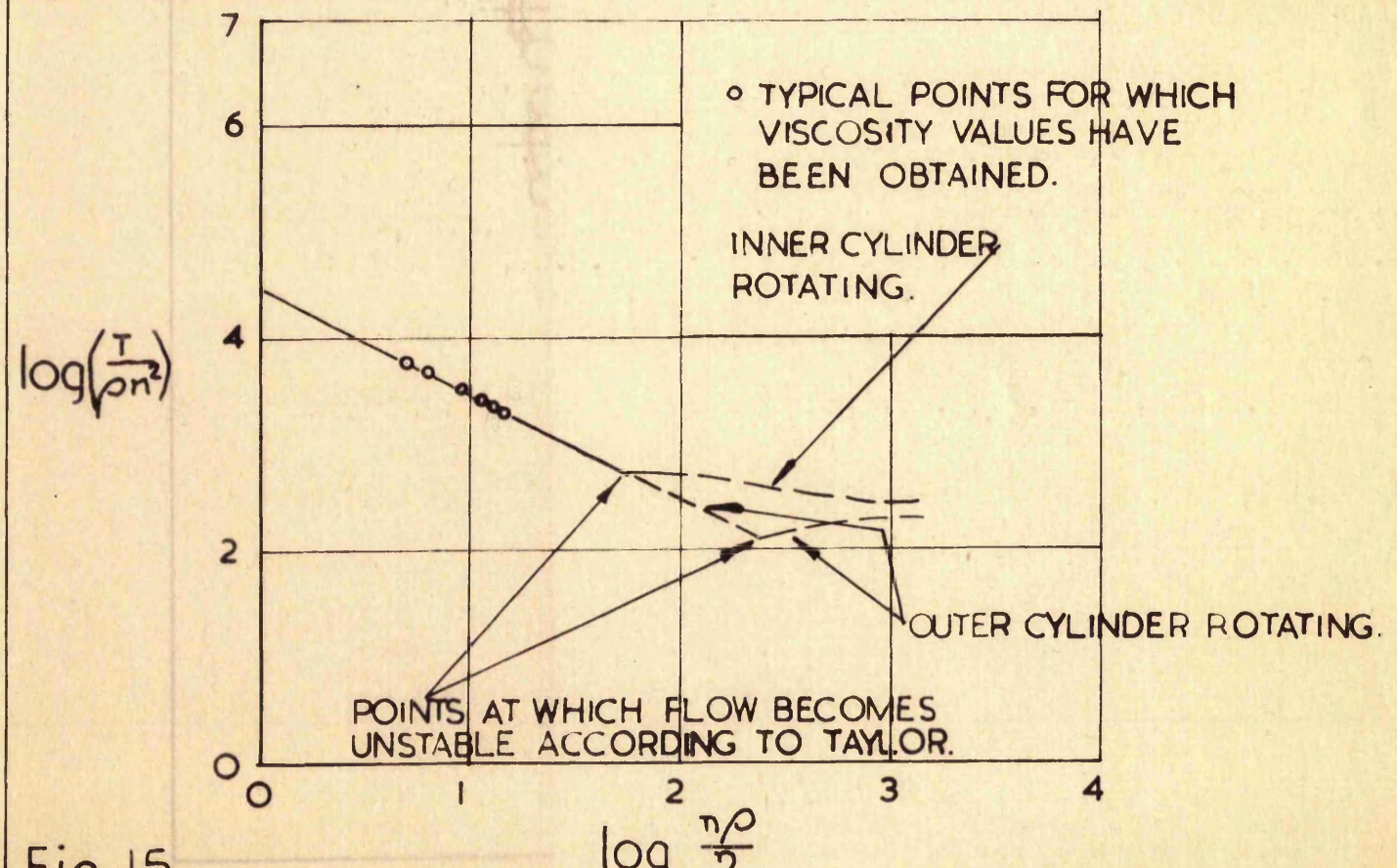

Fig. 15.

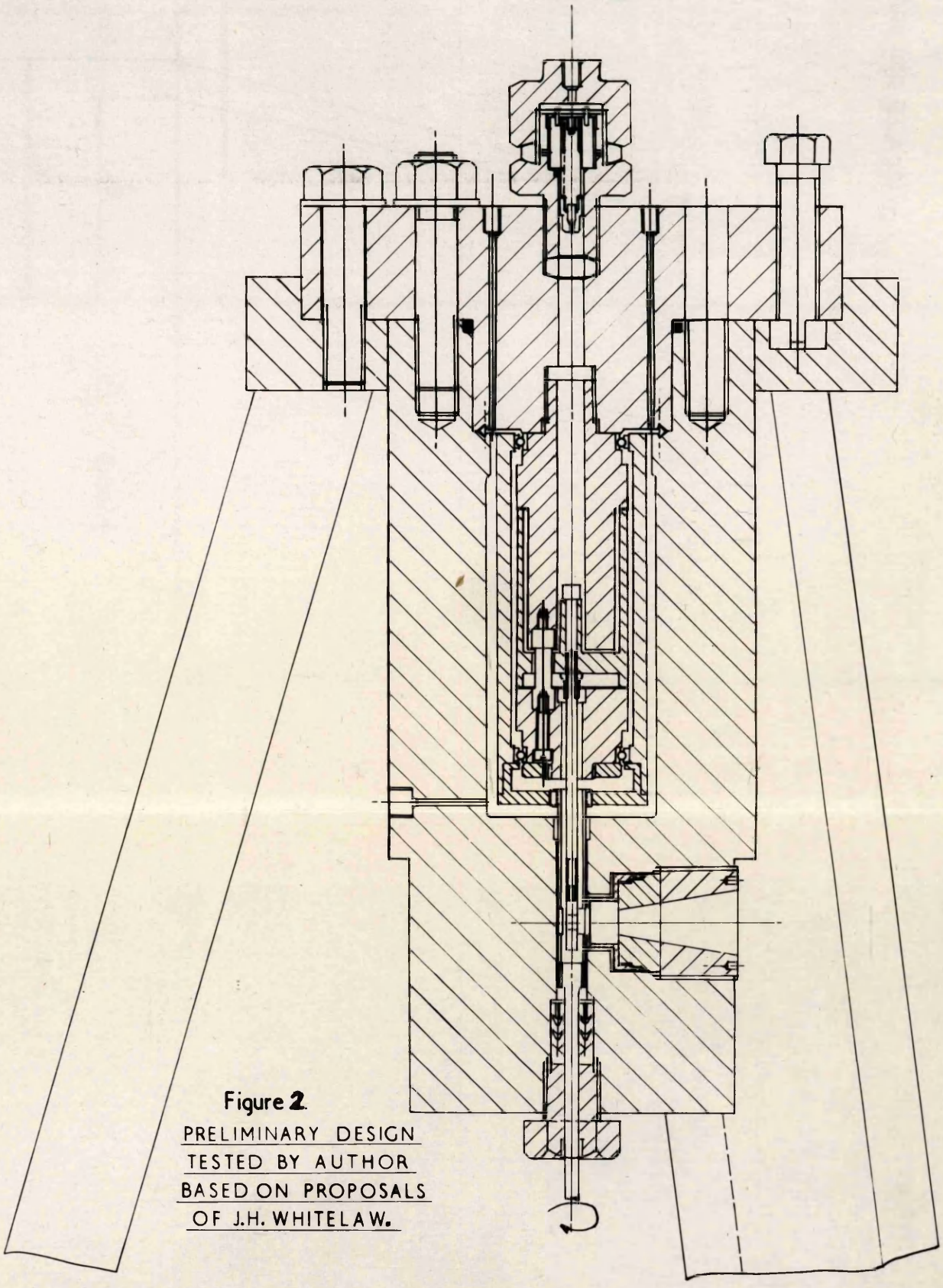

Figure 2.
PRELIMINARY DESIGN
TESTED BY AUTHOR
BASED ON PROPOSALS
OF J.H. WHITELAW.

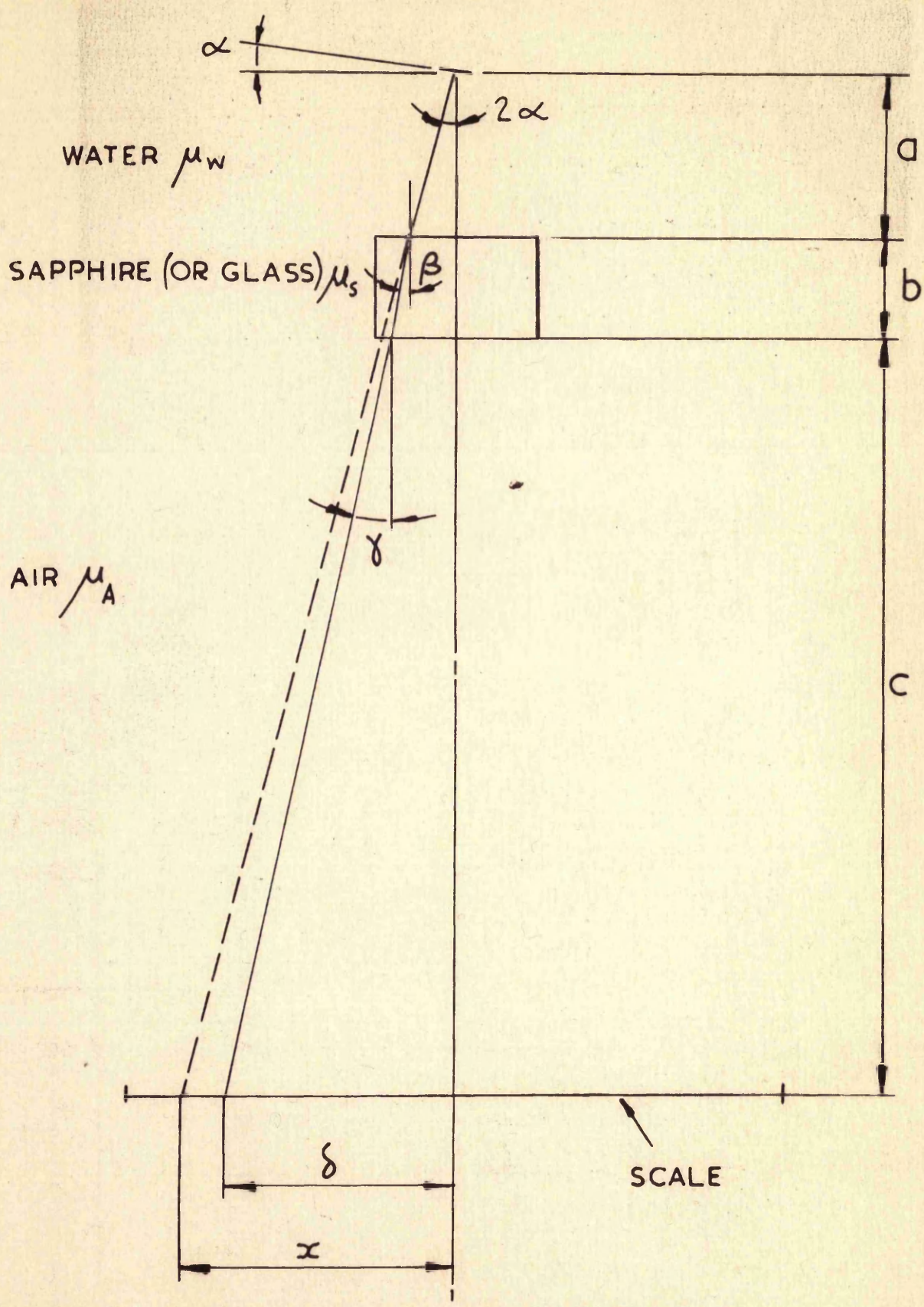

Fig. 3. Effect of refractive index μ
(preliminary design of viscometer.)

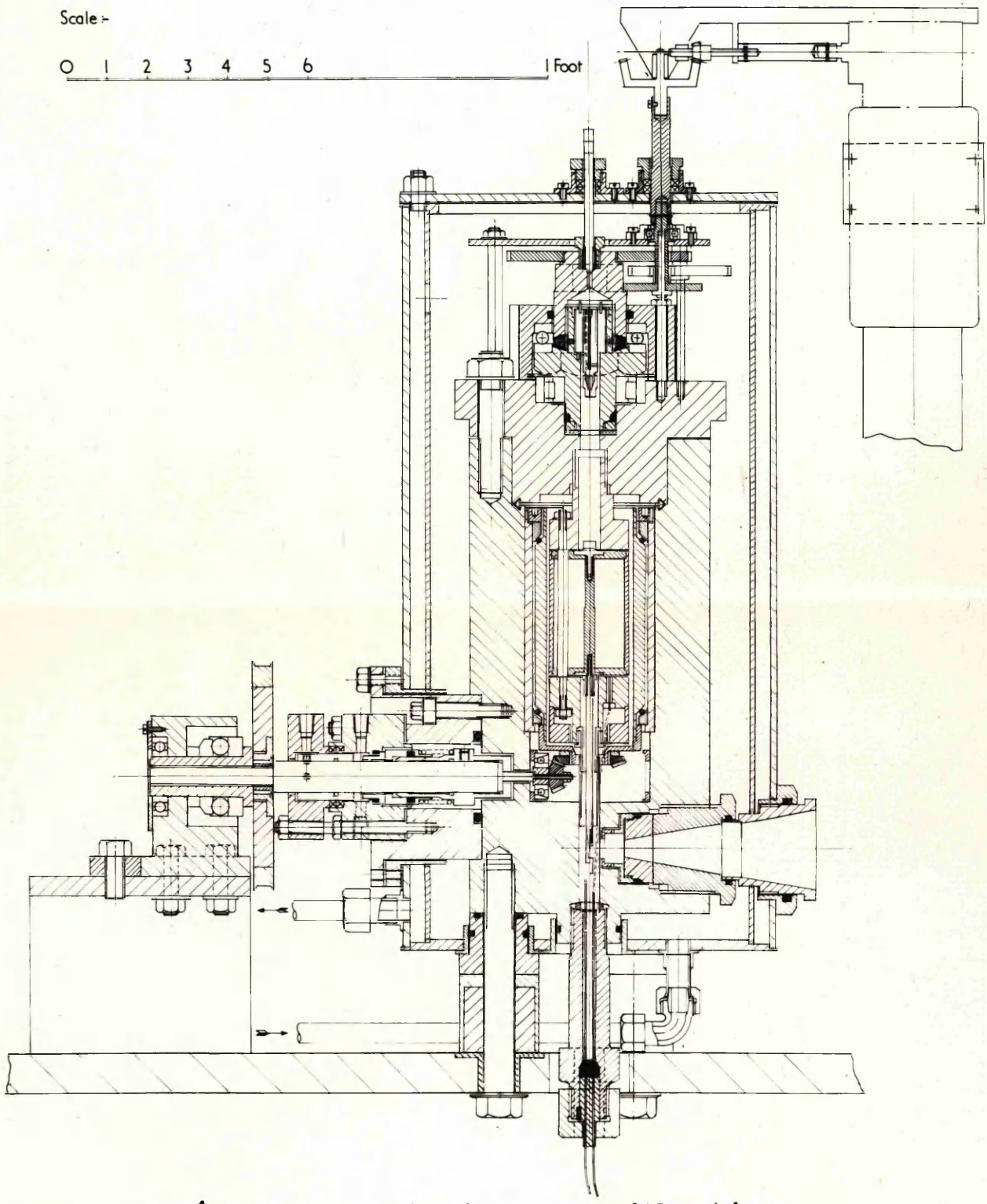

Figure 4. First viscometer - suitable for pressures up to 240 kg/cm²

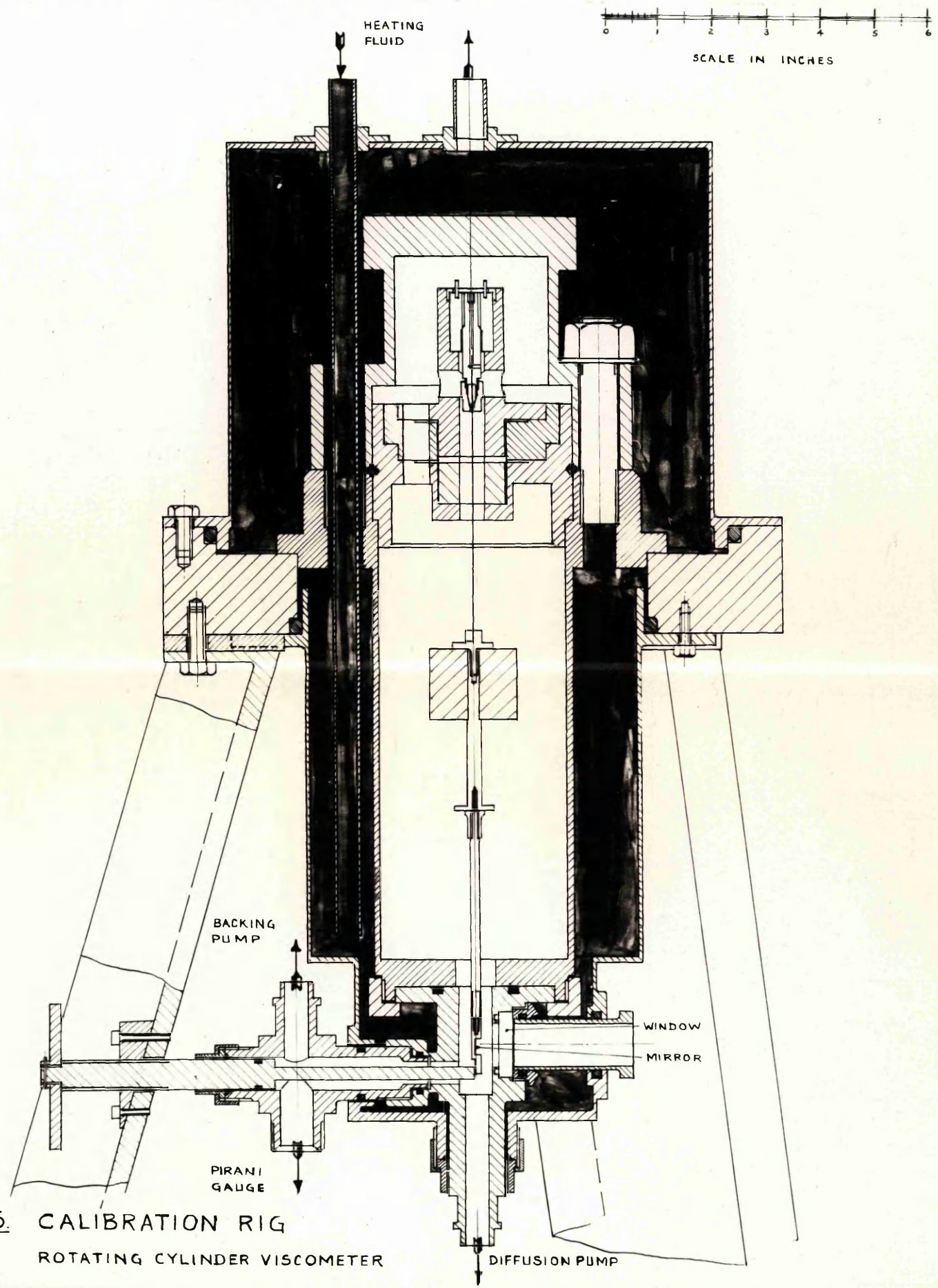

FIG 5. CALIBRATION RIG

ROTATING CYLINDER VISCOMETER

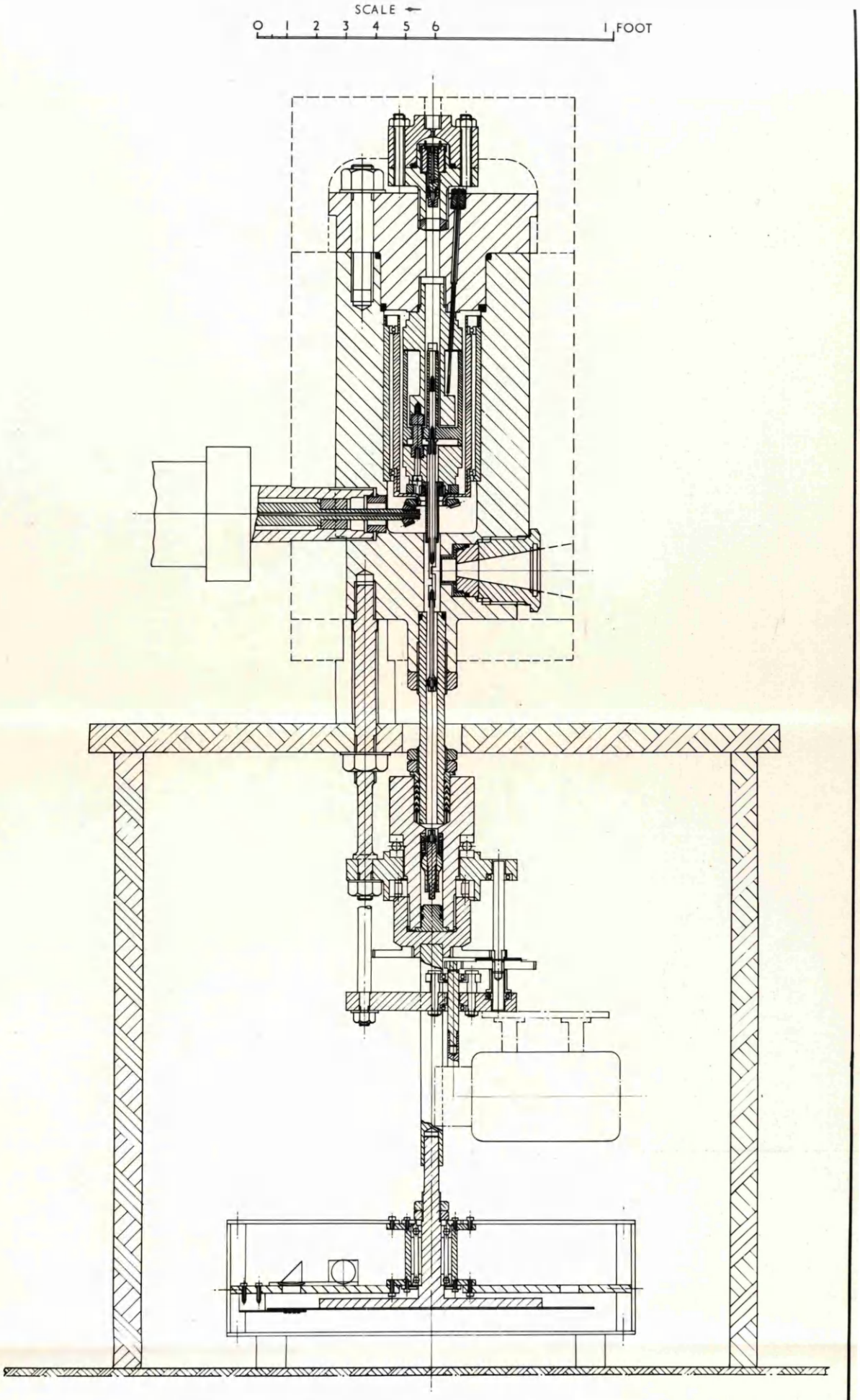

FIG. 6. VISCOMETER FOR MEASUREMENT AT 1000 bar

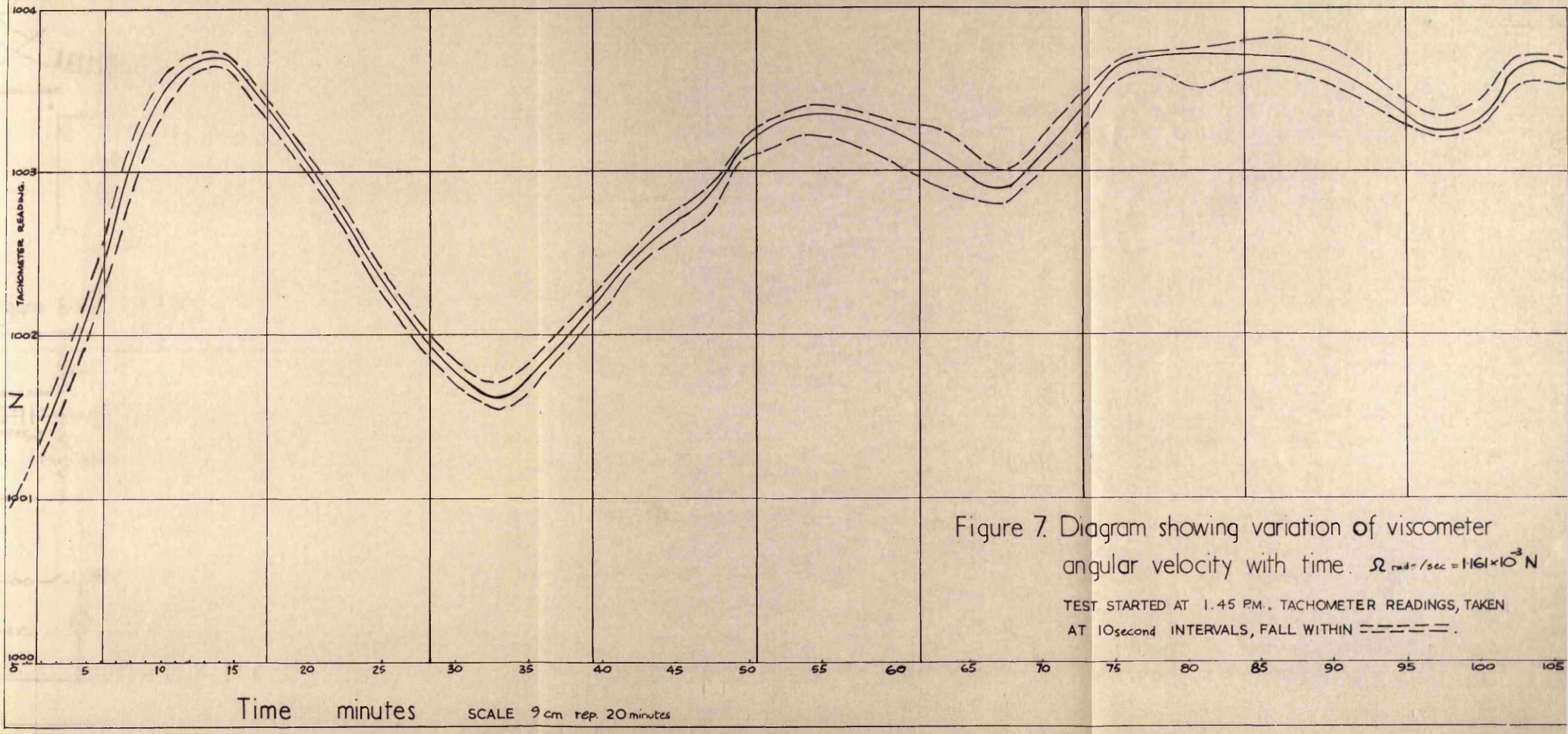

Figure 7. Diagram showing variation of viscometer angular velocity with time. $\Omega_{rad^{-}/sec} = 1.161 \times 10^{-3} N$

TEST STARTED AT 1.45 P.M. TACHOMETER READINGS, TAKEN AT 10second INTERVALS, FALL WITHIN = = = = = = .

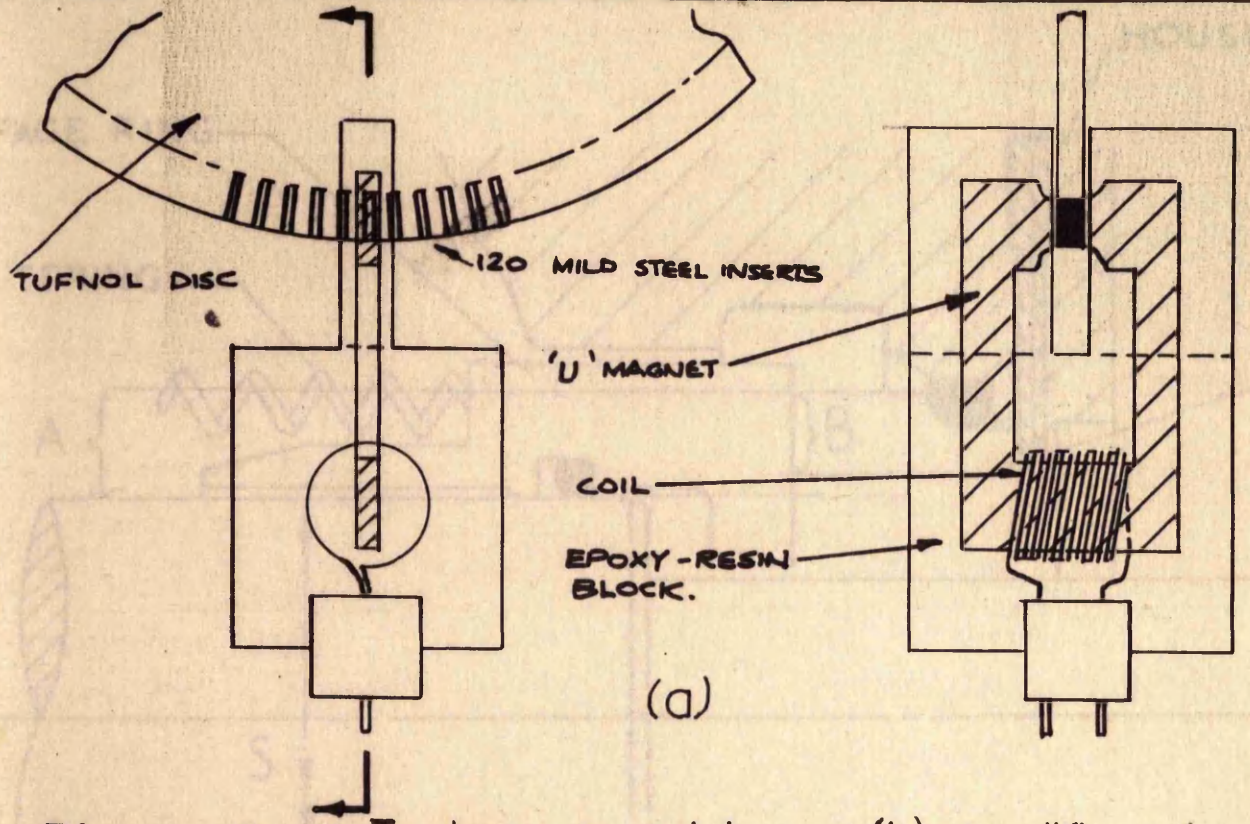

Figure 8. (a) Tachometer pick-up. (b) Amplifier circuit.

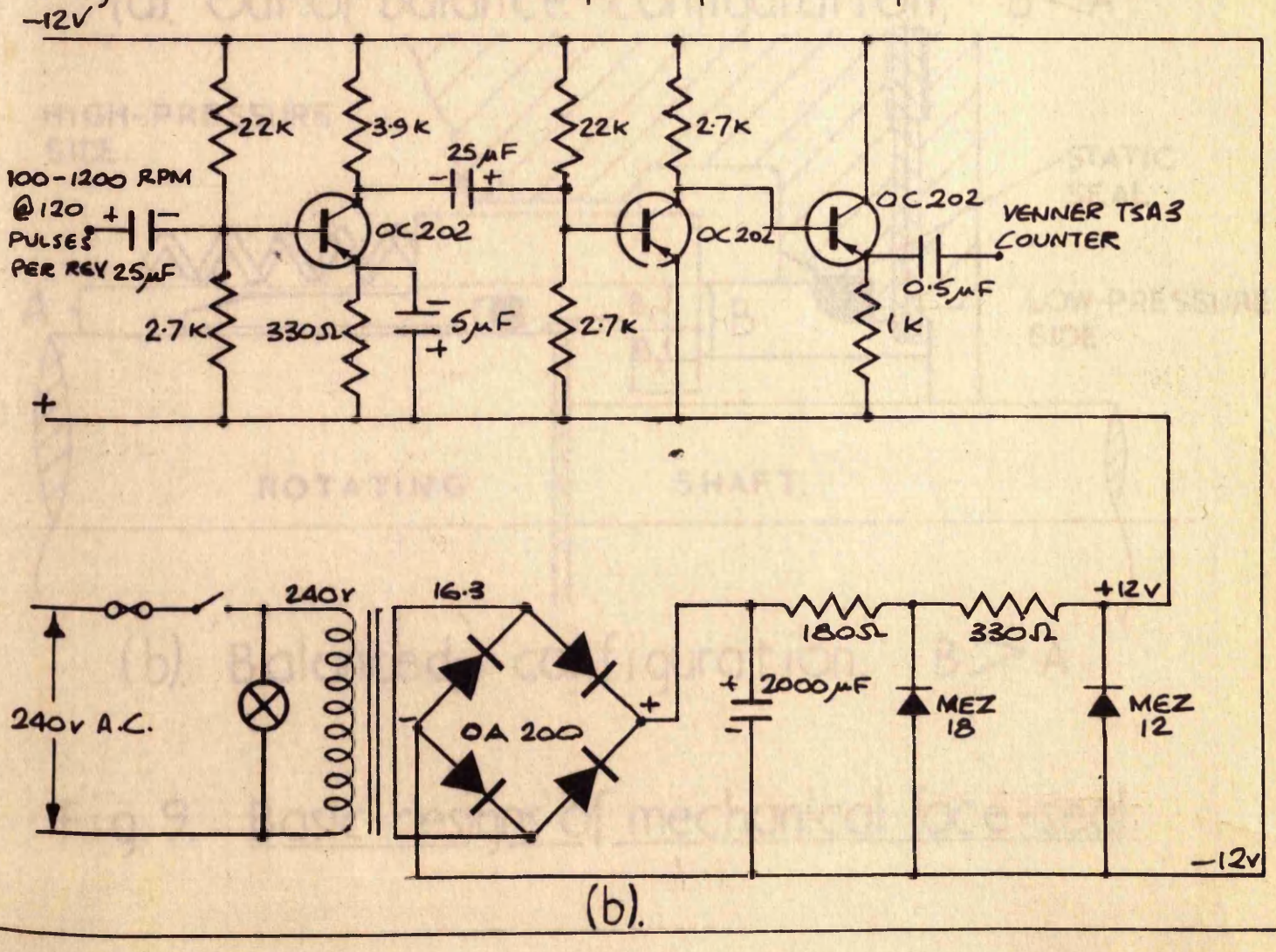

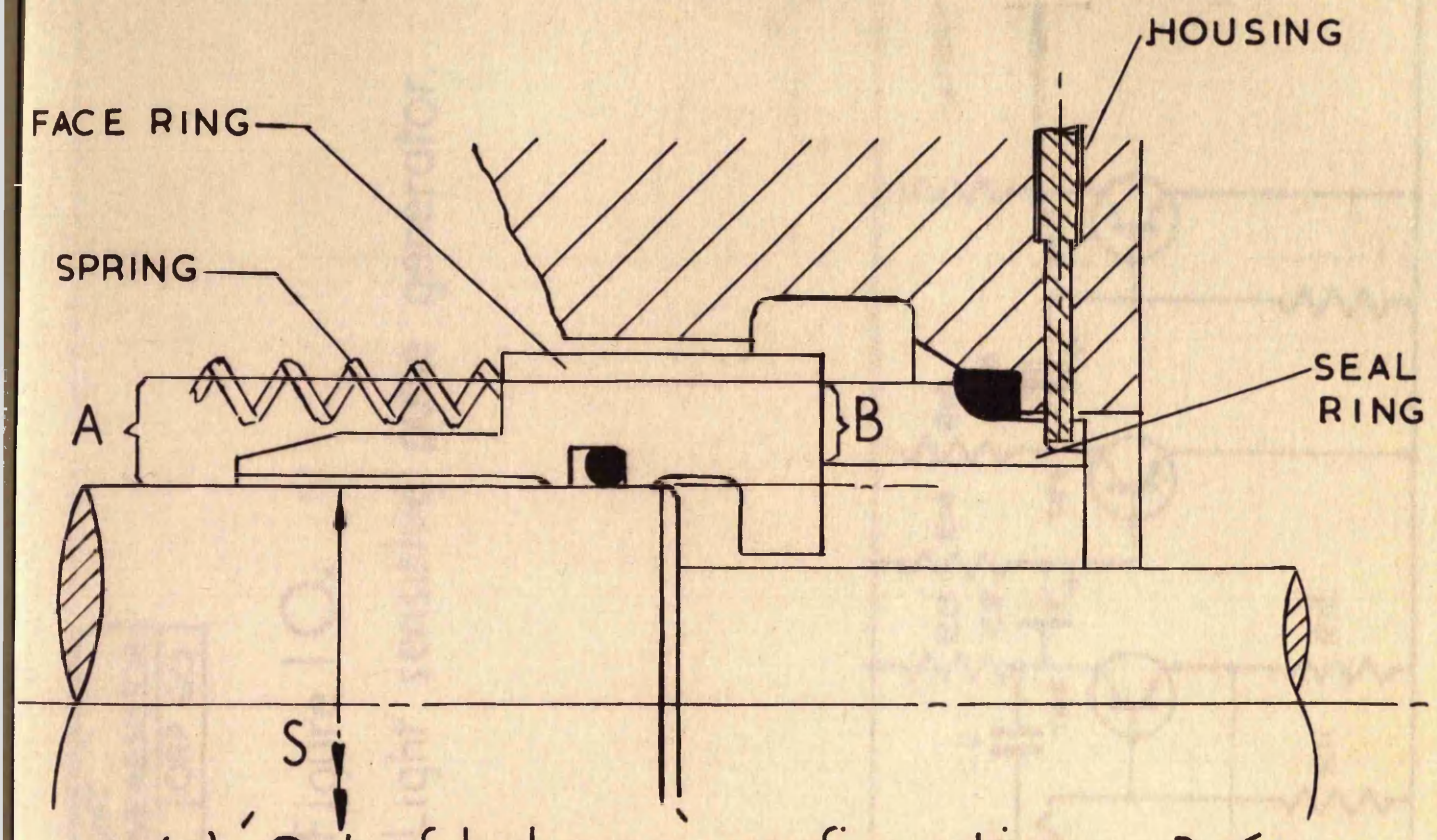

(a). 'Out of balance' configuration, B<A.

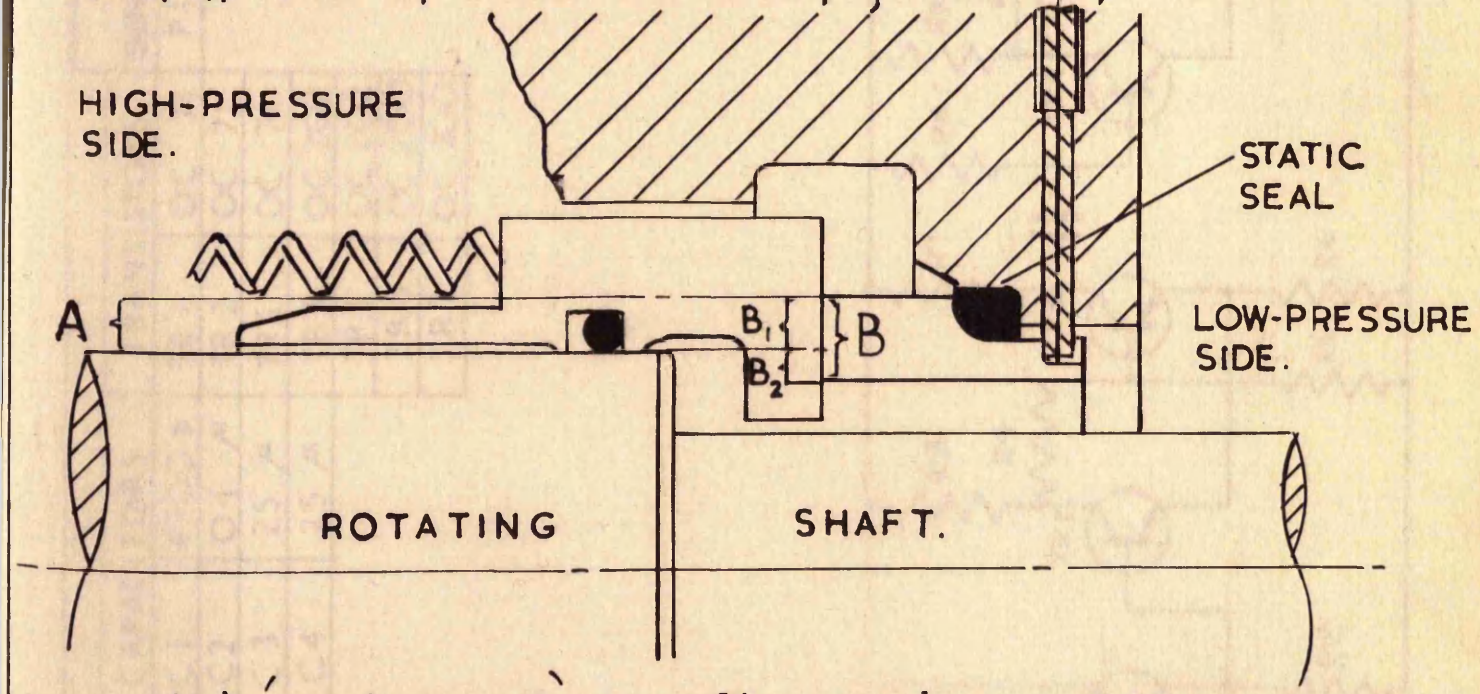

(b). 'Balanced' configuration, B>A.

Fig. 9. Basic designs of mechanical face-seal.

RESISTORS	
R1	33 k
R 2	1·2 k
R 3	4·7 k
R 4	18 k
R 5	6·8 k
R 6	680
R 7	4·7 k
R 8	33 k
R 9	1·5 k
R 10	18 k
R 11	6·8 k
R 12	150
R 13	1·5 k
R 14	18 k
R 15	2·2 k
R 16	10 k
R 17	1 k

CAPACITORS	
C 1	4700 p
C2	0·1 μ
C 3	25 μ
C 4	25 μ

TRANSISTORS	
TR 1	OC 71
TR 2	OC 71
TR3	OC 71
TR 4	OC 202
TR 5	OC 202
TR 6	OC 200
TR 7	OC 200

LIGHT SENSITIVE RESISTOR	
P 1	ORP 60

Figure 10.

Light sensitive pulse generator.

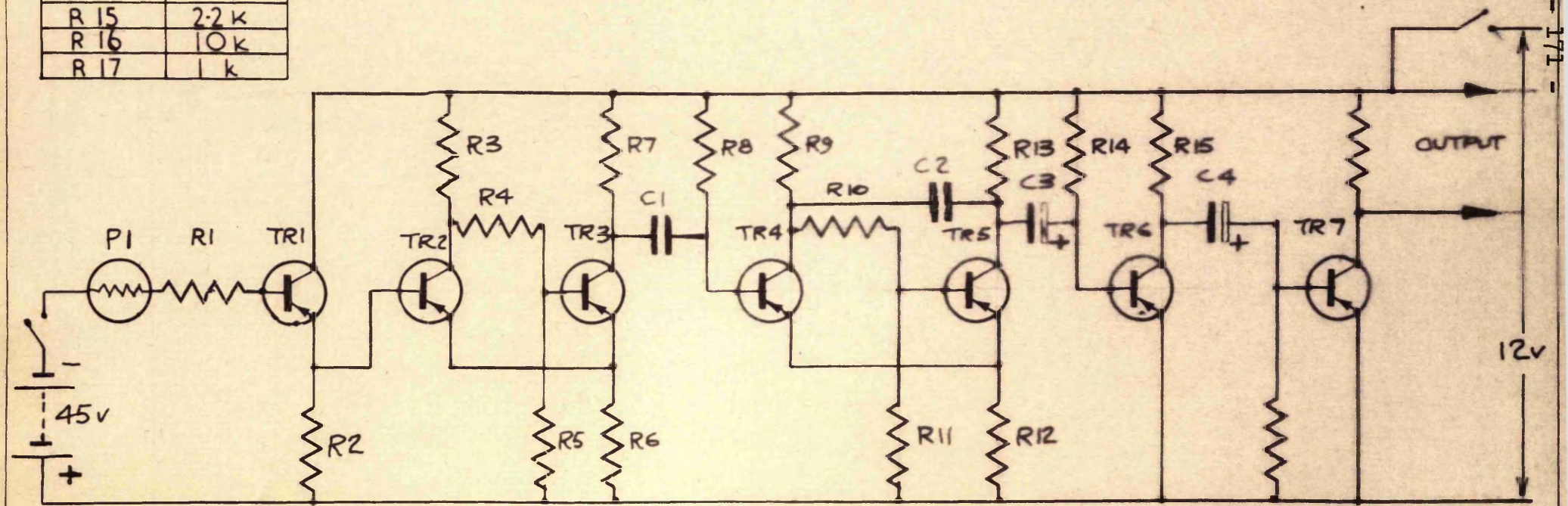

Fig. 11 Diagram of heating circuit for first viscometer.

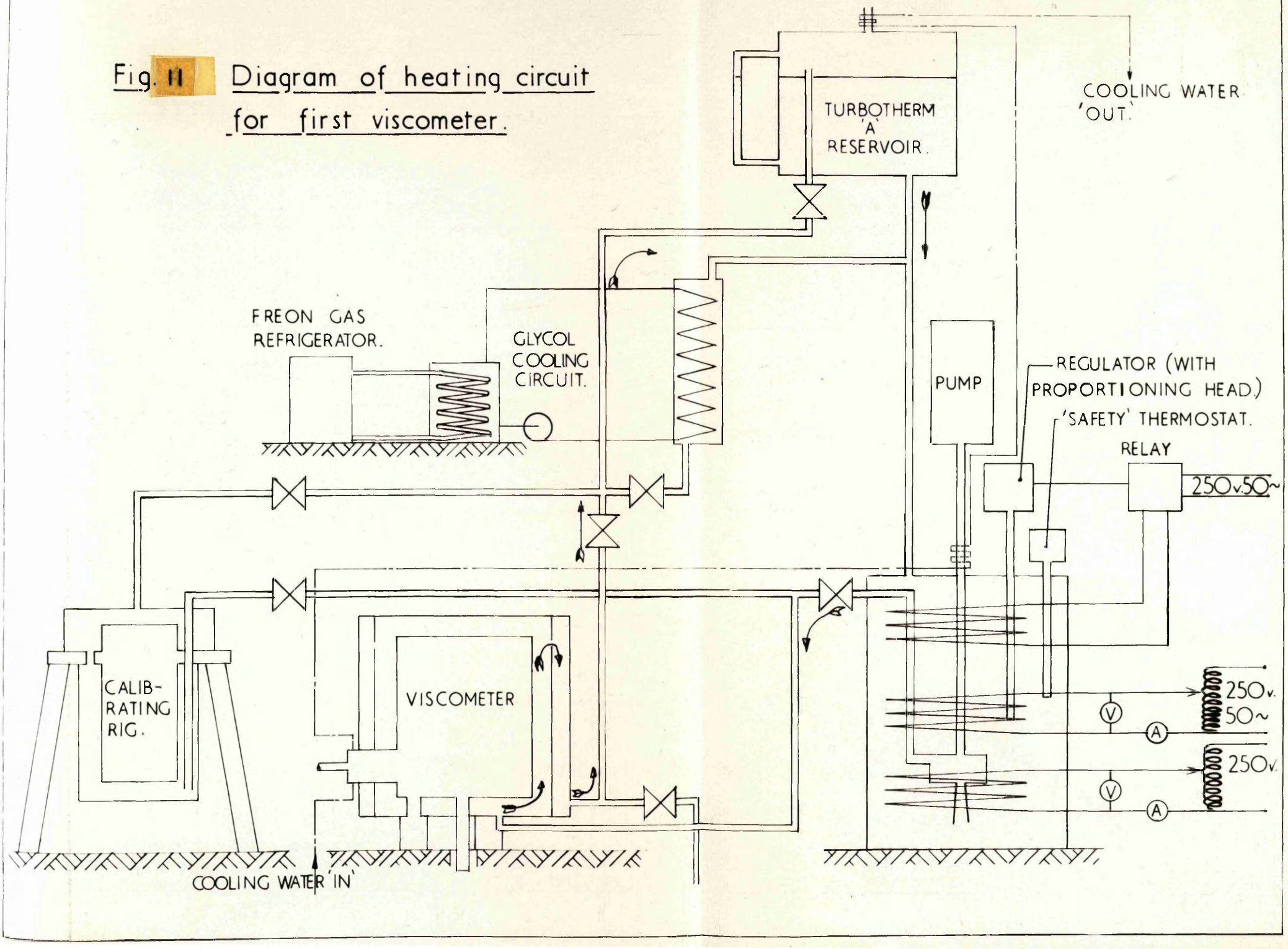

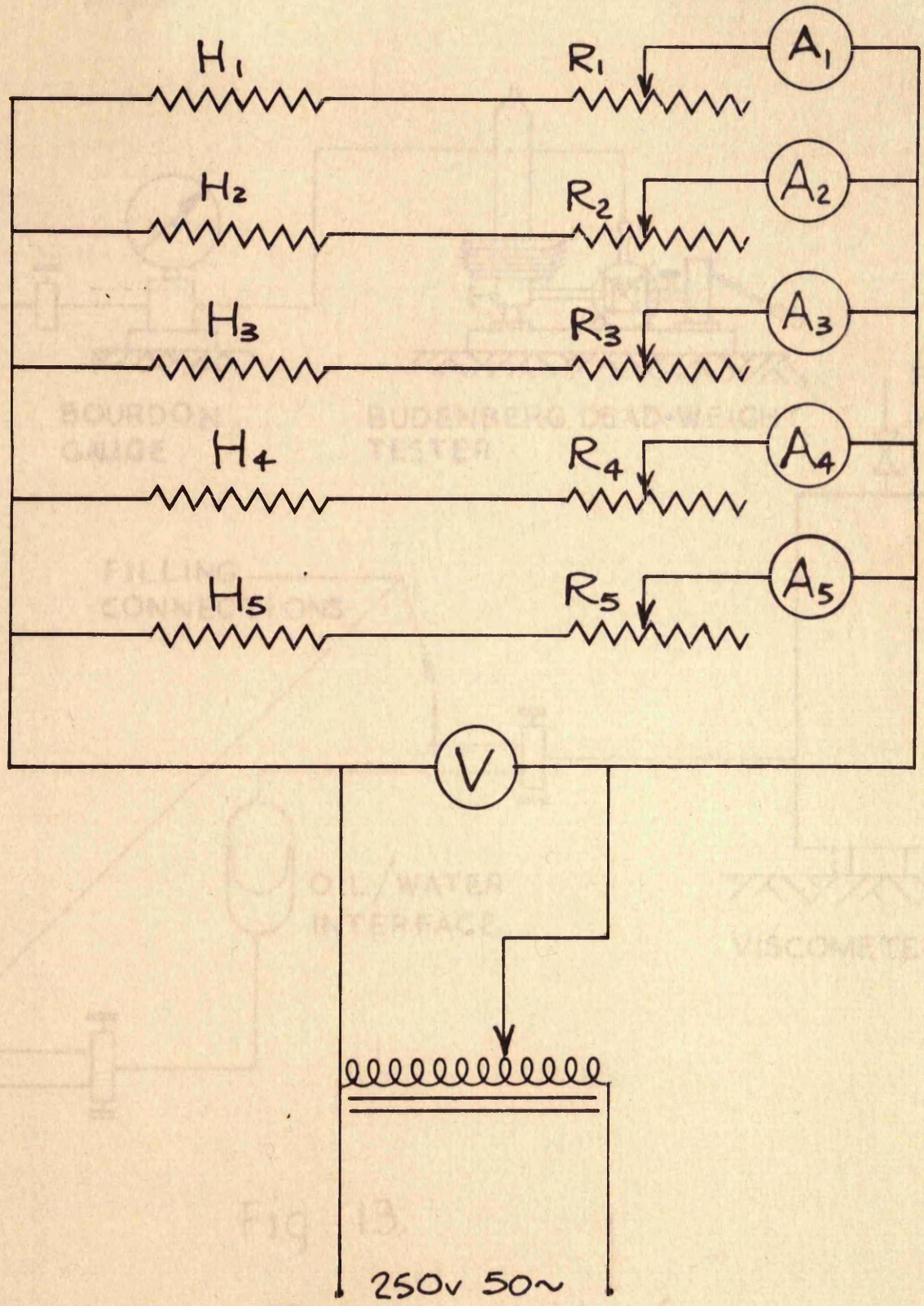

Figure 12. Heating circuit for Second Viscometer.

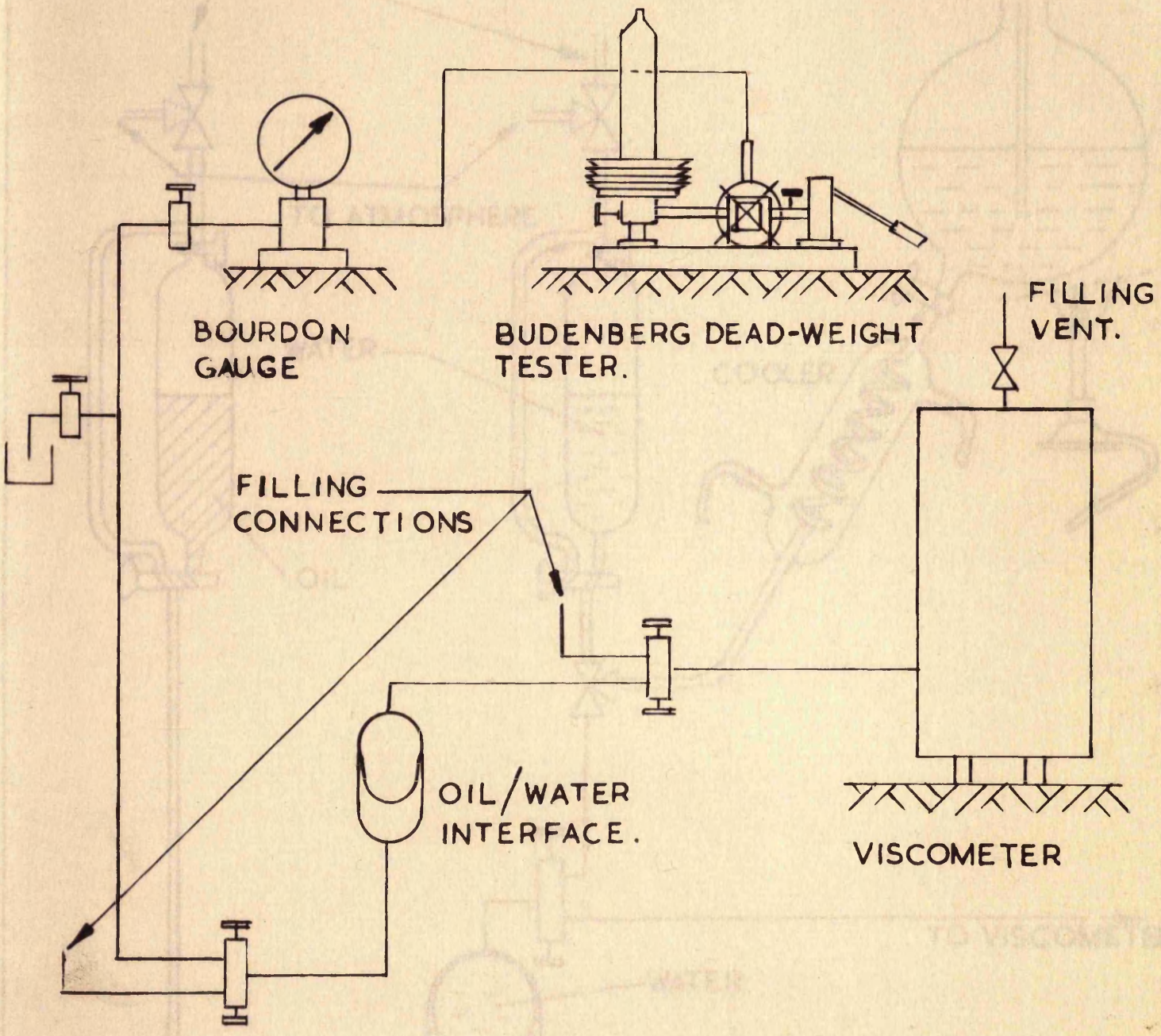

Fig. 13.

Pressure System suitable for 400 kg/cm^2

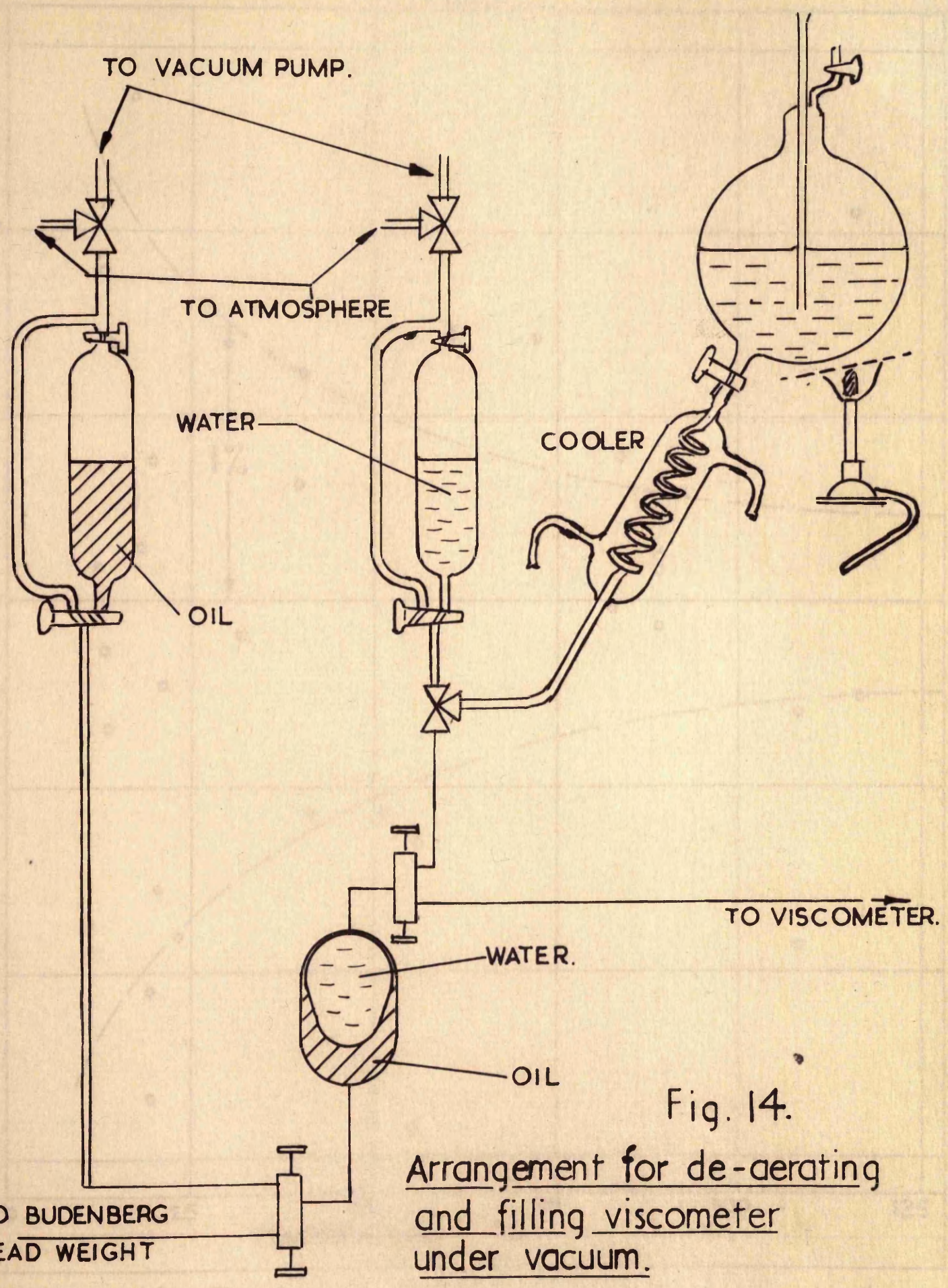

Fig. 14.

Arrangement for de-aerating and filling viscometer under vacuum.

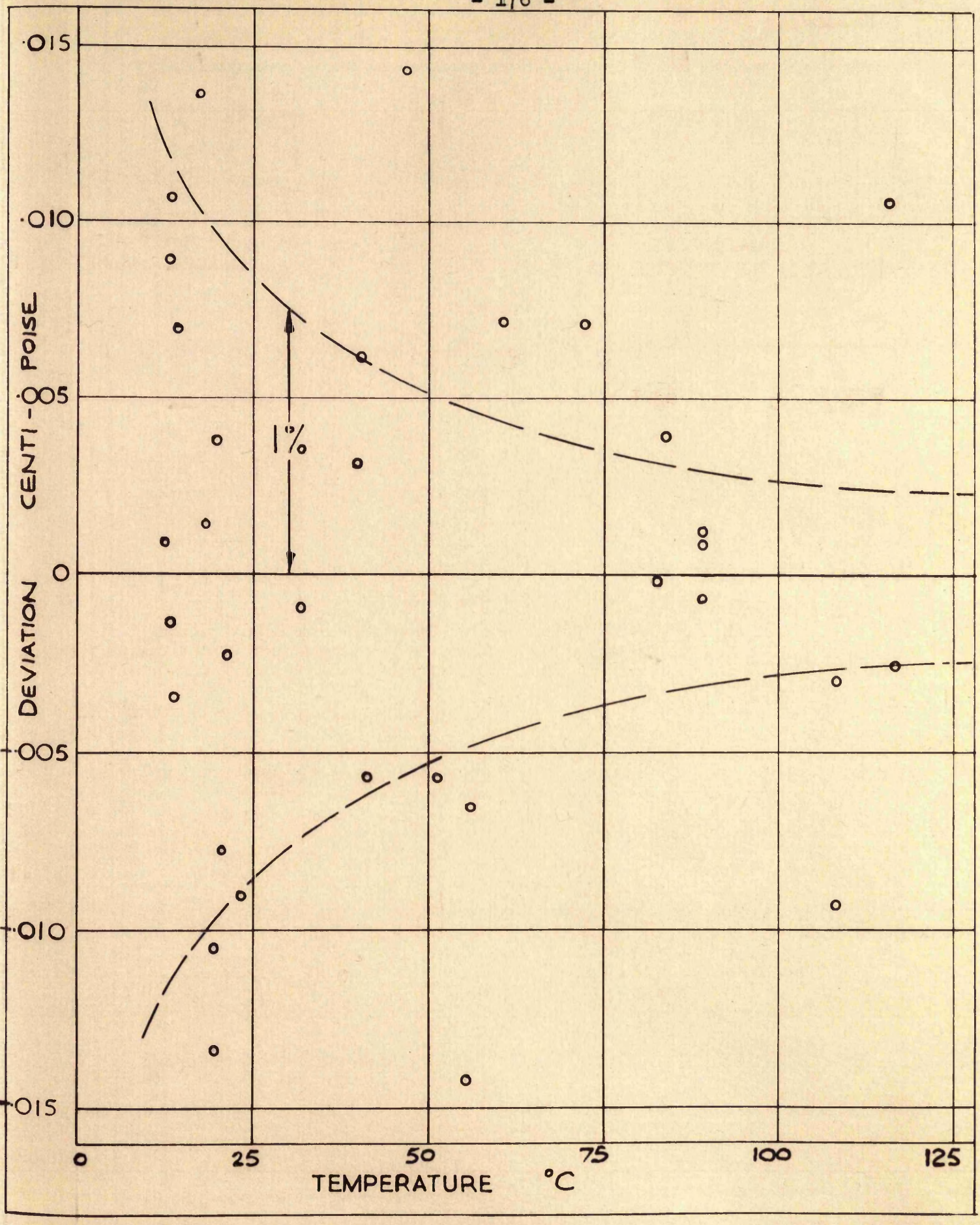

Figure 16. Deviation of experimental points at 1 atm. from smoothed curve.

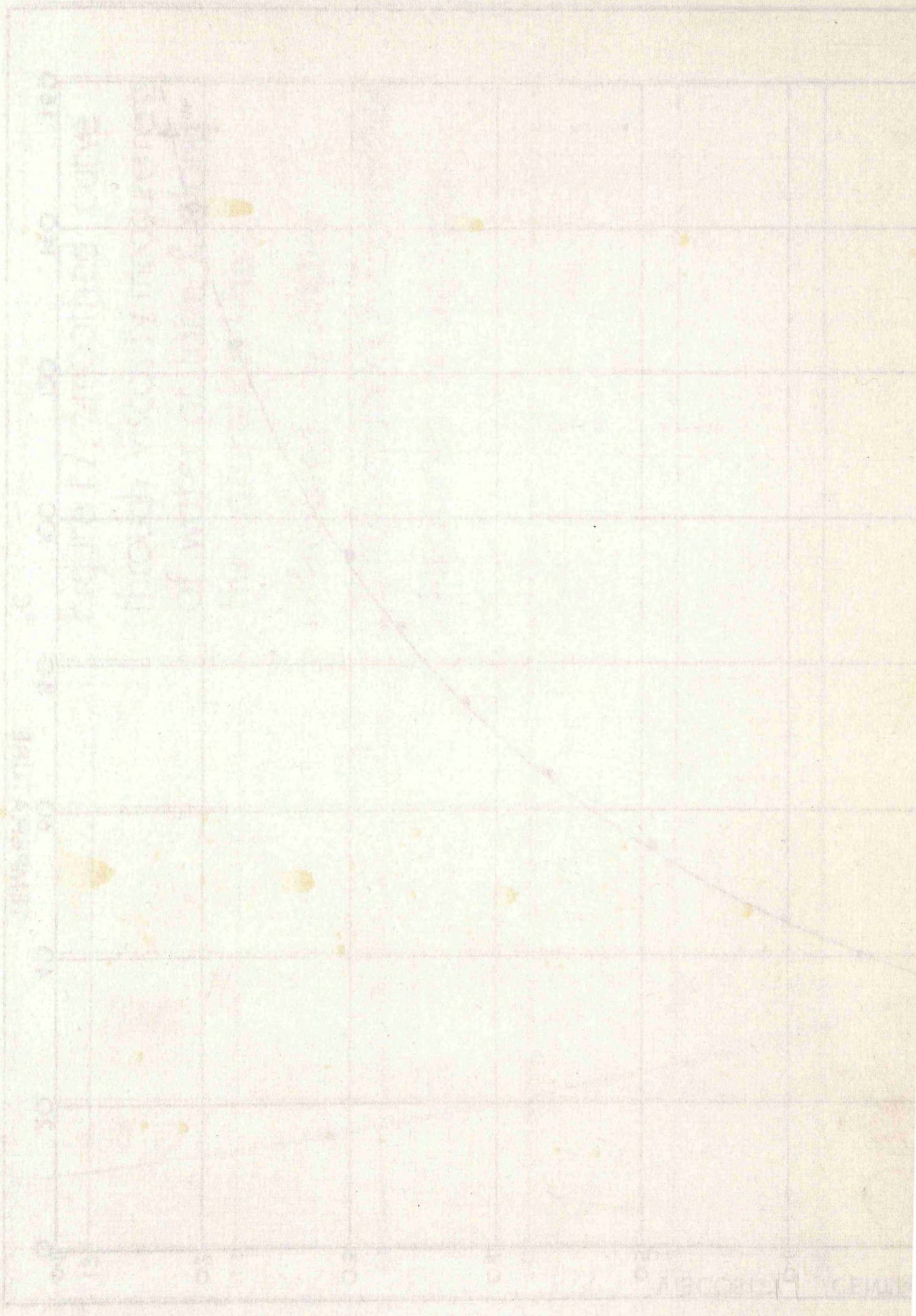

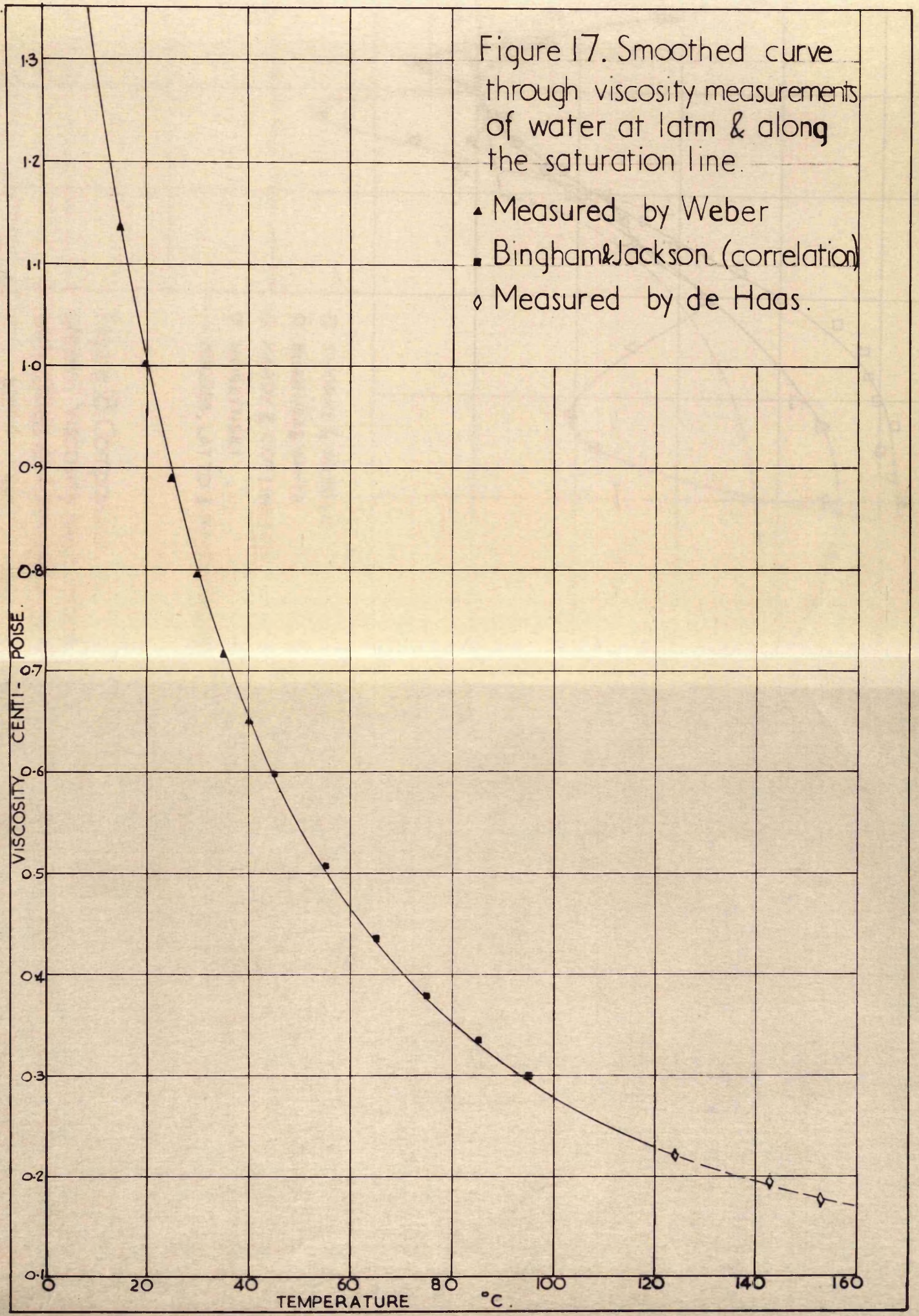
Figure 17. Smoothed curve through viscosity measurements of water at latm & along the saturation line.
▲ Measured by Weber
■ Bingham & Jackson (correlation)
◊ Measured by de Haas.
VISCOSITY CENTI-POISE.
1·3
1·2
1·1
1·0
0·9
0·8
0·7
0·6
0·5
0·4
0·3
0·2
0·1
0
20
40
60
80
100
120
140
160
TEMPERATURE °C.

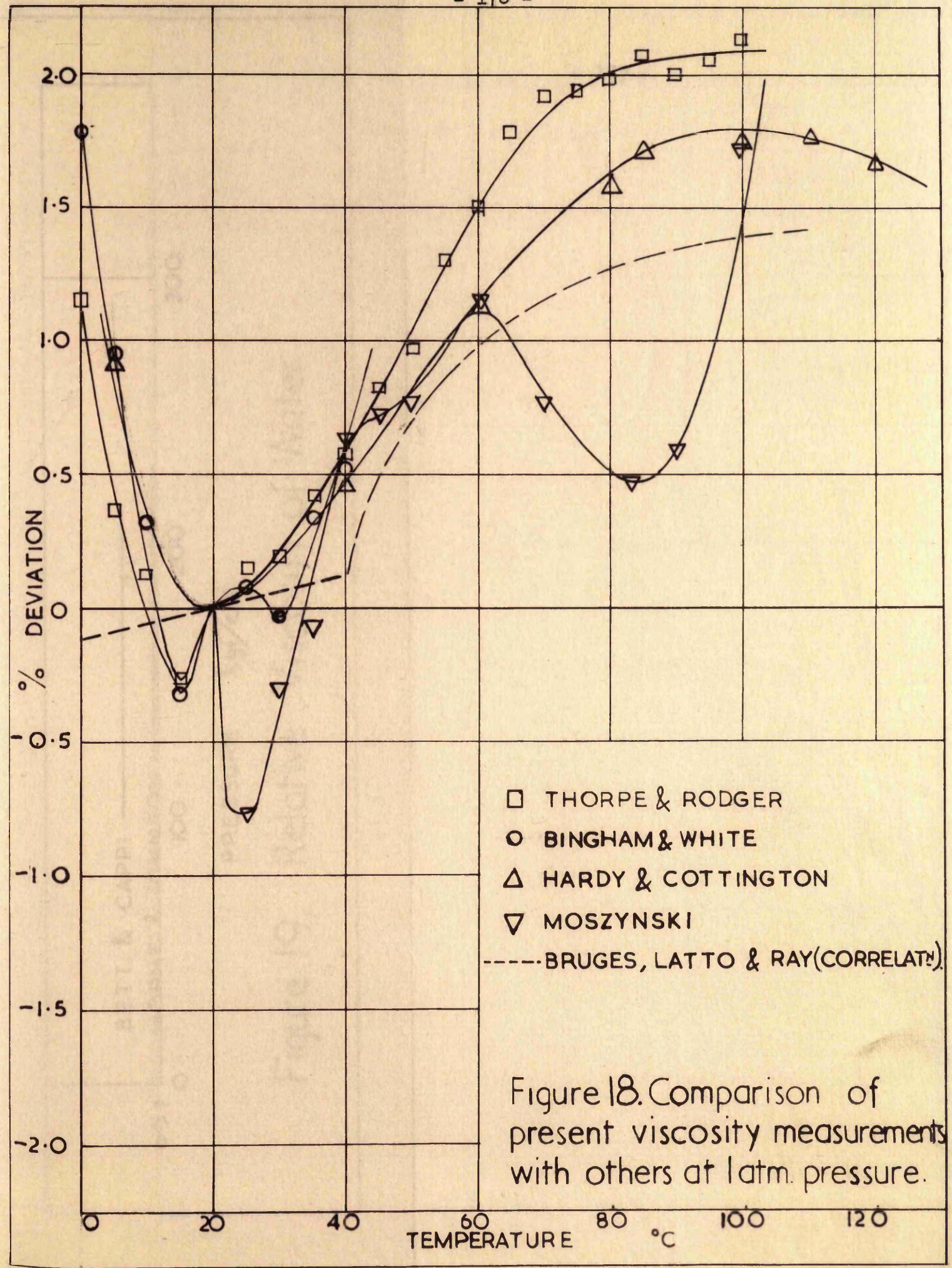

Figure 18. Comparison of present viscosity measurements with others at 1atm. pressure.

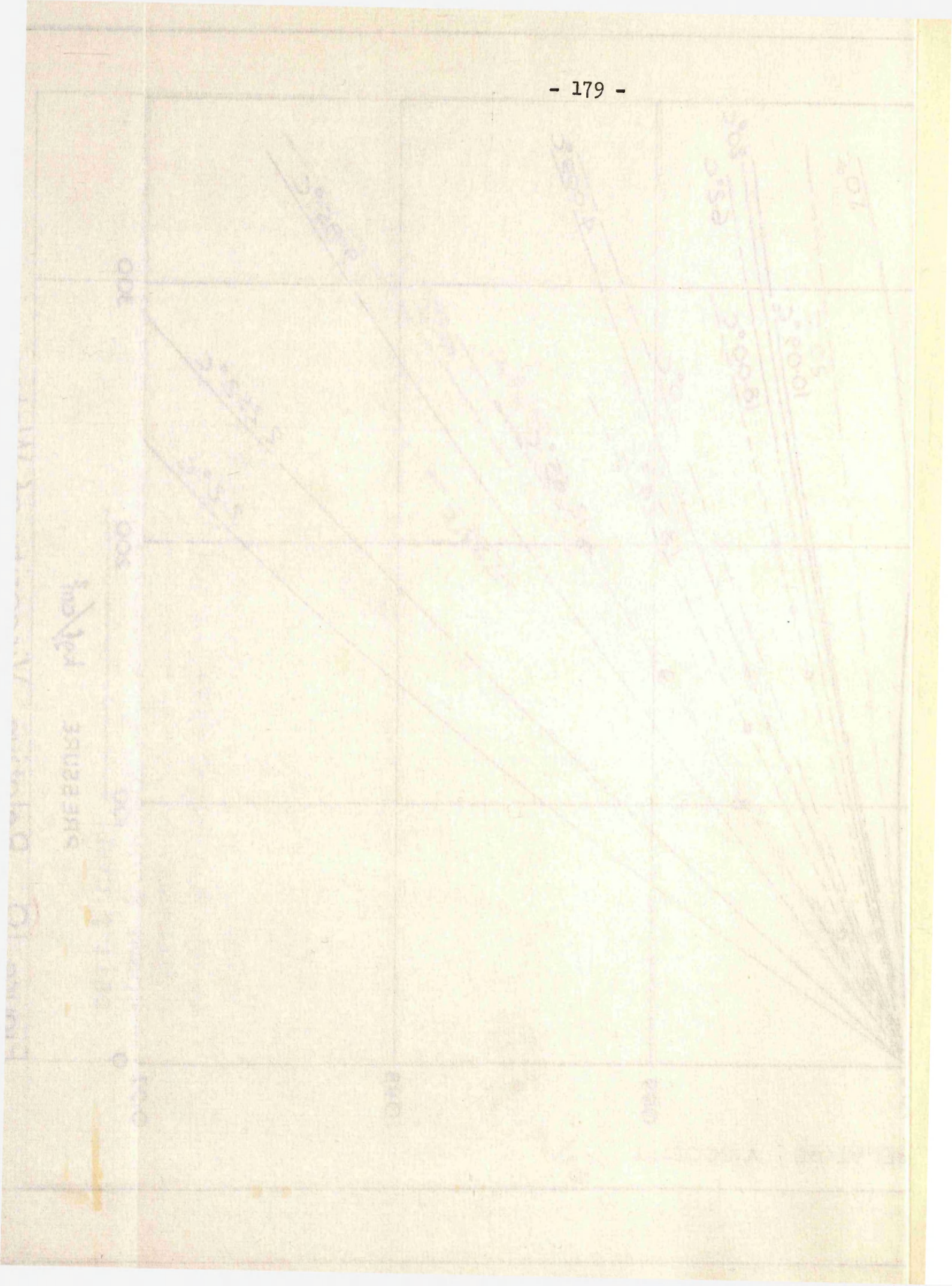

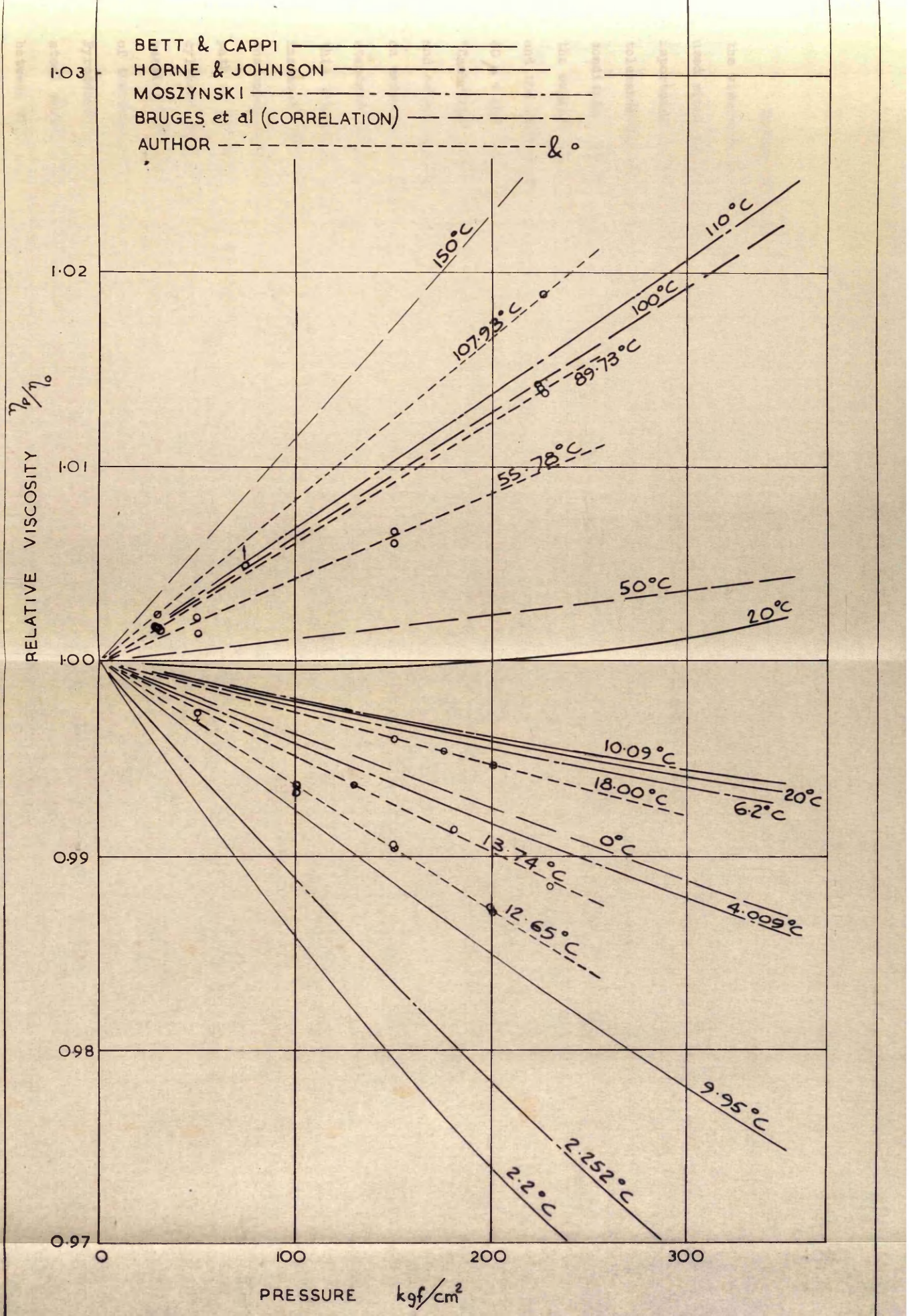

Figure 19. Relative Viscosity of Water.

APPENDIX A

CALIBRATION OF THERMOCOUPLES

During the initial tests with the viscometer to determine the viscosity of air, uncalibrated chromel/alumel thermocouples were used since the general behaviour of the instrument was of greater importance at this stage than absolute accuracy. The recommended tolerance for these thermocouples was ± 3°C in the uncalibrated condition. At this period of the development of the viscometer the expense of precious metal thermocouples did not seem justifiable and the favourable emf generated by Cr/Al thermocouples (approximately 40 μv per °C) made it possible to continue using an available "Cambridge" vernier potentiometer with direct reading to 1 μv and other standard laboratory equipment. Before commencing the tests on water it was decided to calibrate these thermocouples against a standard platinum resistance thermometer since, in many respects, this type of instrument was ideally suited for the purpose. For instance, the points at which the temperature is measured i.e. along the upper surface of the lower guard cylinder, requires that the path of the thermocouple leads is through the bottom of the rotating cylinder and between the mirror stem and the pressure vessel before passing out through the seal at the bottom. The most suitable form of thermocouple was considered to be that produced by Messrs. Pyrotenax in which the two conductors are contained in a stainless steel sheath with magnesium oxide powder acting as an insulator, between wires and sheath. The outside diameter of the sheath is only 0.021 in. and the fact that the wires were sheathed allowed the

thermocouples to follow the fairly complicated path, by suitably manipulating the sheath, without danger of the wires becoming tangled with the cylinders.

It was discovered during the calibration, however, that the peculiar construction of this type of thermocouple assembly gave rise to inaccuracies. Namely, the emf generated was found to be not only a function of the hot junction temperature but also of the temperature of the "pot", which is the small cylindrical block at the termination of the sheath from which the thermocouple conductors emerge. It was easy to demonstrate that only the heat of a hand on the pot, for a few seconds, was sufficient to move the galvanometer pointer the equivalent of about 0.5°C across the scale. Sectioning of the "pot" revealed that the thermocouple wires inside the sheath were soldered to the emerging conductors and that this joint was constituting another thermocouple. This meant that the thermocouple was sensitive to ambient temperature as well as the temperature at the hot junction.

An obvious solution to this problem was to arrange for the "pots" to be embedded in a block of large thermal inertia which would not respond to every small change in ambient temperature. However, since the temperature of the laboratory was not controlled sufficiently to prevent fluctuations of about ± 3°C over a 24 hour period, a block of this sort would experience considerable changes in temperature unless made very large, especially when, by necessity, it is in the close proximity of the heated apparatus. The procedure finally adopted was to mount the thermocouples with the pots between two Tufnol blocks which were sealed inside a small packet by immersion

in paraffin wax. This water-proof assembly was kept permanently immersed in an ice-bath during calibration of the thermocouples and in subsequent viscosity measurements.

Six thermocouples were calibrated against a standard platinum resistance thermometer using a small low-temperature furnace. This furnace consisted of a solid copper cylinder with deep holes drilled axially in which the thermocouples and resistance thermometer could be fitted. The whole cylinder was immersed in a vessel of paraffin and heated electrically. The vessel was surrounded, except at the top by a layer of cork-chippings. The lid consisted of a 2 in. thickness of polystyrene with small holes for the thermocouples to pass through. The heater was manually controlled, but by first of all heating steadily and then greatly reducing the power supplied it was possible to arrange for the temperature-time relationship to pass through a very shallow peak. At this point, the six thermocouple emf's were recorded and a Smith Bridge was used to record the resistance of the standard thermometer. It was necessary to take readings before and after the maximum readings occurred but only the peak value was taken as a calibration point, the rest of the readings were later discarded. This procedure was repeated at 25 temperatures between 17°C and 150°C at approximately 5° intervals. The temperature-emf observations were fitted to equations of the form

$$= A + Bt + Ct^2 + \ldots\ldots$$

using the method of least squares and a digital computor. By also determining the standard deviation of the observed results from these equations it was possible to select the best fit.

In all cases the fit given by cubic equation was a great improvement over the quadratic, but increasing the form of the equation to higher powers in t had only a minimal effect on the standard deviation. Table A.1 lists the standard deviations obtained with the different equations fitted.

Form of equation / T/C	Standard deviation of fit μV					
	1	2	3	4	5	6
$e = A + Bt + Ct^2$	7.06	7.36	10.3	6.88	7.07	6.80
$e = A + Bt + Ct^2 + Dt^3$	2.24	3.92	6.78	2.61	2.34	1.93
$e = A + Bt + Ct^2 + 11 + Et^4$	2.17	3.85	6.30	2.59	2.31	1.92
$e = A + Bt + Ct^2 + Dt^3 + Et^4 + Ft^5$	2.15	3.30	6.04	2.59	2.31	1.92

Table A.1

It is apparent from Table A.1 that the Thermocouple No. 3 has the greatest standard deviation which can be partly explained by the fact that it had a shorter stainless steel sheath than the rest and, because it was shorter than the rest, it did not penetrate the copper block in the furnace to the same extent as the other thermocouples. From the first computor results it was possible to see where any errors had been made in the selection of "peak" values from the initial readings. The data was adjusted to take account of these corrections and Table A2 shows the standard deviation of observations from the least squares fit of equations with the form

$$e = A + Bt + Ct^2 + Dt^3$$

Thermocouple	Standard deviation μv
1	2.00
2	4.06
3	6.71
4	2.25
5	1.84
6	1.62

Table A.2

The computed equation of this form was used as the basis for measurements made with these thermocouples and a print out of the generated emf at 1C intervals was computed for additional ease of interpolation. Applying a tolerance of $\pm 2\sigma$ to all computed temperatures, for thermocouples 1, 4, 5 and 6 the tolerance is less than $\pm$ 0.1°C in all cases. Thermocouple 3 was rejected.

After several test runs, in which viscosity measurements were made on water, it was decided to replace one of the Cr/Al thermocouples with a Pt/Pt - 10% Rh thermocouple. This thermocouple, as supplied by Messrs. Johnson Matthew, was sheathed in stainless steel with an outside diameter of 0.064 in. This sheath, in the annealed state, was sufficiently flexible to fit into the lower guard cylinder in the same way as the Cr/Al thermocouples already described.

Since it was planned to carry out viscosity measurements between 0° and 20°C it was essential that the calibration should be valid over this range. It was decided, therefore, to calibrate this thermocouple in the viscometer jacket since by this means the temperature could be varied over a similar range to that anticipated

for viscosity measurement. At the same time the thermostatic control of the viscometer was an advantage over the manually controlled furnace previously used. In fact a few calibration points were observed near $0^{\circ}C$ by immersing the thermocouple and standard platinum resistance thermometer in a Dewar flask containing glycol, which was temperature controlled by an immersion-type refrigerating coil. The Smith Bridge was no longer available for this calibration since it was permanently housed in a separate room. The resistance of the standard thermometer Rt was therefore obtained by means of the circuit shown in Figure A1. Using a photocell galvanometer amplifier this resistance was found from the ratio of the p.d.'s across the thermometer and a 25 Ω standard resistor respectively. The resistance R_o was also obtained, when the resistance thermometer was immersed in a mixture of ice and water, in the same way. (Note: A calibration certificate for the 25 Ω resistor allowed variations of ambient temperature from $20^{\circ}C$ to be taken into consideration). Although a Tinsley thermal compensator was incorporated in the thermocouple circuit a test for spurious emf's was carried out at every calibration point and the emfs recorded were adjusted to take this into account.

The Standard Platinum Resistance Thermometer No. 153384 was used for the calibration. This had been calibrated by N.P.L. at 5/8/66. The temperature was calculated from

$$t = \frac{R_t - R_o}{0.00392682R_o} + 1.4926 \left(\frac{t}{100} - 1 \right) \frac{t}{100}$$

where $t = {}^{\circ}C$.

For convenience, the calibration results were interpolated graphically in the form $e_t - e : e$ where e_t was obtained from the reference tables (1).

Owing to the very small emf generated per °C for a Pt/Pt-10% Rh thermocouple, a more sensitive vernier potentiometer and galvanometer were required. Fortunately these were temporarily available with other necessary equipment. The Tinsley vernier potentiometer used could be read directly to 0.1 μ v and by using a photocell galvanometer amplifier, the additional sensitivity of this apparatus counteracted the fact that the emf's to be measured were much smaller. All but about the first ten of the results recorded in Chapter 6 were obtained using the Pt/Pt-10% Rh thermocouple, the others having been calculated from the average of three Cr/Al thermocouple readings.

Reference:

(1) American Institute of Physics. Temperature, Its Measurement and Control in Science and Industry. Published by Reinhold Publishing Corp. N.Y., U.S.A. (1941)

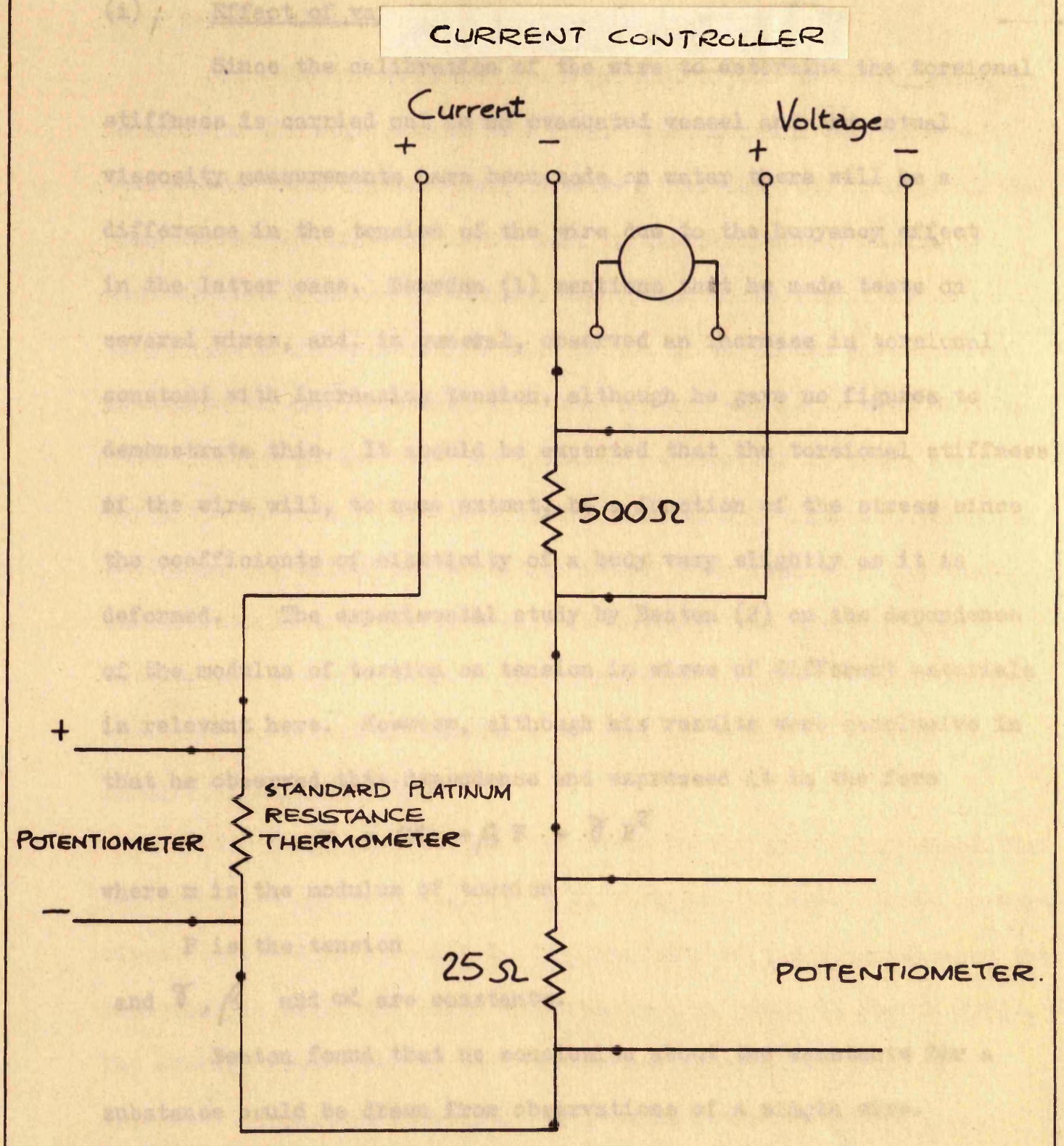

Figure A1. Circuit used to obtain R_t when calibrating the Pt/Pt-10% Rh thermocouple in the viscometer thermostat.

APPENDIX B

(i) Effect of varying tension in the torsion wire

Since the calibration of the wire to determine the torsional stiffness is carried out in an evacuated vessel and the actual viscosity measurements have been made on water there will be a difference in the tension of the wire due to the buoyancy effect in the latter case. Bearden (1) mentions that he made tests on several wires, and, in general, observed an increase in torsional constant with increasing tension, although he gave no figures to demonstrate this. It should be expected that the torsional stiffness of the wire will, to some extent, be a function of the stress since the coefficients of elasticity of a body vary slightly as it is deformed. The experimental study by Benton (2) on the dependence of the modulus of torsion on tension in wires of different materials is relevant here. However, although his results were conclusive in that he observed this dependence and expressed it in the form

$$m = \alpha + \beta P + \gamma P^2$$

where m is the modulus of torsion

P is the tension

and γ, β and α are constants.

Benton found that no conclusion about the constants for a substance could be drawn from observations of a single wire. However, by observations on a series of wires of the same substance and different diameters he was able to present his findings in the above form. He found that the modulus decreased with increasing

tension for steel and brass with low Cu content, but that the opposite effect occurred with Nickel. The tension was varied between zero and the elastic limit.

In order to estimate the magnitude of the effect of changing tension on the stiffness of the wire, inertia rings were made with varying mass but approximately constant inertia. The inertia is the same as for the inner cylinder used in the preliminary design of viscometer; this had previously been found to be 1822.1 gm cm^2. Simple calculation indicated that 47 cc. of water are displaced by immersion of this cylinder, i.e. the tension change in wire will be less by about 47 gmf when the cylinder is immersed in water at 20°C. Thus, the tension in the wire varies between 297.7 gmf and 347.5 gmf including the effect of the mirror stem. Five inertia rings were therefore made with the same inertia but with the mass varying between 275 gm and 355 gm. The changes in tension produced should simulate the effect of buoyancy, if such an effect is appreciable.

Details of Inertia Rings

The rings were turned from brass in the best lathe available. The precision achieved was not as high as for the more recent inertia rings described in Appendix E. The geometry of the rings showing the positions at which the rings were measured is given in Figure B2(b). The average dimensions of the 5 rings are recorded in table B1. Accurate micrometers were used but a temperature controlled gauge room was not available at the time.

Measurement of the rings was repeated when the gauge room had been completed using precision slip gauges and "Sigma" comparator.

These results are listed in table B2. It can be seen that the result for ring D_L shows the most noticeable change from that given in table B1.

TABLE B1

Inertia Ring	Mass gm	D_1 in	D_2 in	d in	L_1 in	L_2 in	I gm in^2	I gm cm^2
A_L	275.73	0.2490	2.9005	0.1875	1.0386	0.3002	288.02	1858.2
B_L	294.17	0.2502	2.7906	0.1875	0.9777	0.3472	284.84	1837.7
C_L	313.76	0.2503	2.6992	0.1875	0.9277	0.3964	284.63	1836.3
D_L	333.93	0.2505	2.6172	0.1875	0.9759	0.4492	286.56	1848.8
E_L	353.02	0.2505	2.5425	0.1875	0.8205	0.5044	284.84	1837.7

TABLE B2

Inertia Ring	Mass gm	D_1 in	D_2 in	d in	L_1 in	L_2 in.	I gm in^2	I gm cm^2
A_L	275.73	0.2491	2.90062	0.1875	1.03853	0.30027	288.037	1858.30
B_L	294.17	0.2503	2.79035	0.1875	0.97794	0.34736	284.797	1837.33
C_L	313.76	0.2503	2.69922	0.1875	0.92800	0.39640	284.633	1836.34
D_L	333.93	0.2505	2.61722	0.1875	0.87626	0.44904	285.441	1841.55
E_L	353.02	0.2504	2.54247	0.1875	0.82069	0.50421	284.865	1837.83

Experimental. The 5 rings were suspended, in turn, from a Nimonic 90 wire inside the calibration rig but without the vacuum system operating. The resulting periodic times, listed in table B4, were taken at random amplitude and each is the average of several timings of 50 oscillations. For example, timings made on A_L are listed in table B3 to show the precision obtained using stop-watch, telescope, mirror and scale technique.

* The result for 10 oscillations has been included to illustrate the improved precision resulting from timing over a longer period. During the last four timings the amplitude was steadily decreasing and there appears to be a tendency for the periodic time to increase as a result of this. Although this phenomena was not pursued for Nimonic 90 wires the amplitude effect is discussed more fully for tungsten wires in part (iii) of this appendix.

TABLE B3

No. of Oscillations timed	Time Recorded		Time for 1 Oscillation
	min	sec	sec
* 10	3	59.1	23.91
66	26	16.6	23.888
50	19	53.8	23.876
52	20	41.9	23.883
50	19	53.9	23.878
53	21	5.9	23.885

TABLE B4

Inertia Ring	Mass gm	I gm cm^2	I gm cm^2	I_{TOTAL} gm cm^2	τ	τ^2	I/τ^2
A_L	275.73	1858.30	0.91	1859.21	23.882	570.350	3.260
B_L	294.17	1837.33	0.91	1838.24	23.774	565.203	3.252
C_L	313.76	1836.34	0.91	1837.25	23.761	564.585	3.259
D_L	333.93	1841.55	0.91	1842.46	23.776	565.298	3.253
E_L	353.02	1837.83	0.91	1838.74	23.777	565.346	3.252

At a later date, using a slightly different length of Nimonic 90 wire, the experiment was repeated using the photocell circuit shown in Figure 10 to actuate a Venner T.S.A.3 timer. The experiment was performed in a vacuum of 10^{-2} torr with random amplitude. The average period obtained from repeating the timing of 10 oscillations 10 times has been used to calculate I/τ^2. The times recorded are given in table B5 and the torsional stiffness calculated is given in table B6. Note that a different mirror stem was used to that indicated in table B4.

TABLE B5

Inertia Ring	Ave. time for 10 oscillations. sec										Mean	STD Dev. σ
	1	2	3	4	5	6	7	8	9	10		
A_L	23.6809	803	780	781	793	794	791	792	791	797	23.6793	0.0010
B_L	23.5241	53	43	60	57	70	14	57	69	68	23.5253	0.0016
C_L	23.5362	73	70	71	90	82	85	73	90	70	23.5377	0.0009
D_L	23.5543	40	40	45	45	45	46	43	52	50	23.5545	0.0003
E_L	23.5541			23.5541			23.5539			39	23.5540	0.0001

TABLE B5

Inertia Ring	I gm cm^2	Δ I gm cm^2	I_{TOTAL} gm cm^2	τ	τ^2	I/τ^2
A_L	1858.30	1.73	1860.03	23.679	560.965	3.3174
B_L	1837.33	1.73	1839.06	23.525	553.426	3.3230
C_L	1836.34	1.73	1838.07	23.538	554.037	3.3176
D_L	1841.55	1.73	1843.28	23.555	554.838	3.3222
E_L	1837.83	1.73	1838.56	23.554	554.791	3.3158

Conclusions.

The average standard deviation for the timing of 10 oscillations is only ± 0.0008 seconds, i.e. 0.0034% which is negligible. From an analysis of error to assess the accuracy with which the plain inertia rings A_1 and A_2 were made it was found that σ_I = ± 0.065%. This series of rings were made by the same machine and using the same measuring methods but these are subject to two errors since they are made in two parts of different diameter. Therefore for rings A_L to E_L the error is assessed to be

$$\sigma_I = \sqrt{2\,\sigma_{A_1}{}^2} = 0.092\%,$$

i.e. a standard deviation of approximately 0.1% should be expected in the results.

The results for I/k^2 listed in tables B4 and B6 have been shown plotted in Figure B1(a) and B1(b) as a % deviation for the mean. It can be seen that although both sets of results fall within a band of ± 0.1% there appears to be no definite trend in either set of results. Surprisingly, the results are dissimilar in other respects. The lightest ring gave the highest torsional constant in the first experiment but was among the lowest in the second. This could mean that other effects are entering the experiment which have not been accounted for, in theerror assessment. However, it may be deduced, within the limitations of the experiment, that the mass of the inertia ring has no significant effect on the torsional constant. From this is may also be inferred that the changes in tension in the wire due

to buoyancy effect of immersion in water will not affect the initial calibration of the wire.

References.

(1) Bearden, J.A. Phys. Rev. 56, 1023 (1939)

(2) Benton, J.R. Phys. Rev. 12, 100 (1901)

Appendix B(ii) Investigation of the effect of varying period of oscillation on the observed torsional constant of the wire.

Since the success of measuring the viscosity by this method depends upon the behaviour of the wire during calibration it was felt that the possible effect of varying period of oscillation should be assessed. This has been achieved by making seven rings of different angular moment of inertia ranging from 800 to 12600 gm cm^2. Each can be fitted to the mirror stem without disturbing the collets which grip the wire. Several of these rings were too large to be oscillated in the vacuum vessel and the results quoted were obtained with the pendulum set up on the bench with the only precautions that vibrations and draughts were kept to a minimum.

In order that there was no possible effect of varying tension in the wire (although the previous section would suggest that period is not affected appreciably by tension), the rings were made of constant mass. An exception was the ring of largest inertia which was aluminium compared with brass for the rest. The mass of this ring was about 20% less than the others. In fact the rings were designed to have the same mass as the inner cylinder of the viscometer, so that the direct stress in the wire was similar during these tests to that in subsequent viscosity measurements.

The first ring in the series was a plain cylinder with a central hole for the mirror stem. Other rings consist of a small diameter part and a large diameter part. The small diameter part is really only a spacer which allows the ring to be gripped firmly

on the mirror stem. The accuracy with which the larger rings could be made was limited by the manufacturing facilities available. The largest rings tended to have a slight taper in the section of largest diameter, this part being slightly deeper at the outside than at the centre of the ring. This was allowed for, as near possible, by plotting the changing thickness graphically and calculating the inertia of the ring in two parts, one part being a flat plate and the other a ring with wedge-shaped cross-section.

A rigorous assessment of accuracy has not been made, since it is thought that insufficient precautions were taken to provide a good environment for the tests, which, in itself, could introduce errors difficult to account for. However, the previously made assessment of error for the rings (see previous section) would suggest a standard deviation for the calculated inertia of approximately 0.1%. A technique using a telescope, mirror and scale was used to start and stop a stop-watch at the turning point of the oscillations which were taken as the beginning and end of each test. Since the accuracy of the stop-watch was not taken into account in the determination of the period of oscillation, each ring was timed over a similar period of about 20 minutes. However, some of the scatter in the results was due to error in the stop-watch since the above procedure could not be rigidly adhered to on every occasion.

The measurements from which the inertia of the rings were calculated are given in table B7 and the results from timing the rings are given in table B8. Micrometers reading to 0.0001 in. were used to measure the dimensions except for the ring designated A_1 for

which slip gauges and comparator were used. More accurate methods of measurement were not used for the other rings because of the limited time available. However, it is felt that this type of experiment should be repeated with much greater care in order to ascertain that the torsional behaviour can be regarded independent of the period of oscillation with even greater certainty.

TABLE B7

Inertia Ring	A_1	B_1	C_1	D_1	E_1	F_1	G_1
Mass gm	372.53	372.40	372.52	372.25	375.91	376.10	288.27
D_1 in	1.6256	0.5045	0.5007	0.5010	0.4991	0.3502	0.3504
D_2 in	-	1.8468	2.1842	2.8589	4.0129	4.7338	7.4011
d in	0.1875	0.1875	0.1875	0.1875	0.1875	0.1875	0.1875
L_1 in	1.3240	0.3288	0.6505	0.9219	1.1225	1.1731	1.1748
L_2 in	-	1.0022	0.6980	0.3981	0.2025	0.1519	0.1487
I gm cm^2	124.70	157.34	215.22	360.62	707.13	1032.6	1954.6
I gm cm^2	804.50	1015.07	1388.52	2326.57	4562.1	6662.2	12610.1

TABLE B8

Inertia Ring	A_1	B_1	C_1	D_1	E_1	F_1	G_1
I_{TOTAL}	806.23	1016.80	1390.25	2328.30	4563.82	6663.89	12611.8
Period "τ" sec	11.437	12.847	15.033	19.478	27.192	32.899	45.306
I/τ^2	6.1635	6.1608	6.1521	6.1369	6.1723	6.1569	6.1441

A deviation plot of the values for the torsional constant listed in table B8 is given in Figure B2(a). The standard deviation is 0.18% and there would appear to be no definite trend in the results.

Appendix B(iii)

During the measurements of periodic time, which were necessary in the previous parts of this appendix, it was observed that to some extent the period of oscillation was a function of the amplitude. This phenomenon had been observed by Bearden during the calibration of the wires for his viscometer, and also by Benton in his investigation of the effect of direct stress on the torsional modulus. That such variations should occur may be deduced from theoretical considerations, as Zener (3) has shown in his volume "Elasticity and Anelasticity of Metals". The deviation of metals from elastic behaviour at high stress levels is to be expected and one would anticipate some permanent 'set' in metal subjected to this treatment. However, even at extremely low stress levels a metal deviates from perfect elastic behaviour, without necessarily incurring permanent deformation. An-elasticity is a term which has been coined to denote the property by which stress and strain are not single-valued functions of one another in the low stress range and in which no permanent set occurs. This behaviour is more obviously a problem inherent in the oscillating disc viscometers, where part of the decay of vibrations is due to the viscosity of the fluid and part due to internal friction of the wire material. In this context internal friction is an expression of the anelasticity of the wire and experiments must be performed in a good vacuum to discover how much of the decrement is due to this effect. The work of Kestin and Moszynski (4) on wires of platinum-tungsten alloy indicate that the internal friction of a wire can be

reproduced with reasonable accuracy, the scatter in their experimental points being in the order of 20%. However, it appeared that the period of oscillation was subject to slight changes from one test to another for which they offered no explanation. It would seem to the author that the change in periodic time observed by Moszynski was an amplitude-dependent effect. The explanation which seems most likely is that even at low stress levels the stress-strain relation is not linear, i.e. there is some deviation from Hooke's Law.

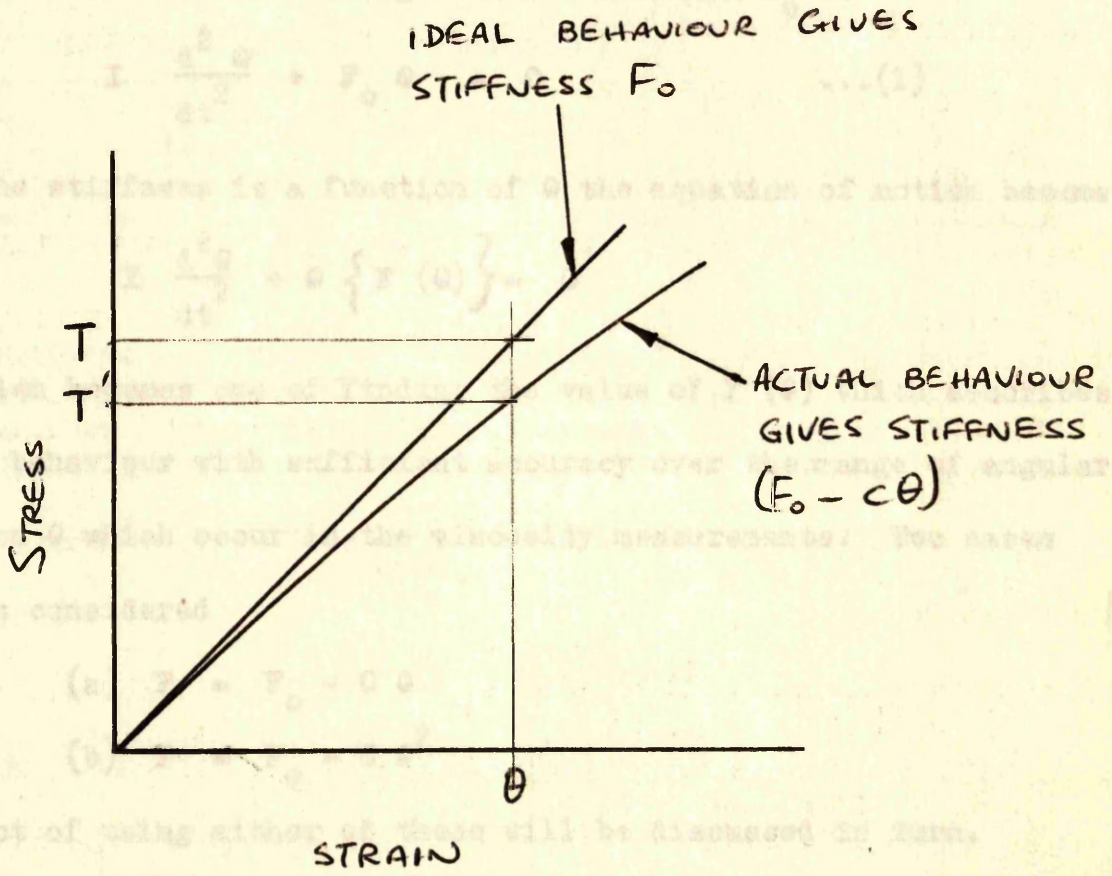

This non-linear behaviour can be expected to have an effect both in the static and dynamic performance of the wire. In the former circumstance it will result in a larger deflection for a given torque T, i.e. assuming that torsional stiffness of wire remained

constant at F_o, then the torque to produce a deflection θ would be given by

$$T = F_o \theta$$

However, if the torsional stiffness has changed to some new value which is a function of θ, say $F(\theta)$, then the torque to produce a deflection θ would be given by

$$T' = \{F(\theta)\}\theta$$

Considering the effect of this on the dynamic performance of the wire, the equation of motion assuming constant siffness F_o is

$$I \frac{d^2\theta}{dt^2} + F_o \theta = 0 \qquad \ldots(1)$$

and if the stiffness is a function of θ the equation of motion becomes

$$I \frac{d^2\theta}{dt^2} + \theta \{F(\theta)\} = 0$$

The problem becomes one of finding the value of $F(\theta)$ which describes the wire behaviour with sufficient accuracy over the range of angular deflection θ which occur in the viscosity measurements. Two cases have been considered

(a) $F = F_o - C\theta$

(b) $F = F_o - C\theta^2$

the effect of using either of these will be discussed in turn.

(a) The equation of motion becomes

$$I \frac{d^2\theta}{dt^2} + \theta(F_o - C\theta) = 0 \qquad \ldots(2)$$

this can be re-written

$$\frac{d^2\theta}{dt} + \frac{F_o}{I}\theta(1 - K\theta) \quad \text{where} \quad \frac{C}{F_o} = K \qquad \ldots(3)$$

For very small θ the assumption can be made that $(1 - K\theta)$ is constant in which case equation (3) becomes identical to equation (1) and the solution is that of S.H.M.

i.e.
$$\theta = A \sin \left\{ \sqrt{\frac{F_o}{I}(1 - K\theta)} \cdot t \right\}$$

i.e. when the amplitude is θ_a the modified frequency ω_a is given by

$$\omega_a = \sqrt{\frac{F_o}{I}(1 - K\theta_a)}$$

whereas the frequency given by equation (1) is

$$\omega_o = \sqrt{\frac{F_o}{I}}$$

$$\therefore \quad \frac{\omega_a}{\omega_o} = \sqrt{1 - K\theta_a}$$

$\therefore$ the ratio of the period of oscillation, τ_a, when the amplitude is θ_a to the period when the amplitude is zero, τ_o, is

$$\frac{\tau_a}{\tau_o} = \frac{1}{(1 - K\theta_a)^{\frac{1}{2}}}$$

$$= (1 + \tfrac{1}{2} K \theta_a - \ldots\ldots)$$

$$\therefore \quad \frac{\tau_a - \tau_o}{\tau_o} = \frac{K}{2} \cdot \theta_a = \frac{C}{2F_o} \cdot \theta_a \qquad \ldots(4)$$

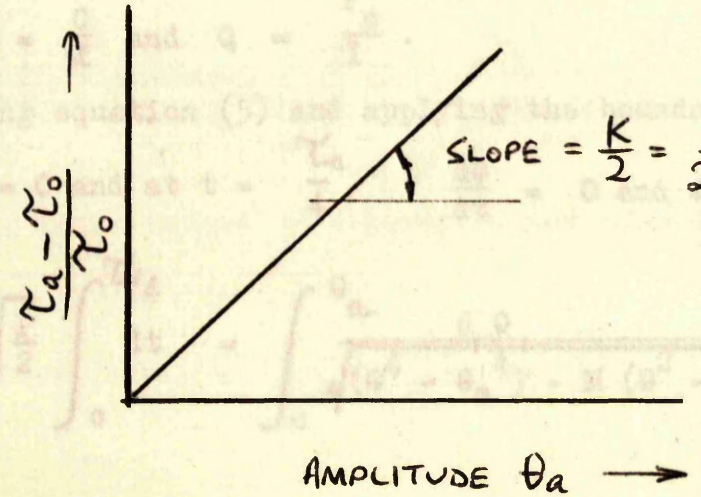

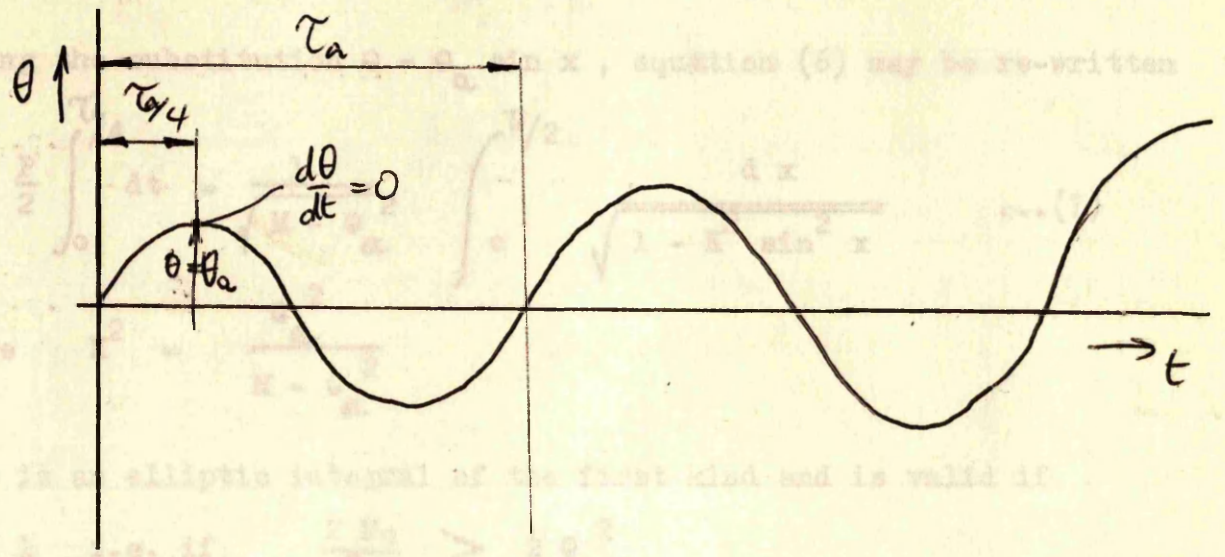

Thus if the period of oscillation is plotted against the amplitude θ_a the slope can be used to obtain the constant C which enables the correct torsional stiffness F to be used in the static application of the wire i.e. $F = F_o - C\theta_a$.

(b) Considering now the effect of modified torsional stiffness given by $F = F_o - C\theta^2$ the equation of motion becomes

$$\frac{d^2\theta}{dt^2} = P\theta^3 - Q\,\theta \qquad \ldots.(5)$$

where $P = \frac{C}{I}$ and $Q = \frac{F_o}{I}$.

Integrating equation (5) and applying the boundary conditions at $t = 0$, $\theta = 0$ and at $t = \frac{\tau_a}{4}$ $\frac{d\theta}{dt} = 0$ and $\theta = \theta_a$ we get

$$\sqrt{\frac{P}{2}} \int_0^{\tau_a/4} dt = \int_0^{\theta_a} \frac{d\theta}{\sqrt{(\theta^4 - \theta_a^4) - M(\theta^2 - \theta_a^2)}} \qquad \ldots(6)$$

where $$M = \frac{2Q}{P}$$

Making the substitution $\theta = \theta_a \sin x$, equation (6) may be re-written

$$\frac{P}{2}\int_0^{\tau/4} dt = \frac{1}{\sqrt{M - \theta_a^2}} \int_0^{\pi/2} \frac{dx}{\sqrt{1 - K^2 \sin^2 x}} \qquad \ldots(7)$$

where $$K^2 = \frac{\theta_a^2}{M - \theta_a^2}$$

This is an elliptic integral of the first kind and is valid if

$K^2 < 1$ i.e. if $\frac{2F_o}{C} > 2\theta_a^2$

$$\therefore \frac{\tau_a}{4}\sqrt{\frac{P}{2}} = \frac{1}{\sqrt{M - \theta_a^2}}\left[\frac{\pi}{2}\left(1 + \frac{\theta_a^2}{4(M - \theta_a^2)} + \frac{9}{64}\frac{\theta_a^4}{(M - \theta_a^2)^2} + \ldots\right)\right]$$

$\ldots.(8)$

Now when $\tau_a = \tau_o$ $\theta_a = 0$

$$\therefore \frac{\tau_o}{4}\sqrt{\frac{P}{2}} = \frac{1}{\sqrt{M}}\ \frac{\pi}{2}\ (1 + 0 + 0 + \ldots.)$$

$$\therefore \tau_o = 2\pi\sqrt{\frac{I}{F_o}}$$ which is the solution to equation (1)

and at amplitude θ_a $\tau = \tau_a$

$$\therefore \frac{\tau_a}{4}\sqrt{\frac{P}{2}} = \frac{1}{\sqrt{M - \theta_a^2}}\left[\frac{\pi}{2}\left(1 + \frac{\theta_a^2}{4(M - \theta_a^2)} + \frac{9\,\theta_a^4}{64(M - \theta_a^2)} + \ldots..\right)\right]$$

Neglecting terms raised to a power higher than 2 and dividing each side by τ_o gives

$$\frac{\tau_a}{\tau_o} = \left(1 + \frac{3C}{8F_o}\theta_a^2 + \ldots\ldots\right)$$

i.e.

$$\frac{\tau_a - \tau_o}{\tau_o} = \frac{3C}{8F_o}\theta_a^2 + \ldots\ldots\ldots\ldots \quad \ldots(9)$$

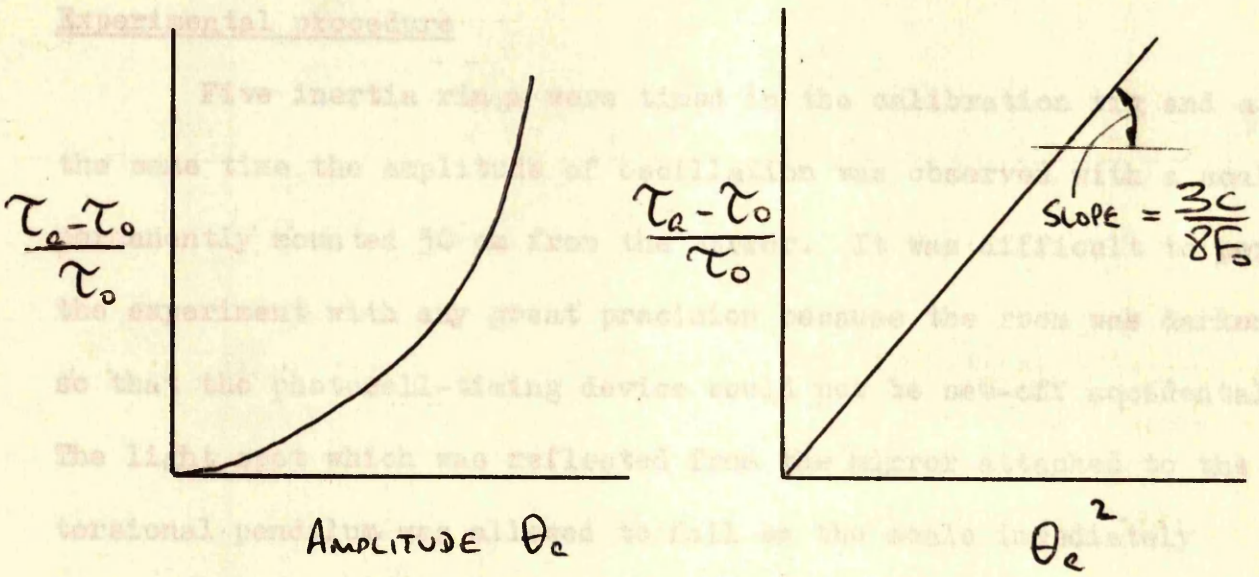

If this assumption gives the form of the deviation from Hooke's Law a plot of $\frac{\tau_a - \tau_o}{\tau_o}$ against θ_a^2 should allow the constant C to be determined from the slope so that the torsional stiffness at deflection θ_a is given by

$$F = F_o - C\,\theta_a^2$$

These solutions have been described because both results have been used at some time to describe the amplitude dependence of the frequency of a torsional pendulum. A solution of the type (a) was used by Benton (2) and was found to apply at amplitudes up to 50^o for a wire of total length 3 metres. A solution of the type (b) was

used by Bearden (1) who found the relationship true for amplitudes up to 100' using tungsten wire.

After many attempts to fit the small amplitude periodic times observed to an equation of the second type, the author's conclusion was that the linear relationship given by the first equation is more applicable to this work where the amplitudes are up to 10° of arc.

Experimental procedure

Five inertia rings were timed in the calibration rig and at the same time the amplitude of oscillation was observed with a scale permanently mounted 50 cm from the mirror. It was difficult to perform the experiment with any great precision because the room was darkened so that the photocell-timing device would not be set-off accidentally. The light spot which was reflected from the mirror attached to the torsional pendulum was allowed to fall on the scale immediately after the counter had been started and the amplitude was recorded. The scale was then pivotted away from the path of the spot so that the signal to stop the counter (after the required number of oscillations had occurred) would not be interfered with. The effect of amplitude has not been exactly reproduced from one test to the next as can be seen from the standard deviation of the results. In this respect these are regarded as preliminary measurements. When it is considered that the effect of non-linear behaviour of the wire is likely to necessitate a correction of not more than 0.5%, a certainty of $\pm$ 10% in determining this effect is sufficient at present.

Results Observations of periodic time have been plotted against amplitude and the best straight line has been drawn through these points. Figures B4, B5 and B6 show typical sets of results. The scale reading 'a' cm can be converted to the amplitude θ_a in radians by the relation $\theta_a = 5 \times 10^{-3} a.$, where θ is in radians

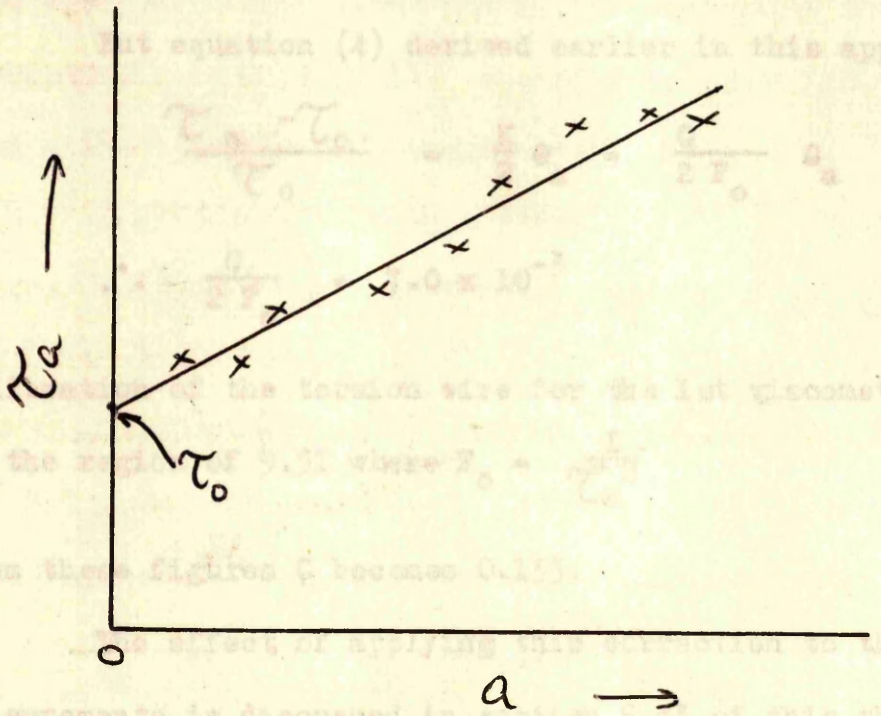

The point at which the line through the results cuts the τ_a - axis is taken to be the period at zero amplitude, from which F_o has been calculated.

The ratio $\frac{1}{a}\left(\frac{\tau_a - \tau_o}{\tau_o}\right)$ was obtained for each ring tested. The mean value for this ratio was found to be 3.501×10^{-5} and the standard deviation of the results was $\pm 0.337 \times 10^{-5}$ which amounts to $\pm$ 9.9%

i.e.
$$\frac{\tau_a - \tau_o}{\tau_o} = 3.5 \times 10^{-5} \times a$$
$$= 3.5 \times 10^{-5} \times 200\, \theta_a$$
$$= 7.0 \times 10^{-3}\, \theta_a$$

where θ_a is in radians.

But equation (4) derived earlier in this appendix gives

$$\frac{\tau_a - \tau_o}{\tau_o} = \frac{K}{2}\theta_a = \frac{C}{2F_o}\theta_a$$

$$\therefore \frac{C}{2F_o} = 7.0 \times 10^{-3}$$

Calibration of the torsion wire for the 1st viscometer gives F_o in the region of 9.51 where $F_o = \frac{I}{\tau_o^2}$

From these figures C becomes 0.133.

The effect of applying this correction to the viscosity measurements is discussed in section 5.33 of this thesis.

Addendum to Appendix B(iii)

Considering again the equation of motion when $F = F_o - C\theta$

i.e.

$$I \frac{d^2\theta}{dt^2} + \theta (F_o - C\theta) = 0 \qquad \ldots(1)$$

This was previously solved making the assumption that $(1 - K\theta)$ is a constant when θ is small. An exact solution follows which may be used without making this assumption.

Equation (1) can be written

$$\frac{d^2\theta}{dt^2} + \frac{F_o}{I} \theta - \frac{C}{I} \theta^2 = 0$$

let $\frac{F_o}{I} = P$ and $\frac{C}{I} = Q$

$$\therefore \frac{d^2\theta}{dt^2} + PQ - Q\theta^2 = 0$$

$$\therefore 2 \frac{d\theta}{dt} \frac{d^2\theta}{dt^2} = 2 \frac{d\theta}{dt} Q\theta^2 - 2 \frac{d\theta}{dt} P\theta$$

$$\therefore \left(\frac{d\theta}{dt}\right)^2 = \frac{2Q\theta^3}{3} - P\theta^2 + A$$

at $t = \frac{T_a}{4}$ $\frac{d\theta}{dt} = 0$ and $\theta = \theta_a$

$$\therefore 0 = \frac{2Q}{3} \theta_a^2 - P\theta_a + A$$

$$\therefore A = P\theta_a^2 - \frac{2Q}{3} \theta_a^3$$

$$\therefore \left(\frac{d\theta}{dt}\right)^2 = \frac{2Q}{3} (\theta^3 - \theta_a^3) - P (\theta^2 - \theta_a^2)$$

$$\therefore dt = \frac{d\theta}{\sqrt{\frac{2Q}{3} (\theta^3 - \theta_a^3) - M (\theta^2 - \theta_a^2)}}$$

where $\frac{3P}{2Q} = M$

but $t = \frac{\tau_a}{4}$ at $\theta = \theta_a$ and $t = 0$ at $\theta = 0$, let $\tau_a = T$

$$\therefore \sqrt{\frac{2Q}{3}} \int_0^{T/4} dt = \int_0^{\theta_a} \frac{d\theta}{\sqrt{(\theta^3 - \theta_a^3) - M(\theta^2 - \theta_a^2)}} \qquad \ldots(2)$$

$$\sqrt{\frac{2Q}{3}} \int_0^{T/4} dt = \frac{1}{\theta_a^{3/2}} \int_0^{\theta_a} \frac{d\theta}{\sqrt{\left[\left(\frac{\theta}{\theta_o}\right)^3 - 1\right] - \left\{\frac{M}{\theta_o}\left\{\left(\frac{\theta}{\theta_o}\right)^2 - 1\right\}\right\}}}$$

let $x = \frac{\theta}{\theta_a}$ $\therefore$ $dx = \frac{1}{\theta_a} d\theta$

$$\therefore \sqrt{\frac{2Q}{3}} \int_0^{T/4} dt = \frac{1}{\theta_a^{\frac{1}{2}}} \int_0^1 \frac{dx}{\sqrt{(x^3 - 1) - \frac{M}{\theta_a}(x^2 - 1)}}$$

$$= \frac{1}{\theta_a^{\frac{1}{2}}} \int_0^1 \frac{dx}{\sqrt{(x - 1)(x^2 + x + 1) - \frac{M}{\theta_a}(x - 1)(x + 1)}}$$

$$= \frac{1}{\theta_a^{\frac{1}{2}}} \int_0^1 \frac{dx}{\sqrt{(x - 1)(x^2 - \left[\frac{M}{\theta_a} - 1\right]x - \left[\frac{M}{\theta_a} - 1\right])}}$$

let $a = \left[\frac{M}{\theta_a} - 1\right]$

then $\sqrt{\frac{2Q}{3}} \int_0^{T/4} dt = \frac{1}{\theta_a^{\frac{1}{2}}} \int_0^1 \frac{dx}{\sqrt{(x - 1)(x^2 - ax - a)}}$

$$= \frac{1}{\theta_a^{\frac{1}{2}}} \int_0^1 \frac{dx}{\sqrt{(x - 1)(x - \gamma_1)(x - \gamma_2)}}$$

where $\gamma_1 = \frac{a + \sqrt{a^2 + 4a}}{2}$ and $\gamma_2 = \frac{a - \sqrt{a^2 + 4a}}{2}$

let $u = (x - \nu_2)^{\frac{1}{2}}$ $\therefore$ $x = u^2 + \nu_2$

$$du = \frac{dx}{2(x - \nu_2)^{\frac{1}{2}}}$$

$$\therefore \sqrt{\frac{2Q}{3}} \int_0^{T/4} dt = \frac{1}{\theta_a^{\frac{1}{2}}} \int_{(-\nu_2)^{\frac{1}{2}}}^{(1-\nu_2)^{\frac{1}{2}}} \frac{2(x - \nu_2)^{\frac{1}{2}}\, du}{(x - \nu_2)^{\frac{1}{2}} \sqrt{\left[u^2 + (\nu_2 - 1)\right]\left[u^2 - (\nu_1 - \nu_2)\right]}}$$

let $u = (1 - \nu_2)^{\frac{1}{2}} v$

$\therefore$ $du = (1 - \nu_2)^{\frac{1}{2}} dv$

$$\therefore \sqrt{\frac{2Q}{3}} \int_0^{T/4} dt = \frac{2}{(\nu_1 - \nu_2)^{\frac{1}{2}} \theta_a^{\frac{1}{2}}} \int_{\left(\frac{\nu_2}{\nu_2 - 1}\right)^{\frac{1}{2}}}^{1} \frac{(1 - \nu_2)^{\frac{1}{2}}\, dv}{\sqrt{1 - \nu_2} \sqrt{\left[(1 - \nu_2)v^2 + (\nu_2 - 1)\right]\left[(1 - \nu_2)v^2 - (\nu_1 - \nu_2)\right]}}$$

$$\therefore \sqrt{\frac{2Q}{3}} \int_0^{T/4} dt = \frac{2}{(\nu_1 - \nu_2)^{\frac{1}{2}} \theta_a^{\frac{1}{2}}} \int_{\left(\frac{\nu_2}{\nu_2 - 1}\right)^{\frac{1}{2}}}^{1} \frac{dv}{\sqrt{(v^2 - 1)\,(1 - \nu_2)v^2 - (\nu_1 - \nu_2)}}$$

$$\therefore \sqrt{\frac{2Q}{3}} \int_0^{T/4} dt = \frac{2}{(\nu_1 - \nu_2)^{\frac{1}{2}} \theta_a^{\frac{1}{2}}} \int_{\left(\frac{\nu_2}{\nu_2 - 1}\right)^{\frac{1}{2}}}^{1} \frac{dv}{\sqrt{(1 - v^2)\left[1 - \left(\frac{1 - \nu_2}{\nu_1 - \nu_2}\right) v^2\right]}}$$

let $k^2 = \left(\frac{1 - \nu_2}{\nu_1 - \nu_2}\right)$

$$\therefore \sqrt{\frac{2Q}{3}} \int_0^{T/4} dt = \frac{2}{\theta_a^{\frac{1}{2}}(\nu_1 - \nu_2)^{\frac{1}{2}}} \int_0^1 \frac{dv}{(1 - v^2)(1 - k^2v^2)} - \int_0^{\left(\frac{\nu_2}{\nu_2 - 1}\right)^{\frac{1}{2}}} \frac{dv}{(1 - v^2)(1 - k^2v^2)}$$

This is an elliptic integral of the first kind, so that

$$\sqrt{\frac{2Q}{3}} \int_0^{T/4} dt = \frac{2}{\theta_a^{\frac{1}{2}}(\nu_1 - \nu_2)^{\frac{1}{2}}} \left[F\left(k, \frac{\pi}{2}\right) - F(k, \phi) \right]$$

where $\phi = \sin^{-1} \left(\frac{\nu_2}{\nu_2 - 1} \right)^{\frac{1}{2}}$

$$(\nu_1 - \nu_2) = \frac{a}{2} + \frac{\sqrt{a^2 + 4a}}{2} - \frac{a}{2} + \frac{\sqrt{a^2 + 4a}}{2} = \sqrt{a^2 + 4a}$$

$$(1 - \nu_2) = 1 - \frac{a}{2} + \frac{\sqrt{a^2 + 4a}}{2}$$

$$\therefore \frac{\nu_2}{\nu_2 - 1} = \frac{\frac{a}{2} - \frac{\sqrt{a^2 + 4a}}{2}}{\frac{a}{2} - 1 - \frac{\sqrt{a^2 + 4a}}{2}} = \left[\frac{\frac{\sqrt{a^2 + 4a}}{2} - \frac{a}{2}}{1 + \frac{\sqrt{a^2 + 4a}}{2} - \frac{a}{2}} \right]$$

$$\therefore \sqrt{\frac{2Q}{3}} \int_0^{\tau_a/4} dt = \frac{2}{\theta_a^{\frac{1}{2}}(a^2 + 4a)^{\frac{1}{2}}} \left[F\left(\sin^{-1} \sqrt{\frac{1 - \frac{a}{2} + \frac{\sqrt{a^2 + 4a}}{2}}{\sqrt{a^2 + 4a}}}, \frac{\pi}{2}\right) \right.$$

$$\left. - F\left(\text{ditto}, \sin^{-1} \sqrt{\frac{\frac{1}{2}\sqrt{a^2 + 4a} - \frac{a}{2}}{1 + \frac{1}{2}\sqrt{a^2 + 4a} - \frac{a}{2}}}\right) \right]$$

By substituting experimental values of τ_a into this equation with the observed amplitude θ_a the value of C can be obtained.

(F_o must also be obtained experimentally).

References:

(1) Bearden, J.A., Phys Rev. 56, 1023, (1939)

(2) Benton, J.R., Phys. Rev. 12, 100, (1901)

(3) Zener, C., Elasticity and Anelasticity of Metals, Univ. of Chicago Press, Illinois (1948)

(4) Kestin, J and Moszynski, J.R., Brown University Report No. AF891/11 "An experimental investigation of the internal friction of thin platinum alloy wires at low frequencies". (1957)

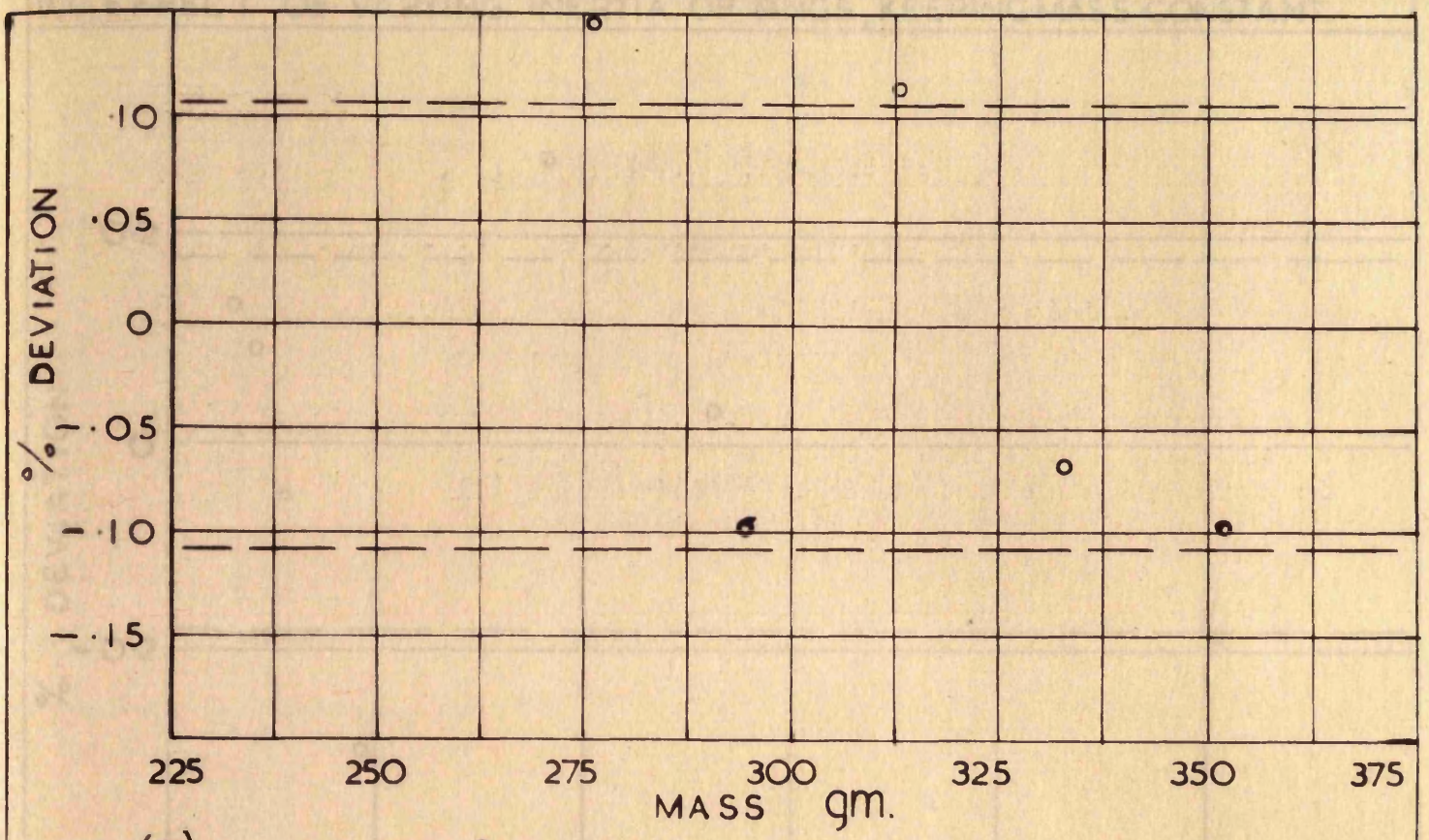

(a) TELESCOPE & SCALE METHOD OF TIMING OSCILLATIONS.

Fig. B1. Results with rings of varying mass & constant inertia.

(b) PHOTOELECTRIC METHOD OF TIMING OSCILLATIONS.

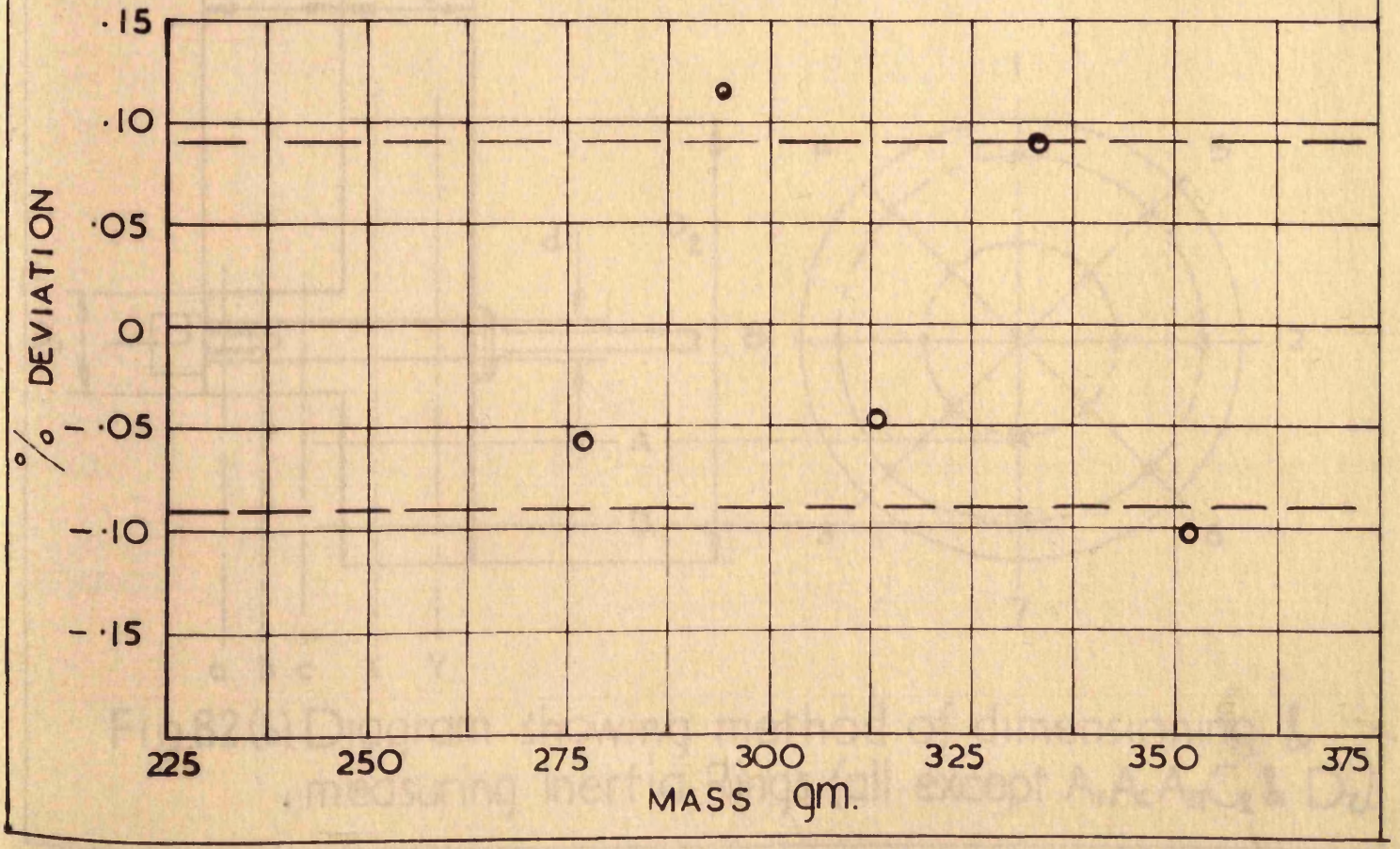

(a). EFFECT OF VARYING INERTIA OF RINGS, KEEPING MASS CONSTANT.

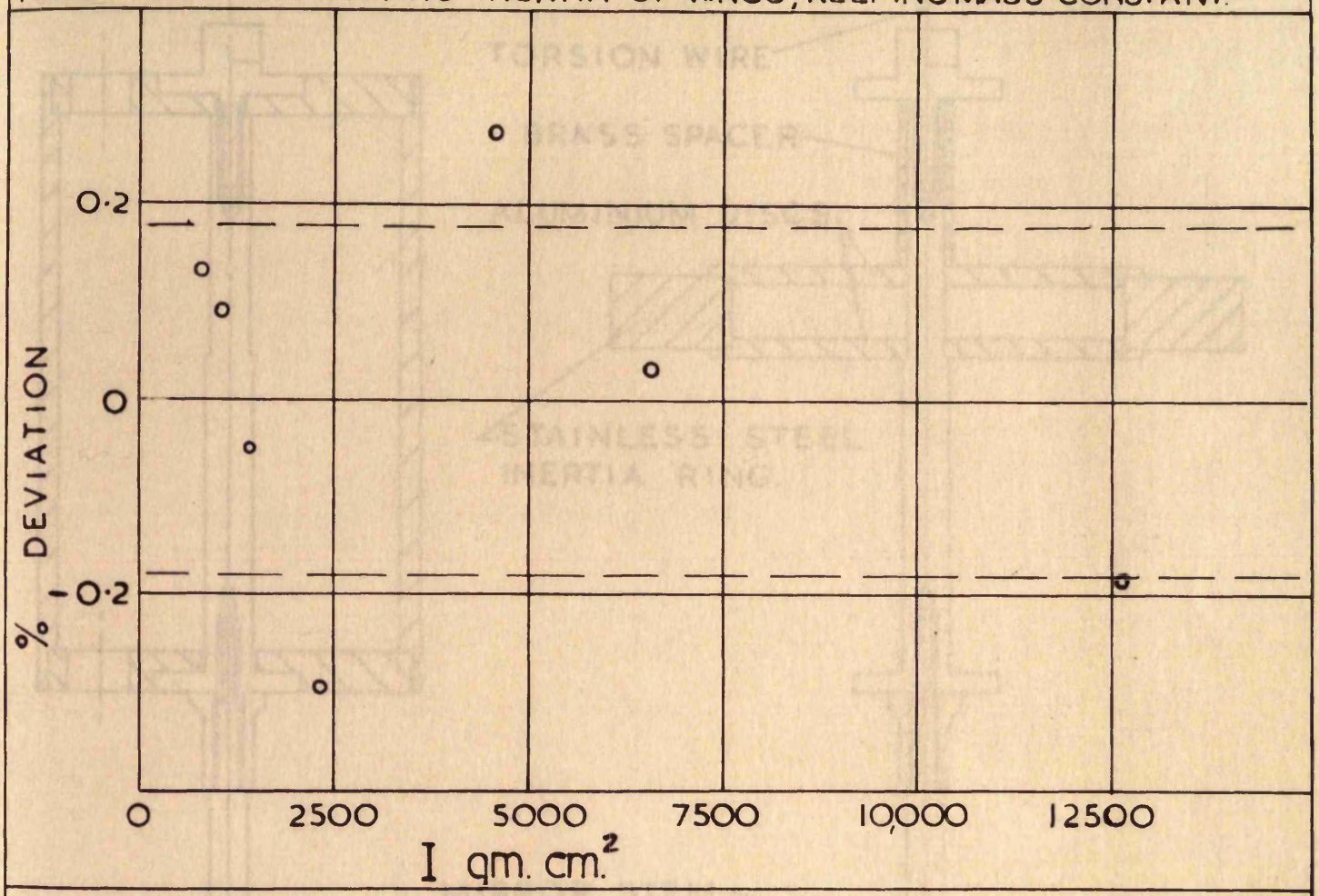

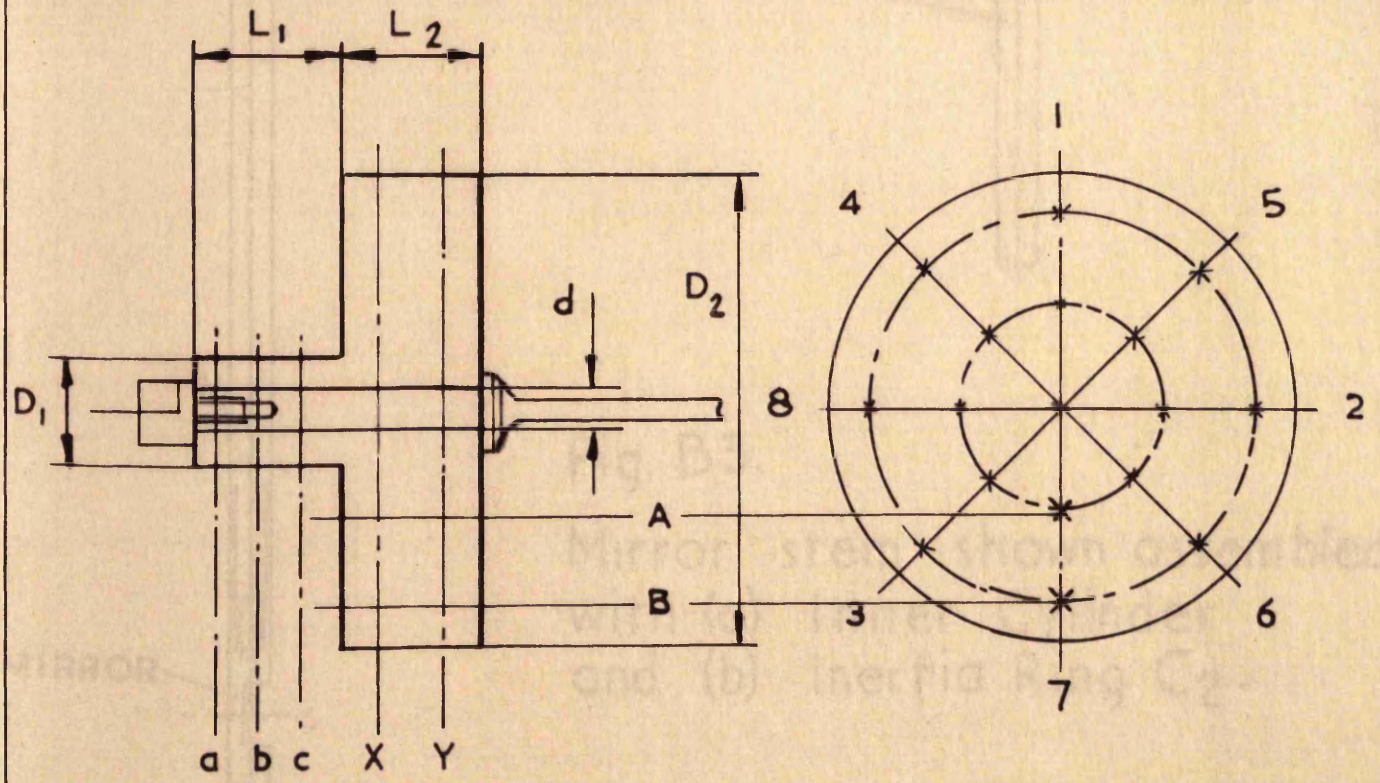

Fig.B2.(b). Diagram showing method of dimensioning & measuring Inertia Rings (all except $A_1 A_2 A_{22} C_2$ & D_2).

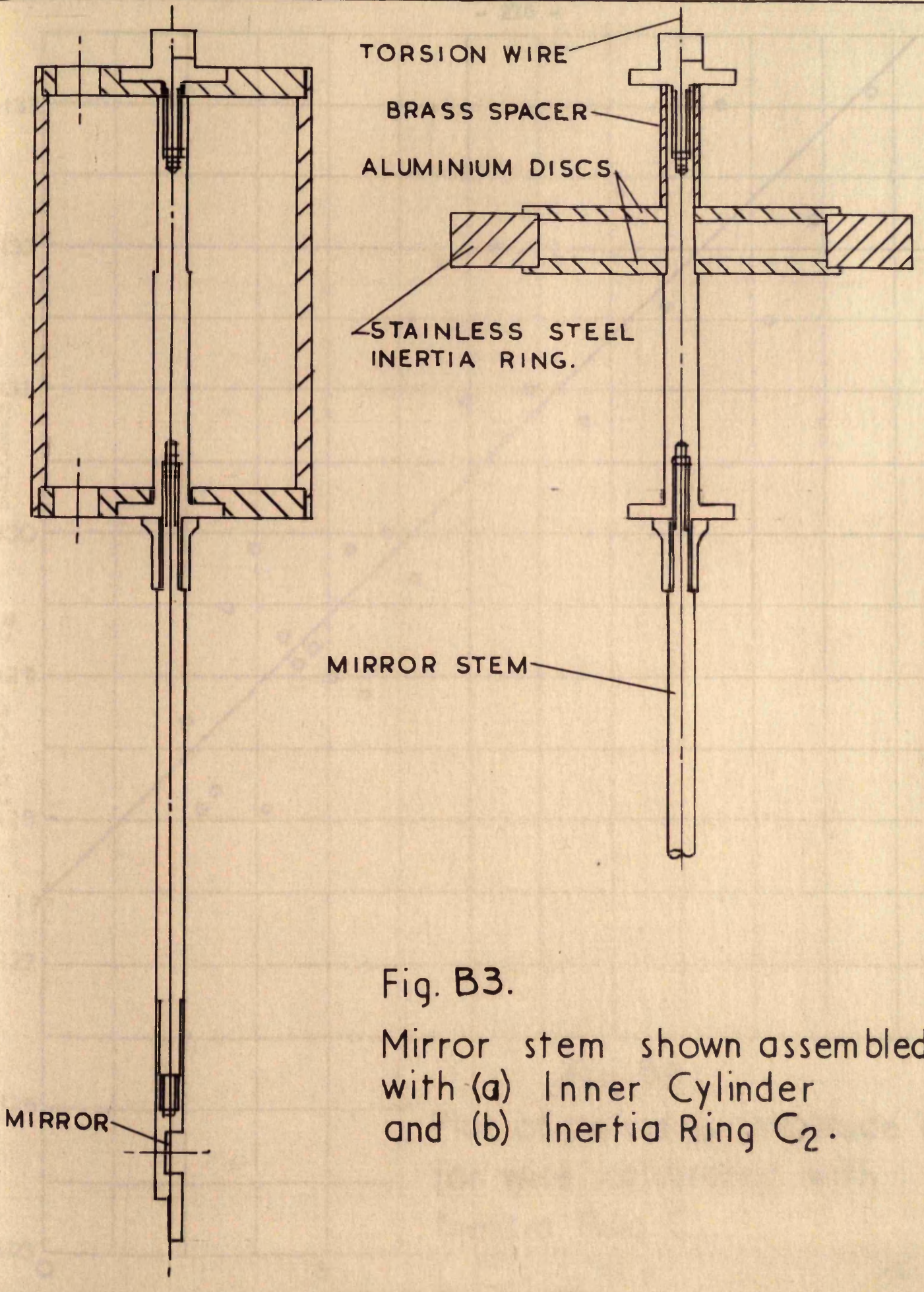

Fig. B3.

Mirror stem shown assembled with (a) Inner Cylinder and (b) Inertia Ring C_2.

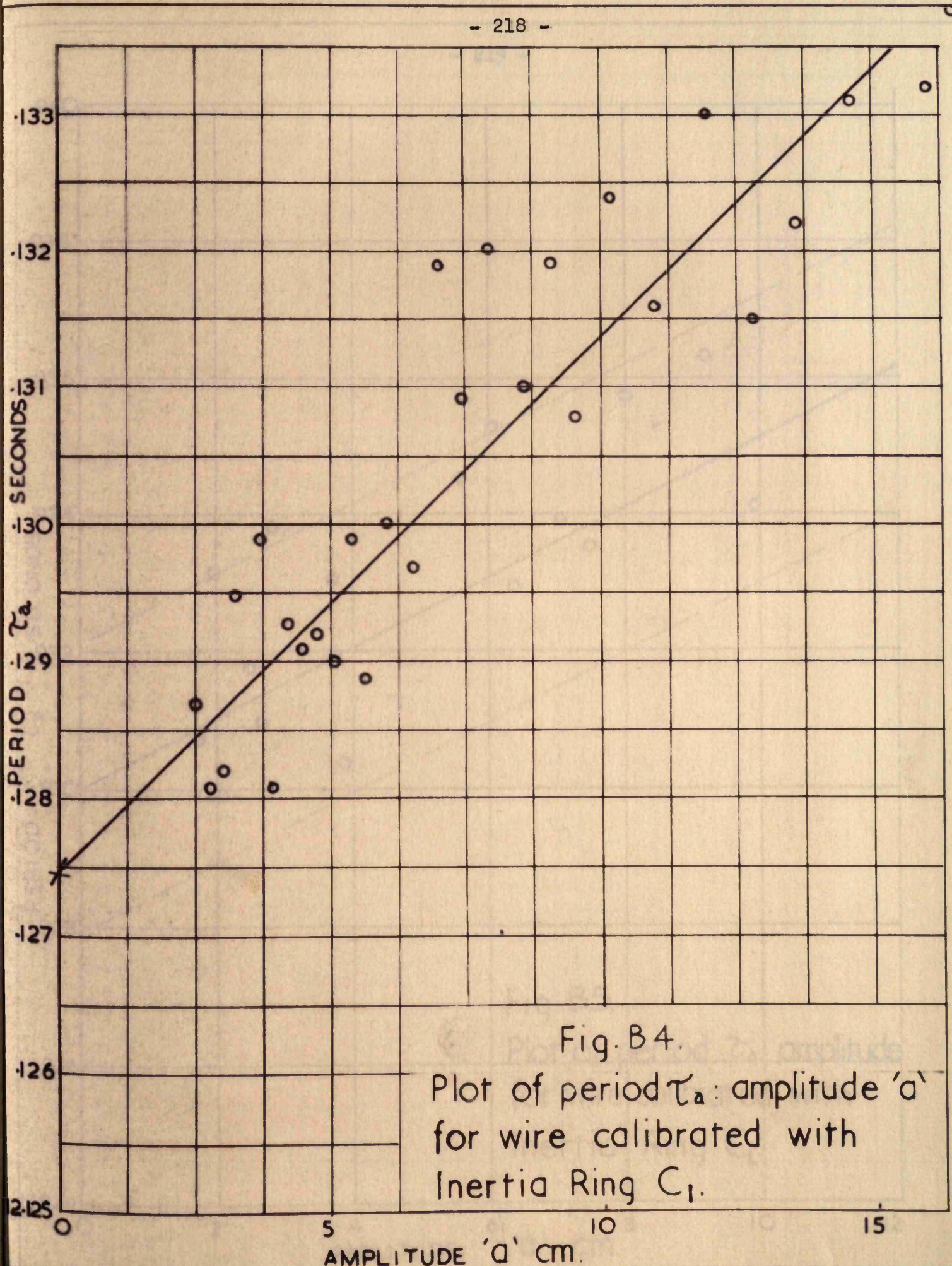

Fig. B4.
Plot of period τ_a : amplitude 'a' for wire calibrated with Inertia Ring C_1.

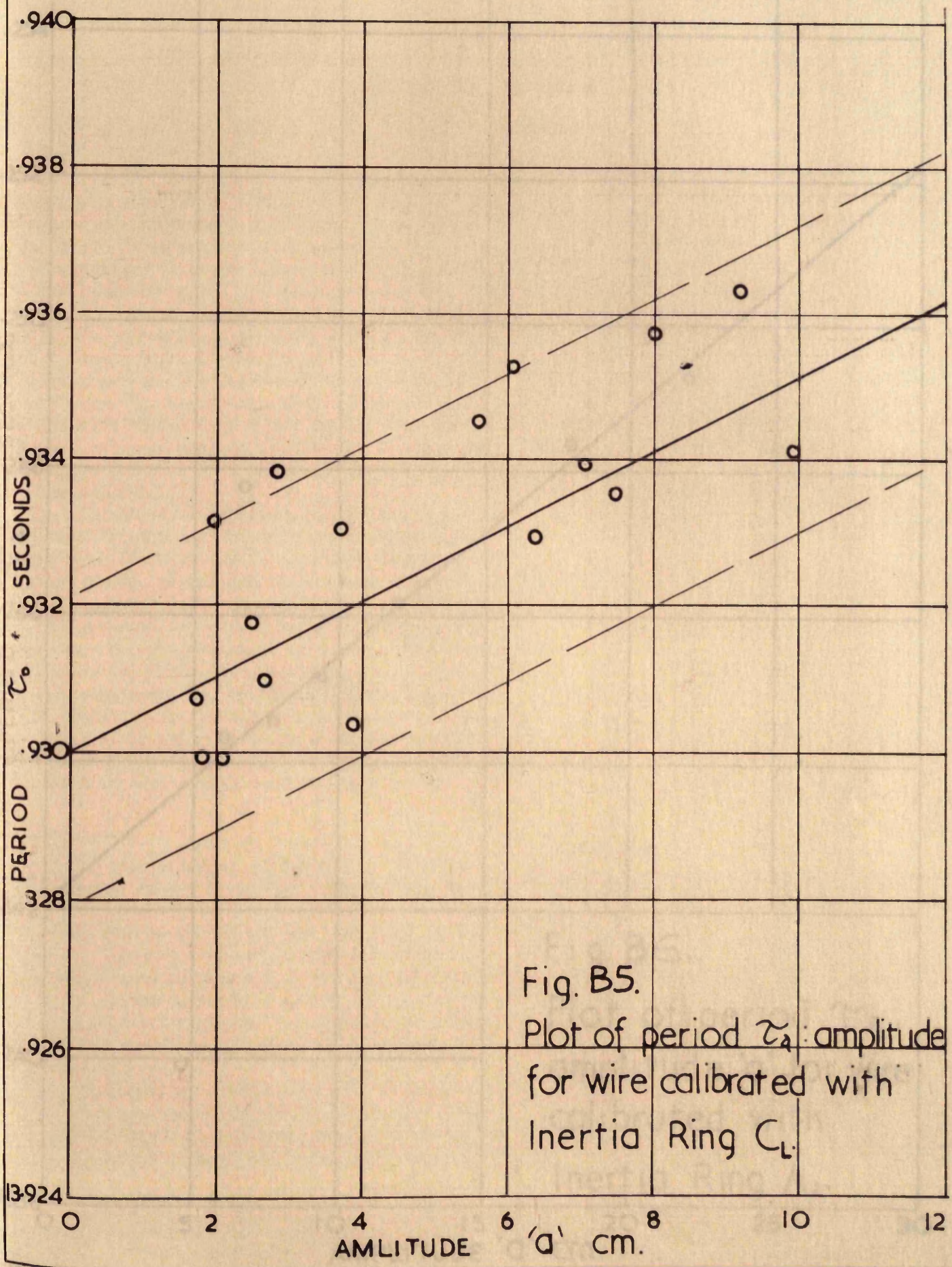

Fig. B5.
Plot of period τ_a : amplitude for wire calibrated with Inertia Ring C_L.

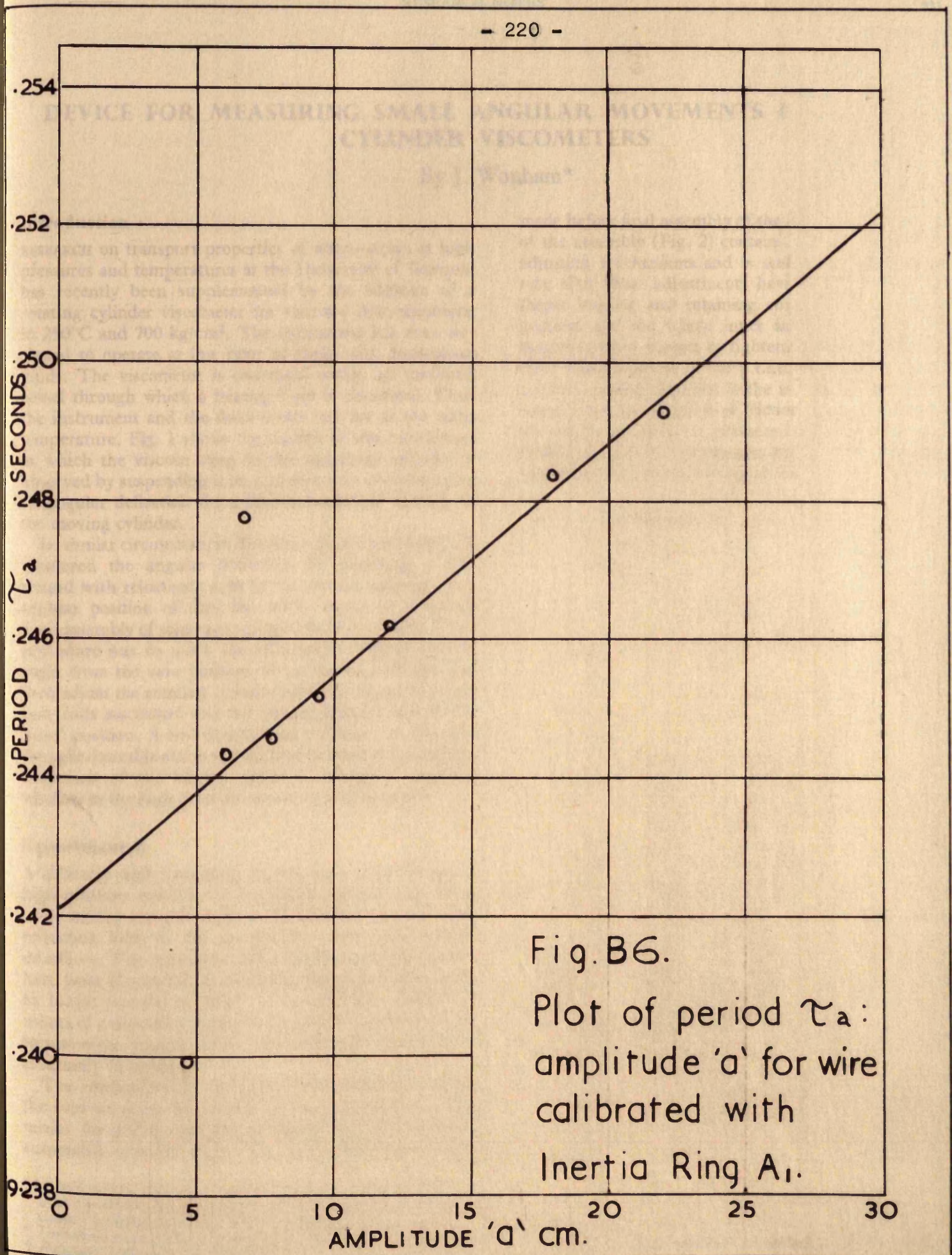

Fig. B6.

Plot of period τ_a: amplitude 'a' for wire calibrated with Inertia Ring A_1.

APPENDIX C

DEVICE FOR MEASURING SMALL ANGULAR MOVEMENTS IN ROTATING CYLINDER VISCOMETERS

By J. Wonham*

Introduction

RESEARCH on transport properties of water–steam at high pressures and temperatures at the University of Glasgow has recently been supplemented by the addition of a rotating cylinder viscometer for viscosity determinations to 250°C and 700 kg/cm^2. The instrument has been designed to operate at low rates of shear with Newtonian fluids. The viscometer is contained within an insulated vessel through which a heating fluid is circulated. Thus the instrument and the fluid under test are at the same temperature. Fig. 1 shows the outline of this instrument in which the viscous drag on the stationary cylinder is observed by suspending it on a torsion wire and observing its angular deflection for a known rotational velocity of the moving cylinder.

In similar circumstances Reamer, Cokelet and Sage (1)† measured the angular deflection by attaching a disc wound with reluctance coils to the torsion cylinder. The angular position of this disc with respect to a second fixed assembly of reluctance gauges could be sensed. Their procedure was to move the reluctance gauges a known angle from the zero position of the torsion cylinder and then adjust the rotating cylinder speed to bring the reluctance coils associated with the torsion cylinder back to the 'zero' position. A less complicated technique to this was thought desirable and it was decided to observe the angular deflection of the torsion cylinder through a sapphire window in the high pressure vessel by optical means.

Experimental

A difficulty with measuring angular movement through a high-pressure window by an optical method (e.g. using scale, mirror and telescope) is the necessity to correct for refraction both at the air–sapphire and sapphire–fluid interfaces. This correction and subsequent possible errors have been eliminated by retaining the torsion cylinder at its initial position as observed through the window by means of a device for adjusting the angular position of the torsion-wire support point. This angular movement is accurately measured.

The mechanism for adjusting the angular position of the support point has in this case been combined with a means for giving vertical and lateral adjustment to the suspended cylinder (these two latter adjustments being made before final assembly of the device). The main body of the assembly (Fig. 2) contains the vertical and lateral adjusting mechanisms and is sealed by means of a lens ring after these adjustments have been completed. The thrust bearing and retaining cover are then placed in position and the whole inner assembly held positively against a p.t.f.e. washer by tightening down eight retaining nuts. The thickness of the p.t.f.e. was adjusted to give a positive vertical restraint to the assembly but freedom to rotate with the minimum of friction. Lateral movement of the whole assembly is prevented by the roller bearing. Sealing is provided by the lens ring at the top and an 'O' ring with anti-extrusion ring at the bottom of the device.

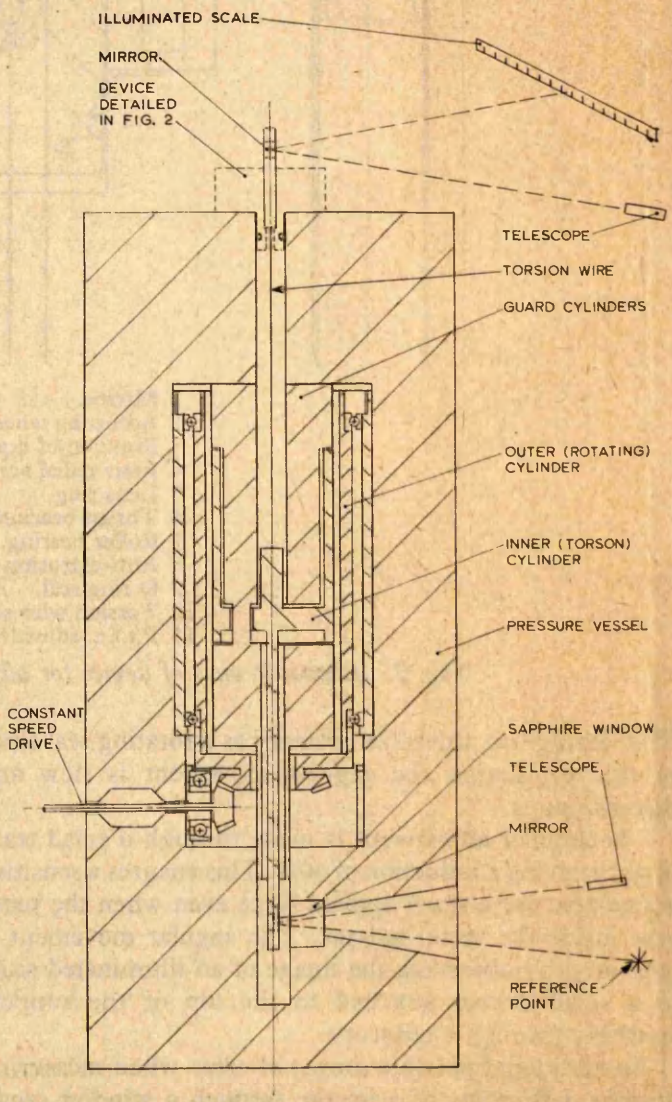

Fig. 1. *Diagrammatic cross-section of viscometer*

The MS. of this Research Note was received at the Institution on 24th September 1964 and in its revised form, as accepted by the Council for publication, on 12th February 1965.

* *University of Glasgow, Mechanical Engineering Research Annexe.*

† *Reference is given at the end of this Note.*

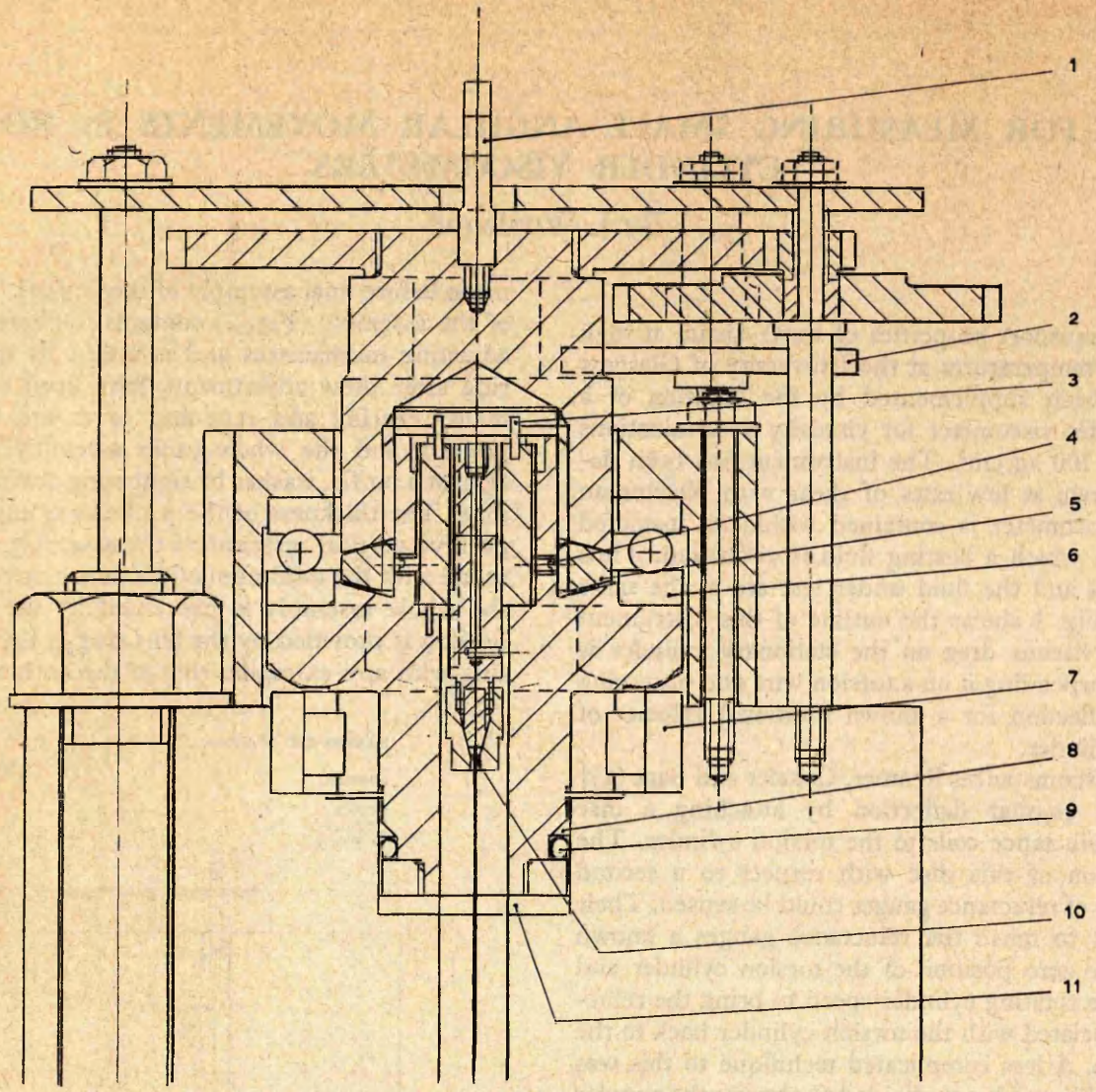

1 Mirror.
2 Adjusting wheel.
3 Rotation of bush by pins gives vertical adjustment.
4 Four radial screws give lateral adjustment.
5 Lens ring.
6 Thrust bearing.
7 Roller bearing.
8 Anti-extrusion ring.
9 O ring seal.
10 Torsion wire support point.
11 P.t.f.e. adjusting washer.

Fig. 2. *Schematic view of device for adjusting the angular position of the torsion cylinder*

This O ring has proved satisfactory as a rotating seal since in this application the angular movement is slow and discontinuous.

The angular adjustment is made through a small train of gears giving a reduction of 40/1. This ensures a sensitive adjustment for a small applied force even when the pressure inside the vessel is large. The angular movement is measured by observing the image of an illuminated scale in a small mirror attached to the top of the support assembly through a telescope.

An additional possible source of error when measuring angular deflections of a mirror through a window could be due to bending of the window as a result of the differential pressure across it. Providing the window is supported symmetrically about its cylindrical axis it is expected that light entering the window along this axis will remain undistorted by bending. Therefore in this device the error does not arise if the telescope and reference point under observation (Fig. 2) are placed in the close vicinity of the window axis.

Results

The device has been tested at ambient temperatures and at pressures up to 330 kg/cm^2 without loss of accuracy. It is limited to this pressure at the moment by the size of the thrust bearing used and the limited space available in

which to locate the assembly on the present apparatus. At all test pressures the support point could be adjusted to within 0°–0′–30″ of the angular position required without difficulty.

It is hoped to extend the pressure range of this type of device to that for which the main pressure vessel of the viscometer has been designed. It is also planned to modify the apparatus for use at temperatures up to 250°C.

Acknowledgement

The present work was performed at the Mechanical Engineering Research Annexe, the University of Glasgow, under the direction of Professor James Small, the James Watt Professor of Mechanical Engineering, with whose consent this note has been submitted. This work has formed a part of the current research investigation on thermodynamic and transport properties now being undertaken by this laboratory and sponsored by C.E.G.B.

REFERENCE

(1) Reamer, H. H., Cokelet, G. and Sage, B. H. *Analytical Chemistry* 1959 **31** (August), 1422.

APPENDIX D

THERMODYNAMICS AND FLUID MECHANICS CONVENTION

Liverpool · 13–15th April 1966

PAPER 9

A rotating cylinder viscometer for measurement at elevated temperature and pressure

J. WONHAM

Advance copy subject to revision. The paper and discussion will be published in Proceedings 1965–66, Volume 180, Part 3J

PUBLISHED BY THE INSTITUTION OF MECHANICAL ENGINEERS
1 BIRDCAGE WALK · WESTMINSTER · LONDON · SW1

The Convention was arranged by the

THERMODYNAMICS AND FLUID MECHANICS GROUP

of the

INSTITUTION OF MECHANICAL ENGINEERS

This paper is intended to be presented for discussion at the Convention, in Liverpool, on 13–15th April 1966. Communications, which should be addressed to R. J. Millson, Editor of Proceedings, must reach the Institution by 27th May 1966.

Paper 9

A ROTATING CYLINDER VISCOMETER FOR MEASUREMENT AT ELEVATED TEMPERATURE AND PRESSURE

By J. Wonham*

This paper records some of the recent experimental methods used to determine the viscosity of water. In drawing attention to the many techniques used (most relying upon calibration of the instrument by a fluid of known viscosity), the conclusion may be drawn that an absolute instrument is required which will produce results over a wide range of temperature and pressure.

It has long been known that the rotating cylinder viscometer is capable of a high degree of accuracy, but technical considerations have, in the past, restrained most workers from pursuing this method at high pressures.

Progress in the development of the rotating cylinder instrument for these conditions is described and specific problems encountered with this method are discussed.

This work is a continuation of the design studies of Kjelland-Fosterud (1)† and Whitelaw (2) who both gave considerable thought to the problems associated with this type of instrument. The first instrument to be tested by the author was based on Whitelaw's design but it was found that certain aspects of this instrument required major alteration. A new instrument was set up and has been found suitable for accurate viscosity determination.

INTRODUCTION

THE MAIN EFFORT IN viscosity measurement of water substance in recent years has been directed towards supercritical steam and also steam at atmospheric pressure and temperatures up to 1100°C. This work has been well described by Whitelaw (2) and Latto (3).

Experimental determination of the viscosity of liquid water is not so comprehensive as that for steam. When considering this region, it is convenient to divide it into two parts:

(1) Viscosity of liquid water in the range 0°–100°C at 1 atmosphere pressure and along the saturation line above 100°C.

(2) Viscosity of compressed liquid in the temperature range 0°–300°C, and at pressures up to 800 kg/cm^2.

Notable contributions in this field are listed in Table 9.1. The measurements of Moszynski with the oscillating sphere instrument may be considered absolute, and are claimed to have an accuracy of ± 1 per cent, but these results would seem to be about 2 per cent low when extrapolated to 20°C and compared with the N.B.S. value.

Bruges (12) points out that more experimental work is needed in this region to remove the inconsistencies. These make correlation of the existing data extremely difficult without resorting to 'weighting' certain of the measurements. Bruges's report also indicates that the works of Weber and Swindells *et al.* permit the tabulation of values from 0° to 40°C with an uncertainty of ± 1 part in 500. Measurements made with rotating cylinder viscometers by Bearden (13) and other workers measuring the viscosity of air, indicate that this level of accuracy can be achieved by the rotating cylinder method.

There are at least two rotating cylinder instruments which have been used at high temperatures and pressures. Thomas, Ham, and Dow (14) tested lubricating oils up to 3000 kg/cm^2 and 250°C with an accuracy of about 4 per cent. The drive motor for the rotating cylinder was completely immersed in the pressure vessel, and the heat generated by the motor appears to have made accurate temperature control difficult. The angular deflection of

The MS. of this paper was first received at the Institution on 29th October 1965 and in its revised form, as accepted by the Council for publication, on 28th December 1965.

* *Mechanical Engineering Research Annexe, University of Glasgow, Glasgow 3.*

† *References are given in Appendix 9.II.*

Table 9.1

Author	Reference	Method	Pressure, atm	Temperature, °C	Comments
Swindells, Coe, and Godfrey.	4	Capillary	1	20	Quoted accuracy for water at 20°C, 0·05 per cent
Roscoe and Bainbridge.	5	Oscillating spherical vessel	1	20	A value for water of 1·0025 ± 0·0005 cP at 20°C
Timrot and Khlopkina.	6	Capillary	90–500	18–300	—
Weber	7	Falling ball	0–500	0–160	—
Moszynski	8	Oscillating sphere	3–340	20–185	Quoted accuracy ±1 per cent
Schmidt and Mayinger	9	Capillary	57–741	78–300	—
Tanaka *et al.*	10	Capillary	1–232	12–263	Probable accuracy 1·6 per cent
Cappi	11	Falling body	0–10 000	0–100	—

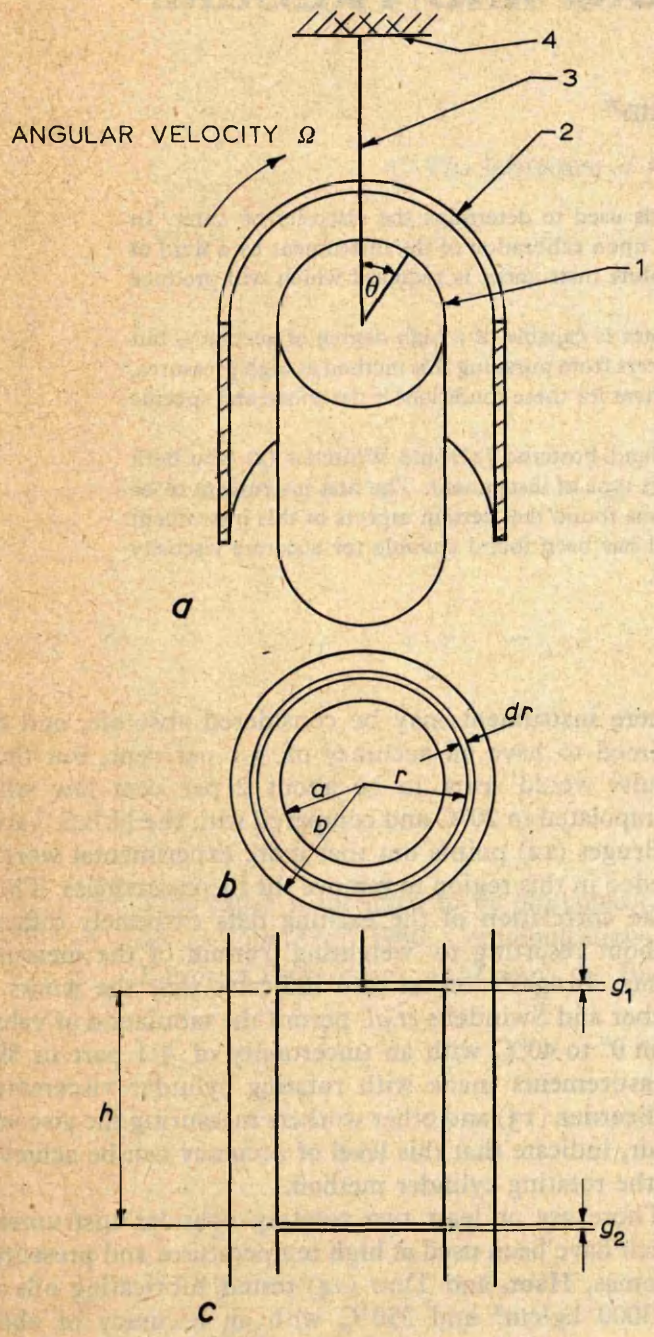

a Principle of operation.
b Arrangement for Couette flow.
c Guard cylinders.

Fig. 9.1

the inner cylinder was measured externally by observing the change of resistance of an alloy resistance wire. This was fastened into the cylinder in such a way that the measured resistance increased proportionally with the angle of displacement.

More recently, Reamer, Cokelet, and Sage (**15**) have measured the viscosity of *n*-pentane at pressures up to 5000 lb/in^2 and between 0°–500°F with a rotating cylinder instrument claiming a probable accuracy not exceeding 0·4 per cent. This is a highly developed instrument, and this claim appears to be justified.

With these experiments in mind, it would appear that the technical difficulties are not insurmountable.

METHOD

The principle of operation is shown in Fig. 9.1*a*. A cylindrical sleeve 2 clears the inner cylinder 1 by a radial distance of approximately 2 mm. Cylinder 2 is rotated at constant angular velocity by means not illustrated.

The inner cylinder is supported by a Nimonic 90 suspension wire shown as 3. This in turn is attached to the support 4. The entire instrument is submerged in the fluid, the viscosity of which is to be measured.

As a result of rotation of cylinder 2 about the inner cylinder 1, a drag is produced upon the latter. This induced torque on cylinder 1 results in an angular deformation of the suspension 3. Therefore the rotation of cylinder 2 is reflected as an angular displacement of cylinder 1, shown by the angle θ. As long as laminar flow exists in the annular space between cylinders 1 and 2, and the deformation of the suspension wire obeys Hooke's law, the angular displacement θ is directly proportional to the absolute viscosity.

SIMPLE THEORY

Only the elementary treatment of this method of flow is given here. Fig. 9.1*b* shows the arrangement for Couette flow where a volume element is indicated at some radius r.

From the definition of viscosity, it follows that for a Newtonian fluid the shear at any point may be related to the viscosity and the velocity gradient by equation (9.1).

$$\tau = \eta r \frac{d\omega}{dr} \quad . \quad . \quad . \quad . \quad (9.1)$$

but $$\tau . 2\pi rh . r = T$$

where T is the torsional moment attributable to the viscous drag.

$$\therefore \frac{T}{2\pi r^2 h} = \eta r \frac{d\omega}{dr}$$

$$\therefore \frac{d\omega}{dr} = \frac{T}{2\pi r^3 h\eta}$$

Integrating across the annular gap and applying boundary conditions

$$\omega = 0 \quad \text{when} \quad r = a$$

and $$\omega = \Omega \quad \text{when} \quad r = b$$

$$\int_0^{\Omega} d\omega = \frac{T}{2\pi h\eta} \int_a^b \frac{1}{r^3} dr$$

$$\therefore \Omega = \frac{T}{4\pi h\eta} \left[\frac{b^2 - a^2}{a^2 b^2}\right]$$

i.e. $$\eta = \frac{T}{4\pi h\Omega} \left[\frac{b^2 - a^2}{a^2 b^2}\right] \quad . \quad . \quad (9.2)$$

Guard cylinders have been included in the design, see Fig. 9.1*c*, to eliminate the torsional drag on the end surface of the inner cylinder. Nevertheless, a correction must be applied owing to the gaps g_1 and g_2 between the inner cylinder and the guards. The end correction for rotation viscometers derived by Roscoe (**19**) is not relevant where guard cylinders are provided, although it would be a useful exercise to verify his theoretical solution experimentally.

A correction for these gaps has been arrived at theoretically by Houston (**16**) who concluded that 0·47 of the sum of the gaps should be added to the inner cylinder length to give the effective length of the inner cylinder L. In this case the sum of the gaps is 0·05 cm where the length of the inner cylinder is 8 cm. Only a very small error is introduced if the effective length, making allowance for the gaps, is taken to be L, where

$$L = 0{\cdot}5(g_1 + g_2) + h$$

i.e. this infers that the viscous drag owing to the gap is shared equally between the suspended cylinder and the guard cylinder at each end.

Thus

$$\eta = \frac{T}{4\pi L\Omega} \left[\frac{b^2 - a^2}{a^2 b^2}\right] \quad . \quad . \quad . \quad (9.3)$$

A convenient way of using this viscosity equation is to introduce two constants F and K, where F is the torsional constant of the suspension wire:

$$\frac{T}{\theta} = F$$

and where K is dependent on the dimensions of the instrument,

$$K = \frac{1}{L} \left[\frac{b^2 - a^2}{a^2 b^2}\right]$$

Assuming the time for one revolution of the outer cylinder as t, then

$$t = \frac{2\pi}{\Omega}$$

Substituting for F, K, and Ω in equation (9.3) gives

$$\eta = \frac{KF\theta t}{8\pi^2} \quad . \quad . \quad . \quad . \quad (9.4)$$

The determination of viscosity by this method will therefore depend on the accuracy of obtaining K, F, θ, and t.

EXPERIMENTAL ARRANGEMENT

The detailed arrangement of the viscometer is shown in Fig. 9.2. The rotating cylinder 1 runs in bearings located in a sleeve 2. This sleeve is a sliding fit into the bore of the cylindrical pressure vessel 3. A bevel gear 4 is fitted to the bottom of the rotating cylinder which transmits the constant speed drive provided by the shaft and pinion 5.

A heavy steel table 6 is weighted with sand-bags. The pressure vessel is fixed to the table by three studs and is adjusted to stand vertically by introducing packing shims under three equally spaced legs 7. A high pressure sapphire window 8 allows a mirror 9 to be observed from some suitable position.

Also standing on the legs is a double-walled copper jacket 10 which is to provide a constant temperature bath for heating the instrument and the test fluid contained therein. The parts so far described can be assembled and need little attention once assembly has been satisfactorily achieved. The remaining parts are also assembled as a complete unit and final assembly can then take place. This unit comprises the cover-plate 11 held by eight studs 12 and sealing on a Delta-ring 13. Screwed into the lower side of the cover is the guard cylinder assembly 14 which is in two parts held accurately together by three equally spaced distance pieces 15. The inner cylinder has first to be suspended from the support assembly before the lower guard can be placed in position.

The lower guard is extended downwards to protect the mirror-holding stem from any turbulence in the fluid caused by the moving parts. This guard also allows thermocouples 18 to be introduced through the bottom of the instrument and into the fluid under test, although this has proved a difficult assembly problem.

The radial position of the support assembly is adjustable through a small chain of reduction gears 19. An adjusting spindle emerges through a rotating seal in the top cover of the fluid-bath as does the upper mirror stem 20. (These details are not shown.) The details of this support assembly have been previously described (**17**).

Heating system

The bath around the instrument is double walled. Heating fluid is circulated such that it enters through the bottom of the jacket at three positions A (see Fig. 9.2) passing up between the inner wall and the outer surface of the pressure

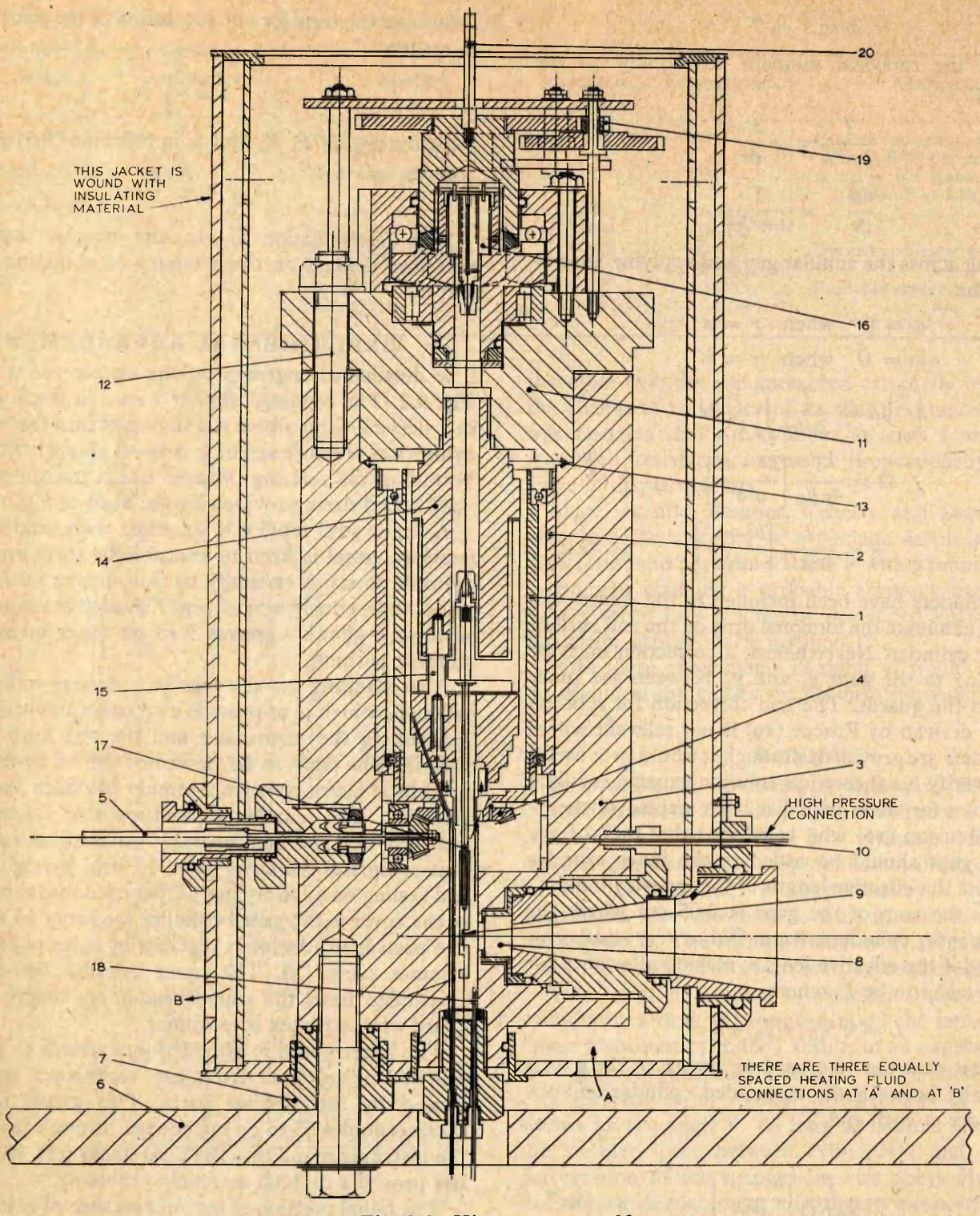

Fig. 9.2. Viscometer assembly

vessel. At the top it passes through ports into the space between the two walls of the vessel, and out at three equally spaced positions *B*. This arrangement has been designed to keep the flow of fluid evenly about the instrument, thus ensuring a well-distributed heating effect.

Up to the present, water has been used for heating the apparatus, thus limiting the present measurements to 100°C (see Appendix 9.I). The static seals can be easily modified using polytetrafluorethylene (p.t.f.e.) O-rings for operating the instrument up to 250°C with Thermex heating fluid. The rotating seals, which are at present of a rubber compound are to be changed for small stuffing boxes making use of braided p.t.f.e. Most rubber compounds cannot be used with Thermex.

The circulating fluid is heated in a separate vessel by means of a 3-kW immersion heater made as a single unit but with separate terminals for each of the three 1-kW elements. The elements are sheathed in 'Inconel' tube and

are suitable for temperatures above 250°C. At present the upper 1-kW element is supplied by power switched by a toluene regulator. The other two elements are controlled manually using a Variac. Maximum power for these elements is only required during initial heating to the working temperature; at this stage power is reduced to the level where the thermostatic control of the toluene regulator can best meet the remaining heat requirement.

TEMPERATURE MEASUREMENT

The importance of accurate measurement of temperature cannot be overstressed. Initial heating tests on the apparatus have depended entirely upon two sheathed chromel–alumel thermocouples which are located on the upper face of the lower guard cylinder. These are introduced through a Conax-type seal at the bottom of the instrument, and along slots cut into the sides of the mirror-stem guard extension. At present tests are being carried out with thermometers (mercury in glass) fitted into wells from the top cover of the heating jacket.

It is thought that, since the apparatus is almost completely enclosed within the thermostatically controlled bath, the test fluid and the heating fluid around the instrument will be at the same temperature. If this is the case less importance may be attached to thermocouple readings taken at points within the test fluid and more accurate measurements can be made either with a Beckman thermometer or with a platinum resistance thermometer. These will be located in the bath near the wall of the pressure vessel.

THE PRESSURE SYSTEM

This is basically the same as that used by Whitelaw and by Venart (**18**) in his thermal conductivity rig. A Budenberg dead-weight gauge is used to pressurize oil on one side of a rubber interface (a hydraulic accumulator cylinder containing a rubber bulb has been modified for this purpose). The pressure is also indicated by a Bourdon gauge fitted in the line. The pressure connection is into the side of the vessel but the top mirror stem can be removed to facilitate initial evacuation of the vessel and to act as a bleed for any air which remains in the system during filling.

The constant speed drive

Although individual readings are made at a constant angular velocity of the rotating cylinder, it is desirable to make readings at several different speeds and also when rotating in the reverse direction. This eliminates the effect of any 'set' in the suspension wire which could cause error in the value obtained for θ. With these considerations in mind, an infinitely variable speed hydraulic gear was obtained driven by a three-phase synchronous motor through a timing-belt. The speed of this unit can be varied from 0 to 1000 rev/min in either direction. The angular velocity of this output shaft is measured by an electric tachometer which produces 120 pulses for each revolution of the shaft.

These are counted by an electronic counter, and experiments have shown that the speed remains remarkably steady—not varying by more than 1 or 2 parts in 2000 over several minutes. This speed is reduced by a 10:1 reduction gear and a further 2:1 reduction is produced by the bevel gears inside the vessel. Thus the actual speed of the outer cylinder can be varied from 0 to 50 rev/min in either direction.

METHOD OF MEASURING θ

A 'null' method of measuring the angular movement of the inner cylinder has been developed. This technique entails that the inner cylinder be kept at its initial position (as seen through the window in the pressure vessel) by rotating the support-assembly of the suspension wire. The angular movement of this assembly is measured by means of a telescope, mirror, and scale. This mirror is attached to the top mirror stem as previously described.

This procedure has the advantage that no angular measurements are made through the window, thus eliminating the need for corrections owing to refraction. A 2-metre, machine-divided precision scale has been mounted such that it forms an arc of radius 300 cm about the centre of the instrument. This was achieved by mounting the scale in clamps at accurately drilled points along the arc on a rigid table. Once the scale had been set up, the position of the table was adjusted until the centre and ends of the scale were equidistant from the centre of the viscometer. This was achieved by mounting a rod 300 cm long horizontally in a suitable stand. Observation of the position of the inner cylinder is by a second telescope, mirror, and scale arrangement, this mirror being attached to a stem extending from the bottom of the inner cylinder. Both scales are illuminated so that the divisions are clearly visible.

EXPERIMENTAL PROCEDURE

Considering again equation (9.4)

$$\eta = \frac{KF\theta t}{8\pi^2}$$

the procedure will be outlined for the determination of each of these parameters.

K: This is a constant depending upon the dimensions of the instrument. The external diameter and length of the inner cylinder have been accurately measured using an electrical comparator and slip gauges. The bore of the rotating cylinder has been measured with an internal micrometer at several positions and the mean diameter calculated. At present this dimension is known with the least accuracy and will be checked using other methods. Measurements are made at intervals along the cylinders and around the circumference. The mean and standard deviations are then calculated. The distance between guard cylinders has been measured and the faces checked for parallelism and alignment, using a travelling microscope and shadow-graph techniques. Deviations as small as 0·000 05 in can be determined in this way. Roundness

checks have been made using a Talyrond instrument. All the measurements have been made in a gauge room maintained at 68°F.

F: The inner cylinder and suspension wire can be oscillated torsionally. The torsional constant for the wire may be derived from the simple formula:

$$F = \frac{4\pi^2 I_c}{T_c^2}$$

where F is the torsional constant; I_c the moment of inertia of the inner cylinder; and T_c the periodic time of torsional oscillations of the system.

This formula does not consider the effect of damping on the system. It was decided to reduce the effect of damping to a negligible amount by timing the oscillations in a vacuum vessel. This apparatus is shown in Fig. 9.3. Evaluation of I_c has also been made using torsional oscillations. The procedure is described by Bearden (13), in

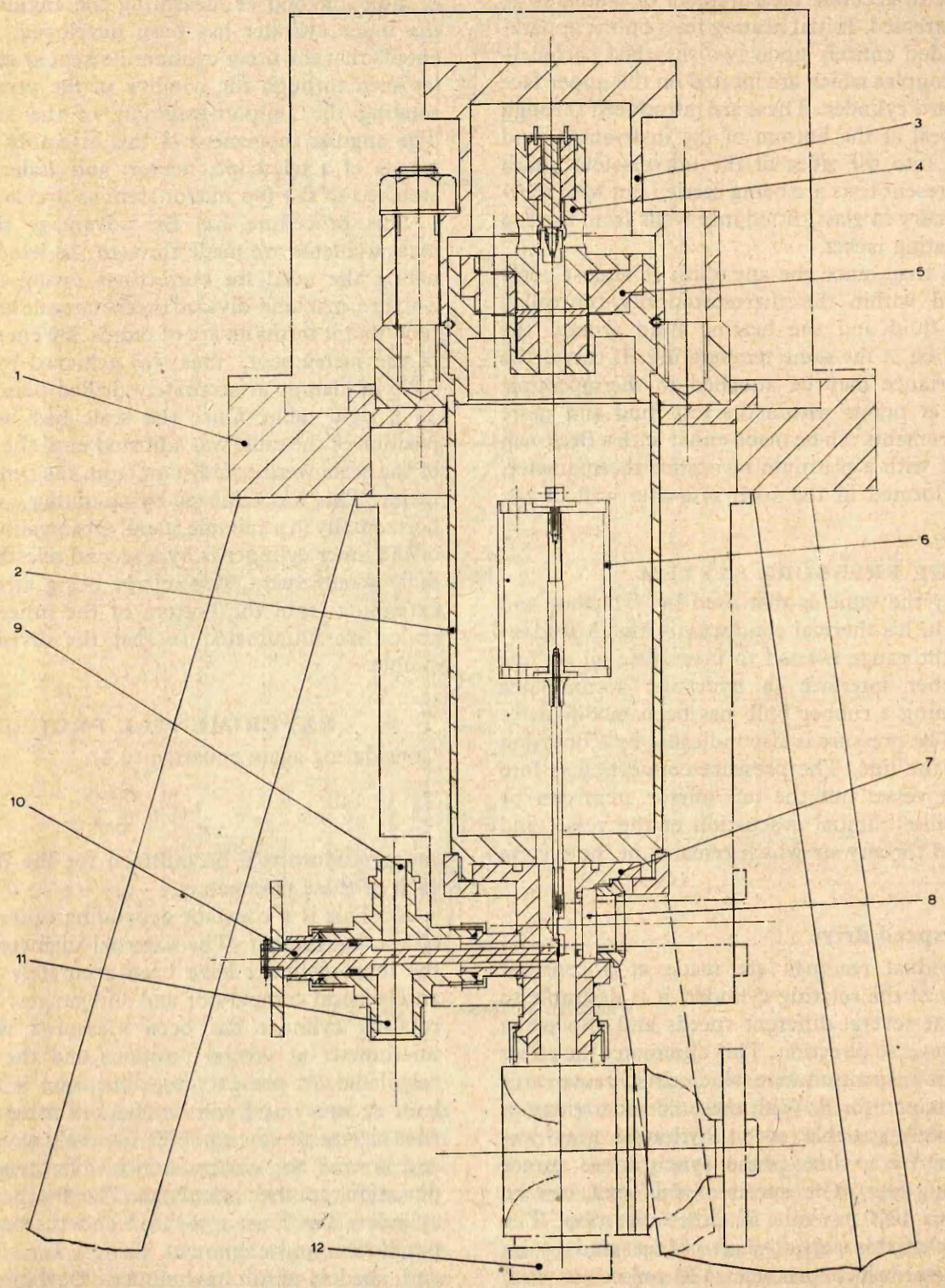

Fig. 9.3. Vacuum vessel for calibrating the suspension wire, vacuum better than 10^{-4} torr

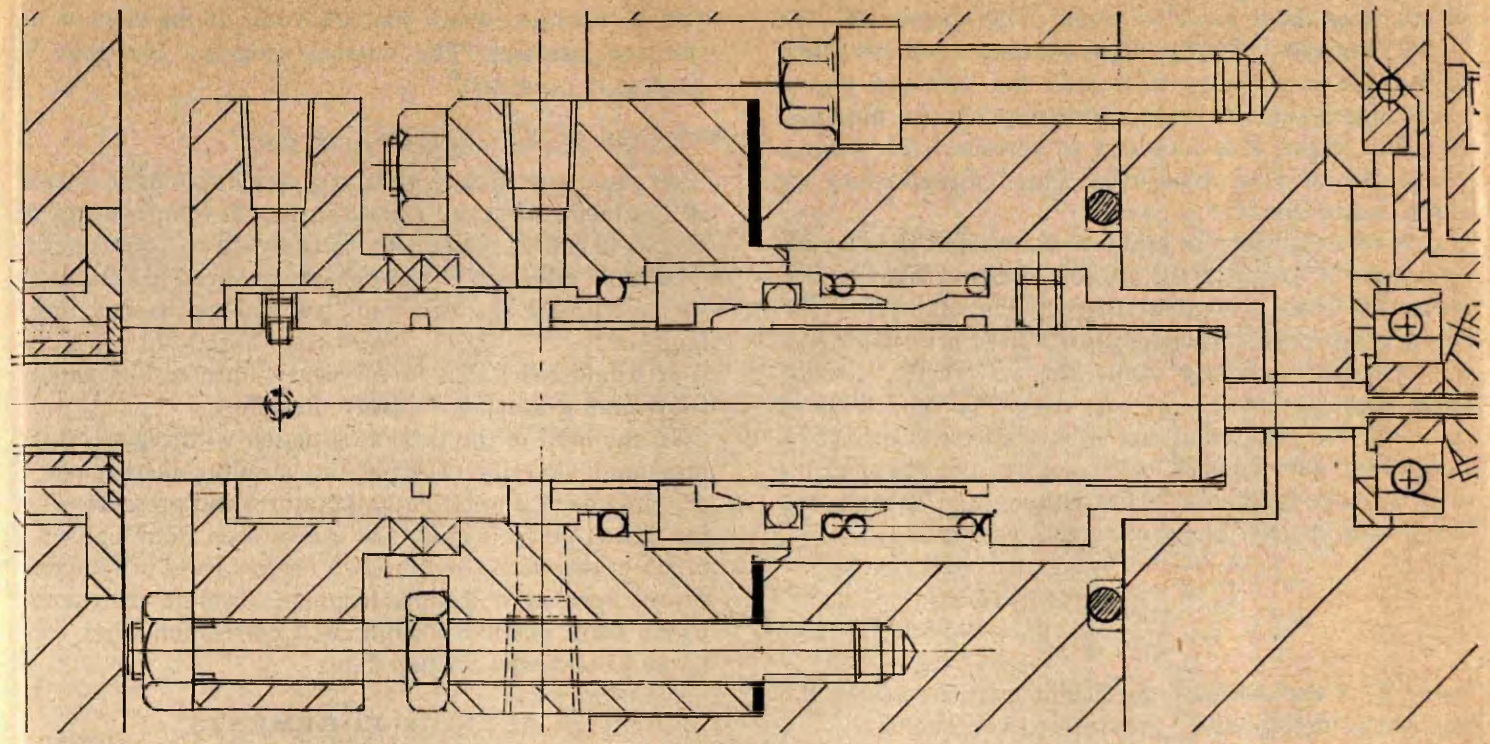

Fig. 9.4. Mechanical seal for operation at 3500 lb/in², 250°C, and speeds up to 100 rev/min

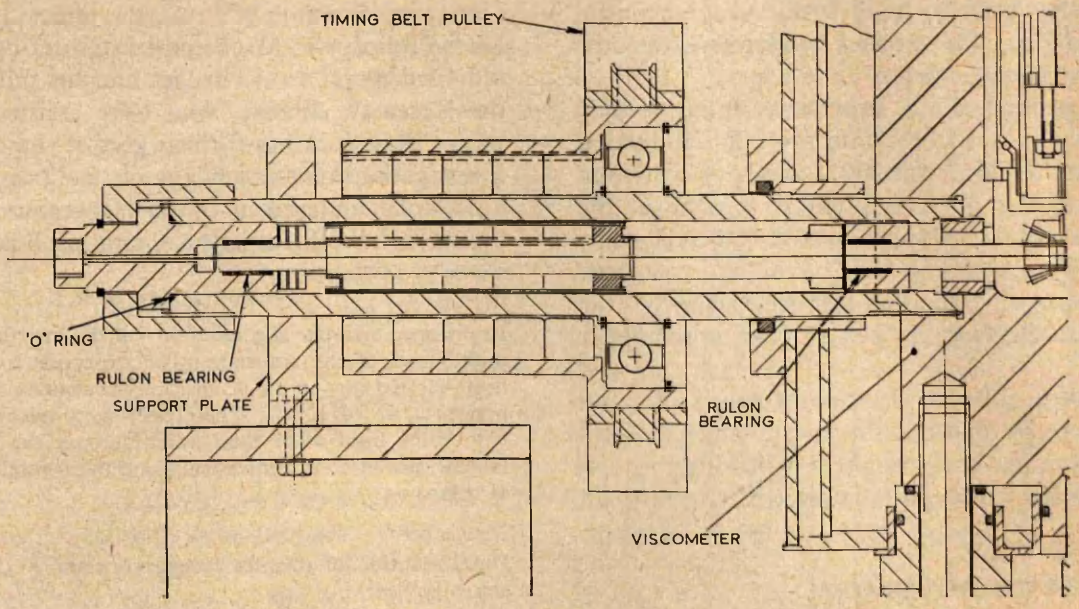

Fig. 9.5. Magnetic drive

which the period of oscillation is measured for objects of calculable moments of inertia. Hence the torsional stiffness of the wire becomes known and can be used to obtain the moment of inertia of a more complex shape, where the periodic time is measured for this object also.

$$F = \frac{I_c}{T_c^2} = \frac{I_k}{T_k^2}$$

$$I_c = I_k \left[\frac{T_c}{T_k}\right]^2$$

Thus I_c can be found if I_k is of known moment of inertia.

This procedure is slightly complicated by the presence of the stem which is used to locate the suspended objects and which holds the small mirror at the lower end. The value of I for this can either be calculated or found experimentally and must then be included in the total moment of inertia of any suspended system under test. The times of torsional oscillations have been measured using the amplified pulse from a photo-electric cell to start and stop an electronic timer. This method is accurate to 1 part in 10^5. Experiments have been carried out to investigate the possible effects of varying the periodic times, and the mass, of bodies of calculated moments of

inertia upon the torsional constant of the suspension wire. It has been concluded that these changes in the behaviour of the wire are likely to be so small that only with precise temperatures control can any exact results be obtained. For this reason it is intended to surround the vacuum vessel with an isothermal bath. This is indicated by the chain-dotted line in Fig. 9.3.

It is also necessary to calibrate the torsion wire for the temperatures at which the viscosity measurement is to be made. Up to the present, at elevated temperature, oscillation timings of the suspended system have been made with the cylinder oscillating inside the viscometer. Ideally, these measurements on the wire should be carried out in the evaluated calibration rig, although by measuring the logarithmic decrement of oscillations in the viscometer a fairly accurate estimation of the damping can be made and thus F can be determined using the relationship:

$$T_c = \frac{2\pi}{\left(\frac{F}{I_c} - \frac{K^2}{4I_c^2}\right)^{1/2}}$$

where K is the damping coefficient calculated from the logarithmic decrement of the damped oscillations.

At the start of a test, the initial positions of the top and bottom mirror stems are recorded. The required angular velocity of the outer cylinder is set by the manual control on the hydraulic gear. The value t is obtained from the reading given by the tachometer.

The angular position of the support assembly is then adjusted by means of a 4·75 rev/min reversible induction motor, which acts through the 200:1 chain of reduction gears. Thus, once the outer cylinder is rotating at the desired speed the inner cylinder can be returned to its initial position by controlling this motor and watching through the telescope. Once this has been achieved, the angle θ can be deduced from the new reading on the upper scale.

This procedure is repeated for several values of t and θ in both directions of rotation. The mean values of t and θ can be taken from the best straight line passing through a plot of the recorded values and the value of viscosity can be calculated.

FUTURE DEVELOPMENT

The drive shaft seal illustrated in Fig. 9.2 is unsuitable for high pressures. For this reason it is soon to be replaced by the mechanical seal shown in Fig. 9.4. This has been designed by the makers for operation up to 250°C and 240 kg/cm². With this modification completed, results should soon be available over this range of test conditions. A further development is to be introduced with a new viscometer, having a slightly larger diameter pressure vessel. This is the magnetic drive illustrated in Fig. 9.5. The new instrument with this drive will have tremendous advantages over the present arrangement and has been designed for measurements to 1000 kg/cm².

By surrounding the suspension wire calibration vessel with an isothermal bath, considerably more information will be obtained about the behaviour of the wire at the test temperatures. The torsional constant can then be accurately predicted.

CONCLUSION

This paper describes an apparatus which should be capable of producing viscosity measurements at temperatures up to 250°C and at pressures ultimately up to 1000 kg/cm². The main effort up to the present has been in setting up the instrument and overcoming initial mechanical problems.

It would seem that in the near future results will be forthcoming which will justify this effort.

In the light of the present situation with regard to the measured viscosity of water, an absolute instrument is certainly needed to cover temperatures and pressures over the widest possible range. As can be seen from Table 9.1 much of the work covers only a narrow band of temperature or pressure. Results from an absolute instrument would make possible a more exact correlation when considered beside the existing data.

ACKNOWLEDGEMENTS

The present work was performed at the Mechanical Engineering Research Annexe, University of Glasgow, under the direction of Professor James Small, the James Watt Professor of Mechanical Engineering. The author is indebted to Dr E. A. Bruges and his other colleagues at the Research Annexe, who have assisted him in many ways. This work has formed part of the current research investigations on thermodynamic and transport properties now being undertaken by this laboratory and sponsored by the Central Electricity Generating Board.

APPENDIX 9.I

In order to estimate the suitability of the instrument and to make initial tests of the accuracy to be expected, measurements have been carried out on air at ambient conditions and at a few temperatures up to 100°C. These tests were necessarily carried out with some fluid other than water because the first bearings obtained were in non-stainless steel and there would have been a risk of corrosion.

Results

Determination of the instrument constant K (linear dimensions are in inches):

Inner cylinder diameter $(2a)$ = 1·9686
Outer cylinder diameter $(2b)$ = 2·1649
Inner cylinder length = 3·1534
Distance between cylinders = 3·1696
$L = 3{\cdot}1534 + \frac{1}{2}(3{\cdot}1696 - 3{\cdot}1534) = 3{\cdot}1615$

$$K = \frac{1}{L}\left[\frac{b^2 - a^2}{a^2 b^2}\right] = 3{\cdot}4486 \times 10^{-3}$$ converted to cm units.

Determination of F:

The moment of inertia of the mirror stem has been determined by comparing times of torsional oscillations with two inertia rings, designated A_1 and A_2. The moments of inertia of these rings, notation I_{A1} and I_{A2}, have been calculated from the mass M and the measured outer diameter D and inner diameter d where it can be shown that

$$I = \frac{M}{8}(D^2 + d^2)$$

These values are listed in Table 9.2.

Discussion

Dr D. J. Ryley, M.Sc.(Eng.), C.Eng., M.I.Mech.E.—Referring to paper 9, I would suggest that as a consequence of the relative movement of the walls bounding the test liquid, paddle work will be done on the liquid. This will tend to cause a rise in temperature and a consequent modification to the viscosity. Has the author considered the error thus introduced, or is the effect too trivial to merit a correction?

Mr J. Wonham—Dr Ryley has raised a pertinent question regarding shear heating in the annular space between the cylinders. The temperature rise may be calculated using the method described by Bjørnståhl* and the differential equation giving the temperature distribution across the annular gap has been solved by Weltmann and Kuhns† using a method of successive approximations. However, with the low rates of shear occurring in this instrument the calculated shear heating effect is extremely small and, with the frictional heat of the bearings, is likely to be conducted into the large mass of metal constituting the cylinders and pressure vessel with negligible effect on the temperature of fluid under test. Nevertheless, it is considered necessary to locate the thermometer as near as possible to the fluid sample under test. Mehrishi and Lorimer‡ have described rotating contact thermocouples attached to the rotating cylinder, the electromotive forces being conducted away through concentric mercury troughs in the base of the instrument. Such a technique as this would be difficult to apply in the limited space available within a pressure vessel and it is likely that mercury vapour would contaminate the sample at elevated temperatures.

In the apparatus described here, overall temperature stability has been achieved by surrounding the instrument with a thermostatic jacket. Thermocouples have been introduced into the close proximity of the fluid sample under test (i.e. at the top surface of the lower-guard cylinder) giving an accurate record of the temperature at which the viscosity is measured. Under these experimental conditions the effects of shear heating are considered to be accounted for reasonably well.

* BJÖRNSTÅHL, Y. *Z. Phys.* 1942 **119**, 245.
† WELTMANN, R. N. and KUHNS, P. N. *J. Colloid Sci.* 1952 **7**, 218.
‡ MEHRISHI, J. N. and LORIMER, J. W. *J. Sci. Instrum.* 1965 **42**, 173.

Table 9.2

Inertia ring	Mass, g	D, in	d, in	I, g cm^2
A_1	372·53	1·6256	0·1875	804·50
A_2	305·58	1·4716	0·1875	542·34

Table 9.3

Suspended system	Periodic time	
	Notation	Sec
Mirror stem + A_1 . . .	T_1	13·925
Mirror stem + A_2 . . .	T_2	11·443
Mirror stem	$T_{\Delta I}$	1·244

The two inertia rings were assembled with the mirror stem and suspended in turn from a suitable torsion wire. Then torsional oscillations were timed.

The mirror stem forms part of the oscillating system in each case and its moment of inertia ΔI can be calculated by measuring the period of oscillation of this stem alone. These times are listed in Table 9.3.

Using the times listed in Table 9.3 and the values of I recorded in Table 9.2, ΔI has been calculated from:

$$\Delta I = I_{A1}\frac{T_{\Delta I}}{T_1^2 - T_{\Delta I}^2} = 6{\cdot}468 \text{ g cm}^2$$

$$\Delta I = I_{A2}\frac{T_{\Delta I}}{T_2^2 - T_{\Delta I}^2} = 6{\cdot}482 \text{ g cm}^2$$

ΔI has been taken as the average of these two values:

$$\Delta I = 6{\cdot}475 \text{ g cm}^2$$

[N.B.—When this value of ΔI is added to I_{A1} and I_{A2} to give the moments of inertia I_1 and I_2 of the two suspended systems, the values of I_1/T_1^2 and I_2/T_2^2 agree to within 0·2 per cent. Thus ΔI is considered to be known with sufficient accuracy.]

Having now determined ΔI, the moment of inertia of the inner cylinder assembly, I_c, can be calculated from

$$I_c = I_2\left[\frac{T_c}{T_2}\right]^2$$

where T_c is the periodic time of torsional oscillations of assembly I_c

$$T_c = 19{\cdot}133 \text{ sec}$$

giving $$I_c = 1532{\cdot}7 \text{ g cm}^2$$

A different wire to the one used in the above tests was used in the following viscosity determination. The periodic time used to calculate F in this case is for the inner cylinder assembly, inertia I_c

$$T = 17{\cdot}230 \text{ sec}$$

The angular deflection of the inner cylinder is given by the movements of the scale image observed in the mirror attached to the top of the suspension assembly. The electronic tachometer gives a value N to the counter-reading. Values of δ and N are recorded in Table 9.4.

Evaluation of viscosity from results:

$$\eta = \frac{KF\theta t}{8\pi^2}$$

$$= \frac{KI\theta t}{2T^2}$$

where $$\theta = \frac{\delta}{600} \quad \text{and} \quad t = \frac{2400}{N}$$

Table 9.4

Direction of rotation	N	Deflection, δ, cm
First run—clockwise	404	2·10
	795	4·10
	1198	6·30
anti-clockwise	403	2·00
	803	4·10
	1202	6·20
	1603	8·25
	2000	10·35
Second run—anti-clockwise	651·2	3·30
	1049	5·30
	1375	7·10
	1727	8·80
	1948	10·0
clockwise	1869	10·0

Thus η reduces to

$$\eta = \frac{2K\delta I}{NT^2}$$

Substituting the values recorded for K, I, and T and the mean value of δ and N obtained from a graphical plot of $\delta:N$ gives:

First run: $$\frac{\delta}{N} = \frac{10{\cdot}46}{2000} = 5{\cdot}230 \times 10^{-3}$$

giving $$\eta = 186 \times 10^{-6} \text{ P}$$

Second run: $$\frac{\delta}{N} = \frac{20{\cdot}88}{4000} = 5{\cdot}220 \times 10^{-3}$$

giving $$\eta = 185 \times 10^{-6} \text{ P}$$

The values of δ and N were recorded at an air-temperature of 20·6°C, thus a value in the region of 184×10^{-6} P would be expected.

The viscometer was dismantled and reassembled with the heating jacket in position. This procedure entailed fitting a new torsion wire and the periodic time was remeasured giving $T = 16{\cdot}60$ sec.

Deflections were recorded in only one direction of rotation.

N	Deflection, δ, cm
497	2·45
997	5·40
1499	8·05
2008	10·95

From the plot of $\delta:N$

$$\frac{\delta}{N} = \frac{12{\cdot}4}{2000} = 6{\cdot}2 \times 10^{-3}$$

giving $$\eta = 216 \times 10^{-6} \text{ P}$$

The temperature, this time given by an uncalibrated chromel–alumel thermocouple located near the upper face of the lower guard cylinder, was 82°C.

At this temperature the accepted viscosity for air is approximately 209×10^{-6} P. Bearing in mind that uncalibrated thermocouples of this type have an absolute accuracy of ±3 per cent this could account for the error in η.

Greater accuracy would not be expected in this case where the deflections produced are so small compared with those for which the instrument is designed, viz. a maximum deflection δ of 100 cm in either direction. Nevertheless the plots of $\delta:N$ indicate good inherent behaviour of the instrument and are of sufficient value to proceed with the manufacture of stainless steel bearings which are illustrated in Figs 9.3 and 9.4.

Initial tests with water in the modified instrument indicate that improved accuracy can be expected owing to the larger angular deflections.

APPENDIX 9.II

REFERENCES

(1) KJELLAND-FOSTERUD, E. Ph.D. Thesis, University of Glasgow, 1958.

(2) WHITELAW, J. H. Ph.D. Thesis, University of Glasgow, 1960; also T.R. 1 and T.R. 3, Mechanical Engineering Department, University of Glasgow, 1960.

(3) LATTO, B. Ph.D. Thesis, University of Glasgow, 1964; also T.R. 16, Mechanical Engineering Department, University of Glasgow.

(4) SWINDELLS, J. F., COE, J. R. and GODFREY, T. B. *J. Res. natn. Bur. Stand.* 1952 **48**, 1.

(5) ROSCOE, R. and BAINBRIDGE, W. *Proc. Phys. Soc.* 1958 LXXII, 4.

(6) TIMROT, D. L. and KHOPKINA, A. V. 'Experimental investigation of the viscosity of water and steam at high pressures and temperatures', Moscow', Thesis by A. V. Khopkina, 1954.

(7) WEBER, W. *Z. Physik.* 1955 **7** (2), 96; also *Z. Physik.* 1963 **15** (4), 342.

(8) MOSZYNSKI, J. R. *J. heat Trans., Am. Soc. mech. Engrs* 1961 **83**, 111.

(9) SCHMIDT, E. and MAYINGER, F. *Techn. Hochschule* (Munich) *Report*, 1961.

(10) TANAKA, K. *et al.* J. C. P. S. Report No. 10.

(11) CAPPI, J. B. Ph.D. Thesis, University of London, 1964; also BETT, K. E. and CAPPI, J. B. *Nature*, 1965 **207**, (Aug.) 620.

(12) BRUGES, E. A. T.R. 9A, Mechanical Engineering Department, University of Glasgow, 1963.

(13) BEARDEN, J. A. *Phys. Rev.* 1939 **56**, 1023.

(14) THOMAS, B. W., HAM, W. R. and DOW, R. B. *Ind. Engng Chem.* 1939 **31**, 1267.

(15) REAMER, H. H., COKELET, G. and SAGE, B. H. *Analyt. Chem.* 1959 **31** (Aug.), 1422.

(16) HOUSTON, W. V. *Phys. Rev.* 1937 **52**, 751.

(17) WONHAM, J. *J. mech. Engng Sci.* 1965 (June) **7** (2), 230.

(18) VENART, J. E. S. Ph.D. Thesis, University of Glasgow, 1964; also T.R. 14, Mechanical Engineering Department, University of Glasgow, 1965.

(19) ROSCOE, R. *Brit. J. appl. Phys.* 1962 **13** (July), 362.

MADE AND PRINTED IN GREAT BRITAIN BY WILLIAM CLOWES AND SONS, LIMITED, LONDON AND BECCLES

APPENDIX E

(i) Initial testing of the viscometer was carried out using Nimonic 90 torsion wires, mainly because of the good high temperature properties of this material, especially with regard to creep. However, it was felt that since more is known of the behaviour of tungsten suspension wires, advantage should be taken of its reproducible torsional behaviour. Bearden (1) pointed out in his work that tungsten annealed at approximately 1200°C for 10 minutes behaved better than material which had received no treatment since being drawn and coiled.

During initial tests with the tungsten wire a phenomenon immediately observed from plotting deflection against angular velocity was the occurrence of solid contact or coulomb friction within the system, giving rise to the characteristic hysteresis loop. This is illustrated in Figure E2(i). It was discovered that hysteresis effects can be allowed for (at the same time maintaining a fair accuracy) by taking readings both for ascending and descending values of the input ('N' in this case) and then re-plotting the arithmetic average. Alternatively, the slope of the $\zeta : N$ plot can be obtained by taking either the ascending or descending sides of the loop. Either of these procedures could have been applied at all times had it been possible to reverse the direction of rotation of the motor. However, at elevated pressures, rotation of the seal is limited to one direction unless the R.H. coiled spring which loads the seal faces is changed for one oppositely coiled. It was therefore decided to set up a small rig for the purpose of annealing the wire in the

hope that this might eliminate the friction by allowing the cylinder to hang perfectly straight at all times. The most likely cause of the friction is thought to be the residual set in the wire produced during coiling.

The improvement in the results is illustrated by Figure E2(ii) in which the results of annealed wire are shown for comparison. The annealing rig is shown in Figure E1. It consists of a quartz tube in which the wire is allowed to hang under tension of about 100 gm. Connecting wires pass through sealed holes in the ends of the tube and these are connected to a Variac. Pure hydrogen was allowed to pass through the tube from a hydrogen bottle for about 15 minutes prior to heating the wire. The temperature of the wire was obtained with a disappearing filament type optical pyrometer. The temperature was held at approximately 1200°C for 10 minutes with a steady stream of hydrogen passing through the tube to prevent oxidation. Subsequently all wires used in the instrument have been given this treatment.

Appendix E(ii) Determination of the temperature effect on the torsional properties of tungsten wire.

If accurate measurements are to be made at elevated temperatures it is essential that the temperature dependence of torsional stiffness of the wire be accurately known. There is little information in the handbooks of physical constants except for phosphor bronze, which is commonly used in galvanometer and other sensitive instrument suspensions. The treatise on tungsten by Smithells (2) quotes the relation between the modulus of torsion G and temperature for single crystal tungsten wires as

$$G_T = G_o \left(\frac{T_s - T}{T_s} \right)^{0.263}$$

where G_T is the modulus at T^oK, T_s is the absolute melting point of tungsten and G_o = 17,100 ± 300 Kg. per sq. mm. at 300^oK.

However, the properties of single crystal wires and ordinary drawn wire is shown to differ considerably in another part of this treatise; the amount by which the wire is drawn is also a critical factor, for instance the torsion modulus values at room temperature can vary from 9000 to 22000 Kg/mm^2. Measurements on the modulus of elasticity at elevated temperatures have been made by Koch and Dannecker (3) and Dodge (4) but these were considered insufficient evidence to apply a correction to the viscometer suspension, since the effect of temperature is a function of the degree of cold work and can also be altered by annealing the wire. A more satisfactory solution is to carry out the dynamic method of determining torsional stiffness at varying temperatures with the wire to be used in viscosity

measurements. This technique is similar to that used by Rode, Reamer and Sage (5) who measured the variation in torsional elastic constant with temperature for a 10% tungsten-platinum wire.

The apparatus for this experiment consists of a vacuum vessel within a thermostatically heated jacket in which a torsional pendulum can be oscillated (see Figure 5). Means are provided for starting the body oscillating and the periodic time is recorded photoelectrically. The inertia ring dimensions vary due to thermal expansion and thus modify the value of I for the ring. The same heating fluid used for heating the first viscometer is circulated through the jacket. The temperature is recorded by mercury in glass thermometers which fit into 'wells' in the top cover of jacket and although not in close contact with the wire are just outside the wall of the vacuum vessel at the required level. It was discovered that the system needed a number of hours at the test temperature for the pendulum to reach the temperature of the surroundings without the vacuum system operational. Only when the rig was considered to be reasonably isothermal was the rig evacuated and tests commenced.

Results Using the relationship $F = \frac{I}{\tau^2}$ for torsional stiffness, the values of I and τ have been determined over the temperature range 17° to 152°C.

For a disc $I = \frac{1}{2} M R^2 = \frac{M D^2}{8}$

For yellow brass the coefficient of linear expansion is 19×10^{-6}. If D_{20} is the diameter of the inertia ring at 20°C, then

at some temperature $(20 + t)^{o}C$.

$$D_{(20+t)} = D_{20}(1 + \alpha t)$$

and

$$I_{(20+t)} = \frac{M}{8} D_{(20+t)}^{2} (1 + \alpha t)^{2}$$

$$= I_{20}(1 + \alpha t)^{2}$$

For inertia ring A_2, I_{20} = 541.151 gm cm^2. The results are listed in Table E.1 and are shown plotted graphically in Figure E3

TABLE E.1

Temp. ^{o}C	t	$\tau_{(20+t)}$ sec	$\tau_{(20+t)}^{2}$	$I_{(20+t)}$ gm cm^2	$I_{TOTAL\ (20+t)}$ gm cm^2	$\left(\frac{I_{TOTAL}}{\tau^2}\right)_{20+t}$
17	-3	7.56330	57.2035	541.090	547.565	9.5722
20	0	7.56564	57.2389	541.151	547.626	9.5674
23	3	7.56730	57.2640	541.212	547.687	9.5642
90	70	7.60806	57.8826	542.806	549.281	9.4896
140	120	7.63845	58.3489	543.625	550.100	9.4278
145	125	7.6403	58.3742	543.724	550.199	9.4254
152	132	7.6445	58.4384	543.864	550.339	9.4174

Conclusions

The graph shows the linear relationship between the torsional stiffness and temperature of the wire. No attempt has been made to calculate this effect in terms of the modulus of rigidity of the material

since this would require an accurate knowledge of the length and diameter of the wire, neither of which need to be known in the present experiment.

If the slope of the graph is denoted as χ where $\chi = \frac{dF}{dt}$ then the torsional stiffness F_t at a temperature of $(20 + t)^{\circ}C$ is given by

$$F_t = F_o + \frac{dF}{dt} \cdot t$$

$$= F_o + \chi t$$

The value for χ obtained in this experiment is $- 1.196 \times 10^{-4}$. All measurements of viscosity above and below $20^{\circ}C$ have been corrected using this factor.

The value at $17^{\circ}C$ was obtained after a period of about 1 month had elapsed from completion of the other measurements. The precision in the timings was not as high as during the main experiment, however, the average of three timings of 50 oscillations gave $\tau = 7.5633$ sec $\pm$ 0.0020 sec. This result confirms the previous values obtained, there being only a slight increase in stiffness compared with low temperature values obtained at the start of the test. The result at $140^{\circ}C$ is given in Table E2 to illustrate the precision obtained.

TABLE E2

No. of oscillations timed	Total time recorded		Periodic Time
	mm.	sec	
50	6	21.8874	7.63775
50	6	21.8833	7.63767
50	6	21.9100	7.63820
50	6	21.9720	7.63944
50	6	21.9331	7.63866
50	6	21.9183	7.63837
50	6	21.9109	7.63822
50	6	21.9454	7.63891
50	6	21.9426	7.63885

Appendix E(iii) Specimen calibrations of torsional constant of wire.

From the conclusions drawn in Appendix B it might be deduced that although the timing of oscillations of the torsional pendulum can be carried out with a precision better than 1 part in 10^4 there remains an uncertainty of at least ± 0.2% in the torsional constant when several rings are tested with the same wire. There may be several reasons for this. For instance, when the work described in Appendix B was carried out, the magnitude of the amplitude effect had not been appreciated and was not taken into account. Furthermore, towards the latter part of the experimental programme described in this thesis several modifications to the calibration arrangement were made which have improved the precision. An example being that in the first calibration experiments using a photocell to switch the counter, a collimating lamp was used to reflect a spot of light from the mirror on the pendulum in such a way that this light spot was focused by a lens onto the photocell, as shown below.

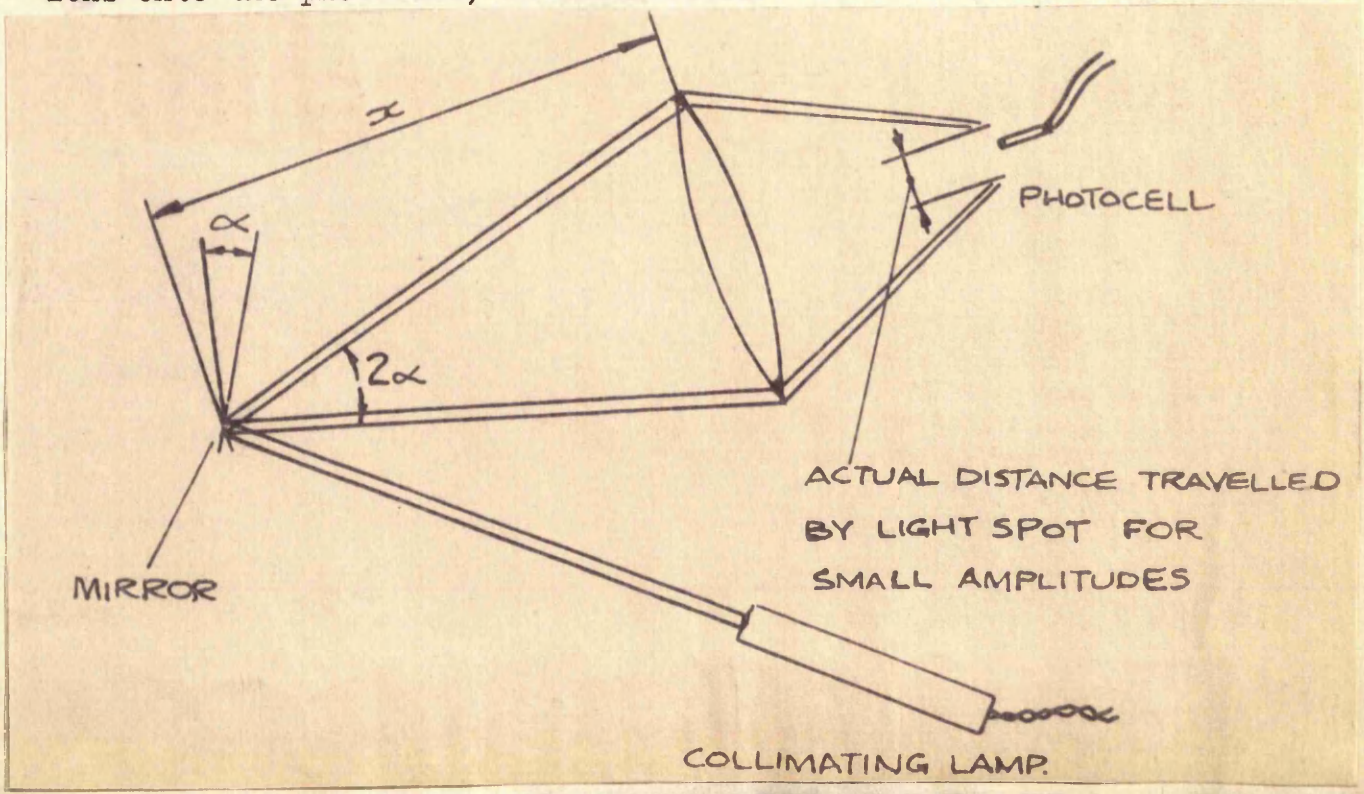

The focusing was necessary to give the required light intensity for triggering the timing circuit, but has the disadvantage that the distance travelled by the focused light is much smaller than the distance travelled across the lens and therefore the velocity with which the light passes the cell is much slower. The time constant of the photocell is a function of this velocity in that for large amplitudes the light spot passes the photocell in a fraction of a second but for small amplitudes the light spot may dwell on the cell for more than a second causing the triggering signal to be modified slightly. The system has since been altered using two lens as shown below.

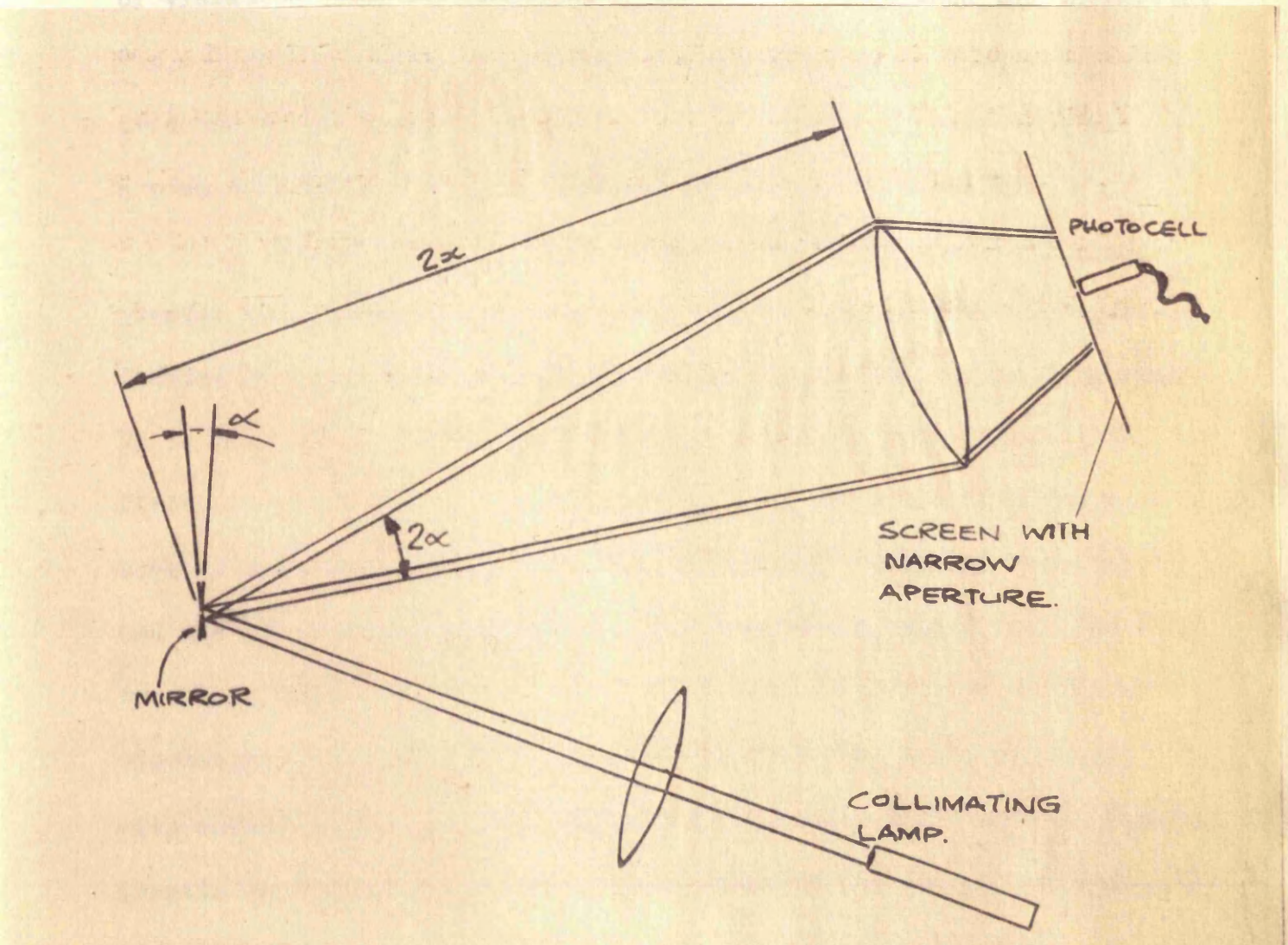

By using a lens to focus the collimated light onto the mirror a much brighter reflected light spot is obtained. This allowed the pick-up lens to be moved about twice the previous distance from the mirror so that, for the same amplitude as before, the velocity of the light spot was effectively doubled. A further precaution was to place a screen immediately in front of the photocell with an aperture approximately 0.03 in. wide. These two simple modifications greatly improved the precision and made it possible to time much smaller amplitude oscillations. A third modification was to fix the calibration rig to a much heavier stand in order to reduce the effect of vibration from the vacuum pump and in the cases when the thermostat was operating, vibration from the circulating pump. Vibration very effectively increases the scatter in the results by causing the system to move as a simple pendulum as well as torsionally.

In the latter part of these tests it was also felt that greater care in manufacturing the inertia rings and more stringent imspection methods could further reduce the uncertainty in obtaining I. Up to this time, three sets of inertia rings had been made. The first set of seven rings designated A_1 to G_1 were made with the same mass as the inner cylinder for the preliminary design of viscometer, and are slightly heavier than the rings A_2 and B_2 which were the only two rings having the same mass as the inner cylinder for the first viscometer. In addition five rings designated A_L to E_L were made with constant angular inertia but varying mass. Since neither varying inertia or varying mass (within the limits of the present experiments)

would appear to affect the calibration of the wire. Several of these rings were used to calibrate the wire prior to using the wire in the viscometer. The results of testing the wire with rings A_1, B_1 and C_1; A_2 and B_2; and C_L are given in Table E3. Note that the presence of an amplitude effect had been recognised and that the value of stiffness quoted is F_o which was calculated from the period at zero amplitude.

TABLE E3

Inertia Ring	Total Mass gm	I_{TOTAL} gm cm^2	Period τ_o sec	$I/\tau_o^2 = F_o$
A_1	417.99	810.98	9.2421	9.4945
B_1	417.86	1021.55	10.3658	9.5072
C_1	417.98	1395.00	12.1275	9.4848
A_2	350.77	548.82	7.5970	9.5092
B_2	346.73	1992.45	14.4917	9.4874
C_L	359.22	1842.82	13.9300	9.4968

The average value of F_o for these rings is $F_o = 9.4967 \pm 0.0114$ where 0.0114 is 1 standard deviation which can also be written as $\pm$ 0.12%. This deviation is similar in magnitude to that recorded in Appendix B, where amplitude was not recorded and the periodic times used in calibrations were the average of 6 or more timings taken at varying amplitudes. This was taken to infer that the deviation was due to the quality of the rings. To test this conclusion

a ring was made (designated A_{22}) with the same basic dimensions as A_2 but with greater precision in the manufacturing procedure, i.e. the faces of the ring were polished to very near optical flatness and the diameter was measured using slip gauges and electronic comparator. The difference in F_o from that given by A_2 was less by 0.05% and the difference from the mean value quoted above is also 0.05%.

TABLE E4

Inertia Ring	Total Mass gm	I_{TOTAL} gm cm^2	Period τ_o sec	I/τ_o^2
A_{22}	351.93	550.49	7.6115	9.5018

If anything, the results obtained with the first six rings suggest that the scatter is less with rings of larger diameter. This is to be expected since an error in measuring the diameter then has a proportionally smaller effect on the calculated value of I. For this reason two more rings were made designated C_2 and D_2 which differ fairly radically from the previous shape of high-inertia rings illustrated in Appendix B. Figure B3 shows inertia ring C_2 mounted on the mirror stem in place of the inner cylinder. Two aluminium discs hold the ring in the horizontal position and a small brass spacer allows the assembly to be nipped tightly together. In the case of inertia ring D_2 one aluminium ring was found to be sufficient to provide a firm support. The rings are made from S.80 stainless steel

with great care, the faces being ground flat and then polished on a surface block. The outside diameter was measured by electronic comparator and slip-gauges and the bore by "Tesa" three pronged internal micrometer with a vernier scale reading to 0.0001 in. The mass of the rings was measured by a precision chemical balance and calibrated weights, the error being only ± 0.1 mg in a mass of 274.0254 gm for ring C_2. Individual readings have not been recorded here but the calculated inertia of each component is listed in Table E5.

TABLE E5

Ring	Inertia gm cm^2	
	C_2	D_2
Inertia Ring	2898.55	4479.61
Aluminium carrier ring (i)	58.47	169.41
Aluminium carrier ring (ii)	57.87	-
Brass spacer	0.24	0.29
Mirror stem	6.475	6.475
Total assembly	3021.61	4655.78

NOTE Some timings of ring C_2 were made without the second aluminium carrier, in which case the total moment of inertia is 2963.85 gm cm^2.

The results of timing these two rings, again taking into account the amplitude effect, is given in table E6.

TABLE E6

Inertia Ring	Total Mass gm	I_{TOTAL} gm cm^2	Period τ_o sec	I/τ_o^2
C_2	312.16	2963.85	17.660	9.5033
D_2	382.08	4655.78	22.126	9.5101

The results obtained from timing all 9 rings with the same torsion wire can be seen graphically in Fig. E4(b). The results from A_{22}, C_2 and D_2 lie within a band of 0.07% and are an obvious improvement on the previous 6 results. It is thought that the accuracy obtained with these rings (the assessment of errors has concentrated on rings C_2 and D_2 in particular) is quite adequate for the present requirements.

Figure E4 has been drawn to show in graph (a) the % deviation of the first six rings about the mean and (b) the % deviation of all nine rings about the mean. It might have been inferred from the results of the first six rings that the torsional stiffness was decreasing with increasing moment of inertia of the suspended system. However, the results of all the rings show that there would appear to be no particular trend, thus confirming the findings of Appendix B.

References.

(1) Bearden, J.A. Phys. Rev. 56, 1023 (1939)

(2) Smithells, C.J., Tungsten, A Treatise on its Metallurgy, Properties and Applications. 3rd Edition. Published By Chapman and Hall Ltd., London (1952).

(3) Koch and Dannecker. Ann. der Phys. 47, 197-227 (1915)

(4) Dodge, Phys. Rev. 11, 311 (1918)

(5) Rode, J.S. Reamer, H.H. and Sage, B.H., Rev. of Sci. Instrum. 30, 11, 1062 Nov (1959)

Fig.E1. Apparatus used to anneal tungsten wire in an atmosphere of hydrogen.

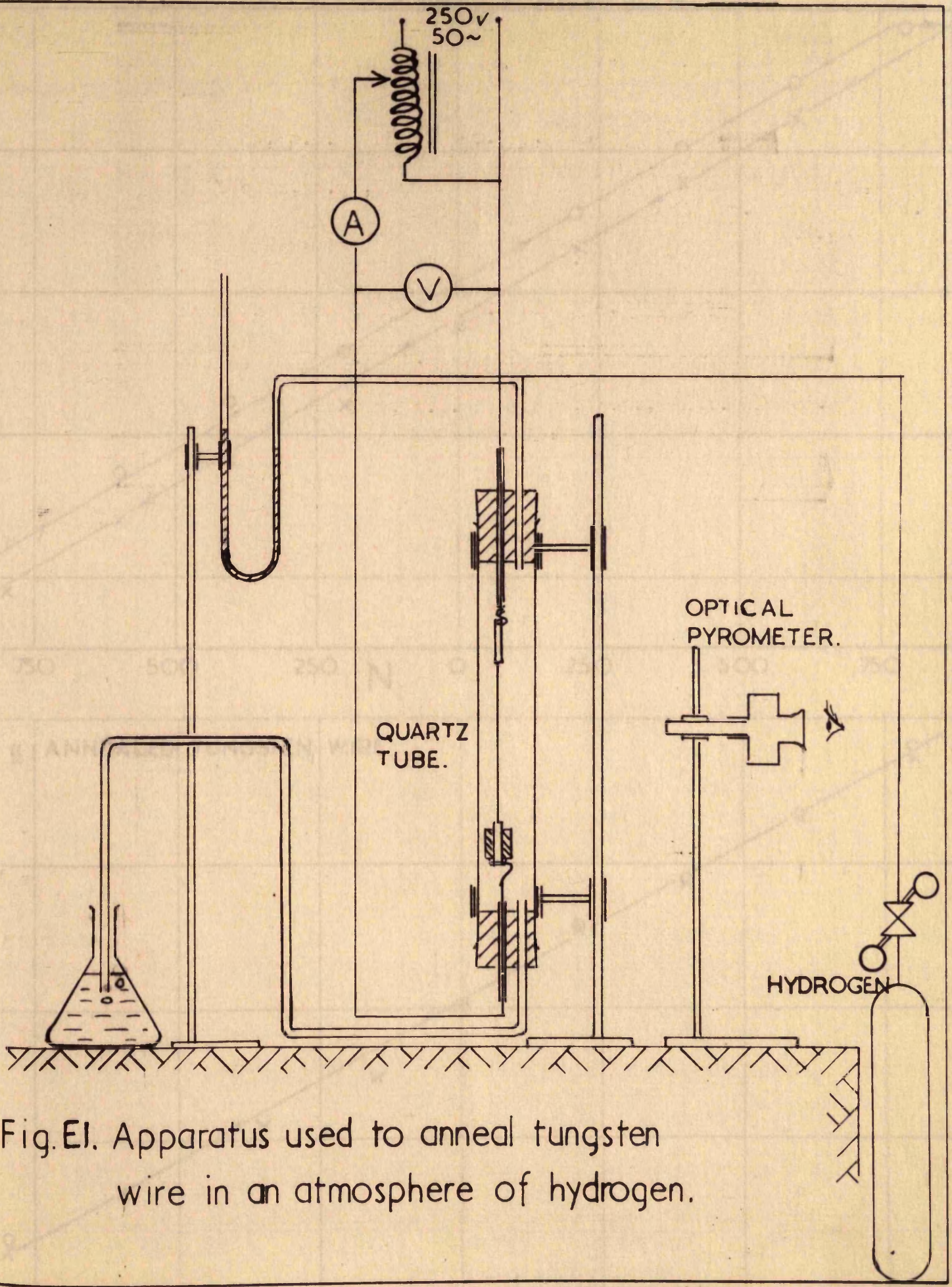

Fig. E1. Apparatus used to anneal tungsten wire in an atmosphere of hydrogen.

FIG. E2 i PLOT OF δ : N FOR UNANNEALED TUNGSTEN WIRE.

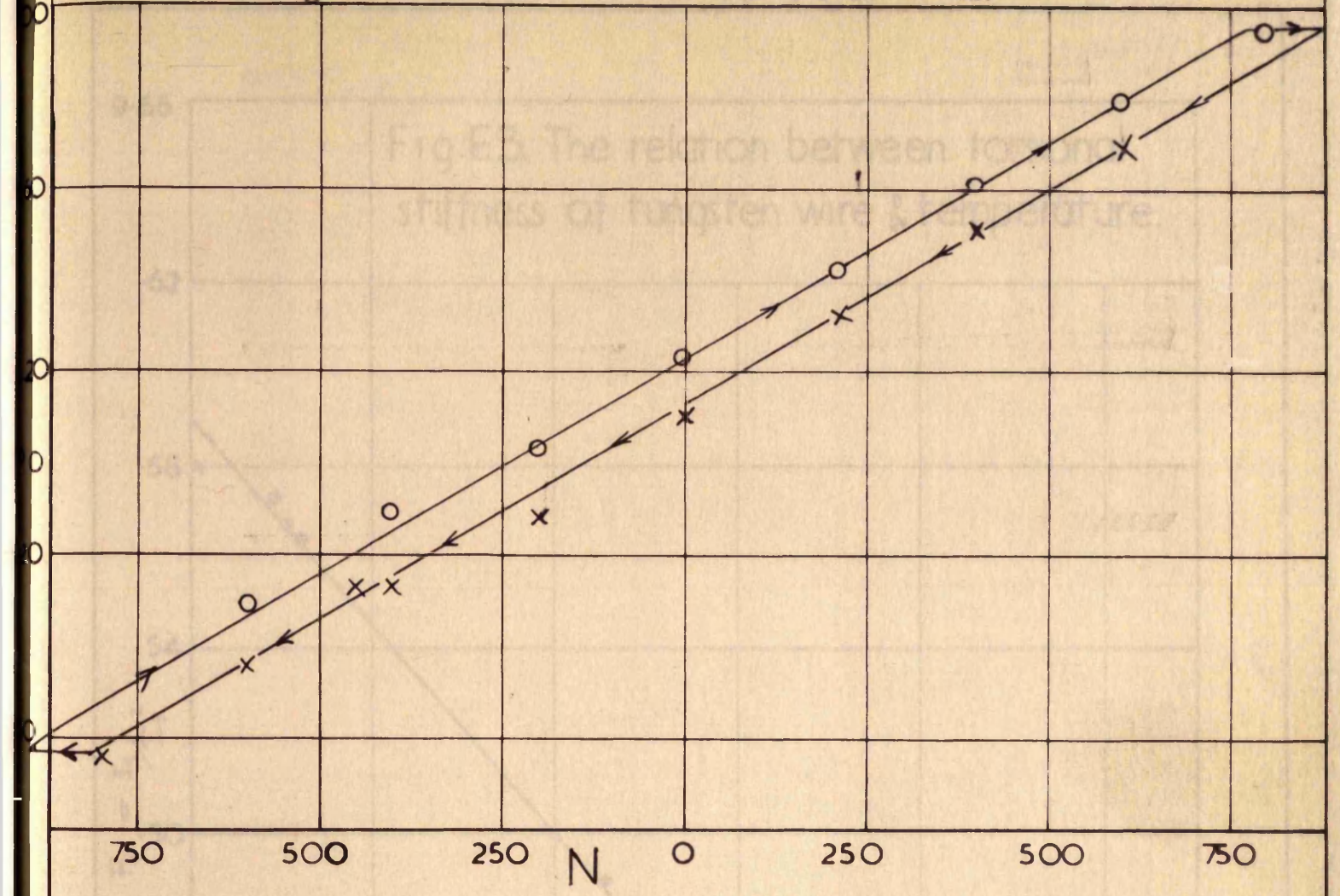

ii ANNEALED TUNGSTEN WIRE.

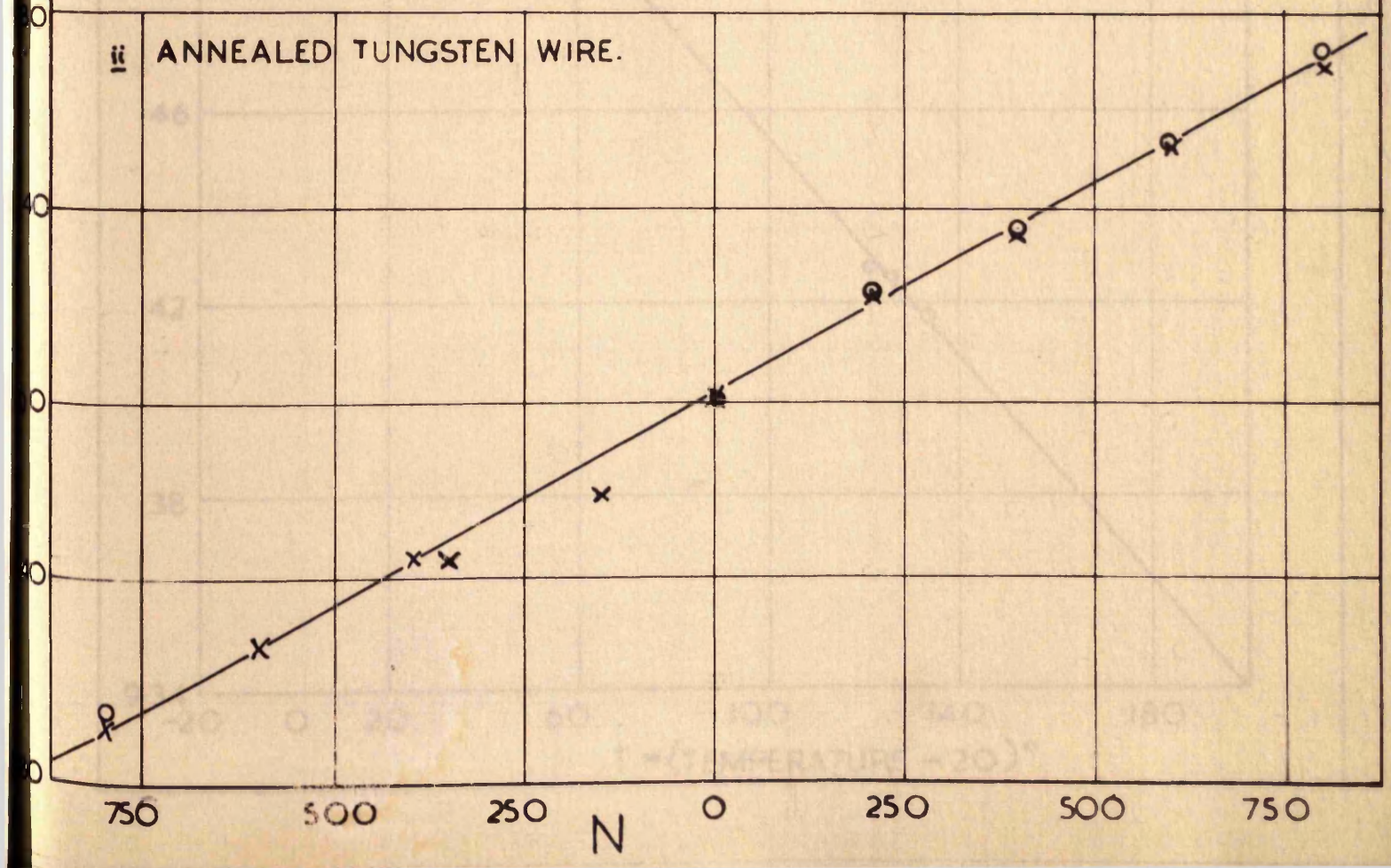

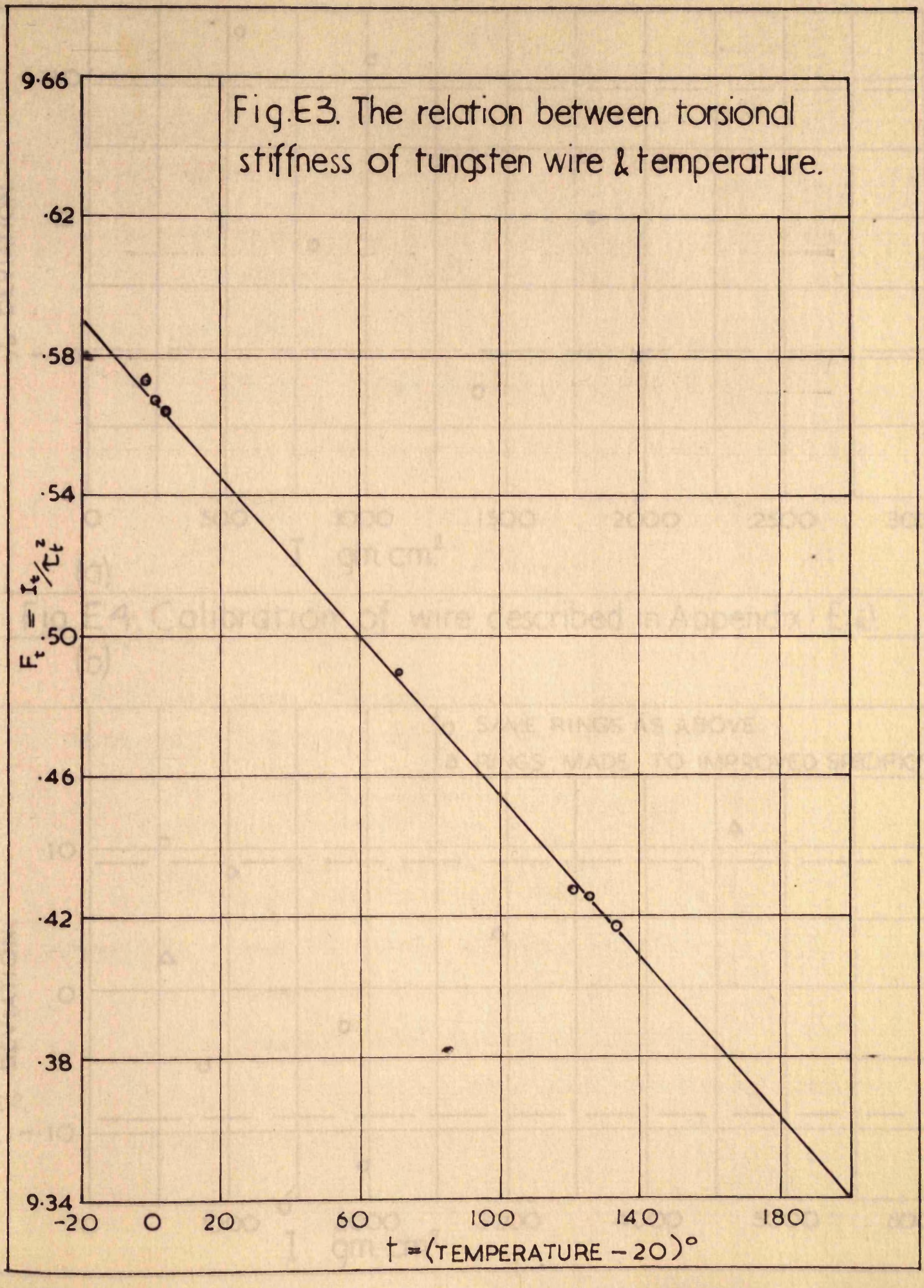
Fig.E3. The relation between torsional stiffness of tungsten wire & temperature.
9·66
·62
·58
·54
·50
·46
·42
·38
9·34
$F_t = I_t/\pi t^2$
-20
0
20
60
100
140
180
t = (TEMPERATURE - 20)°

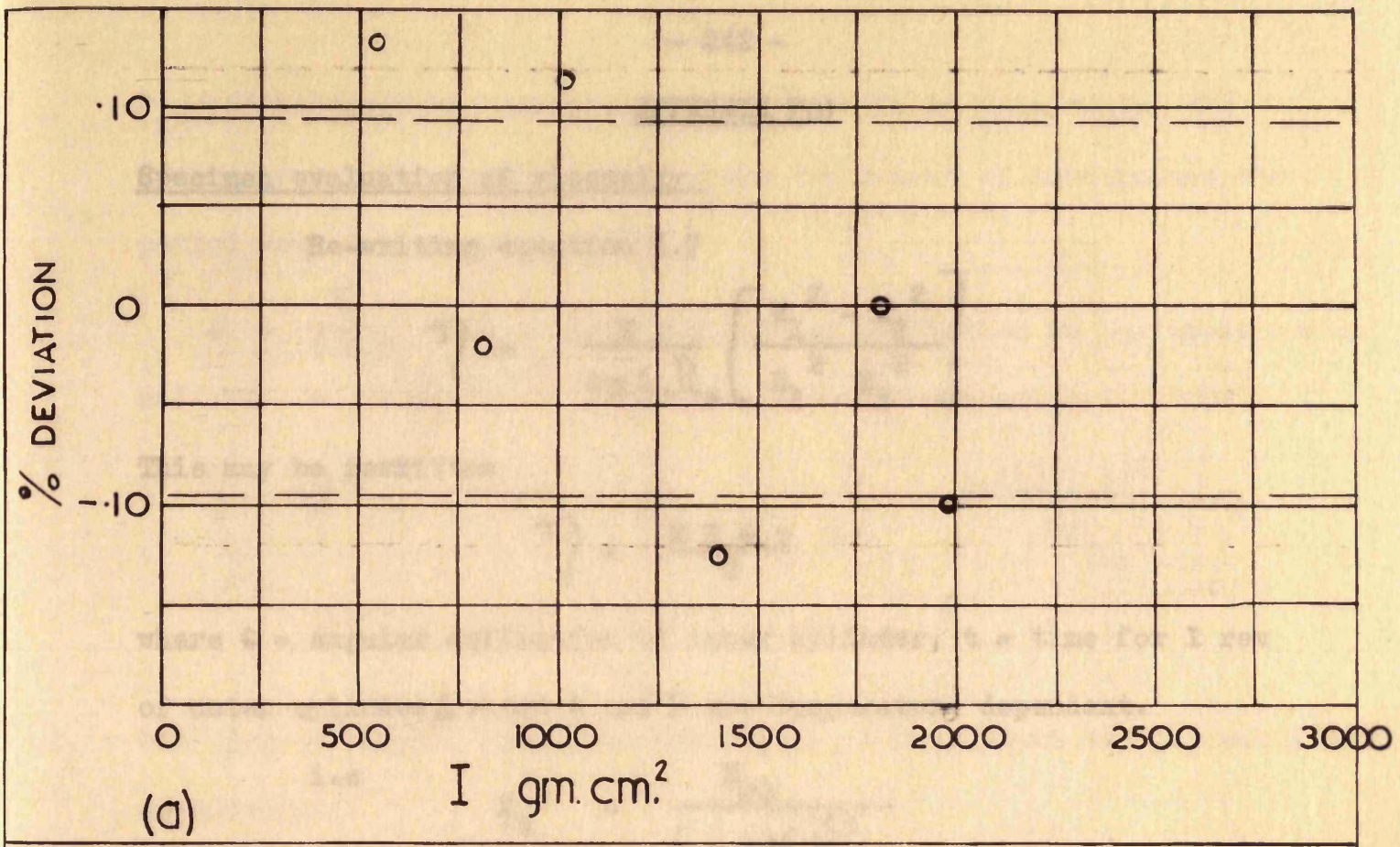

(a)

Fig. E4. Calibration of wire described in Appendix E(iii).

(b)

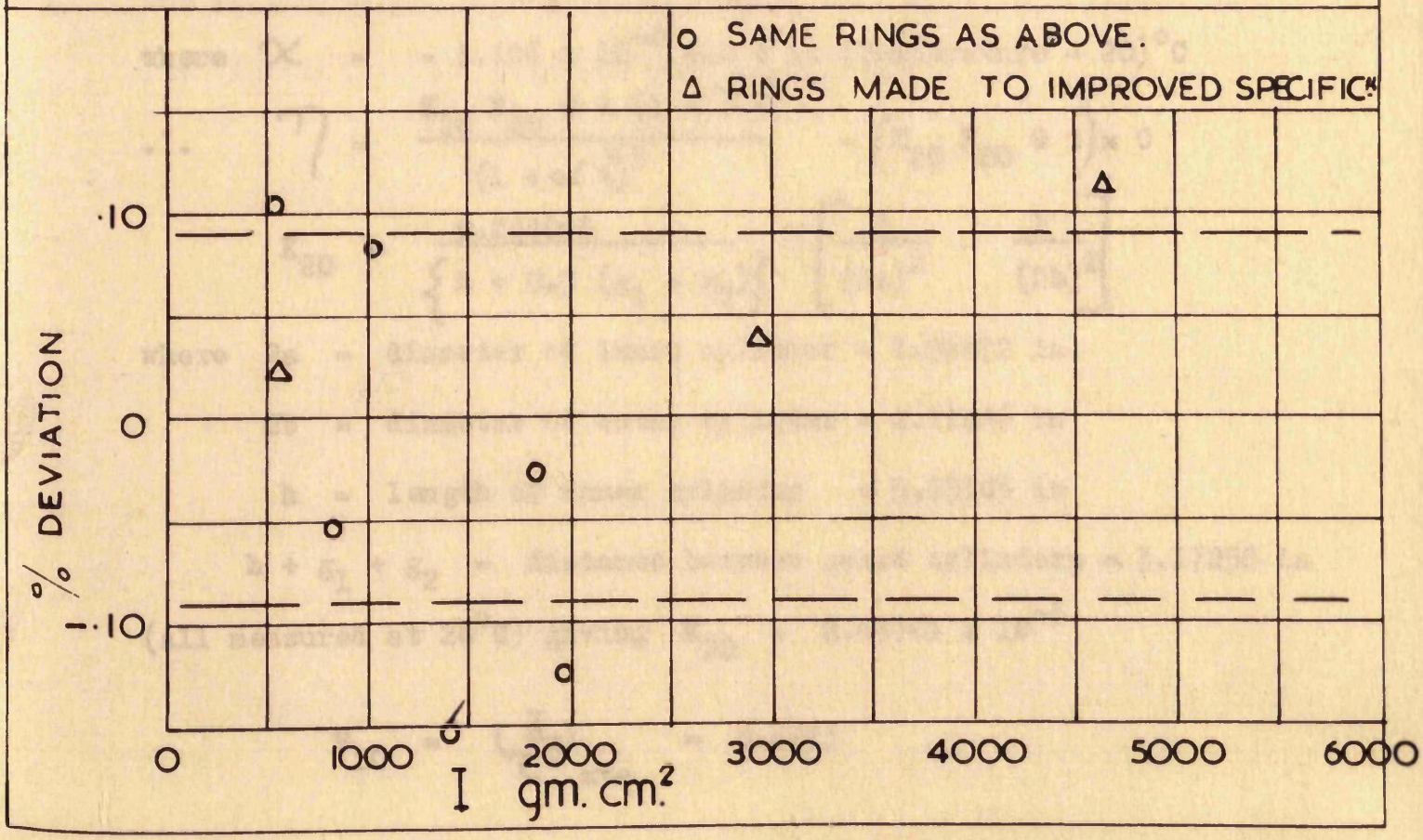

APPENDIX F(i)

Specimen evaluation of viscosity

Re-writing equation 3.7

$$\eta = \frac{T}{4\pi L \Omega_o}\left[\frac{R_1^2 - R_2^2}{R_1^2 R_2^2}\right]$$

This may be rewritten

$$\eta = \frac{K F \theta t}{2}$$

where θ = angular deflection of inner cylinder, t = time for 1 rev of outer cylinder & where K and F are temperature dependent.

i.e
$$K_t = \frac{K_{20}}{(1 + \alpha t')^3}$$

where $\alpha = 16 \times 10^{-6}$

and
$$F_t = F_{20}(1 + \chi t')$$

where $\chi = -1.196 \times 10^{-4}$ and t' is (Temperature - 20)°C

$$\therefore \quad \eta = \frac{K_{20} F_{20} \theta t (1 + \chi t')}{(1 + \alpha t')^3} = (K_{20} F_{20} \theta t) \times C$$

$$K_{20} = \frac{0.244095}{\{h + 0.5 (g_1 + g_2)\}} \cdot \left[\frac{1}{(2a)^2} - \frac{1}{(2b)^2}\right]$$

where 2a = diameter of inner cylinder = 1.96872 in.

2b = diameter of outer cylinder = 2.11486 in

h = length of inner cylinder = 3.15106 in

$h + g_1 + g_2$ = distance between guard cylinders = 3.17258 in

(all measured at 20°C) giving $K_{20} = 2.65761 \times 10^{-3}$

$$F_{20} = \left(\frac{I}{\tau^2}\right)_{ave} = 9.4973$$

F_{20} is the torsional stiffness of the wire found from taking the average value for several rings where the moment of inertia and the period were determined at 20°C.

$\theta = \frac{\delta}{600.0}$ where δ is the angular deflection on the upper scale.

and $t = \frac{1.624 \times 10^4}{3N}$ where N = tachometer reading.

$$\therefore \eta = 10^{-3} \times 2.65761^5 \times \frac{I}{\tau^2} \times \tfrac{1}{2} \times \frac{\delta}{600} \times \frac{1.624 \times 10^4}{3N} \times C$$

$$= 10^{-1} \times 2.65761^5 \times \frac{I}{4\tau^2} \times 0.180444 \times \frac{\delta}{N} \times C$$

but $\frac{I}{\tau^2} = 9.4973$ (for the wire calibration relevant to this particular measurement)

$$\therefore \eta = 0.113860 \times \frac{\delta}{N} \times C$$

The following readings were taken to obtain a typical single value for viscosity. The pressure was 125 Kgf/cm^2.

N		Reading of Upper Scale	Thermocouple emf μV	Time
Beginning	End			
0		74.10	108.5	14.10
198.6	198.7	102.25	108.7	14.15
299.5	299.5	117.65	108.9	14.25
399.6	399.4	132.10	109.3	14.30
499.8	499.8	146.55	109.6	14.40
599.6	599.1	161.10	109.9	14.50
501.0	501.6	147.05	110.2	15.00
399.2	399.2	132.65	110.5	15.10
299.7	298.6	117.20	110.6	15.15
200.6	200.7	101.90	110.7	15.25
99.5	99.5	88.10	110.75	15.30

The average value for the thermocouple emf was 109.59 μV = e

From the calibration curve for this thermocouple

$$e_t - e = + 2.0\ \mu V$$

$$\therefore\ e_t = 111.59 \mu V$$

Referring to the standard reference table

$$\text{Temperature} = 17.7 + \frac{11.59}{100} \times 16.7$$

$$= 19.636$$

$$\text{say} = \underline{19.64^\circ C}$$

$$\therefore\ t' = (19.64 - 20) = - 0.06^\circ C$$

$$\therefore\ C = \frac{(1 + 0.06 \times 1.196 \times 10^{-4})}{(1 - 0.06 \times 16 \times 10^{-6})^3} \approx 1.0000$$

The mean value of N and the corresponding upper scale reading have been fitted to the best straight line curve by the method of least squares. The slope of this line is $\frac{\delta}{N}$ which in this case evaluated

to 1.4636×10^{-1}; the standard deviation ofscale readings from the linear fit being 0.436 cm. A factor of 0.6 has to be introduced because of a calibration error in the counter.

$\therefore \eta = 0.113860 \times 1.4636 \times 1 \times 0.6 \times 10^{-1}$

$= 0.00999804$ poise

say $\eta = 0.9998$ cP

The pressure coefficient at 20°C is $- 2.8 \times 10^{-5}$ cP/atm. (experimental value given by Moszynski).

$\therefore$ At 1 atm. $\eta = 0.9998 + 0.0035 = \underline{1.0033 \text{ cP}}$

Appendix F(ii)

The viscosity measurements used to construct the viscosity: temperature relationship at 1 atm. pressure were almost invariably the results of several observations of deflection with different outer cylinder velocities. However, the procedure followed to obtain the viscosity values at elevated pressures was somewhat simpler in that the pressure was changed inside the instrument, keeping the speed approximately constant, and the new angular position of the inner cylinder was then observed. This did not necessarily involve rotating the torsion head to the null point each time the pressure was changed. When, for instance, the change in deflection of the inner cylinder was only, say, 2.5 mm (as seen on the lower scale) the upper scale reading could be modified by plus or minus 5.0 mm whichever was the case, since the upper scale is twice the distance from the viscometer than the lower scale. To start with, measurements were made at temperatures below 20°C since it is known that as the temperature decreases the pressure coefficient of viscosity for water increases negatively. Since the affect of pressure on the viscosity of water is small it was felt that initial success was more likely to be obtained where the pressure coefficient is greatest.

The temperature was usually varying slightly during the time that measurements were being made. This was due to the frictional heat produced by the mechanical face seal during the period when the cylinder speed was being increased incrementally to give the required deflection. Observations taken during this period and in the running

down period were used to calculate some of the absolute values of viscosity quoted in section 6.1. However, the temperature changes were small in most cases and the procedure was firstly to calculate the viscosity at the observed temperature and then to apply a correction to bring the viscosity to some datum temperature (using values for $\frac{d\eta}{dt}$ calculated from Bingham and White's correlation). The datum temperature was normally taken as that obtained during the initial stages of the experiment.

The first viscosity measurements made at varying pressure were encouragingly consistent and are shown plotted in Figure E2. At once it can be seen that the temperature recorded during the measurements is above the datum of 12.65°C so that the viscosity values corrected to this temperature are somewhat higher. There is, however, no appreciable change in the slope which would suggest that the thermocouple was giving a consistent value of the temperature of the test-fluid.

At a later date, however, measurements were being repeated at approximately the same conditions but this time measurements were continued over a longer period to assess the long-term effect of frictional heat from the seal on the accuracy of the instrument. One would expect the temperature rise resulting from the frictional heat to cause a fall in the measured viscosity. Observed values for viscosity show exactly this, for instance, results 1, 2 and 3 are consistent with each other when considered as a group, and so are results 4, 5, 6 and 7. At this point it is apparent that the temperature

is rising in the test fluid so that without applying a correction to bring the results to a common temperature, the pressure effect is not obvious. However, when the correction for the observed temperature change is now applied, the slope of corrected values does not agree with the slope of initially observed values. This is due to the fact that the thermocouple, being slightly nearer to the mechanical seal than the test fluid, experiences a rise in temperature sooner than the test-fluid so that the observed temperature is higher than the actual fluid temperature. The difference between the two will be increasing as the temperature gradient in the instrument builds up when the seal is operating at high pressures.

This illustrates an obvious limitation with this instrument using the face-seal. Results over the pressure range must be made before the temperature recorded is affected by frictional heat. If this precaution is observed consistent results may be obtained, as can be seen by comparing the initial results from the two sets of data represented in Figures F2 and F3. In all measurements recorded in Chapter 6, the results were not appreciably affected by the time-dependent instrument behaviour described above. The use of a magnetic drive in the second viscometer should completely eliminate the effect in future measurements with this instrument.

At higher temperatures, for instance at 89.73°C the pressure was cycled between 25 and 225 Kgf/cm^2 in order to obtain the results recorded. This was because over this limited range the pressure effect is almost linear and intermediate points were considered to be of little value.

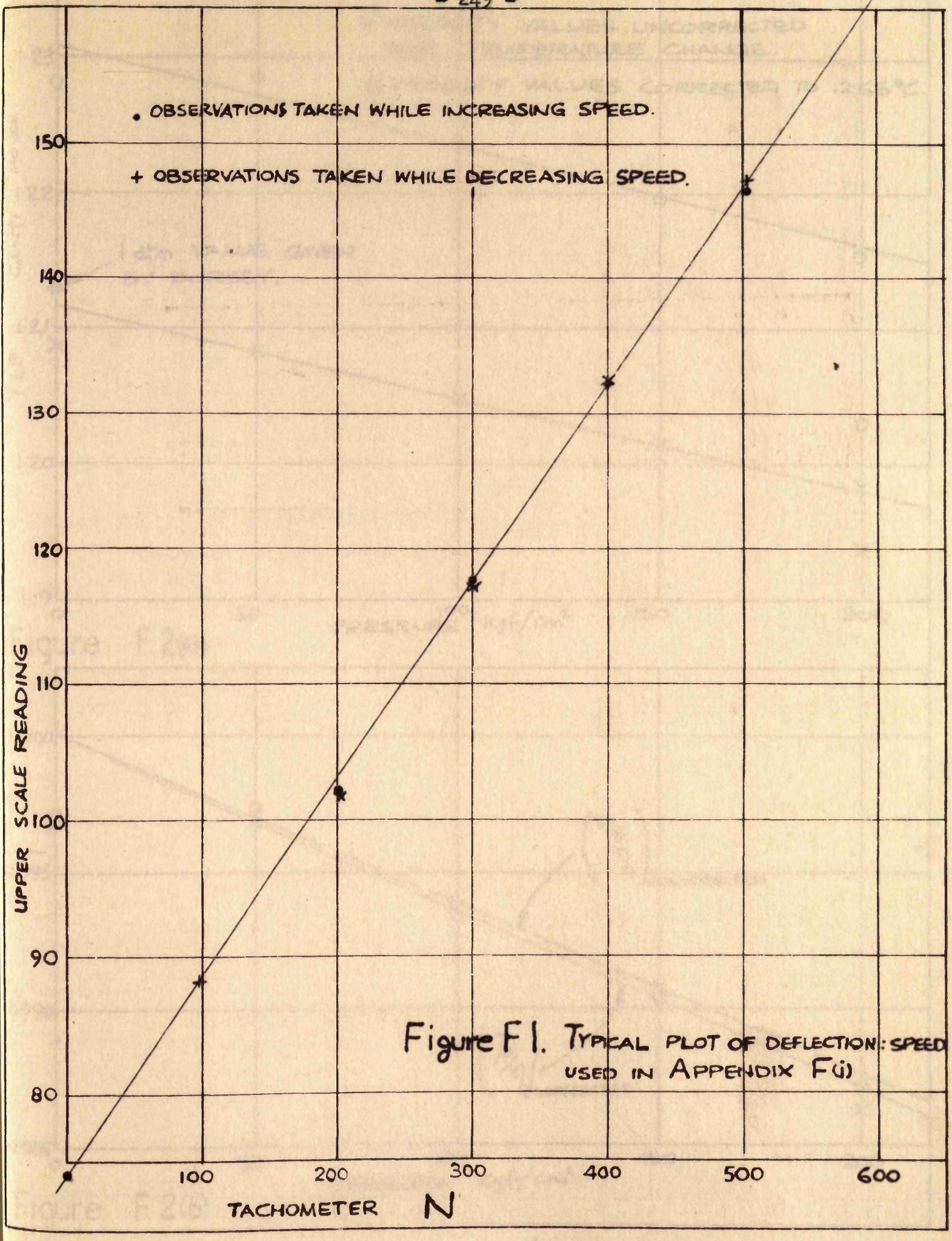

Figure F1. TYPICAL PLOT OF DEFLECTION: SPEED USED IN APPENDIX F(i)

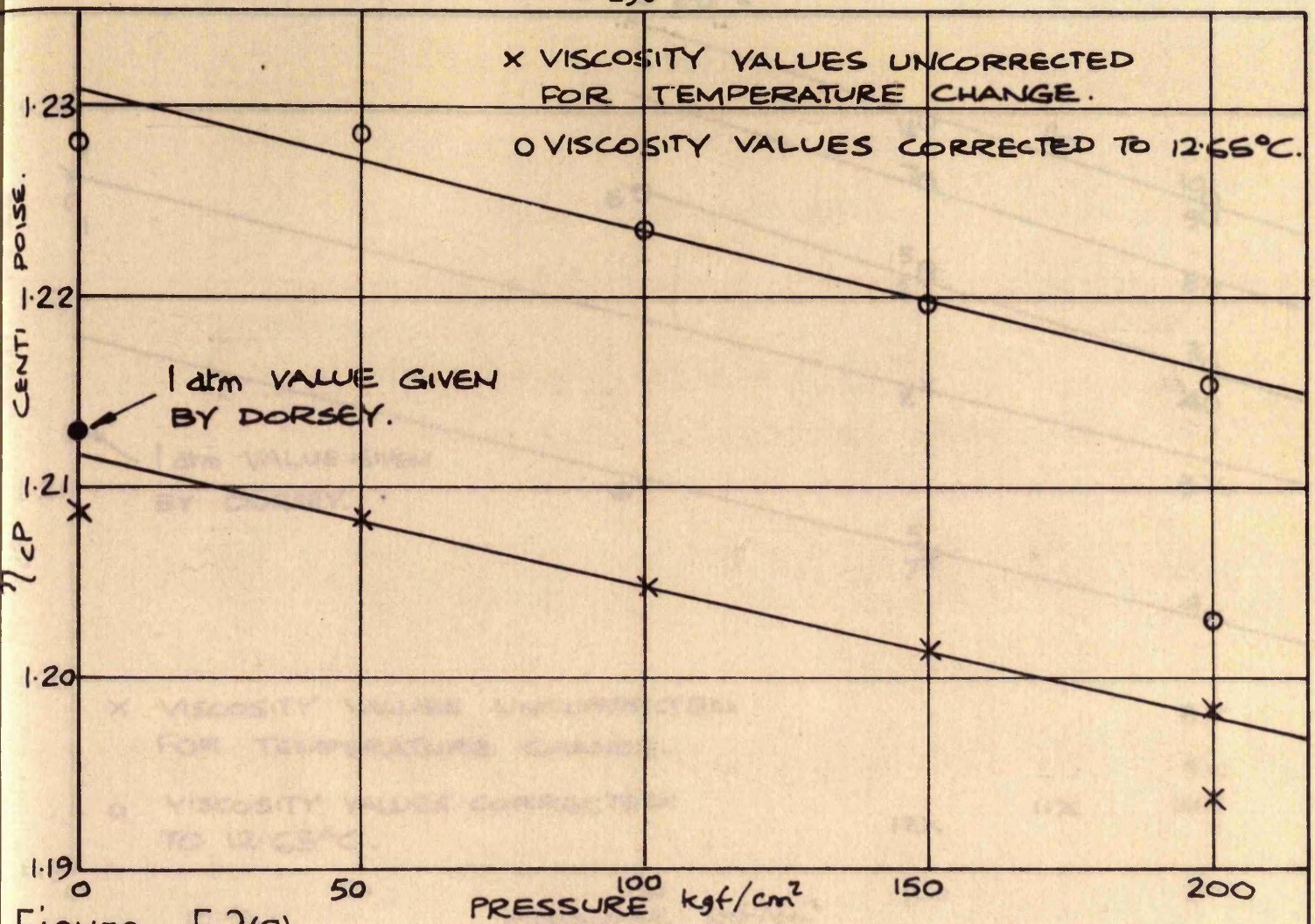

Figure F 2(a)

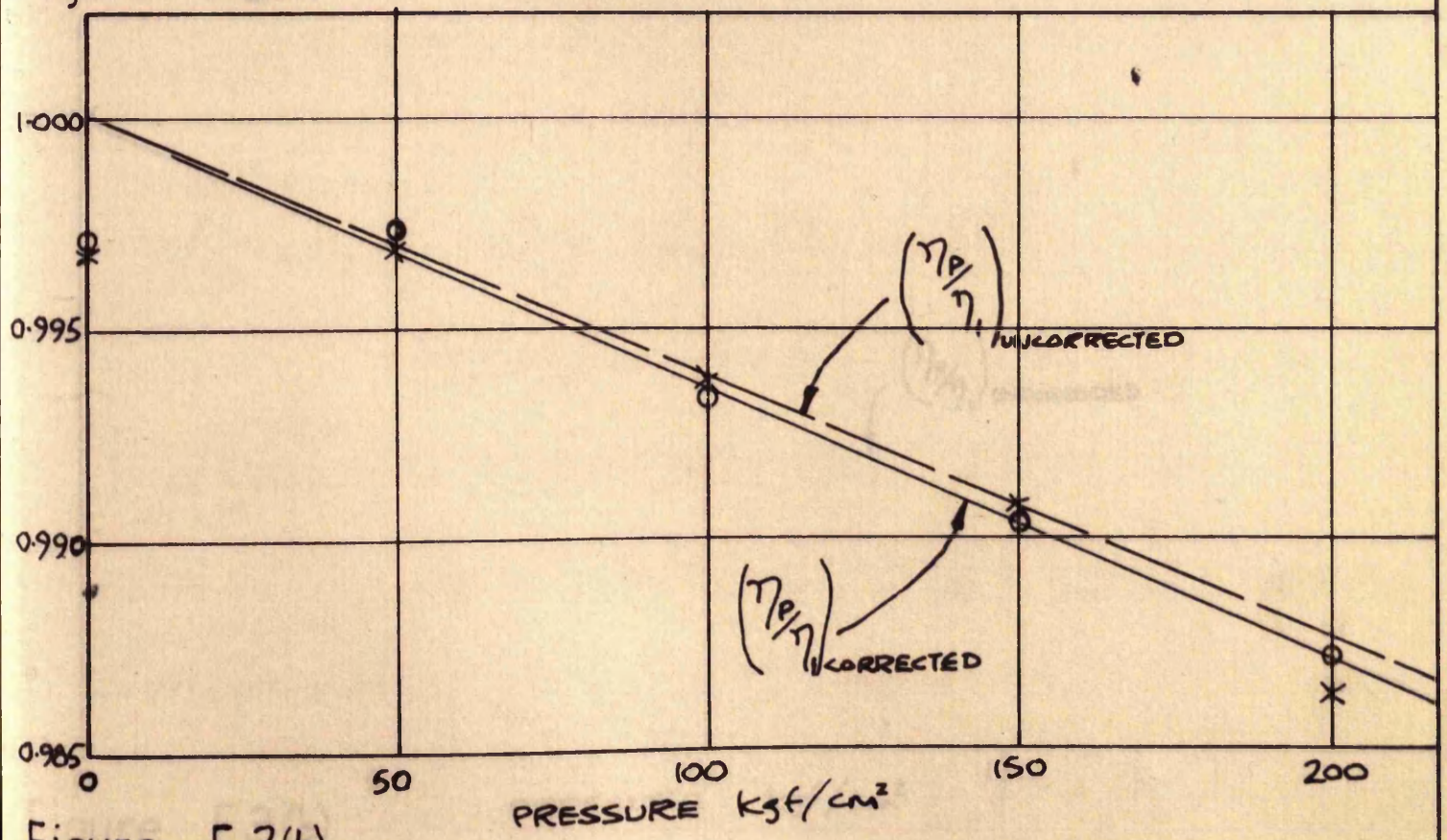

Figure F 2(b)

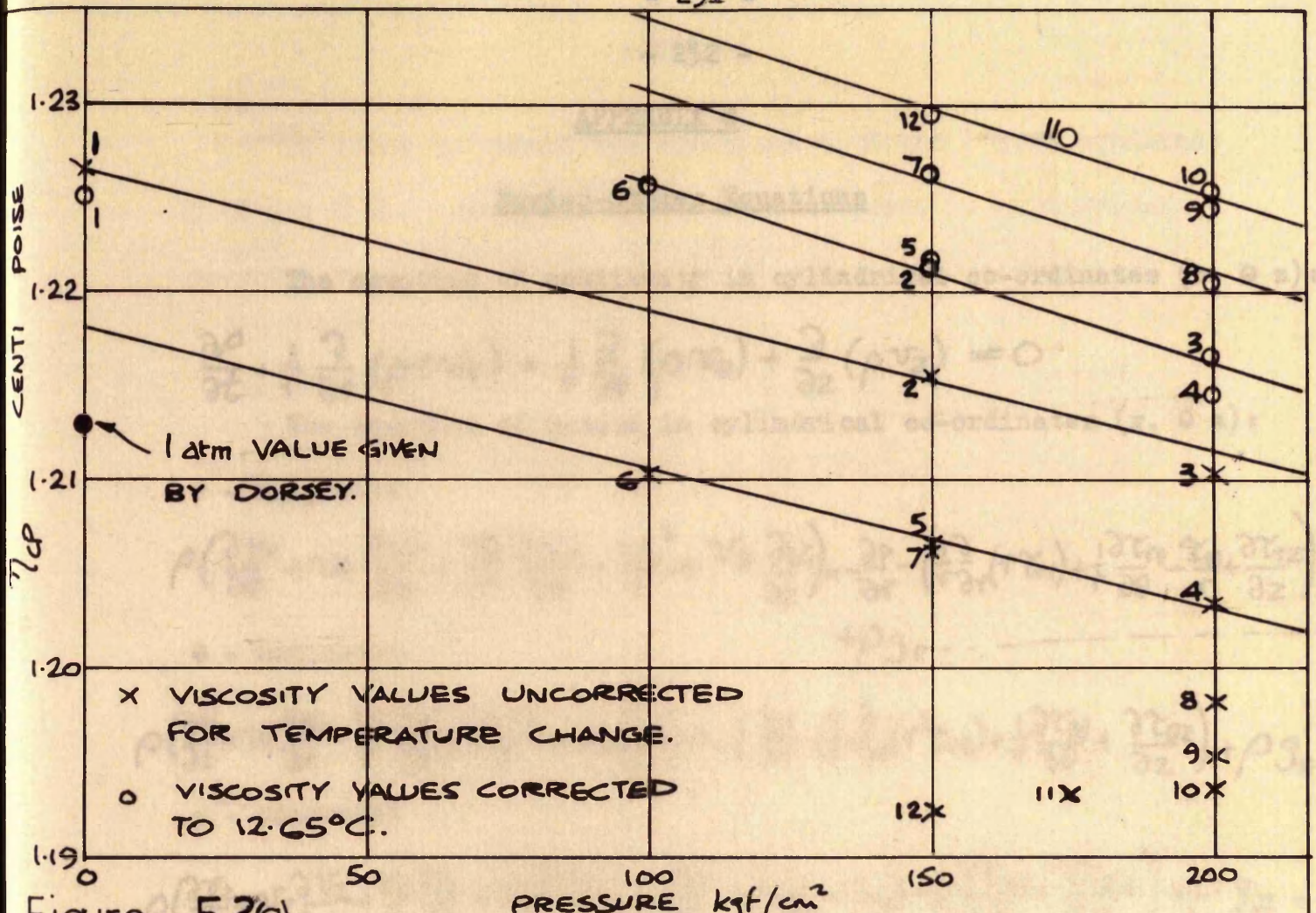

Figure F 3(a)

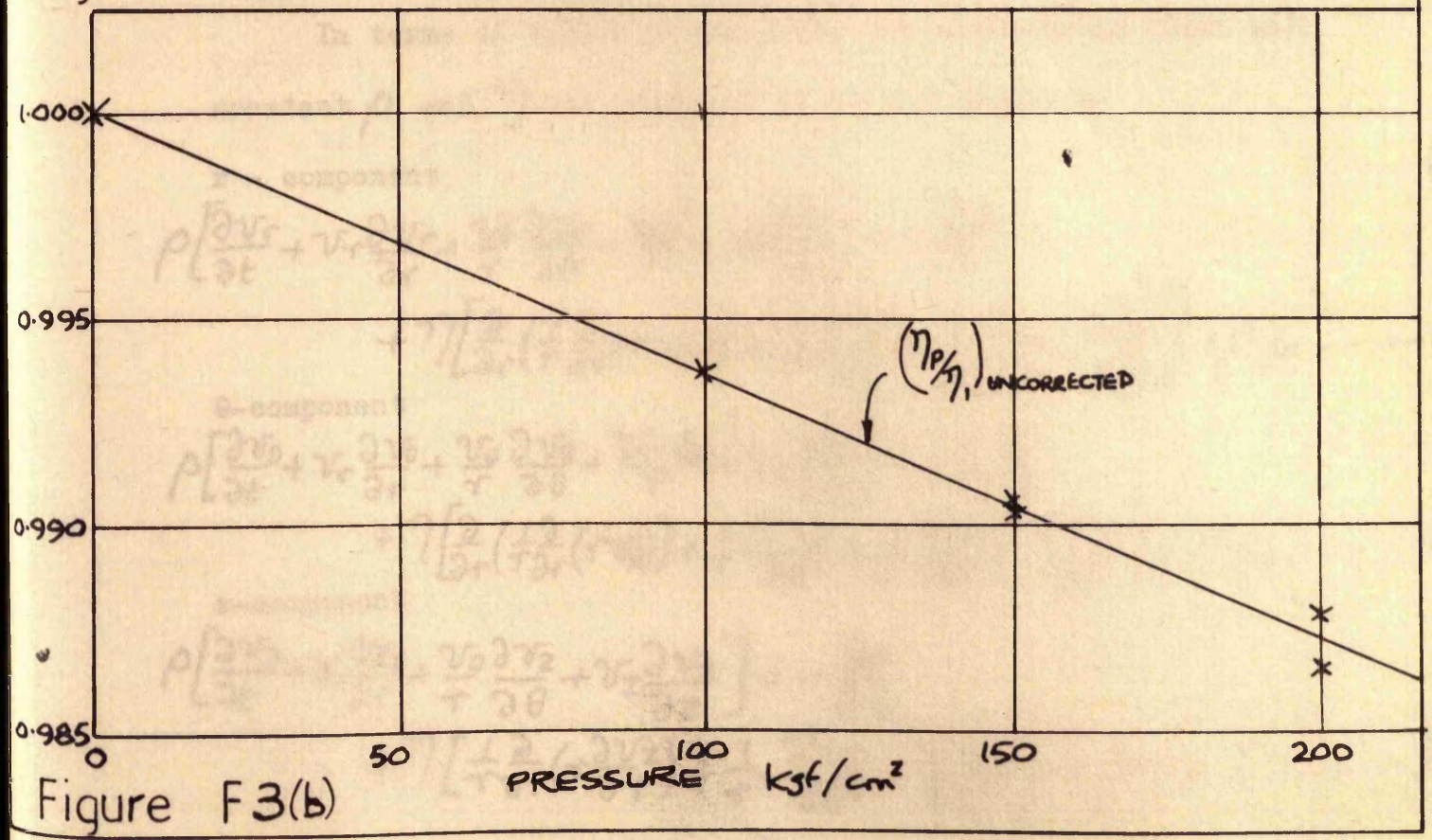

Figure F 3(b)

APPENDIX G

Navier-Stokes Equations

The equation of continuity in cylindrical co-ordinates (r, θ z):

$$\frac{\partial \rho}{\partial t} + \frac{1}{r}\frac{\partial}{\partial r}(\rho r v_r) + \frac{1}{r}\frac{\partial}{\partial \theta}(\rho v_\theta) + \frac{\partial}{\partial z}(\rho v_z) = 0$$

The equation of motion in cylindrical co-ordinates (r, θ z):

r - component

$$\rho\left(\frac{\partial v_r}{\partial t} + v_r\frac{\partial v_r}{\partial r} + \frac{v_\theta}{r}\frac{\partial v_r}{\partial \theta} - \frac{v_\theta^2}{r} + v_z\frac{\partial v_r}{\partial z}\right) = -\frac{\partial p}{\partial r} - \left(\frac{1}{r}\frac{\partial}{\partial r}(r\tau_{rr}) + \frac{1}{r}\frac{\partial \tau_{r\theta}}{\partial \theta} - \frac{\tau_{\theta\theta}}{r} + \frac{\partial \tau_{rz}}{\partial z}\right) + \rho g_r \quad \text{---A}$$

θ - component

$$\rho\left(\frac{\partial v_\theta}{\partial t} + v_r\frac{\partial v_\theta}{\partial r} + \frac{v_\theta}{r}\frac{\partial v_\theta}{\partial \theta} + \frac{v_r v_\theta}{r} + v_z\frac{\partial v_\theta}{\partial z}\right) = -\frac{1}{r}\frac{\partial p}{\partial \theta} - \left(\frac{1}{r^2}\frac{\partial}{\partial r}(r^2\tau_{r\theta}) + \frac{1}{r}\frac{\partial \tau_{\theta\theta}}{\partial \theta} + \frac{\partial \tau_{\theta z}}{\partial z}\right) + \rho g_\theta \quad \text{---B}$$

z - component

$$\rho\left(\frac{\partial v_z}{\partial t} + v_r\frac{\partial v_z}{\partial r} + \frac{v_\theta}{r}\frac{\partial v_z}{\partial \theta} + v_z\frac{\partial v_z}{\partial z}\right) = -\frac{\partial p}{\partial z} - \left(\frac{1}{r}\frac{\partial}{\partial r}(r\tau_{rz}) + \frac{1}{r}\frac{\partial \tau_{\theta z}}{\partial \theta} + \frac{\partial \tau_{zz}}{\partial z}\right) + \rho g_z \quad \text{---C}$$

In terms of velocity gradients for a Newtonian fluid with constant ρ and η the equation of motion becomes:-

r - component

$$\rho\left[\frac{\partial v_r}{\partial t} + v_r\frac{\partial v_r}{\partial r} + \frac{v_\theta}{r}\frac{\partial v_r}{\partial \theta} - \frac{v_\theta^2}{r} + v_z\frac{\partial v_r}{\partial z}\right] = -\frac{\partial p}{\partial r} + \eta\left[\frac{\partial}{\partial r}\left(\frac{1}{r}\frac{\partial}{\partial r}(r v_r)\right) + \frac{1}{r^2}\frac{\partial^2 v_r}{\partial \theta^2} - \frac{2}{r^2}\frac{\partial v_\theta}{\partial \theta} + \frac{\partial^2 v_r}{\partial z^2}\right] + \rho g_r \quad \text{---D}$$

θ-component

$$\rho\left[\frac{\partial v_\theta}{\partial t} + v_r\frac{\partial v_\theta}{\partial r} + \frac{v_\theta}{r}\frac{\partial v_\theta}{\partial \theta} + \frac{v_r v_\theta}{r} + v_z\frac{\partial v_\theta}{\partial z}\right] = -\frac{1}{r}\frac{\partial p}{\partial \theta} + \eta\left[\frac{\partial}{\partial r}\left(\frac{1}{r}\frac{\partial}{\partial r}(r v_\theta)\right) + \frac{1}{r^2}\frac{\partial^2 v_\theta}{\partial \theta^2} + \frac{2}{r^2}\frac{\partial v_r}{\partial \theta} + \frac{\partial^2 v_\theta}{\partial z^2}\right] + \rho g_\theta \quad \text{---E}$$

z-component

$$\rho\left[\frac{\partial v_z}{\partial t} + v_r\frac{\partial v_z}{\partial r} + \frac{v_\theta}{r}\frac{\partial v_z}{\partial \theta} + v_z\frac{\partial v_z}{\partial z}\right] = -\frac{\partial p}{\partial z} + \eta\left[\frac{1}{r}\frac{\partial}{\partial r}\left(r\frac{\partial v_z}{\partial r}\right) + \frac{1}{r^2}\frac{\partial^2 v_z}{\partial \theta^2} + \frac{\partial^2 v_z}{\partial z^2}\right] + \rho g_z \quad \text{---F}$$

In order to obtain the equations D, E and F from equations A, B and C the components of the stress tensor in cylindrical co-ordinates (r, θ, z) are required. These are as follows:-

$$\tau_{rr} = -\eta\left[2\,\frac{\partial v_r}{\partial r} - \frac{2}{3}\,(\nabla.\,v)\right] \qquad \ldots.G$$

$$\tau_{\theta\theta} = -\eta\left[2\left(\frac{1}{r}\,\frac{\partial v_\theta}{\partial \theta} + \frac{v_r}{r}\right) - \frac{2}{3}\,(\nabla.\,v)\right] \qquad \ldots.H$$

$$\tau_{zz} = -\eta\left[2\,\frac{\partial v_z}{\partial z} - \frac{2}{3}\,(\nabla.\,v)\right] \qquad \ldots.I$$

$$\tau_{r\theta} = \tau_{\theta r} = -\eta\left[r\,\frac{\partial}{\partial r}\left(\frac{v_\theta}{r}\right) + \frac{1}{r}\,\frac{\partial v_r}{\partial \theta}\right] \qquad \ldots.J$$

$$\tau_{\theta z} = \tau_{z\theta} = -\eta\left[\frac{\partial v_\theta}{\partial z} + \frac{1}{r}\,\frac{\partial v_z}{\partial \theta}\right] \qquad \ldots.K$$

$$\tau_{zr} = \tau_{rz} = -\eta\left[\frac{\partial v_z}{\partial r} + \frac{\partial v_r}{\partial z}\right] \qquad \ldots.L$$

where

$$(\nabla.\,v) = \frac{1}{r}\,\frac{\partial}{\partial r}\,(r\,v_r) + \frac{1}{r}\,\frac{\partial v_\theta}{\partial \theta} + \frac{\partial v_z}{\partial z} \qquad \ldots.M$$

APPENDIX H

Observed fluctuations in rotating cylinder angular velocity due to changes in main's frequency

The results of observing the tachometer reading at 10 second intervals is shown in Figure 7. This indicates maximum fluctuations of 0.4% at early and late afternoon, corresponding to peaks in industrial and domestic demand being met by the changing loading of power station turbines and alternators. However, periods of up to an hour with maximum deviation of ± 0.05% occurred in the off-peak period of the day.

This sort of fluctuation in main's frequency is to be expected. However, it is significant that the Carter hydraulic gear has not lessened the accuracy obtained from the sunchronous motor (which will follow closely main's frequency). This was anticipated when choosing this type of variable speed device, especially when a steady running temperature has been reached.

A print-out device could be fitted to the tachometer giving a continuous recording of speed variations during any given test. This would be a valuable addition where accuracy exceeding ± 0.05% is required for the speed of the rotating cylinder.

A point to notice is that most thyristor controlled electric motors available commercially are not normally constant in speed to better than ± 0.1%.

APPENDIX J

Precise angular measurement using radial diffraction gratings and moire fringe techniques.

Moire fringes are the bands of light and shade which appear when a beam of light passes successively through a pair of periodic structures, or regularly spaced grids, having the same, or nearly the same, pitch. Although these bands were accurately described as long ago as 1874 by Lord Rayleigh, and have had a limited application for measuring purposes since about 1930, the rapid development of measurement by this method did not begin until about 1950 when a technique was developed by N.P.L. for mass producing large and accurate diffraction gratings inexpensively. In fact the complete theory of moire fringes, which takes into account the wave propagation of light, did not appear until 1956 when it was given by Guild (1).

In 1960 an account of the progress made in the use of diffraction gratings as measuring scales was given by Guild (2). This work is already out-dated by more recent developments. For instance, since about 1958 the photographic method of producing gratings has replaced the grooved diffraction type. The latter type required a 'spectroscopic reading head' which necessitated the light to be collimated before passing through the gratings and then to be de-collimated in order to focus the fringe onto the photocell. The photographic diffraction grating employs what is known as a 'normal incidence reading head'. This is illustrated below, where

a light from source S is collimated by the lens L and falls upon a Grating G.

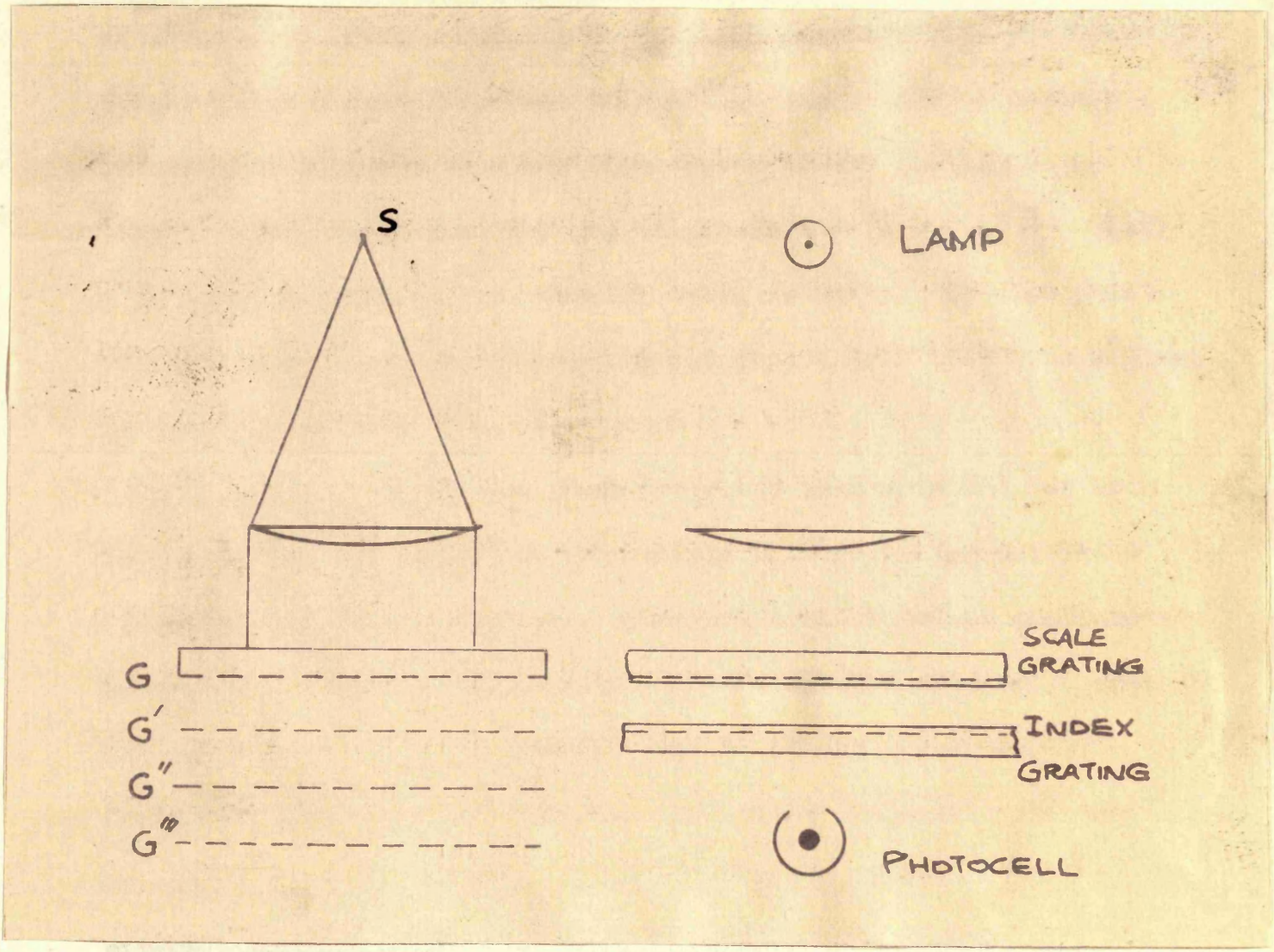

The images of the grating are formed by Fresnel diffraction images in the planes G', G", G"', etc., and a second, similar, grating will form moire fringes if placed in any one of these planes, though G' is generally used because inevitable imperfections in collimation results in degradation of the most distant images. The distance between scale and index gratings when this type of reading head is used can be shown, under ideal conditions, to be $\frac{w^2}{\lambda}$ where w is

the grating spacing and λ is the wave-length to which the photocell responds. However, for most photographic variable density gratings of about 1000 lines per inch, the emulsion surface also possesses slight phase corrugations and this brings the planes of optimum intensity modulation to a position closer to the grating G. Birch (3) has shown that the gap thickness $t = (n - 0.1)\frac{w^2}{\lambda}$ where n is a small integer, i.e. usually taken as unity. He also points out that the second grating should not depart from the optimum plane by more than $\pm\ 0.15\ \frac{w^2}{\lambda}$.

It is only during the last few years that a method has been developed for producing radial gratings with a similar precision achieved with linear gratings. When two similar radial gratings are superposed, circular moire fringes are formed the spacing of which is inversely related to the eccentricity of the two gratings. The fringes become wider and fewer as the centre distance decreases until, for perfect concentricity, one moire fringe occupies the whole circle. If one grating is rotated relative to the other under these conditions the whole overlapping area passes from light to dark and back to light again for a rotation equal to one grating spacing. When, under these circumstances, light passing through the whole annulus is made to fall upon a photocell, the resulting output of the cell provides a very accurate measure of the angle turned by the moving grating since every line contributes to the measurement and any small errors in the spacing of the lines disappears by the effect of averaging. The application of this averaging principle

in the manufacture of gratings means that the gratings are of such a high order of accuracy that a simpler and more convenient method can be used to measure the angle moved by the grating in practice which takes into account imperfections of the bearing on which the grating rotates. This method consists of two normal incidence reading heads disposed at opposite ends of a diameter and connected in parallel.

Reading heads with more than one photocell

Although reading heads employing a single photocell may prove adequate when angular displacement is to be measured by simply counting fringes, and where measurement is to be made in one direction of rotation only, the use of multi-cell reading heads facilitates the interpolation of fringes and allows the direction of the movement of the grating to be sensed. It is usual, therefore, to employ a group of four photocells equally spaced over the width of a single fringe. Each cell then generates an alternating current each cycle of which measures a movement equal to one grating spacing. Each of the four signals approaches the zero axis at each cycle and is thus equivalent to an alternating current superimposed upon upon a steady direct current. However, it is usual to derive from the reading head two purely alternating currents in quadrature relationship. This may readily be done by connecting photocells 1 and 3 together in opposition and photocells 2 and 4 similarly. Not only are the D.C. components of the signals thus eliminated but the magnitude of each of the combined signals is double that of

any one photocell.

If the two alternating signals obtained by the above procedure are applied, one to the X axis and the other to the Y axis, of a C.R.O. the two acting together cause the spot to trace a circular Lissajois figure. Relative grating movement in one direction causes the spot to revolve in a clockwise direction while grating movement in the reverse direction causes rotation of the spot in a counter-clockwise direction. Assuming gratings of perfect accuracy and the maximum size of Lissajois circle on a very large C.R.O. tube with a sharply focused spot according to Sayce (4) it would be possible to read its position to $1/3^{\circ}$ and thus make angular measurements with a 21,600 line radial grating to 1/18 of a second. Such accuracy is possible (a) if the X and Y signals are truly sinusoidal (b) if they are maintained in exact quadrature (c) if they are completely free from D.C. component and (d) if their magnitude is constant. Conditions to give a similar accuracy have been achieved by McIlraith (5), who, with linear gratings, has successfully interpolated to 0.001 fringe using a sine-cosine potentiometer. However, it is generally accepted that sub-division to 1/20 fringe is relatively easy by fitting a protractor, divided into 18° intervals, to the tube face. Thus, since each complete rotation of the spot corresponds to a grating movement of 1 minute of arc in the present apparatus, it is possible to obtain an accuracy of $\pm$ 3 seconds of arc using this method.

Experimental.

The second viscometer has been designed to operate using radial gratings to measure the rotation of the torsion head necessary to achieve the null position. This can be seen in Figure 6 which illustrated the complete viscometer. Progress so far has been in the setting up of the grating and in devising a method of registering fringes in separate counters when the torsion head is reversed. The C.R.O. method of fringe interpolation has been adopted using 4-photocell normal incidence reading heads. The counter triggering signal has been taken from the tube face rather than from the reading head. This technique involves attaching a photocell to the C.R.O. screen at a point on the Y axis where the Lissajois figure crosses. This photocell transmits a signal to the appropriate counter for the movement of each complete fringe past the reading head.

The method used to switch the signal from one counter to the other is shown in Figure J1. The + counter receives the fringe signals when the torsion head is rotated "forward" and the - counter receives signals when it is rotating in the "reverse" direction. The method of operation is obvious from reference to the diagram. Each time the torsion head is stopped there is a fraction of a fringe which must be interpolated using the C.R.O. screen protractor and recorded with the appropriate counter reading. The position of the torsion head can easily be obtained from these readings.

Adjustments of the torsion head must obviously be made in

conjunction with a sufficiently sensitive method of observing the null position of the inner cylinder. A Hilger and Watts model TA 130 Angle Dekkor auto-collimator has been chosen for this purpose. It has a displacement range of 60 minutes of arc in the horizontal direction and can be directly read to 30 sec. of arc. The setting accuracy is quoted as a standard deviation of 1 second and the overall accuracy is quoted as less than 6 sec. of arc. The combination of photographic diffraction gratings and auto-collimator should result in a precision almost an order of magnitude greater than was obtainable with the first viscometer.

Some notes on experimental procedure are listed below

(a) The spindle to which the scale grating is attached has been mounted in Barden type 103 H5 precision angular contact bearings. These have been mounted in the back to back configuration which gives the best "overturning moment" rigidity and thermal compensation. The spacing sleeves between the bearings has been adjusted to give the recommended axial loading of 15 to 17 lb. The placing of the scale grating on the spindle is extremely critical and must be finely adjusted to remove eccentricity. Preliminary adjustment is made by observing the indexing line on the grating with a microscope. Final positioning can best be made by comparing the signals from two diametrically opposed reading heads. The signals remain in the same phase relationship for perfect centering.

(b) As mentioned earlier, the index grating must be placed at a distance t from the scale where

$$t = (n - 0.1)\frac{w^2}{\lambda} \pm 0.15\frac{w^2}{\lambda}$$

For a 21,600 line radial grating 10 in. diameter w can be considered as 0.00145 in.

λ is the wavelength to which the photocell responds which for the silicon photocell used is 0.8 micron, i.e. 32×10^{-6} inch. When n = 1 this equation therefore gives t = 0.0590 in. ± 0.0098 in.

(c) Two reading heads are used located at opposite sides of the scale grating. The radial position of the index gratings must be such that the tangent to the fringes at the centre of the field should be approximately perpendicular to the rulings. This will be so if the mid-point of the index grating is on the diametral line of the fringes, i.e. the centres of the gratings are equidistant from this point so that the pitches there are equal. If the index grating is moved radially inward or outward its effective pitch is increased or reduced and the fringe direction is changed. This is indicated in the following diagram.

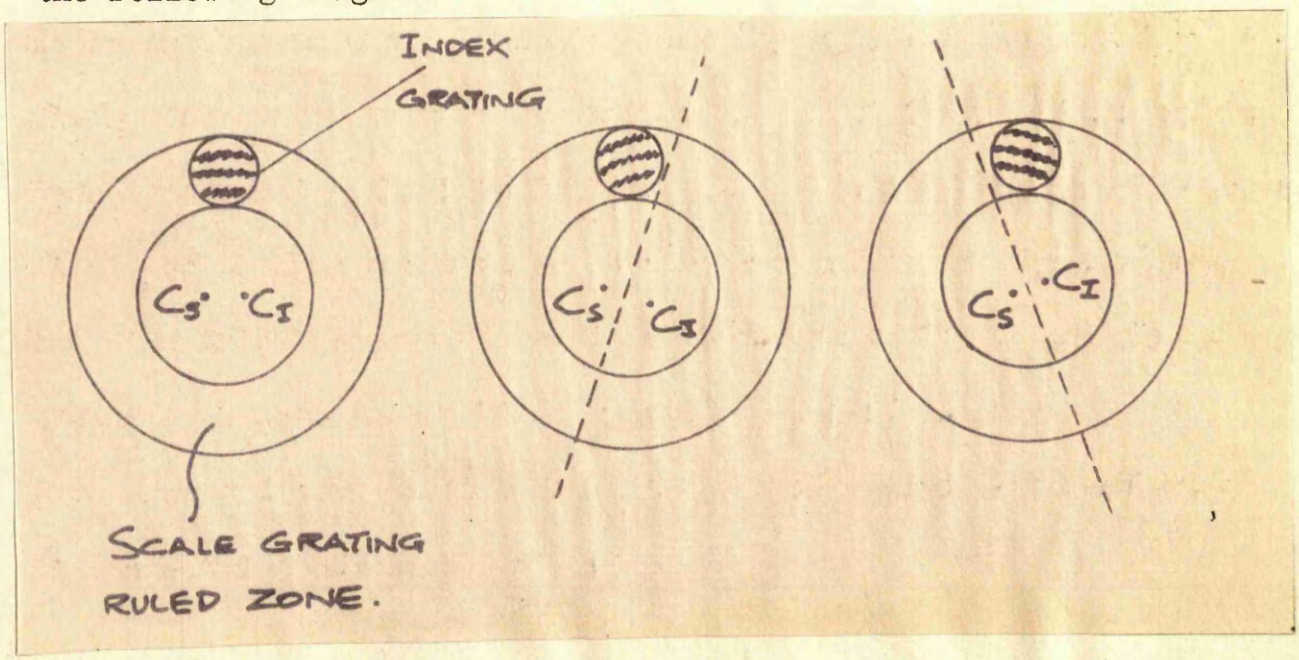

Having set the index gratings to the correct radial position they can be inclined to the scale grating to give the desired fringe distance. At this stage, providing the centering procedure has been followed correctly as described in (a), the quadrature signals from both reading heads can be connected in parallel to the X and Y axes of the C.R.O. The present work was considerably assisted by the availability of "Minirack" electronic equipment from a previous project. This contained balanced amplifiers which have allowed a circular Lissajois figure to be obtained without difficulty.

References:

(1) Guild, J. "The Interference Systems of Cross Diffraction Gratings" Oxford Clarendon Press (1956)

(2) Guild, J. "Diffraction Gratings as Measuring Scales". Oxford, University Press (1960)

(3) Burch, J.M. Progress in Optics, Vol. II. "The Metrological Applications of diffraction gratings". Published by North-Holland Publishing Co., Amsterdam (1963).

(4) Sayce, L.A. "Automatic Measurement", Penguin Technology Survey, (1967).

(5) McIlraith, A.H., J.Sci. Instrum., 41, 34, (1964)

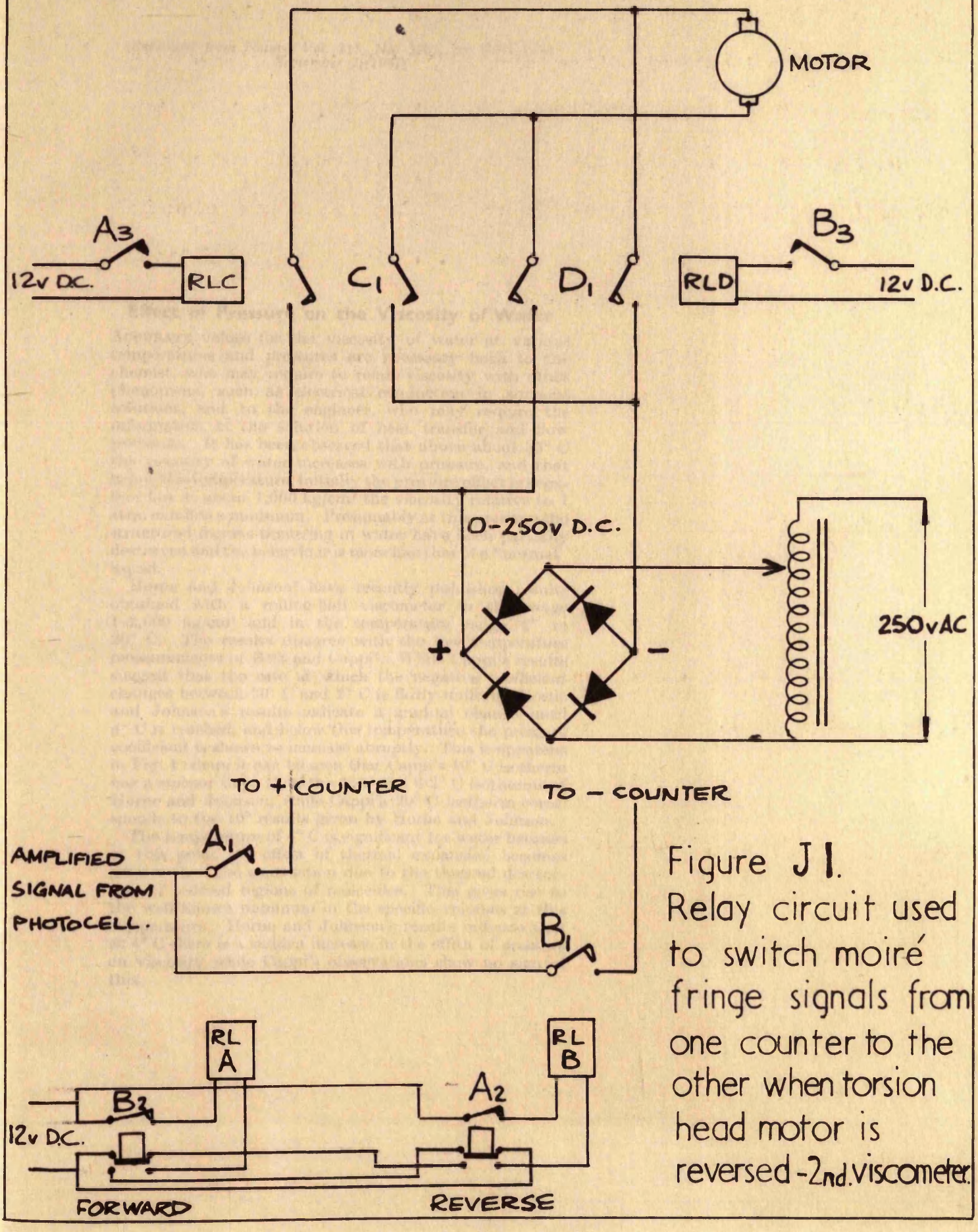

Figure J1.
Relay circuit used to switch moiré fringe signals from one counter to the other when torsion head motor is reversed - 2nd. viscometer.